Light after death : the importance of spectral composition in litter decomposition processes

Marta Pieristé

Faculty of Biological
and Environmental Sciences
University of Helsinki

UFR Sciences et Techniques
Université de Rouen-
Normandie

AGFOREE
Doctoral Programme in Sustainable
Use of Renewable Natural Resources

EdNBISE
Ecole doctorale Normande
de Biologie Intégrative, Santé,
Environnement

LIGHT AFTER DEATH:

THE IMPORTANCE OF SPECTRAL COMPOSITION IN LITTER DECOMPOSITION PROCESSES

Marta Pieristè

DOCTORAL DISSERTATION

To be presented for public discussion with the permission of the Faculty of Biological and Environmental Sciences of the University of Helsinki and of the UFR Sciences et Techniques Université de Rouen-Normandie, in Porthania hall P674 University of Helsinki and room A69 Université de Rouen-Normandie, on the 16th of June 2020 at 9.30 am CET (10.30 am EET).

Rouen/Helsinki 2020

Doctoral candidate: Marta Pieristè

Thesis supervisors:
Dr T Matthew Robson
University of Helsinki (Finland)

Prof. Matthieu Chauvat
University of Rouen (France)

Co-supervisors:
Dr. Estelle Forey
University of Rouen (France)

Dr. Alan G Jones
Scion Research Institute (New Zealand)

Pre-examiners:
Prof Christiane Gallet
University Savoie (France)

Dr Tarja Lehto
University of Eastern Finland (Finland)

Opponents:
Prof Laura Llorens Guasch
University of Girona (Spain)

Dr Stephan Hättenschwiler
CNRS Montpelier (France)

Custos :
Prof Kurt Fagerstedt
University of Helsinki (Finland)

President:
Prof M P (Matty) Berg
Vrije Universiteit Amsterdam
(The Netherlands)

Members of advisory committee Finland:
Dr. Mar Cabeza
University of Helsinki (Finland)

Prof. Anna Lintunen
University of Helsinki (Finland)

Prof. Anna-Liisa Laine
University of Helsinki (Finland)

Members of advisory committee France:
Prof. Frank Le Foll
Université. du Havre (France)

Asst. Prof. James Weedon
Vrije Universiteit Amsterdam
(The Netherlands)

Dr. Annabel Porté
INRA - Université de Bordeaux
(France)

Dr. Marc Ropitaux
University of Rouen (France)

Cover picture: Marta Pieristè (Rouen, Forêt Verte)
ISBN 978-951-51-6137-6 (paperback)
ISBN 978-951-51-6138-3 (PDF)

Unigrafia
Helsinki 2020

Normandie Université

THÈSE EN CO - TUTELLE INTERNATIONALE

Pour obtenir le diplôme de doctorat

Spécialité 4200005 SCIENCES DE L'UNIVERS

Préparée au sein de Université de Rouen Normandie et de « University of Helsinki »

LIGHT AFTER DEATH: THE IMPORTANCE OF SPECTRAL COMPOSITION IN LITTER DECOMPOSITION PROCESSES

Présentée et soutenue par

Marta PIERISTÈ

Thèse soutenue publiquement le 16 Juin 2020 devant le jury composé de		
M Kurt FAGERSTEDT	Professeur, University of Helsinki	Président (Finlande)
M MP (Matty) Berg	Professeur University of Amsterdam	Président (France)
M^me^ Tarja LEHTO	Directeur de recherche, University of Eastern Finland	Rapporteur
M^me^ Christiane GALLET	Professeure, Université Savoie Mont Blanc	Rapporteur
M^me^ Laura LLORENS GUASCH	Professeure, Universitat de Girona	Examinateur
M Stephan HATTENSCHWILER	Directeur de recherche, Cefe – CNRS, Montpellier	Examinateur
M Matthieu CHAUVAT	Professeur, Université de Rouen-Normandie	Directeur de thèse
M T Matthew ROBSON	Directeur de recherche, University of Helsinki	Directeur de thèse
M^me^ Estelle FOREY	Directeur de recherche, Université de Rouen-Normandie	Codirecteur de thèse

Thèse dirigée par

M **Matthieu CHAUVAT** Université de Rouen Normandie

M **T Matthew ROBSON** University of Helsinki

UNIVERSITÉ DE ROUEN NORMANDIE

ED 497 NBISE Normande de Biologie Intégrative, Santé, Environnement

ECODIV

HELSINGIN YLIOPISTO HELSINGFORS UNIVERSITET UNIVERSITY OF HELSINKI

AGFOREE

CanSEE

CONTENTS

LIST OF PUBLICATIONS

This thesis is based on the following publications:

I Pieristè, M., Chauvat, M., Kotilainen, T.K., Jones, A.G., Aubert, M., Robson, T.M. and Forey, E., 2019. Solar UV-A radiation and blue light enhance tree leaf litter decomposition in a temperate forest. Oecologia, 191(1), pp.191-203. DOI 10.1007/s00442-019-04478-x

II Pieristè, M.*, Neimane, S.*, Solanki, T., Nybakken, L., Jones, A.G., Forey, E., Chauvat, M., Ņečajeva, J. and Robson, T.M., 2020. Ultraviolet radiation accelerates photodegradation under controlled conditions but slows the decomposition of senescent leaves from forest stands in southern Finland. Plant Physiology and Biochemistry, 146, pp. 42-54. https://doi.org/10.1016/j.plaphy.2019.11.005
**Joint first author contribution*

III Pieristè, M., Forey, E., Lounès-Hadj Sahraoui, A., Meglouli, H., Laruelle, F., Delporte, P., Robson, T.M. ✦ and Chauvat, M.✦ Spectral composition of sunlight affects the microbial functional structure of beech leaf litter. Plant Soil (2020). https://doi.org/10.1007/s11104-020-04557-6
✦Joint last author contribution

IV Pieristè, M., Wang, Q., Kotilainen, T.K., Forey, E., Chauvat, M., Kurokawa, H., Robson, T.M. and Jones, A.G. Crucial role of blue light as a driver of photodegradation in terrestrial ecosystems on the global scale: a meta-analysis. Manuscript

The publications are referred to in the text by their Roman numerals.

TABLE OF CONTRIBUTIONS

	I	II	III	IV
Original idea	MP, TMR	MP, SN	MP	MP, QW
Study design	MP, EF, MC, AGJ, TMR	MP, SN, TMR	MP, EF, MC, TMR	MP, QW
Data collection /experiment	MP, EF, MC, TMR	SN, TMR, TS	MP, PD	MP
Lab analysis	MP	LN	MP, PD, ALHJ, HM, FL	
Data analysis	MP, MC, TMR, TKK	MP, TMR	MP	MP, QW
Manuscript preparation	MP, EF, MC, AGJ, TMR	MP, SN, TMR, EF, LN, MC, TS, JN	MP, EF, MC, TMR, ALHJ, HM, FL	MP, QW, TMR, HK, MC, AGJ, EF, TKK

AGJ = Alan G Jones
ALHJ = Anissa Lounès-Hadj Sahraoui
EF = Estelle Forey
FL = Frédéric Laruelle
HM = Hacène Meglouli
JN = Jevgenija Ņečajeva
LN = Line Nybakken
MC = Matthieu Chauvat
MP = Marta Pieristè
PD = Philippe Delporte
QW = Qing-Wei Wang
SN = Santa Neimane
TKK = Titta K Kotilainen
TMR = T Matthew Robson
TS = Twinkle Solanki

ABSTRACT

This dissertation focuses on the effect of sunlight on leaf litter decomposition. Sunlight can affect litter decomposition positively or negatively through the process known as photodegradation. Photodegradation is the ensemble of direct, indirect and mediated mechanisms. Short-wavelength solar radiation, carrying high energy, has the capacity to directly break down relatively stable components of plant tissues, such as lignin and cellulose, through photochemical mineralization causing the release of volatile carbon compounds into the atmosphere. Photochemical mineralization produces more-labile molecules, which can enhance the activity of microbial decomposers through a process known as photofacilitation or photopriming. Solar radiation has also the ability to indirectly alter decomposition through negative effects (photoinhibition) on both the activity and community composition of decomposer organisms.

We examined the process of photodegradation under forest canopies in a temperate and a boreal environment. Through two field experiments, we tested the effects of photodegradation on mass loss and carbon content during leaf litter decomposition in each environment (I in France and II in Finland). We also studied these processes under controlled conditions in a filter experiment (II). In France, we performed an additional field experiment, in the same forest as the first, to analyse the effect of photodegradation on microbial assemblages colonizing the litter (III). In these experiments, we employed "photodegradation-litterbags", bespoke litterbags adapted from classical litterbags used in litter decomposition studies incorporating different types of film filter-material, allowing us to manipulate the spectral composition of sunlight. Finally, we conducted a meta-analysis (IV) to summarise the effect of photodegradation driven by different spectral regions of solar radiation at the global scale, and across different biomes, and to test whether the photodegradation rate is modulated by initial litter traits.

This dissertation highlights the importance of blue light as a major driver of photodegradation in a temperate mid-latitude forest understorey,

with the potential to enhance both litter mass loss and carbon loss. However, at a higher latitude, the full spectrum of sunlight decreased mass loss, suggesting that the effect of photodegradation is specific to each biome. Forest canopies not only modify the amount of incoming solar radiation and its spectral composition, but also shape the microclimate of the understorey, producing unique combinations of temperature, moisture and snow-pack depth. Hence, each canopy generates novel interactions of solar radiation and other environmental factors which act on leaf litter to determine the photodegradation rate. At both boreal and temperate latitudes, our spectral manipulations revealed the effect of photodegradation to be litter species-specific, with recalcitrant litter experiencing higher rates of photodegradation. In terms of microbial decomposition, we highlighted how blue light, UV-A radiation and green light, act synergistically to shape the structure of microbial decomposer communities, with bacteria tending to dominate in sunlight and fungi in dark conditions.

The results of our meta-analysis show that the direction and magnitude of photodegradation are dependent on the spectral region considered. We highlight the crucial role of blue light and UV-A radiation as drivers of photodegradation across biomes. Blue light has a positive effect in enhancing mass loss, while UV-A radiation has a negative effect. Moreover, our meta-analysis shows that the rate of photodegradation at the global level is modulated by climate and ecosystem type; whereby arid and semiarid ecosystems with low canopy cover experience the highest photodegradation rates. On the other hand, initial litter traits failed to predict the rate of photodegradation on the global scale, despite being important at the local level; suggesting that different traits could be important in different biomes.

Photodegradation is known to have a role in the carbon cycle, as the process of photochemical mineralization causes the release of volatile carbon compounds into the atmosphere. Therefore, we can expect photodegradation to reduce the amount of carbon sequestered by ecosystems. However, further research is needed to estimate the actual contribution of photodegradation to the global carbon cycle. Moreover, this contribution is likely to be affected by climate change, which modifies environmental factors such as temperature

and the amount and pattern of precipitation; these factors together with spectral irradiance determine the photodegradation rate.

Overall, our results show that the process of photodegradation has an effect on litter decomposition in the understorey of mid- and high- latitude forests, despite the low irradiance to which litter in these ecosystems is exposed. Blue light appears to be more important than other spectral regions in driving photodegradation in these habitats. However, the photodegradation rate is modulated by both climate and ecosystem type.

RÉSUMÉ

Cette thèse s'interesse à l'effet du rayonnement solaire sur la décomposition des litières. La lumière du soleil peut impacter la décomposition des litières de manière positive ou négative grâce au processus connu sous le nom de photodégradation. On définit la photodégradation comme l'ensemble des mécanismes directs et indirects par lesquels le rayonnement solaire peut impacter la décomposition des litières. Au sein du spectre solaire, les rayonnements à courtes longueurs d'ondes mais fortes énergies peuvent accélérer la décomposition au travers de la dégradation directe de la matière organique (ex: lignine, cellulose) via le processus connu sous le nom de « dégradation photochimique» provoquant ainsi la libération de composés de carbone volatils dans l'atmosphère. La dégradation photochimique peut également améliorer la décomposition microbienne grâce à la production de molécules plus labiles. Ce second processus est appelé « photofacilitation » (ou « photopriming »). Enfin, le rayonnement solaire a également la capacité d'impacter négativement la décomposition au travers de l'inhibition de l'activité des organismes décomposeurs et de la modification des communautés microbiennes (« photoinhibition »).

Nous avons étudié le processus de photodégradation sous différentes canopées forestières en milieu tempéré et boréal. Au travers deux études de terrain nous avons testé les effets de la photodégradation sur la perte en masse et la teneur en carbone lors de la décomposition de la litière dans chaque environnement (I en France et II en Finlande). Nous avons également étudié ces processus dans des conditions contrôlées dans le laboratoire (II). En France, nous avons réalisé une étude de terrain supplémentaire dans la même forêt que la première, pour analyser l'effet de la photodégradation sur les communautés microbiennes colonisant la litière (III). Nous avons utilisé des «photodegradation-litterbags» qui sont des sachets de litières permettant de filtrer différentes compositions du spectre solaire. Nous avons ensuite réalisé une méta-analyse (IV) afin de comprendre l'effet des différentes parties du spectre sur la photodegradation à l'échelle mondiale et dans différents biomes.

Dans cette étude, nous avons aussi cherché s'il existait des corrélations entre les traits initiaux des litières et leur taux de photodegradation pour prédire cette photodégradation.

Les résultats de cette thèse montrent que malgré des niveaux relativement faibles d'irradiations (sous-bois d'une forêt tempérée), la photodegradation reste importante dans le processus de décomposition de la litière. Cette thèse met également en évidence l'importance de la lumière bleue en tant que principal moteur de la photodégradation qui peut dans ces milieux tempérés de moyenne latitude, augmenter la perte de masse de litière et la perte de carbone. Cependant, à des latitudes plus élevées, le spectre complet de la lumière solaire limite la perte de masse suggérant ainsi que l'effet de la photodégradation soit dépendant du biome. De plus, l'effet des différentes régions spectrales est modulé par l'espèce constituant la canopée. En effet, des différences de canopées peuvent modifier la quantité du rayonnement solaire entrant et sa composition spectrale, mais également le microclimat du sous-étage, caractérisé par des combinaisons uniques de température, d'humidité et de hauteur de manteau neigeux. Cela suggère que l'interaction de la photodégradation avec d'autres facteurs environnementaux joue un rôle dans la détermination du taux de photodégradation. Par ailleurs, aux deux latitudes étudiées, l'effet de la photodégradation semble être spécifique à l'espèce de litière étudiée, avec un taux de photodegradation plus élevée pour les litières récalcitrantes. En termes de décomposition microbienne, nous avons mis en évidence l'effet de la lumière bleue, du rayonnement UV-A et de la lumière verte, agissant en synergie, sur la structuration des communautés microbiennes. Les bactéries ont tendance à dominer au soleil tandis que les champignons sont favorisés par l'absence de lumière bleue, verte et rayonnement UV-A.

Les résultats de notre méta-analyse montrent que le taux de photodegradation dépend de la partie du rayonnement solaire considérée. Nous soulignons le rôle très important de la lumière bleue et du rayonnement UV-A en tant que moteurs de la photodégradation dans différents biomes, bien que le rayonnement UV-B soit considéré depuis longtemps comme la principale région spectrale responsable de ce processus. La lumière bleue a un

effet positif sur la perte de masse et le rayonnement UV-A a un effet négatif. Nos résultats montrent que le taux de photodegradation à l'échelle mondiale est fonction du climat et de la typologie d'écosystème. D'autre part les traits initiaux de la litière ne semblent pas expliquer le taux de photodégradation, indiquant que différents traits pourraient être importants dans différents biomes.

La photodégradation peut jouer un rôle dans le cycle du carbone car le processus de dégradation photochimique provoque la libération de composés de carbone volatils dans l'atmosphère. Cependant, des études supplémentaires sont nécessaires pour comprendre pleinement la contribution de la photodégradation sur le cycle du carbone à l'échelle mondiale. Enfin, dans un contexte de changements climatiques, la modification des facteurs environnementaux tels que la température, la quantité et le régime des précipitations, est susceptible de modifier le taux et l'importance de la photodégradation.

TIIVISTELMÄ

Tämä väitöskirja keskittyy auringonvalon vaikutukseen karikkeen hajoamisprosessissa. Auringonvalo voi vaikuttaa karikkeen hajoamiseen positiivisesti tai negatiivisesti valon vaikutuksesta tapahtuvan hajoamisprosessin kautta (engl. photodegradation), joka koostuu suorista, epäsuorista ja välillisistä mekanismeista. Lyhytaaltoinen ja korkeaenerginen auringonsäteily voi suoraan hajottaa kasvisolukon komponentteja, kuten ligniiniä, fotokemiallisen mineralisaation avulla, aiheuttaen haihtuvien hiiliyhdisteiden vapautumista ilmakehään. Tämä prosessi tuottaa labiileja molekyylejä, jotka voivat parantaa mikrobihajottajien aktiivisuutta valoaltistuksen seurauksena. Auringonsäteily voi muuttaa karikkeen hajoamista myös epäsuorasti, vaikuttamalla negatiivisesti hajottajaorganismien aktiivisuuteen ja hajottajayhteisöjen rakenteeseen.

Tutkimme valon vaikutuksesta tapahtuvaa karikkeen hajoamisprosessia sekä kenttä- että laboratoriokokeiden avulla lauhkeassa (Ranska) ja boreaalisessa (Suomi) metsäympäristössä. Hyödynsimme klassisissa karikkeen hajoamistutkimuksissa käytettyjä karikepusseja, joihin liitettiin erityyppisiä kalvoja, joiden avulla manipuloitiin auringonvalon spektrikoostumusta. Lisäksi teimme meta-analyysin kootaksemme aurinkonvalon eri spektrialueiden vaikutukset valon aiheuttamassa karikkeen hajoamisessa globaalissa mittakaavassa ja erilaisissa biomeissa ja selvittääksemme, muuttavatko karikkeen alkuperäiset ominaisuudet hajoamisnopeutta.

Tämä väitöskirja korostaa sinisen valon merkitystä valon vaikutuksesta tapahtuvassa karikkeen hajoamisessa keskileveysasteilla sijaitsevan lauhkean vyöhykkeen metsien pohjakerroksessa, mikä voi edistää sekä karikkeen hajoamisnopeutta että hiilen kiertoa. Korkeammilla leveysasteilla kaikki auringonvalon aallonpituudet kuitenkin vähensivät karikkeen hajoamista, mikä viittaa siihen, että valon aiheuttama karikkeen hajoaminen vaihtelee biomikohtaisesti. Metsien latvustot muokkaavat pohjakerrokseen tulevan auringonsäteilyn määrään ja laatuun, mutta ne muovaavat myös

pohjakerroksen mikroilmastoa tuottaen ainutlaatuisia lämpötilan, kosteuden ja lumipeitteen syvyyden yhdistelmiä, joilla puolestaan on merkitystä valon aiheuttamaan karikkeen hajoamiseen. Sekä boreaalisella että lauhkealla vyöhykkeellä spektrikoostumuksen manipulaatiot osoittivat että valon vaikutuksesta tapahtuva hajoaminen riippui karikkeen lajista ja oli suurempi hitaasti hajoavaan karikkeeseen. Mikrobihajotustoiminnan osalta havaittiin että sininen valo, UV-A-säteily ja vihreä valo vaikuttivat synergistisesti, muokaten mikrobiyhteisöiden rakennetta niin, että bakteerien osuus korostui auringonvalossa ja sienten valottomissa olosuhteissa.

Meta-analyysimme tulokset osoittavat, että valon vaikutuksesta tapahtuva hajoaminen on riippuvainen tarkasteltavasta spektrialueesta. Sinisen valon ja UV-A-säteilyn merkitys valon vaikutuksesta tapahtuvaan hajoamiseen on ratkaiseva eri biomeissa. Sinisellä valolla on positiivinen ja UV-A-säteilyllä negatiivinen vaikutus karikkeen hajoamiseen. Meta-analyysimme osoittaa, että valon vaikutuksesta tapahtuvan hajoamisen nopeuteen globaalilla tasolla vaikuttavat ilmasto ja ekosysteemityyppi; kuivissa ja semiaridisissa ekosysteemeissä, missä on vähän latvuston tarjoamaa suojaa, valon aiheuttamaa hajoamista tapahtuu nopeammin. Toisaalta alkuperäiset karikkeen ominaisuudet eivät ennustaneet tämän prosessin nopeutta globaalissa mittakaavassa, vaikka ne olivat tärkeitä paikallisella tasolla; tämä viittaa siihen, että erilaiset ominaisuudet voivat olla tärkeitä erilaisissa biomeissa.

Valon vaikutuksesta tapahtuvalla hajoamisella tiedetään olevan merkitystä hiilen kierron kannalta, koska fotokemiallisen mineralisaatioprosessin seurauksena ilmakehään vapautuu haihtuvia hiiliyhdisteitä. Siksi voidaan olettaa karikkeen valon vaikutuksesta tapahtuvan hajoamisen vähentävän ekosysteemien sitoman hiilen määrää. Tarvitaan kuitenkin lisätutkimuksia, jotta tosiasiallinen vaikutus globaaliin hiilen kiertoon voidaan arvioida.

Kaiken kaikkiaan tuloksemme osoittavat, että valon aiheuttamalla prosessilla on vaikutusta karikkeen hajoamiseen sekä keskileveysasteilla että korkeilla leveysasteilla sijaitsevien metsien pohjakerroksessa, huolimatta näiden ekosysteemien karikkeen saamasta alhaisesta säteilymäärästä. Sininen

valo näyttää olevan valon vaikutuksesta tapahtuvan hajoamisen edistämisessä muita spektrialueita tärkeämpi näissä elinympäristöissä, mutta hajoamisnopeuteen vaikuttavat myös sekä ilmasto että ekosysteemityyppi.

ABBREVIATIONS

AFDM	Ash-Free Dry Mass
AMF	Arbuscular Mycorrhizal Fungi
B:G	Blue to green ratio
C	Carbon content
CH_4	Methane
C:N	Carbon-to-Nitrogen ratio
CO	Carbon monoxide
CO_2	Carbon dioxide
DNA	Deoxyribonucleic Acid
DOC	Dissolved Organic Carbon
F:B	Fungal-to-Bacterial biomass ratio
FAMEs	Fatty-Acid Methyl Esters
FW	Fresh Weight
DW	Dry Weight
GLI	Global Light Index
Gram-N	Gram-negative bacteria
Gram-P	Gram-positive bacteria
Gram-P:Gram-N	Gram-P bacteria to Gram-N bacteria biomass ratio
HPLC	High-Performance Liquid Chromatography
LAI	Leaf Area Index
Lig:N	Lignin-to-N ratio
N	Nitrogen content
NLFA	Neutral Lipid Fatty Acids
NMDS	Non-metric multidimensional scaling
NPP	Net Primary Production
PAR	Photosynthetically Active Radiation
PLFA	Phospholipid Fatty Acid
SLA	Specific Leaf Area
R:FR	Red to Far-red ratio
ROS	Reactive Oxygen Species
UV	Ultraviolet radiation
UV:PAR	UV to PAR ratio

1. INTRODUCTION

1.1. THE PROCESS OF PHOTODEGRADATION

Decomposition is a key process in forest ecosystems, as it regulates nutrients cycles (Cole 1986) and, consequently, has the potential to affect plants and belowground communities (Sylvain and Wall 2011). Several abiotic (temperature, precipitation, sunlight) and biotic (initial litter traits, decomposers assemblages) factors are involved in the process of decomposition in forest ecosystems, and interactions among them determine the litter decomposition rate (Prescott 2010). Which of these factors contribute most to the process of decomposition depends on the ecosystem and the climate considered (García-Palacios et al. 2013; García-Palacios et al. 2016; Wall et al. 2008).

Sunlight can affect litter decomposition positively or negatively through the process known as photodegradation (Bais et al. 2018). Photodegradation is an ensemble of direct, indirect and mediated mechanisms (Fig. 1). These mechanisms interact and are affected by the suite of environmental factors taking part to the decomposition process (King et al. 2012). The relative importance of these mechanisms depends on the biome and the climate (Almagro et al. 2017; Bais et al. 2018). Moreover, since these processes interact with each other in natural environments, their relative contribution is difficult to quantify.

Despite the effects of climate on litter decomposition being widely studied over several decades (Melin 1930; Olson 1963), the study of photodegradation begun only in the 1990s (Caldwell and Flint 1994; Zepp et al. 1995) and was mainly focused on the effects of UV (ultraviolet radiation, 280-400 nm) and particularly UV-B (280-315 nm) radiation, as a consequence of the Ozone Hole (Barnes et al. 2015; Song et al. 2013). At that time, in order to simulate the effect of ozone depletion, photodegradation research mainly involved litter exposure to enhanced UV or UV-B radiation, often supplemented far beyond what was present under ambient conditions and therefore producing results that were difficult to interpret in the context of

processes occurring in natural environments (Gehrke et al. 1995; Newsham et al. 1997). Only relatively recently, have the relative number of studies performed under ambient sunlight increased (reviewed by King et al. 2012 and Song et al. 2013). Consequently, attention was drawn to the potential of visible light to participate in the photodegradation process (Austin and Ballaré 2010). More specifically, the short wavelength regions of visible light, such as blue (420-490 nm) and green (500-570 nm) light, were shown to have an effect on litter decomposition, both directly and indirectly (Austin and Ballaré 2010; Austin et al. 2016).

As mentioned above, photodegradation involves several mechanisms, for the sake of simplicity, we will divide them into three categories: direct, indirect and mediated, and discuss them in the following subsections (Fig.1).

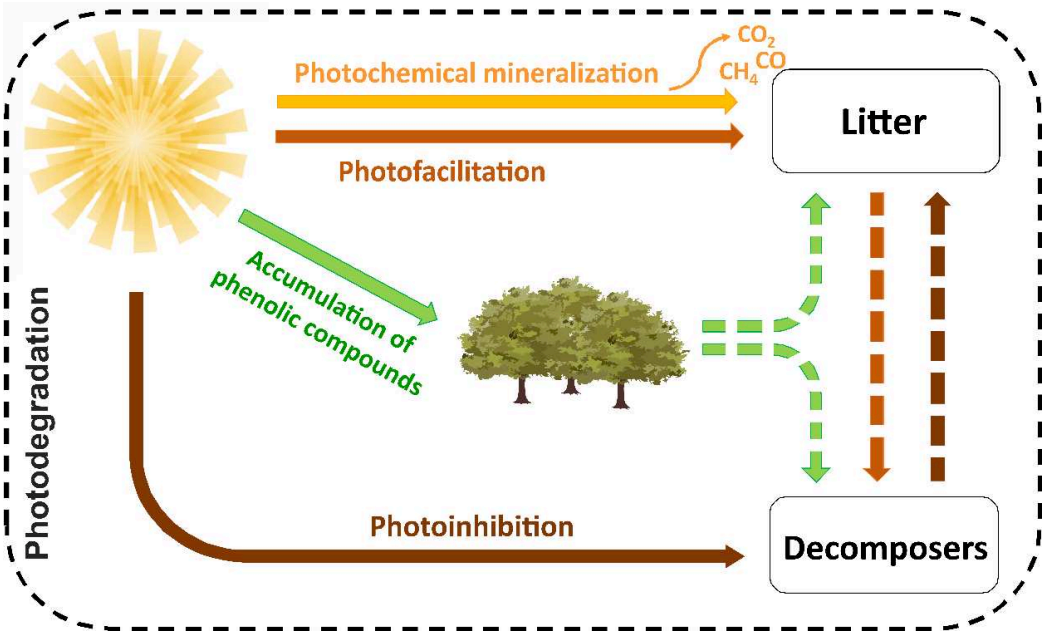

Figure 1 Schematic diagram illustrating the mechanism of photodegradation. Sunlight has three types of effects: direct (yellow arrows); indirect (brown tinted arrows) and mediated (green arrows). Direct effects involve the direct breakdown of organic matter (photochemical mineralization), described in Section 1.1.1. Indirect effects include photofacilitation (light brown) and photoinhibition (dark brown), through which sunlight enhances or inhibits the activity of decomposers (described in Section 1.1.2). Mediated effects include the accumulation of photoprotective pigments in the leaves as a consequence of exposure to sunlight (described in Section 1.1.3). Solid arrows indicate direct effects while dashed arrows indicate subsequent effects.

1.1.1. DIRECT EFFECTS OF SUNLIGHT ON LITTER DECOMPOSITION

Sunlight can increase the rate of litter decomposition by acting directly on litter chemistry through a process known as photochemical mineralization or photolysis (Gallo et al. 2006). This mechanism consists of the direct breakdown of organic matter due to the high energy carried by the short-wavelength part of the solar spectrum: UV radiation and blue and green light (Austin et al. 2016). Photochemical mineralization accelerates litter mass loss and carbon loss, and causes the release of volatile carbon compounds, such as methane (CH_4), carbon dioxide (CO_2) and carbon monoxide (CO), into the atmosphere (Austin et al. 2016; Brandt et al. 2009; Day et al. 2019).

The mechanism of litter photochemical mineralization is highly complex and, at present, not fully understood. Recalcitrant cell-wall polymers, particularly lignin, seem to be the target of direct photochemical mineralization (Austin and Ballaré 2010; Austin et al. 2016). This hypothesis is supported by the capability of lignin to absorb UV radiation, and blue and green light, through its chromophores and undergo the process of direct photolysis (Rahman et al. 2013). However, the formation of reactive oxygen species (ROS), caused by the photolysis of other photosensitive molecules, interacting with lignin (or vice-versa) can be another route to photochemical mineralization (indirect photolysis) (King et al. 2012). The co-existence of these two pathways could explain while several studies have found photochemical mineralization to impact different compounds from lignin.

While some studies have found a decrease in litter lignin content and failed to detect this effect on cellulose (Austin and Ballaré 2010; Austin et al. 2016), other studies have found litter cellulose content, but not in lignin content, to decrease (Baker and Allison 2015; Brandt et al. 2010; Brandt et al. 2007). Some studies have revealed the possibility that photolysis could also target hemicellulose and dissolved organic carbon (DOC) (Baker and Allison 2015; Day et al. 2015; Day et al. 2007; Wang et al. 2015). However, due to contrasting results between studies it is hard to generalize, and the target of photolysis might depend on the interaction of sunlight with other factors, such as litter quality and the pool of microbial decomposers able to utilise more or less complex biomolecules.

Box 1: The solar spectrum

The solar spectrum is an electromagnetic wave which can be divided into several spectral regions covering a discrete range of wavelengths and, consequently, carrying different amounts of energy (Aphalo et al. 2012). The quantity of energy carried by the photons decreases with increasing wavelength (Fig. 1.1). This means that, the shortest-wavelength region of the solar spectrum (UV radiation) transmitted through the atmosphere and reaching the Earth's surface, carries higher energy than visible light. Two region of UV radiation are of biological relevance: UV-B (280-315 nm) and UV-A (315-400 nm), as the wavelengths below 290nm are blocked by the stratospheric ozone layer. Despite representing only about 5% of the solar radiation reaching the Earth surface, UV radiation has a great impact on living organisms due to the large amount of energy carried by its photons (Caldwell et al. 1999). Visible light is divided into several spectral regions, identified by different colours, and includes photosynthetically active radiation (PAR = 400-700 nm) used by plants in the process of photosynthesis (Caldwell 1971). The short-wavelength parts of visible light, violet, blue and green (hereafter, we will refer to violet+blue spectral regions as "blue light"), together with UV radiation, are thought to be involved in photodegradation (Austin et al. 2016).

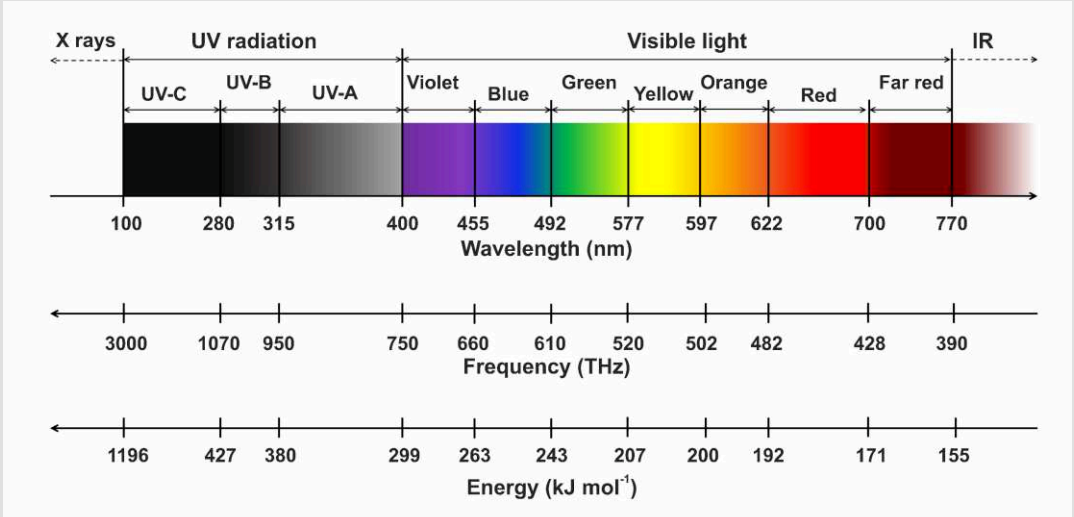

Figure 1.1: Schematic figure showing the different spectral regions that form the solar spectrum according to wavelength (nm), frequency (THz) and energy (kJ mol^{-1}) carried by their photons. Data are extracted from Aphalo et a. 2012.

1.1.2. INDIRECT EFFECTS OF SUNLIGHT ON LITTER DECOMPOSITION

Sunlight can impact litter decomposition indirectly by affecting decomposer organisms in positive or negative ways. Currently, two main opposing mechanisms are known: photofacilitation (also called photopriming) and photoinhibition.

The first process involves the facilitation of microbial decomposition following the photomineralization of complex polymers, such as lignin, otherwise difficult for microbial decomposers to exploit (Baker and Allison 2015; Lin et al. 2018; Yanni et al. 2015).

The second, concerns the inhibition of microbial decomposition, which tends to be specific to different classes of decomposer (fungi, bacteria) and, as consequence, has the potential to alter the community structure of decomposer assemblages (Barnes et al. 2015).

These two processes are often present concomitantly during the decomposition process and are likely to be waveband-dependent, in other words dependent on the spectral composition of sunlight to which litter is exposed (Lin et al. 2018). For example, Austin et al. 2016 reported photoinhibition to occur as a consequence of exposure to UV radiation but not as a consequence of exposure to blue and green light. This segregation might be explained by the higher energy carried by UV photons, which can cause DNA-damage to living organisms (Caldwell et al. 1999). On the other hand, photofacilitation was reported as a consequence of exposure to blue and green light (Austin et al. 2016) during decomposition and of exposure to enhanced UV radiation before the decomposition process (Foereid et al. 2010).

As these two processes very-often interact, it is difficult to differentiate them during photodegradation experiments. Moreover, the relative importance of photofacilitation and photoinhibition seems to depend on the duration of exposure (King et al. 2012; Lin et al. 2018).

As with photochemical mineralization, the study of photodegradation effects on microbial decomposers started as an attempt to understand the effects of ozone depletion by exposing microbes to enhanced UV and UV-B radiation, at irradiances higher than commonly found in natural conditions (Duguay and Klironomos 2000; Moody et al. 1999). These high doses

reportedly reduced spore germination and fungal hyphal length in fungi colonizing leaf litter (Moody et al. 1999; Verhoef et al. 2000), but are not necessarily interpretable in a natural context.

Only recently, have a few studies analysed photofacilitation and photoinhibition in natural conditions in arid and semiarid environments (Ball et al. 2019; Day et al. 2018). The opposite effects were found in arid and semiarid climates, suggesting that photofacilitation and photoinhibition are affected by other environmental variables as well as UV radiation. While ambient UV radiation and blue light enhanced microbial respiration in an arid environment (Day et al. 2018), microbial respiration was reduced by exposure of *Bromus diandrus* litter to UV radiation in a semiarid ecosystem (Lin et al. 2015). These contrasting effects, and the lack of studies in mesic environments and forest ecosystems, make it hard to generalize about the impact of photofacilitation and photoinhibition on the decomposition process. Moreover, it is difficult to distinguish these indirect effects from direct effects and to determine, not only their drivers, but also their relative importance over a range of different biomes.

Although in this thesis we only examined the effects of sunlight on microbial decomposers, the consequences of these effects, as well as direct photo-inhibition, may extend to larger soil fauna, which have a crucial role in the decomposition process (Coleman et al. 2004).

When considering macro and meso-fauna, evaluation of the effects of sunlight in field conditions is challenging due to their high mobility compared to microbial decomposers. Moreover, it is difficult to separate direct effects of sunlight on these groups from the indirect effects due to modification of the food chain (Klironomos and Allen 1995), as the spectral composition impacts microbial-decomposer community structure and biomass (Pancotto et al. 2003).

As an example, the abundance of microbial feeders, such as springtails and non-oribatid mites, was reported to increase under UV-B radiation in controlled conditions due to an increase in microbial biomass (Klironomos and Allen 1995). This effect persisted despite the DNA damage that was found in springtails exposed to enhanced UV-B radiation in a controlled

environment in absence of soil, where DNA repair also occurred after a recovery period in dark conditions (Hawes et al. 2012).

These kinds of studies in controlled environments are likely to overestimate the effect that would occur in natural environments where soil fauna can hide from sunlight, to avoid damaging UV-B exposure and preferentially lay their eggs in the dark (Beresford et al. 2013; Fox et al. 2007). This inconsistency can be illustrated by comparison of the negative effects of UV radiation on earthworm fertility and abundance found in a controlled environment (Hamman et al. 2003) with the lack of effects in a fen ecosystem where earthworms have a greater opportunity to escape direct UV exposure and move between the roots of plants growing under different UV treatments (Zaller et al. 2009).

In summary, the findings from realistic experiments in natural environments suggest that these groups of decomposers are more likely to be impacted indirectly by sunlight as a consequence of the altered soil food web than by direct exposure to solar UV radiation. However, further studies are needed to test this hypothesis.

1.1.3. MEDIATED EFFECTS OF SUNLIGHT ON LITTER DECOMPOSITION

The relationship of sunlight with decomposition is also mediated through plant traits. Leaf structure and biochemistry are influenced by the amount and spectral composition of sunlight received during growth. The exposure of leaves, during the vegetative season, to UV radiation and blue light causes the accumulation of photoprotective pigments, such as flavonoids, in the leaf epidermis (Brelsford et al. 2019; Caldwell et al. 1999; Coffey et al. 2017). These phenolic compounds act as a screen against UV radiation to protect the underlying mesophyll from photodamage (Day et al. 1992; Landry et al. 1995; Rousseaux et al. 1999).

After leaf senescence, these compounds remain in the leaf litter and have the potential to alter decomposition, and the contribution of photodegradation to this process, by reducing UV penetration to the mesophyll (King et al. 2012; Kotilainen et al. 2009; Pancotto et al. 2005). Moreover, they can influence

microbial and fungal succession, through differential effects on the colonisation of leaf litter during the initial stages of decomposition (Aneja et al. 2006; Conn and Dighton 2000). However, the contribution of these mediated effects to decomposition remains relatively unexplored.

Once again research has mainly focused on the effects of elevated UV-B radiation (Gehrke et al. 1995; Hoorens et al. 2004; Newsham et al. 1999; Rozema et al. 1997). Contrasting results were found in these studies, the leaves' exposure to UV-B radiation during growth reduced the subsequent decomposition rate due to an increase in lignin and tannins in litter from a sub-arctic shrubland (Gehrke et al. 1995) and a dune grassland (Rozema et al. 1997). However, in this second environment the effect disappeared in the longer term (Hoorens et al. 2004), suggesting photodegradation-mediated effects to be important only during the initial phase of decomposition or at least to be time-dependent. On the other hand, a study on *Quercus robur* litter found enhanced UV-B radiation to decrease lignin content in the litter and its colonization by basidiomycetes fungi, consequently enhancing the decomposition rate (Newsham et al. 1999). A similar result was reported in a meta-analysis by Song et al. 2013 analysing, amongst others, the effect of UV-B exposure during growth on litter decomposition. It remains to be tested whether these positive and negative effects on decomposition mediated by litter traits are also important under ambient sunlight.

1.2. PHOTODEGRADATION AS FUNCTION OF CLIMATE, ECOSYSTEM AND LITTER TRAITS

Irradiance and the spectral composition of sunlight reaching the Earth's surface change over both spatial and temporal scales (Aphalo et al. 2012; Aphalo 2018). Therefore, we can expect variation in the photodegradation rate across biomes and ecosystems, and assume it to be more relevant at lower latitudes receiving higher UV radiation (Gallo et al. 2009). The photodegradation rate is modified by all the factors that enhance litter exposure to sunlight, including latitude (Moody et al. 2001), season (Brandt et al. 2010; Rutledge et al. 2010), leaf area index (LAI) (Bravo-Oviedo et al. 2017;

Rozema et al. 1999), canopy structure and phenological stage (Rutledge et al. 2010), litter position (surface litter vs standing litter) (Almagro et al. 2015; Brandt et al. 2009) and litter layer thickness (Henry et al. 2008; Mao et al. 2018).

Photodegradation is influenced by various environmental factors during the decomposition process, such as temperature and precipitation (Song et al. 2013). The rate of photodegradation, and particularly the contribution of photochemical mineralization to this process, seems to be enhanced in drier environments where the microbial component of decomposition is low (Brandt et al. 2007). Additionally, photodegradation is also suggested to benefit from diurnal cycles of temperature, which are thought to enhance the mechanism of photofacilitation, creating the ideal conditions for micro-organisms to utilize the bioavailable products of direct photochemical mineralization (Gliksman et al. 2017).

The trade-off between positive (photochemical mineralization, with consequent photofacilitation) and negative (photoinhibition) effects of photodegradation may differ by biome (Huang et al. 2017, Almagro et al. 2017, Gliksman et al. 2017, reviewed by Bais et al. 2018). Whereby, positive effects dominate in arid climates with limited microbial activity, while the negative effects tend to dominate in mesic ecosystems were microbial decomposers play a major role (Bais et al. 2018).

The photodegradation rate has been suggested to depend on initial litter quality (King et al. 2012). For example, recalcitrant litter with high carbon-to-nitrogen ratio (C:N), whereby there is less available nitrogen for microbial decomposers, seems to benefit more from the process of photochemical mineralization (King et al. 2012). On the other hand, Pan et al. 2015 found a positive correlation between photodegradation rate and initial nitrogen (N) content.

As lignin is the supposed target of photodegradation, the magnitude of photodegradation was suggested to increase with lignin content (Austin and Ballaré 2010; Méndez et al. 2019). However, a meta-analysis by King et al. 2012 found no consistent relationship between the rate of photodegradation and initial lignin content of the litter. On the other hand, Pan et al. 2015 found

a positive correlation between photodegradation rate and specific leaf area (SLA).

It is not yet clear what initial litter traits could potentially predict photodegradation, as the classical traits used to predict decomposition rates, such as lignin to nitrogen ratio (Lig:N), or lignin content, fail in this respect (Day et al. 2018). A recent study from Day et al. 2018 analysing the relationship between initial litter traits and photodegradation, found a positive correlation between the rate of photodegradation and the initial content of hemicellulose and cellulose. The differences in results among all these studies suggest the possibility that different traits could predict photodegradation in different biomes, however, this hypothesis remains untested.

Photodegradation represents a relevant driver of litter decomposition not only in arid (Day et al. 2015; Day et al. 2007) and semiarid (Almagro et al. 2015; Austin et al. 2016) biomes at low latitudes but also at high latitudes (Jones et al. 2016; Pancotto et al. 2003; Zaller et al. 2009) and in mesic conditions (Brandt et al. 2010).

Photodegradation has been broadly studied in arid and semiarid environments, in ecosystems characterised by low or absent canopy cover, such as grasslands (Uselman et al. 2011) or open areas (Messenger et al. 2012). On the other hand, the role of photodegradation in forest ecosystems, characterised by a particular light environment that changes through the year according to canopy phenology, remains unexplored. The very few studies employing tree leaf litter, collected this litter in forests, but set up their experiments in nearby open areas (Ma et al. 2017; Messenger et al. 2012; Newsham et al. 2001), making it impossible to extrapolate the results to a forest environment. A recent study from Méndez et al. 2019 only examines the effect of shading on litter decomposition in forest understories, without taking into account the relative importance of each waveband in the process of photodegradation.

At present, little is understood about the role played by photodegradation in litter decomposition in the understorey, under unique characteristics of irradiance and spectral composition changing throughout the year.

1.3. THE FOREST FLOOR: A DYNAMIC LIGHT ENVIRONMENT

Forest ecosystems are spatially complex communities characterized by a composite vertical structure formed by an upper canopy and an understorey layer of shade-loving plants (Oliver and Larson 1996). This multi-layered structure heavily modifies the irradiance and spectral composition of sunlight reaching the forest floor by processes such as transmittance, reflectance and absorption (Aphalo et al. 2012).

The forest canopy modifies the understorey light environment not only spatially but also temporally, through the seasons, according to the combination of several factors such as canopy phenology and solar path length, elevation, latitude and weather conditions (Aphalo et al. 2012). The interaction of these biotic and abiotic processes creates light conditions specific to each geographical location and forest type (Chazdon and Pearcy 1991). As a consequence, the forest floor is subject to a dynamic and ever-changing light environment, constituted by the formation of micro-sites with different light conditions, defined as sunflecks (a sun-patch of direct light reaching the forest floor, Fig.2b) and shades areas (Fig.2c) (Smith and Berry 2013; Way and Pearcy 2012).

The irradiance on the forest floor is lower than in areas without canopy cover and its spectral composition differs greatly from the irradiance characteristic of open areas for the large part of the year. In deciduous forests, understorey irradiance greatly decreases during the period of spring canopy flush and increases again during leaf fall, therefore presenting the opposite annual trend to those of solar UV-B radiation and PAR (400-700 nm) (Ross et al. 1986). Following canopy closure, the light environment on the forest floor is characterized by higher UV to PAR ratios (UV:PAR) compared to open areas, probably largely due to differences in the spectral composition of diffuse radiation compared to direct radiation.

Diffuse radiation in the understorey consists of radiation scattered by the atmosphere and reflected in the canopy: short wavelengths are scattered more than long wavelengths, so are enriched in diffuse radiation (Aphalo et al. 2012; Brown et al. 1994) (Fig.2c). Moreover, the solar radiation reaching the forest

floor is depleted in blue and red (622-700 nm) light, due to the high absorption of these spectral regions used in photosynthesis, and has a lower blue to green ratio (B:G) and red to far-red (700-780 nm) ratio (R:FR) than that found in open areas (Ross et al. 1986) (Fig.2c). These unique characteristics, in terms of spectral irradiance, are likely to impact the contribution of photodegradation to the decomposition process under canopies compared to open areas. For this reason, there are likely to be differences in the contribution of different spectral regions to photodegradation in forested ecosystems compared to open areas, and in the relative contribution of the three different mechanisms constituting photodegradation (described in section 1.1).

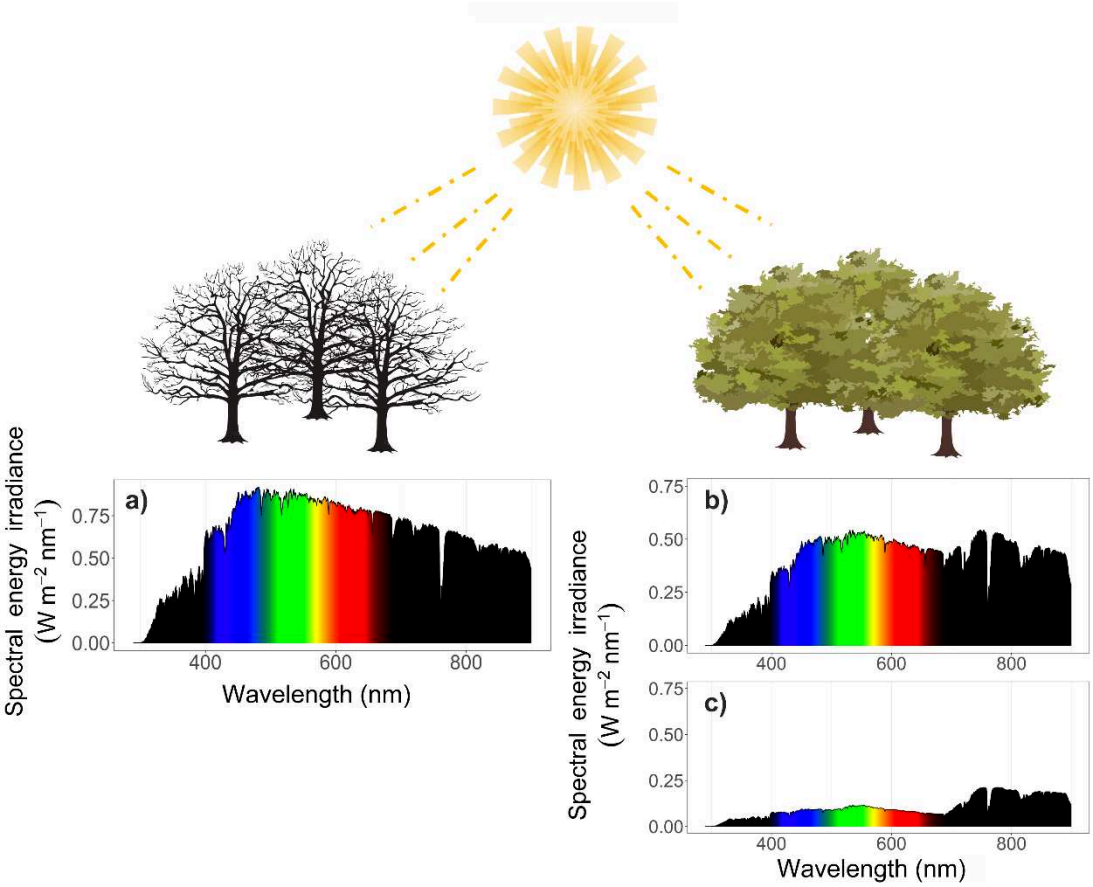

Figure 2 Schematic figure showing the spectral irradiance reaching the forest floor in a deciduous forest a) during dormancy in autumn and winter compared with b) and c) during the vegetative season. During this period, we observe the formation of b) sunflecks and c) shaded areas with different spectral composition and irradiance. Sunflecks (b) are events of very short duration that can last for just a few seconds (Smith and Berry 2013).

Sunlight in a forest understorey, as well as affecting the decomposition process through irradiance, concomitantly impacts the temperature of leaf litter and soil (Smith and Berry 2013). This increase in temperature is likely to increase evaporation of surface moisture and change the microclimate at the soil-litter interface. All of these environmental effects of sunlight interact and are likely to cause a complex final shift on litter decomposition rate.

Forests cover up to 31% of the Earth surface, these ecosystems are responsible for the absorption of about 2 billion tonnes of CO2 per year (FAO 2018). In 2017, forests absorbed about 38% of carbon emissions from industries and fossil fuels (Brack 2019). Therefore, considering the release of carbon compounds into the atmosphere due to photodegradation in these ecosystems is fundamental to understanding the impact of photodegradation on the global carbon sink.

2. AIMS

The first aim of this thesis is to investigate the role of photodegradation in temperate and boreal forest ecosystems. First, by assessing if this process is relevant in litter decomposition in the forest, under low irradiance, and thereafter by determining which spectral regions of sunlight have the most impact on litter decomposition under forest canopies.

In order to do this, we set up several experiments that allowed us to answer to the following questions:

- Does photodegradation have an effect on litter decomposition in the understorey of temperate forests at mid-to-high latitudes where the irradiance is low? And which spectral regions are responsible for photodegradation in forest ecosystems? I-II-III (Assessed in section 4.1)

  Prediction: We expect UV radiation and blue light to enhance litter mass loss, and consequently carbon loss, as a result of both photochemical mineralization and photofacilitation. Moreover, we expect blue light to have a greater effect than UV radiation due to the low UV irradiance at mid-to-high latitudes.

- Does photodegradation impact microbial biomass and community structure, and what spectral regions are the most important in this process? III (Assessed in section 4.2)

  Prediction: We expect treatments excluding UV radiation to have higher fungal and bacterial biomass due to removal of the inhibitory effect of UV-B radiation. We expect the exclusion of UV radiation and blue light to favour fungal decomposers as they tend to prefer darker environments, but to penalise bacterial decomposers which would benefit more from photofacilitation, as they are unable to exploit complex carbon compounds.

Our second aim is to investigate how photodegradation changes across biomes and how the contribution of different environmental factors determines the photodegradation rate across the globe. Additionally, we aim to identify which initial litter traits can predict the rate of photodegradation. In order to do this, we performed a meta-analysis to answer to the following questions:

- What determines the magnitude of photodegradation operated by different spectral regions across the globe? Is it principally dependent on the climate, ecosystem type, decay period, or litter type? IV (Assessed in section 4.3)

  Prediction: Overall, we expect photodegradation to enhance litter decomposition when driven by blue light, due to the capability of this spectral region to achieve photochemical mineralization while having a minimal photoinhibitory effect. On the other hand, we expect a smaller effect of UV radiation, and little-or-no measurable effect of its constituent UV-B radiation, as the capacity of UV radiation for direct photolysis may be counter-balanced by its high photo-inhibition capacity. Furthermore, we expect the rate of photodegradation to contribute more to decomposition in arid than mesic climates, as well as in ecosystems with lower canopy cover, and to change according to the decay period. Moreover, we expect different spectral regions to be of different importance according to climate, ecosystem type and decay phase under consideration.

- What initial litter traits predict the magnitude of photodegradation? IV (Assessed in section 4.4)

  Prediction: We expect the C:N ratio and lignin content to be positively correlated with photodegradation rate, as lignin represents the main target of this process and recalcitrant litter, with lower N availability, benefits the most from the process of photochemical mineralization and consequent photofacilitation. Moreover, we expect photodegradation to have a greater impact on litter with a high surface:volume ratio due to its greater exposure to sunlight.

3. MATERIALS AND METHODS

This dissertation presents the results of three different field experiments (I, II and III), a controlled-environment study (III), and one meta-analysis (IV). The field manipulation in chapter I follows decomposition through its natural time course, in an open canopy from leaf fall through winter, to spring when received irradiance is at its highest, and summer when only occasional sunflecks provide most of the irradiance received in the understorey. Chapter II consists of two parallel experiments, one conducted in the field, concentrating on the open-canopy period from autumn to spring, and one in a controlled environment to explore the mechanisms of photodegradation more precisely. The order of the chapters was chosen because it allows a logical progression through the discussion of the results in that: chapter I and II focus on the impact of photodegradation on litter mass loss and carbon content, while chapter III extends this work to consider the impact of photodegradation on microbial assemblages colonizing the litter. Later, the capacity for these local results to be scaled up to the global level is discussed, accounting for variation in photodegradation rate across biomes (IV).

3.1. STUDY SITES

We conducted the photodegradation experiments in chapters I and III in a mature beech forest (*Fagus sylvatica* L.) in Normandy (France, 49°31'12.6"N 1°07'00.7"E). We chose this location as beech forests form a dense canopy with a large contrast in light environment in the understorey between the growing season and winter season. The study site had the advantage of flat topography and the almost total absence of understorey vegetation meaning the leaf litter is not overgrown and allowing the deployment of many litterbags over large contiguous plots.

In the experiment described in chapter I, we deployed the litterbags on 20th Dec 2016 and collected five replicate litterbags from each treatment

combination after about 3 (4th Apr 2017), 5 (6th June 2017) and 7 (27th July 2017) months for the fast-decomposing ash litter, and 3 (4th Apr 2017), 6 (27th June 2017) and 10 (10th Oct 2017) months for oak and beech litter, which is slower to decompose.

In chapter III we deployed the litterbags on 5th Dec 2017 and collected five replicate litterbags after about 1 (9th Jan 2018), 3 (07th Mar 2018), 6 (7th June 2017) months to measure mass loss and C and N contents. We also collected six replicate litterbags after about 1 (9th Jan 2018), 2 (7th Feb 2018), 3 (07th Mar 2018), 6 (7th June 2017) months to characterized microbial biomass.

To set up the outdoor experiment in chapter II we choose four forest stands in Viikki, Helsinki (II, 60°13'39.7'N, 25°01'09.5'E) characterized by different canopy species: silver birch (*Betula pendula* Roth.); Norway maple (*Acer platanoides* L.); European beech (*Fagus sylvatica* L.) and Norway spruce (*Picea abies* (L.) H. Karst). The presence of different dominant species allowed us to test the effect of the canopy species on the photodegradation rate. We deployed the litterbags on 7th Oct 2016 (silver birch leaves) and 19th Oct 2016 (European beech leaves) and collected them after 6 months (11th Apr 2017) with six replicates for each treatment combination.

We conducted the controlled-environment photodegradation experiment (II) in a fully temperature-controlled growth room at the Viikki Campus of the University of Helsinki, Finland. Lighting in the growth room aimed to capture the key aspects of the light environment outdoors through a combination of broad-spectrum LED lamps installed specifically for the experiments and purpose-built UV-A LED lights. Details on the spectral composition and irradiance in the growth room are given in II. We exposed the litterbags to the light treatments for 6 and 10 weeks and then collected them for the analysis with 16 replicates per each treatment combination.

3.2. LITTER MATERIAL

In each of our experiments, we selected leaf-litter material from several different tree species. This enabled us to compare leaf litter characterized by

different initial traits, such as C content, N content, C:N. Species at different successional stages with leaves known to decompose at different rates were chosen.

In chapter I, we selected leaf litter from three species growing locally in forest stands close to Rouen: pedunculate oak (*Quercus robur* L.); European beech (*Fagus sylvatica* L.) and European ash (*Fraxinus excelsior* L.). We collected fully senescent leaves at the point of abscission directly from trees and we oven dried them at 35°C for a week before deploying them in the field.

In chapter II we selected two contrasting species: silver birch (*Betula pendula* Roth) and European beech (*Fagus sylvatica* L.). We harvested both green leaves and fully senescent leaves of the two species to evaluate the effects of senescence stage on the photodegradation rate. We oven dried the leaves at 37°C until they achieved a constant weight before deploying them in the field. We used fresh litter material of the same origin in the controlled experiment. In this case, half of the leaves were deployed with the adaxial (upper) epidermis facing upwards and half with the abaxial (lower) epidermis facing upwards. This was used as a proxy for the amount of radiation penetrating the leaf to the mesophyll. Typically, the adaxial epidermis in these species has a higher concentration of UV-screening compounds than the abaxial epidermis, and these compounds absorb solar radiation in the shortwave region of the spectrum.

In chapter III we employed fully senescent leaves of European beech (*Fagus sylvatica* L.) collected at the point of abscission and we oven dried them at 35°C for a week before deploying them in the field.

3.3. PHOTODEGRADATION-LITTERBAGS

We employed two types of bespoke litterbags, from hereafter referred as “photodegradation-litterbags”, adapted from classical litterbags used in litter decomposition studies.

The first prototype of photodegradation-litterbags used in II (Fig. 3a), consisted of 8-x-8-cm squares of plastic-film filter material stapled to equal sizes mesh material made from Teflon mosquito netting. Later on, we

developed a second prototype with the addition of plastic straws between the filter and the mesh sheet to prevent the contact between the litter and the filter sheet and reduce the build-up of condensation (Fig. 3b). For technical details concerning photodegradation-litterbags refer to I, II & III.

Photodegradation-litterbags have the advantage of incorporating the attenuating filter directly into the "bag", avoiding additional shade otherwise produced by the mesh material used for the construction of traditional litterbags. This adaptation to avoid an overall reduction in the received irradiance is particularly important in temperate and boreal forests where the incident irradiance is already low. Moreover, the typical Teflon material used for decomposition litterbags can alter the spectral composition of the light treatments by selectively absorbing different wavelengths. Another advantage of our photodegradation litterbags is their ability to hold a single layer of litter, avoiding shading caused by the overlapping of leaves and potential confounding effects that occur when not all the litter material is directly exposed to the radiation treatments.

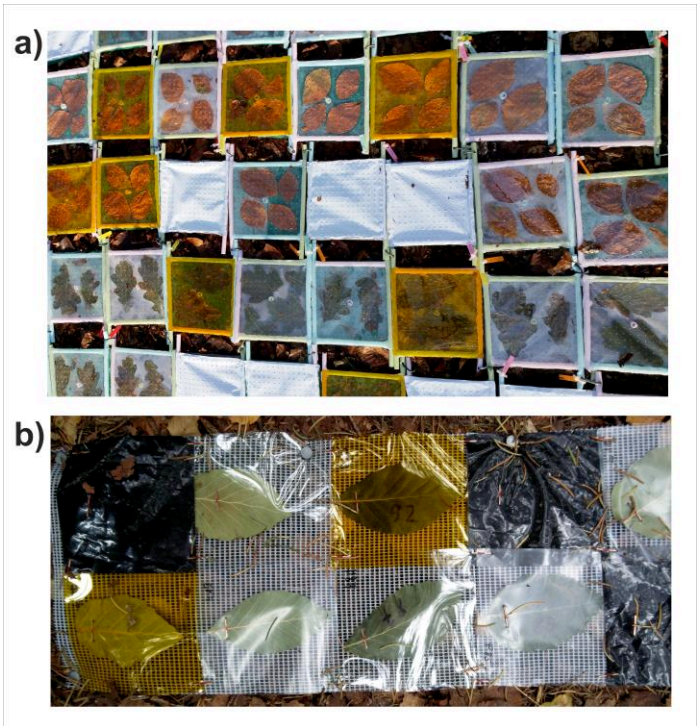

Figure 3 Photographs showing the first (a) and the second (b) prototype of the photodegradation-litterbags.

We used six different plastic-film filters that selectively attenuate solar radiation to create six spectral treatments (Fig.4) in order to analyse the effect of several spectral regions:

- "**Full-spectrum**" treatment (full-spectrum at near-ambient sunlight) of polyethene film (0.05 mm thick, 04 PE-LD; Etola, Jyväskylä, Finland) transmitting > 95% of incident PAR and UV radiation;
- "**No-UV-B**" treatment (attenuating UV-B radiation < 320 nm) using polyester (0.125 mm thick, Autostat CT5; Thermoplast, Helsinki, Finland);
- "**No-UV**" treatment using Rosco #226 (0.2 mm thick, Westlighting, Helsinki, Finland) attenuating UV radiation < 380 nm;
- "**No-UV/Blue**" treatment using Rosco #312 Canary yellow (0.2 mm thick, Westlighting, Helsinki, Finland) attenuating UV radiation and blue light < 480 nm;
- "**No-UV/Blue/Green**" treatment using Rosco #135 deep golden amber (0.2 mm thick, Westlighting, Helsinki, Finland) attenuating UV radiation and blue and green light < 580 nm (this treatment was used only in III);
- "**Dark**" treatment using solid polyethene film, white on the upper-side and solid black on the lower-side (0.15 mm thick, Casado sarl, France and 0.07mm thick, Siemenliike Siren, Helsinki, Finland), attenuating > 95% of PAR and UV radiation.

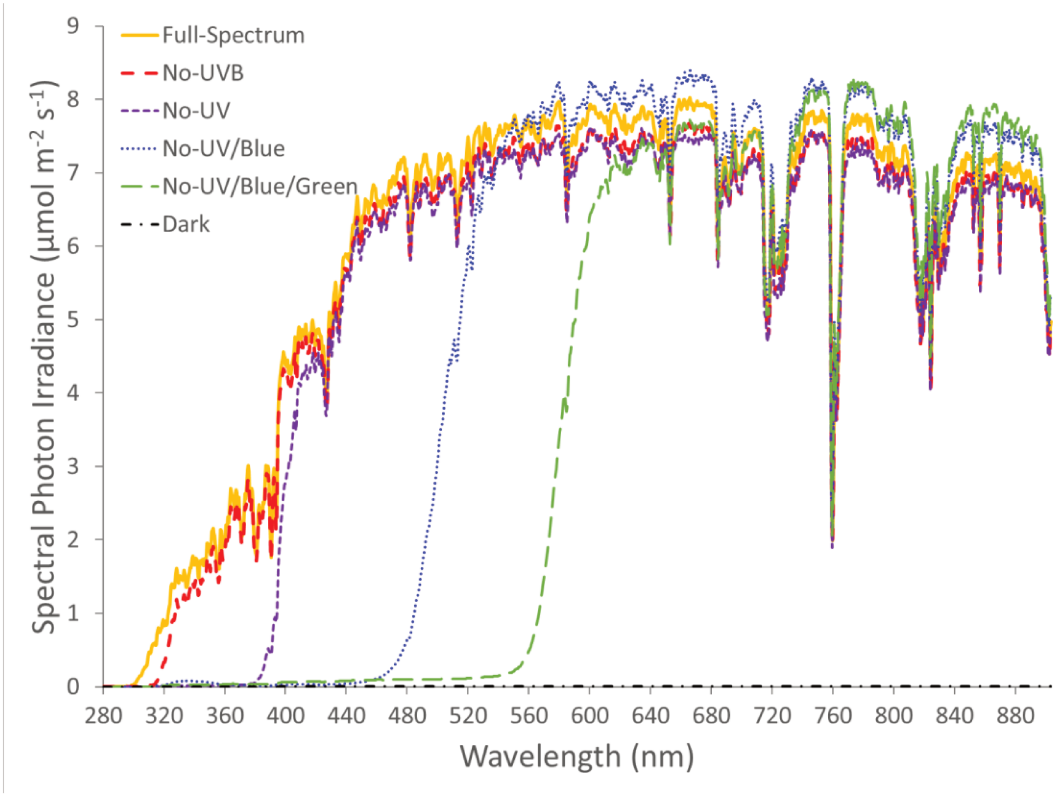

Figure 4 Spectral irradiance measured outdoors under the six filter treatments.

3.4. SPECTRAL IRRADIANCE MEASUREMENTS

Punctual measurements of spectral irradiance were done both outdoors (in the forest site and in a nearby open area) and in the growth room using an array spectroradiometer (Maya2000 Pro Ocean Optics, Dunedin, FL, USA; D7-H-SMA cosine diffuser, Bentham Instruments Ltd, Reading, UK, see I, II & III for details about measurements and calibration).

Canopy flush and light regime in the forest understorey were monitored through hemispherical photographs taken regularly during the experiments and used to calculate the global light index (GLI) with the software Hemisfer (Schleppi et al. 2007; Thimonier et al. 2010) following the protocol of Hartikainen et al. 2018 (see I, II & III for further details). Punctual measurements of the outdoor spectral irradiance and GLI obtained from hemispherical photos were used to model the spectral irradiance in the understorey over the experimental periods and to calculate light doses

received by the litter under each filter treatment (see I, II & III for details about irradiance doses estimation).

3.5. LITTER MASS LOSS AND CARBON AND NITROGEN CONTENT

Litter mass loss was determined as a percentage of initial mass, ash content was calculated to exclude errors due to litter contamination from inorganic material by combustion of a subsample of each replicate in a muffle oven at 550 °C for 12 h. Carbon (C) and nitrogen (N) contents and the carbon-to-nitrogen ratio (C:N) were determined using a CN Soil Analyzer Flash 2000 (Thermo Scientific, Waltham, USA) in I and III and a Vario Micro Cube (Elemental Analysis Systems GmbH, Hanau, Germany) in II.

3.6. MICROBIAL BIOMASS AND COMMUNITY STRUCTURE

We determined microbial biomass and the structure of microbial communities (bacteria and fungi) colonizing leaf litter through PLFA (Phospholipid Fatty Acid) and NLFA (Neutral Lipid Fatty Acid) analyses as in III, using a subsample of 0.15 g of freeze-dried litter from each litterbag. Lipid extraction was performed according to (Frostegård et al. 1991) and the resulting fatty acids were identified by comparing their mass spectra with the standard mass spectra in the NIST MS library.

We determined the amounts of the NLFA 16:1ω5 and the PLFA 16:1ω5 in the litter and used the ratio as indicator of the AMF (Arbuscular Mycorrhizal Fungi) biomass. As an indicator of saprotrophic fungi biomass we used the PLFA c18:2ω6,9 (Frostegård et al. 1991).

We estimated the biomass of Gram-positive bacteria (Gram-P) by the quantification of the PLFA: i15:0, a15:0, i16:0, i17:0, a17:0 and Gram-negative bacteria (Gram-N) by the quantification of the PLFA: cy17:0, c18:1ω7 and cy19:0 in the litter (Frostegård et al. 2011). As an indicator of total microbial biomass in the sample, we used the total amount of PLFA. We chose PLFA and

NLFA analysis over metabarcoding because we were mainly interested on the biomass and on the relations between fungal and bacterial biomass in the litter.

3.7. STATISTICAL ANALYSES

All statistical analyses where performed in R for Windows (ver. 3.6.1., R_Core_Team 2013). Multi-factor ANOVA were used to analyse the difference between filter treatments on mass loss and C and N contents (I, II & III). A multivariate analysis (NMDS) was used to explore the differences in microbial community structures due to our filter treatments (III).

A multi-level meta-analysis was done to evaluate the effects of photodegradation driven by the different spectral region across ecosystems and climates (IV).

Furthermore, we evaluated the potential correlation between photodegradation driven by each spectral region and initial litter traits, through a mixed-effect model (IV), in order to identify traits that could act as predictors of the photodegradation rate. We considered the following traits in our analysis: carbon content (C); nitrogen content (N); carbon to nitrogen ratio (C:N); lignin content; lignin to nitrogen ratio (Lig:N) and specific leaf area (SLA).

Litter type	**I**	**II**	**III**	**IV**
European beech (*Fagus sylvatica* L.)	x	x	x	
European ash (*Fraxinus excelsior* L.)	x			
Pedunculate oak (*Quercus robur* L.)	x			
Silver birch (*Betula pendula* Roth)		x		
Canopy species				
European beech (*Fagus sylvatica* L.)	x	x	x	
Silver birch (*Betula pendula* Roth)		x		
Norway maple (*Acer platanoides* L.)		x		
Norway spruce (*Picea abies* (L.) H. Karst)		x		
Litterbags				
Prototype 1		x		
Prototype 2	x		x	
Measured/collected variables				
Mass loss	x	x	x	x
AFDM	x		x	
C content	x	x	x	
N content	x	x	x	
C:N	x	x	x	
PLFA			x	
NLFA			x	
HPLC		x		
Initial C	x	x	x	x
Initial N	x	x	x	x
Initial C:N	x	x	x	x
Initial SLA	x	x	x	x
Initial Lignin				x
Initial Lig:N				x
Initial Anthocyanin	x	x	x	
Initial Chlorophyll	x	x	x	
Initial Flavonoids	x	x	x	

Table 1: Overview of methods applied and data collected in the four chapters.

4. MAIN RESULTS AND DISCUSSION

4.1. EFFECTS OF PHOTODEGRADATION ON LITTER MASS LOSS AND CARBON CONTENT

We monitored dry mass and carbon content of leaf litter of three tree species: European ash (*Fraxinus excelsior* L.), pedunculate oak (*Quercus robur* L.) and European beech (*Fagus sylvatica* L.) in a mature beech forest in Normandy (France, I).

By the end of the experiment, after 10 months, oak and beech litter exposed to ambient sunlight (full-spectrum) had lost 20% and 30% respectively more mass than when decomposing in dark conditions (pairwise full-spectrum-dark: $p < 0.001$ for both species, I). This result is in agreement with recent findings from a semiarid forest in Argentina, where the full spectrum of sunlight enhanced litter mass loss by 15% after 6 months (of winter) and 57% after 1 year of exposure compared with a treatment excluding wavelengths of 280-580 nm (Méndez et al. 2019). Similar results have been obtained from experiments in other biomes, such as subtropical forests (Ma et al. 2017) and arid shrublands (Pan et al. 2015), as a consequence of artificial shading. Contrarily, our ash litter decomposing in dark conditions over 7 months, had lost a similar proportion of its mass to litter exposed to sunlight (pairwise full-spectrum-dark: $p = 0.462$, I).

The species-specific difference between our results suggests that photodegradation is dependent on initial litter traits. It is likely that recalcitrant litter, with a low content of easily-broken-down simple carbon compounds available to microbial decomposers (Hodge et al. 2000), could benefit most from photofacilitation. This is in agreement with findings in arid (Day et al. 2015) and semiarid (Gaxiola and Armesto 2015) ecosystems, where the photodegradation rate depended on the litter species. However, this effect is thought to be more relevant in mesic ecosystems (Bais et al. 2018), where microbial decomposers are crucial in determining the decomposition rates (Asplund et al. 2018).

In our experiment (I), blue light was the spectral region that most affected litter decomposition by enhancing litter mass loss by 6 to 9%, according to litter-species, over 10 months (pairwise No-UV - No-UV/Blue: p = 0.020 and 0.050 for oak and beech respectively, I). Exposure to blue light also led to a greater carbon loss by the end of the experiment (+6-9%; pairwise No-UV - No-UV/Blue: p = 0.016 and 0.023 for oak and beech respectively, I). This result confirms our hypothesis that blue light is the main driver of photodegradation in a temperate mid-latitude forests and highlight the potential of this spectral region to operate photochemical mineralization. Various studies have suggested that short-wavelength visible light is important in the process of photodegradation (reviewed by King et al. 2012). Austin et al. 2016 reported a 30% increase in mass loss from 23 species' litter in an open semiarid environment after exposure to blue and green light. A similar result was reported by Day et al. 2018 in a study analysing photodegradation of 12 different species' litter under arid conditions. However, in that study in the Sonoran Desert the photodegradation rate depended on the litter type, suggesting once more a role of initial litter trait in determining the rate of photodegradation.

In our experiment (I), UV radiation had no significant effect on mass loss (pairwise full-spectrum – No-UV p = 1.000 ash, p = 0.154 oak and p = 0.377 beech, I), this confutes our hypothesis that UV radiation would enhance litter mass loss in a temperate forest. Moreover, within the UV-region, UV-B radiation had no significant effect on mass loss (p = 1.000 ash, p = 0.057 oak and p = 0.438 beech, I), while UV-A radiation enhanced mass loss by 9% in beech litter (pairwise No-UV – No-UV-B p = 0.031, I). This result could be due to the higher irradiances of UV-A radiation and blue light, compared to UV-B radiation reaching the litter in the understorey; particularly at mid and high latitudes (Aphalo et al. 2012; Hartikainen et al. 2018).

Another possible explanation for the lack of a UV-effect could be a trade-off between the positive and negative effects of UV-driven photodegradation, as UV radiation and particularly UV-B radiation are often reported to inhibit microbial decomposition (Duguay and Klironomos 2000; Moody et al. 1999).

However, it is not possible to disentangle the two opposing mechanisms of photochemical mineralization and photoinhibition under field conditions.

Past studies in arid (Gallo et al. 2009; Gallo et al. 2006) and semiarid (Almagro et al. 2015; Austin and Ballaré 2010) ecosystems reported UV and UV-B radiation to enhance litter decomposition. However, this effect was reversed at high latitudes (Pancotto et al. 2003; Pancotto et al. 2005), suggesting that the impact of photodegradation is dependent on the biome. As an example, in our second experiment, monitoring litter mass loss of leaf litter of two tree species, silver birch (*Betula pendula*) and European beech (*Fagus sylvatica*), in southern Finland in four forest stands results were very different (60°N, II) from those obtained at mid-latitude in northern France (49°N, I). Spectral treatments impacted only litter mass loss of beech litter ($p < 0.001$, while $p = 0.807$ for birch, II), the more recalcitrant of the two species, once again confirming the importance of litter quality in determining the photodegradation rate.

The effects of spectral treatments on beech litter changed according to the stand ($p < 0.001$, II). At this higher latitude, blue light did not have a significant effect on mass loss of beech litter in any of the stands (pairwise No-UV - No-UV/Blue: $p > 0.100$ for all the stands, II). While the full-spectrum of sunlight decreased mass loss by 2.5% over 6 months in the beech stand (pairwise full-spectrum-dark: $p = 0.018$, II), UV radiation increased mass loss by 2.4% in the spruce and by 2.1% in the birch stand (pairwise full-spectrum – No-UV $p = 0.025$ and $p = 0.041$ respectively, II).

This difference among stands can be explained by the capacity of different tree canopies to modify the amount of incoming solar radiation and its spectral composition reaching the forest floor (Hartikainen et al. 2018), and create different microclimates characterised by unique combinations of temperature, moisture, snow pack depth (Augusto et al. 2015; Joly et al. 2017; Kovács et al. 2017; Zellweger et al. 2019). In fact, closed canopies not only intercept and filter more light, but they also intercept more snow and consequently reduce the snow cover on the forest floor exposing the litter to freeze-thaw cycles (Davis et al. 1997; Mellander et al. 2005; Pomeroy and Goodison 1997).

4.2. EFFECTS OF PHOTODEGRADATION ON MICROBIAL ASSEMBLAGES AND ASSOCIATED LITTER DECOMPOSITION PROCESS

We monitored biomass and community structure of microbial decomposers colonizing beech leaf litter during the first 6 months of decomposition in a mature beech forest in Normandy (France, III).

Manipulation of the spectral composition of sunlight had a significant effect on the total microbial biomass (p = 0.022, III) and on both bacterial (p = 0.001, III) and fungal biomass (p = 0.021, III) therein. However, biomass of fungi and bacteria were not significantly affected by individual spectral regions but rather by a combination of them; suggesting multiple spectral regions to act synergistically in determining the effect of sunlight on microbial biomass. A plausible reason why we did not detect a clear overarching effect of each spectral region is that the effects, positive or negative, of different spectral regions on decomposers differ among decomposer species (Kumagai 1988; Pancotto et al. 2005; Paul and Gwynn-Jones 2003).

UV-A radiation and blue and green light, when present altogether, significantly reduced the total microbial biomass (-34%, pairwise No-UV/Blue/Green – No-UVB: p = 0.006, III). This was mainly due to a reduced fungal biomass (-37%, pairwise No-UV/Blue/Green – No-UVB: p = 0.006, III). Even though UV-B radiation tended to increase fungal biomass, its effect was not significant (+19%, pairwise No-UVB – Full-Spectrum: p = 0.279, III). A positive effect of UV-B radiation is not uncommon, as this spectral region was previously documented to favour some fungal decomposers (Pancotto et al. 2005; Robson et al. 2004) by stimulating sexual and asexual morphogenesis (Ensminger 1993). On the other hand, bacterial biomass was significantly increased by the full-spectrum of sunlight (+23%, pairwise Dark – Full-Spectrum: p = 0.024, III).

Our results indicate that different combinations of spectral regions had diametrically opposing effects on fungal and bacterial decomposers. Fungi were reduced by the short-wavelength visible light (blue and green light) and UV-A radiation, whereas bacteria were promoted.

Exposure to green and blue light decreased the biomass and reduced hyphal length of several fungal species under controlled conditions on a synthetic growing medium (Velmurugan et al. 2010). UV-A radiation is known to enhance sporulation in some fungal phytopathogens (Paul and Gwynn-Jones 2003). This effect depends on the dose of UV-A radiation, the length of the exposure, the interaction with UV-B radiation (Fourtouni et al. 1998; Kumagai 1988; Osman et al. 1989) and, most importantly, on the fungal species (Paul and Gwynn-Jones 2003).

In several saprophytic fungi, UV-A radiation can inhibit sporulation and delay germination of conidia (García-Cela et al. 2015; Osman et al. 1989), this finding also supports our results. Bacterial decomposers, on the other hand, were more abundant under the full spectrum of sunlight, suggesting that they prefer light environments. A possible explanation for this result could be the increase of nutrients available to bacterial decomposers as a consequence of photochemical mineralization under the full spectrum of sunlight, the so called photofacilitation effect.

Exposure to both UV radiation and visible light have been proven to stimulate subsequent microbial decomposition in several arid and semiarid environments (Austin et al. 2016; Baker and Allison 2015; Lin et al. 2018). In our results, the existence of a negative correlation between litter carbon content and bacterial biomass would support this assertion ($R^2 = 0.4$, $p < 0.001$, III). However, we did not find that bacterial biomass was impacted by specific spectral regions, this might be due to the fact that photosensitivity of bacteria depends on the species and on traits such as pigmentation (Paul and Gwynn-Jones 2003), thus species-specific differences even out across the entire bacterial community.

The opposing effects of sunlight on bacterial and fungal decomposers could modify the community structure of microbial assemblages even at higher latitudes, with bacteria tending to dominate in sunlight and fungi in dark conditions. Additionally, the competitive relationship between bacteria and fungi, previously observed in microbes colonizing beech litter (Møller et al. 1999), could represent a factor responsible for the segregation of light and dark microbial assemblages.

In our experiment, only a small part of the variation in community structure (10.9%, III), analysed through PLFA biomarkers, was explained by spectral composition; while time, in terms of length of the decomposition period, accounted for 31.9% of the variation (III). This ability of spectral composition to shape microbial communities was previously suggested for litter decomposing under UV-B radiation in a heath ecosystem in Tierra del Fuego (Pancotto et al. 2005). Our results support this conjecture for other spectral regions such as blue light and UV-A radiation.

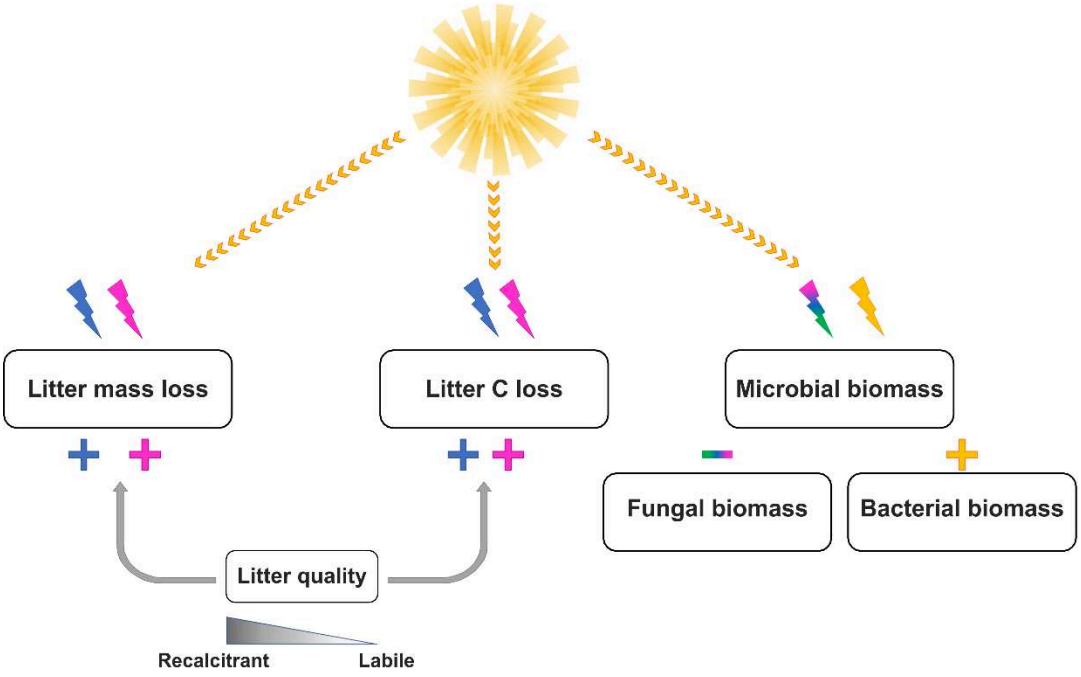

Figure 5: Schematic figure showing the process of photodegradation in a temperate beech forest. The lightening symbols represent the regions of the solar spectrum impacting litter mass loss, C loss and microbial biomass. Blue light (blue lightening) and UV-A radiation (pink lightening) enhance mass and carbon loss in litter. This effect is modulated by litter quality, with a greater effect on recalcitrant litter (section 4.1). The full-spectrum of sunlight (yellow lightening) increases bacterial biomass colonizing the litter, while the synergistic action of UV-A radiation, blue and green light (multicoloured lightening) reduces fungal biomass (section 4.2).

4.3. PHOTODEGRADATION ACROSS ECOSYSTEMS AND CLIMATES

We conducted a meta-analysis of published and unpublished studies analysing the effect of spectral composition on litter mass loss under ambient sunlight conditions.

Across all the studies considered, the full-spectrum of sunlight increased mass loss by 14% (p = 0.040, IV). This confirms the important role of photodegradation in the process of litter decomposition (King et al. 2012).

Different spectral regions had contrasting effects on litter mass loss. Blue light was the spectral region with the biggest impact on mass loss, causing it to increase by 12% over all studies (p = 0.037, IV). On the other hand, UV-A radiation had a negative effect and decreased litter mass loss by 5% (p = 0.019, IV), while UV-B radiation had no significant effect on mass loss overall (p = 0.872, IV). This confirms our hypotheses that blue light would have a positive impact on mass loss while no effect would be detected for UV-B radiation.

The absence of an effect of UV-B radiation is in agreement with results from a previous meta-analysis examining direct and indirect effects of UV-B radiation on mass loss (Song et al. 2013). Interactions among the multiple mechanisms of photodegradation could act to mask the impact of this spectral region. For example, photochemical mineralization and consequent photofacilitation may offset photoinhibition producing no net change in mass loss due to UV-B radiation (Bais et al. 2018).

Several interacting mechanisms may also counter-balance each other over other spectral regions involved in the process of photodegradation. While blue light has proved able to enhance litter decomposition through photochemical mineralization, it has not been shown to produce a photoinhibition effect (Austin et al. 2016). The opposite mechanisms are likely to operate under UV-A radiation, meaning its capability to cause photoinhibition (García-Cela et al. 2015; Osman et al. 1989) outweighs the benefits of photochemical mineralization for microbes.

When considering UV-B, UV-A and blue light, we must remember that these last two spectral regions are present at higher irradiances than UV-B radiation in natural environments, therefore their impact on decomposition

could be enhanced (Aphalo et al. 2012). Solar radiation is enriched in UV-B radiation at low latitudes, and in our meta-analysis we found a significant negative correlation between absolute latitude and UV-B photodegradation rates (slope = -0.003, R^2 = 0.24, p = 0.027, IV). This supports the assertion that UV-B radiation is more important in photodegradation a low latitudes in accordance with its higher proportional contribution to solar radiation (Aphalo et al. 2012).

Finally, the absence of a significant effect of UV radiation on litter mass loss (p = 0.255, IV) could be due to the confounding effects of UV-A and UV-B radiation, which on balance act differently when driving the direct and indirect mechanisms of photodegradation.

Climate modulated the effect of photodegradation driven by the full-spectrum of sunlight (p = 0.001, IV), blue light (p = 0.003, IV) and UV-B radiation (p < 0.001, IV), while it had no significant effect on UV-A-driven photodegradation (p = 0.529, IV). Overall, drier climates experienced higher photodegradation rates than temperate and continental climates. This result confirms our hypothesis and agrees with previous findings suggesting the process of photodegradation to be most relevant in arid environments (Bais et al. 2018; Gallo et al. 2009) under drier conditions (Brandt et al. 2007) where microbial decomposition is reduced (King et al. 2012).

However, when analysing the correlation between the photodegradation rate and the mean annual precipitation (MAP) in our meta-analysis, we only found a significant, but very weak, correlation (slope = 0.001, R^2 = 0.29, p = 0.009, IV) with full-spectrum photodegradation. This is likely due to MAP not being a biologically meaningful predictor. For example, the seasonality of rainfall might prove to be a better predictor as it captures potentially important seasonal fluctuations in precipitation. Additionally, it was suggested that photodegradation would not be reduced under mesic conditions, but simply harder to detect than in drier conditions, simply dwarfed in comparison to the effects of the predominant microbial decomposition (King et al. 2012). For the same reason, it is likely that UV and UV-B and UV-A radiation could have a negative impact on litter

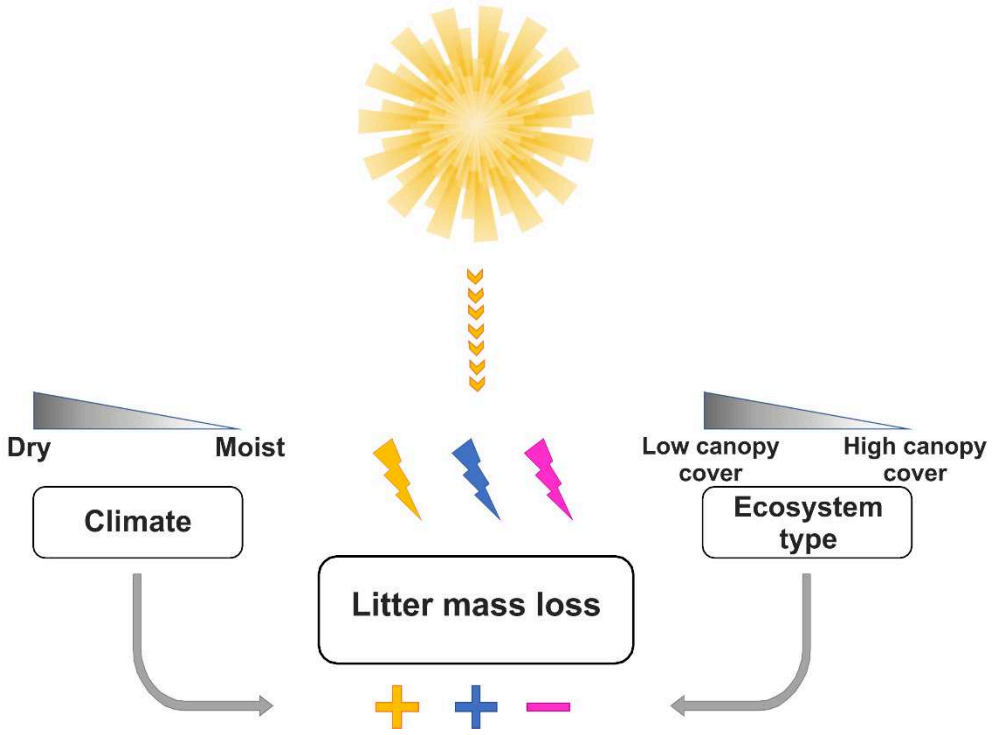

Figure 6: Schematic figure showing the photodegradation across biomes. The lightening symbols represent the regions of the solar spectrum impacting litter mass loss. The full-spectrum of sunlight (yellow lightening) and blue light (blue lightening) enhance litter mass loss, while UV-A radiation (pink lightening) reduces litter mass loss. This effect is modulated by climate and ecosystem type, with drier climates and ecosystems with low canopy cover (such as grasslands and open areas) experiencing higher rates of photodegradation.

decomposition by inhibiting microbial decomposition, which is the main driver of this process (Brandt et al. 2007; Smith et al. 2010).

The importance of the relationship between the photodegradation rate and precipitation it also likely to be dependent on the biome considered. In our field site in France, where we repeated a photodegradation experiment over two consecutive years (I & III), we obtained much lower photodegradation rates the second year. In comparing the two years, we found the second year to have double the precipitation of the first year, potentially explaining the difference in photodegradation rates (III).

Ecosystem type is also able to modulate the rate of photodegradation driven by blue light ($p < 0.001$, IV) and the full spectrum of sunlight ($p < 0.001$, IV). Ecosystem types with lower canopy cover had higher photodegradation rates: this is likely due the higher irradiance to which the litter is exposed in the open, compared for example with woodlands (Rozema

et al. 1999; Rutledge et al. 2010). In our meta-analysis we did not find a significant effect of photodegradation on litter mass loss in woodlands (IV). However, we must keep in mind that the studies were carried out in woodlands located at high latitudes in environments that are characterised by low irradiance and high precipitation.

4.4. PHOTODEGRADATION AND INITIAL LITTER TRAITS

We explored potential correlations between the photodegradation rate and those initial litter traits (IV) traditionally employed to predict decomposition rates such as carbon content (C); nitrogen content (N); carbon to nitrogen ratio (C:N); lignin content; lignin to nitrogen ratio (Lig:N) and specific leaf area (SLA). Unfortunately, due to the small amount of data available, we could not test potential correlations between photodegradation rates and initial content of hemicellulose and cellulose.

Even though the results of two of our experiments (I & II) suggested the importance of C:N in determining the rate of photodegradation in forest ecosystems, these results were not supported by the meta-analysis. In this case, none of the traits considered could predict photodegradation driven by blue light, UV-A radiation or the full spectrum of sunlight, while photodegradation due to UV and UV-B radiation was weakly negatively correlated with initial C content (slope = -0.015, R^2 = 0.08, p = 0.025 for UV and slope = -0.013, R^2 = 0.17, p = 0.043 for UV-B, IV). These results confound our expectations that SLA and lignin content would predict the photodegradation rate.

In the controlled environment experiment (II), where we deployed leaves with different orientation (abaxial or adaxial epidermis facing upwards), we found a significant difference in the photodegradation rate only in one of the two species (*Betula pendula*, p = 0.002, II). Leaves oriented with their abaxial epidermis facing the light source lost mass faster (0.05–0.10% higher daily mass loss depending on the filter treatment) than leaves with their adaxial epidermis facing the light source. This may indicate that the initial content of UV-screening compounds in the litter could affect subsequent decomposition

and photodegradation, as previously found in grey alder (*Alnus incana* (L.) Moench) litter (Kotilainen et al. 2009).

Past studies found photodegradation to be correlated with different litter traits such as initial N content (Pan et al. 2015); C:N (King et al. 2012); SLA (King et al. 2012; Pan et al. 2015); lignin content (Austin and Ballaré 2010; Méndez et al. 2019); hemicellulose and cellulose content (Day et al. 2018). The discrepancies among these results and the lack of correlations in our meta-analysis, suggest that if initial traits are important modifiers of photodegradation then their effects are likely to be specific to different biomes. Therefore, litter quality could be a good predictor at the local level but not at the global scale. However, due to the low number of studies measuring initial litter traits in each biome, we could not test this hypothesis in our meta-analysis (IV).

We must remember, however, that initial litter traits are very often determined by the climatic conditions to which the plants producing the litter are exposed (Fortunel et al. 2009; Oyarzabal et al. 2008), resulting in a correlation between climate (or type of biome) and litter quality, making it difficult to disentangle these two factors. Another issue to bear in mind is how difficult it is to separate the contribution of the various mechanisms of photodegradation, as they interact with each other, and with the microbial pool. It follows that we would be more likely to find litter traits that predict the rate of direct photochemical mineralization in a sterile environment in the absence of microbial decomposition. Additionally, the lack of correlations between photodegradation rates and initial litter traits confirms that we do not completely understand the mechanistic processes behind photodegradation.

5. PERSPECTIVE

5.1. PHOTODEGRADATION IN THE CONTEXT OF CLIMATE CHANGE

Photodegradation has a role in the carbon cycle as the process of photochemical mineralization causes the release of volatile carbon compounds into the atmosphere (Day et al. 2019; Gallo et al. 2009). Those studies that have tried to estimate the amount of CO_2, CO and CH_4 released during photodegradation under both enhanced and ambient solar radiation have obtained a wide range of results, as reviewed by King et al. 2012.

In ambient sunlight, the emission of CO_2 attributable to photodegradation was estimated to range 0.016 and 0.983 g C m^{-2} day^{-1} in grasslands and about 0.093-0.180 g C m^{-2} day^{-1} in peatlands (Brandt et al. 2009; Rutledge et al. 2010). CO emissions from photodegrading litter in studies in ambient sunlight have been estimated to be 2.0–5.5 mg C m^{-2} day^{-1} in a Brazilian shrubland and a savanna ecosystem (Kisselle et al. 2002). Whereas, under controlled conditions in a solar simulator the CH_4 emission from decomposing grass litter was the equivalent of 1.3-4.4 ng C g dw^{-1} h^{-1} (Lee et al. 2012).

The high variability associated with the above-mentioned results underlines how much the emission of volatile carbon compounds through photodegradation, like the rate of photodegradation itself, varies according to the biome. At present, more studies are required to better understand the extent to which photodegradation impacts the global carbon stocks when accounting for differences between biomes. Foereid et al. 2011 attempted to estimate the proportion of that carbon fixed by net primary production (NPP) that is lost through photodegradation at the global scale. According to this model about 0.5-1.6% of the carbon captured as NPP is photodegraded.

Although a low proportion of NPP is degraded at the global scale, Foereid et al. 2011 estimate that the relative contribution of photodegradation is much higher in dry ecosystems, reaching up to 14% of NPP. This suggests that photodegradation is more important at the local level than the global

level. However, the model from Foereid et al. 2011 considers the contribution of photodegradation to be equal for all spectral regions, and simply adjusted for total received irradiance. Additionally, this model fails to account for variation in spectral composition, such as the relative contribution of UV-B radiation, according to geographical location, through elevation, latitude, time of the year, and changing atmospheric factors such as patterns of cloud cover and aerosols. Moreover, data for photodegradation rates at high latitudes are lacking in the model, as well as data for ecosystems with high canopy cover, such as forests; ignoring the role of photodegradation in these kind of ecosystems (I, II & III).

Further studies are required to incorporate photodegradation into models of the global carbon cycle as this will then allow us to assess how the importance of its contribution is likely to vary over the projected global change scenarios (Field and Raupach 2004).

Global changes have the potential to impact photodegradation rates directly and indirectly through changes in the suite of abiotic and biotic factors to which litter is exposed. As an example, ongoing land aridification at low-to-mid latitudes (Kertész and Mika 1999) is likely to enhance the effect of direct photochemical mineralization (Almagro et al. 2015), as we know that this process is promoted by arid conditions (Brandt et al. 2007), resulting in a faster carbon turnover (Chen et al. 2016). Moreover, alteration in rainfall patterns and consequent moisture availability (Fay et al. 2003; Knapp et al. 2002; Miranda et al. 2011), fundamental drivers of the photofacilitation process (Gliksman et al. 2017; Wang et al. 2017), are likely to impact the net contribution of photodegradation to the carbon cycle.

Another aspect of climate change is variation in UV radiation reaching the Earth's surface due to altered clouds patterns and aerosols concentrations in the atmosphere (Zepp et al. 2007; 2011). As we previously mentioned, exposure of leaves to UV radiation determines the accumulation of photoprotective pigments in the leaf upper epidermis (Caldwell et al. 1999; Coffey et al. 2017). This can alter the photodegradation rate of leaf litter (mediated effects of sunlight, see Section 1.1.3) by reducing the penetration of sunlight to the mesophyll (Kotilainen et al. 2009; Pancotto et al. 2005). For

example, in our experiment in controlled-environmental conditions (II), we found a significant effect of leaf orientation, as proxy for phenolic content, on the photodegradation rate. Hence, a change in the amount of UV radiation to which living plants are exposed is likely to cause variation in the photodegradation rate.

But, what about forest ecosystems? Climate change reportedly impacts forest ecosystems in several ways, such as altered: timing of phenology, forest structure and species composition, species distribution; disturbances like fires, drought and insect outbreaks (Best et al. 2007; Dale et al. 2000; Dale et al. 2001; Noce et al. 2017; Seidl et al. 2017). The interactions among these factors make it hard to predict how the rate of photodegradation could potentially change, however, we can speculate on possible consequences. Taking climate change as an example, global warming can cause changes in species distribution, and therefore to the species composition and structure of forest plant communities (Best et al. 2007; Dainese et al. 2017; Nogués-Bravo et al. 2007).

Changes in plant community composition alter litter quality through the suite of traits that potentially determine the photodegradation rate at the local scale and the consequent microbial decomposition (Araujo and Austin 2015; Bosco et al. 2016). Moreover, changes in the forest structure will alter the amount and spectral composition of the irradiance reaching the forest floor due to modification of the multi-layered canopy, as different canopies filter sunlight differently (Hartikainen et al. 2018).

On the other hand, global warming can cause phenological shifts in the timing of bud burst and leaf fall, often leading to an increase in growing season length (Buitenwerf et al. 2015; Gallinat et al. 2015; Piao et al. 2019). This results in a reduction of the period of canopy opening, and as a consequence decreases the potential for photodegradation by reducing the amount of radiation directly reaching the forest floor. Moreover, this change in the light environment in forest understoreys will be accompanied by a modification of the microclimate, exposing litter to a different combination of moisture, temperature, spectral composition and snow-pack depth (Augusto et al. 2015;

Davis et al. 1997; Kovács et al. 2017; Mellander et al. 2005; Pomeroy and Goodison 1997; Zellweger et al. 2019).

Further studies are required to improve our understanding of the impact of climate changes on photodegradation in forests and its consequences on the carbon sink capacity of these ecosystems.

5.2. FUTURE OF PHOTODEGRADATION RESEARCH

There are several questions that remain unresolved in photodegradation research, especially in forest ecosystems. In this thesis we found photodegradation to have a role in the process of litter decomposition even under the low irradiances to which litter is exposed in forest understoreys. However, we only examined photodegradation of surface litter, as that is the layer directly exposed to sunlight.

When considering litter decomposition in forests we must bear in mind that thickness of the litter layer varies according to the forest type (Bens et al. 2006). The surface layer of litter filters shortwave solar radiation (Vazquez-Yanes et al. 1990) responsible for photodegradation, meaning the underlying litter layers avoid exposure to this part of the spectrum. Consequently, we can expect photodegradation to act only on the surface litter, therefore we could argue that the effect of photodegradation is often overestimated, as it affects only a small percentage of the litter on the forest floor. In fact, the photodegradation rate has been shown to decrease with increasing litter layer thickness (Henry et al. 2008; Mao et al. 2018). However, while direct photochemical mineralization is likely to decrease with increasing litter-layer thickness, these studies do not account for the potential for a priming effect to be carried over through the litter profile. In fact, we can expect the priming effect of photofacilitation (section 1.1.2) of surface layer to persist after this litter has mixed or been covered by more litter layers and in doing so initiate to a persistent carry-over effect of photodegradation on decomposition.

The role of the canopy species affecting photodegradation in forest environments proved important in our research (II). Trees of different species, age, and density, filter the sunlight differently in terms of the irradiance and

its spectral composition reaching the understorey (Hartikainen et al. 2018). Photodegradation generally increases with factors that enhance litter exposure to sunlight (King et al. 2012), and these can be mediated through canopy structure (Rutledge et al. 2010). Hence, when canopy density increases, increasing shade decreases the photodegradation rate (Ma et al. 2017; Pan et al. 2015). So, we could expect the rate of photodegradation to change according to LAI and the canopy species composition, while interacting with other environmental factors.

Understanding the relationship, between LAI and photodegradation rate, could be the first step to empirically estimating the photodegradation rate globally and calculating its effect on forest NPP worldwide and on the fertility of forest soils. This kind of approach was previously used to model photodegradation by Foereid et al. 2011, however at that time data on photodegradation rates in forest ecosystem were not yet available.

An important limitation on the estimation of photodegradation at the global scale is the absence of a standard method for doing photodegradation experiments. The highly diverse methods employed, such as litterbags placed under filter screens (Pancotto et al. 2003; Pancotto et al. 2005), litter boxes (Austin and Vivanco 2006), photodegradation-litterbags (Day et al. 2007), shade cloths (Ma et al. 2017), filter tunnels (Messenger et al. 2012), or louvered designs (Brandt et al. 2010), can create very different microclimates and therefore make studies to be difficult to compare. A standard method for the study of photodegradation across biomes is needed to reduce confounding results caused by methodological differences.

As a step towards standardisation of dose-response, a spectral weighting function for photochemical mineralisation was recently published (Day et al. 2019). The spectral sensitivity to UV radiation of biological or biophysical responses vary according to the process of interest. To allow comparison of a response under different conditions the effective irradiance can be calculated by weighting measured irradiance according to the effectiveness of each wavelength in producing this response (Aphalo et al. 2012). After quantifying the response produced by each wavelength, it is

multiplied by a radiation amplification factor (RAF) to obtain the effective dose of radiation over the spectrum of interest.

Formulation of a weighting function for photodegradation is complicated, as several responses should be considered to account for the multiple mechanisms involved (direct, indirect and mediated effect of sunlight) (Barnes et al. 2015). Consequently, most photodegradation studies present unweighted doses of UV radiation, which can create difficulties when comparing the results of these studies (Caldwell et al. 1986; Caldwell and Flint 1997).

The recent development of a BSWF for the component mechanism of photochemical mineralisation by Day et al. 2019, excluding indirect and mediated photodegradation, opens new possibilities in the field of photodegradation research, allowing for better comparison and providing a standard way to present UV doses across studies. This polychromatic spectral weighting function was made by comparing the effects of different regions of the sunlight (280 nm – 650 nm) on several types of litter. Photochemical mineralisation declined exponentially with increasing wavelength but even at the upper limit of this range still had some activity. Applying this weighting function, the relative effectiveness at our field sites (spectra in Figure 2) were compared; for the winter canopy (Fig. 2a): 9% UV-B radiation, 64% UV-A radiation, and 24% blue light; for canopy shade (Fig. 2b) 7% UV-B radiation, 61% UV-A radiation and 27% blue light; and for canopy sunflecks (Fig. 2c) 8% UV-B radiation, 59% UV-A radiation, and 29% blue light. Although the relative differences are small, they are congruent with the heightened importance of blue light in the understorey. According to these calculations, photochemical mineralisation contributes five-times more to photodegradation in the open canopy than in a closed-canopy sunfleck, and a further ten-times more in the sunfleck than in the shade.

6. CONCLUSIONS

The first aim of this thesis was to investigate the role of photodegradation in temperate and boreal forest ecosystems. Our results show that the process of photodegradation is relevant to litter decomposition in the understorey of temperate and boreal forests, even though this litter is exposed to relatively low irradiance.

Moreover, this thesis highlights the importance of blue light as a major driver of photodegradation in temperate forest understoreys, with the potential to both accelerate litter mass loss and carbon loss. At these latitudes, blue light and UV-A radiation proved to contribute more than UV-B radiation as drivers of photodegradation, which runs contrary to their importance in arid and semiarid ecosystems at low latitudes. The direction and magnitude of the effect of photodegradation depend on the litter species and the type of forest canopy, since canopies not only filter sunlight differently, but also create different combinations of temperature, moisture and snow-pack depth.

While mass loss from litter was impacted by specific spectral regions in different ways, litter microbial biomass depended on the interaction of multiple spectral regions. In temperate forests, blue light, acting synergistically with UV-A radiation and green light, was able to impact microbial decomposition. In fact, sunlight had an opposing effect on bacterial and fungal decomposers, modifying the community structure of microbial assemblages, with bacteria tending to dominate in sunlight and fungi in dark conditions.

A second aim of the thesis was to investigate how photodegradation changes across biomes and which initial litter traits could be used to predict the rate of photodegradation. We found that at a global scale the direction and magnitude of photodegradation differ according to the spectral region considered. We highlight the crucial role of blue light and UV-A radiation as drivers of photodegradation across biomes, eclipsing that of UV-B radiation, despite UV-B radiation being regarded for decades as the main spectral region

responsible for this process. While blue light enhances mass loss, when considering several biomes, UV-A radiation decreases mass loss.

UV-A radiation has potentially very interesting effects on decomposition, as it represents a larger fraction of solar spectral irradiance than UV-B radiation and is enriched in canopy shade compared with blue light. Moreover, this spectral region combines the potential for photochemical mineralization, with a strong impact on fungal decomposers, which can be positive or negative according to species, therefore it would deserve more attention in future photodegradation research.

At a global level, our meta-analysis found that the photodegradation rate is modulated by climate and ecosystem type, with dry environments characterised by low canopy cover experiencing the highest photodegradation rates.

Finally, according to our meta-analysis results, classical litter traits such as lignin content, C:N, lig:N, are not good predictors of the rate of photodegradation at the global scale. This does not exclude the possibility that different traits could be important in different biomes, as for example results of our experiments suggested C:N to be important in determining the rate of photodegradation. These discrepancies emphasize how much there remains to discover about the mechanisms underlying the photodegradation process and its relationship with other environmental factors.

7. ACKNOWLEDGEMENTS

Undertaking this PhD has been an incredible experience that enriched both my education and my personal skill and wouldn't have been possible without the help and support of multiple people.

Firstly, I would like to acknowledge the Region Normandy and the "Lammi Biological Station Grant 2016" for the financial support to this project, together with the two universities, the University of Helsinki and the University of Rouen-Normandy, that provided the facilities that allowed me to complete my research.

I am particularly grateful to my supervisors and co-supervisors: Dr Matthew Robson, Prof. Matthieu Chauvat, Dr. Estelle Forey and Dr. Alan Jones, for the guidance and support through these four years.

I am sincerely thankful to Prof Christiane Gallet and Dr Tarja Lehto for accepting to act as pre-examiners of this dissertation and to Prof Laura Llorens Guasch and Prof Stephan Hättenschwiler for accepting to act as opponents during the defence. I would like to thank Prof Kurt Fagerstedt for acting as custos and Prof Matty Berg for accepting to role of President of the French grading committee.

I would like to express my gratitude to the two research groups, CanSEE and ECODIV, that hosted me during the years of my PhD, for giving me this incredible opportunity. I have been very lucky to have the best colleagues both in France and in Finland to share my adventure with. Twinkle, Craig, Titta, Saara, David, Benoit, Marceau, Edouard, Corentin, François, Matthieu, Sylvaine, Philippe, a warm thank you not only for the help with my research but also, and most important, for the lovely times, for your friendship and for the support through the most stressful moments. You all have helped me building up my new life in these two wonderful countries without making me feel alone, despite being far away from my family and friends. A special thanks to Philippe, none of the experiments in my thesis would have been possible without your precious help and bright and innovative ideas.

I am truly grateful to all my co-authors for their fundamental contribution to this thesis. I am particularly grateful to Dr Qing-Wei Wang for the opportunity to create this research collaboration and for inviting me to visit the FFPRI in Japan, in what was an incredible trip and an enlightening travel through Japanese culture. I would equally thank Santa Neimane, joint first author of the second chapter of this thesis, for the help with the experiment.

I would like to thank my advisory board at the University of Helsinki: Prof Anna-Liisa Laine, Dr Mar Cabeza and Prof Anna Lintunen, and my follow-up committee at the University of Rouen: Dr James Weedon, Dr Annabel Porté, Prof Frank Le Foll and Dr Marc Ropitaux for the guidance and advise through these four years.

I gratefully acknowledge the researchers, students and stuff of Lammi Biological Station who made my field work fun despite the grey Finnish days. John, Elena, Albert, Irma, Joose, my time in Lammi wouldn't have been the same without you.

My sincere gratitude to my family who supported and believed in me since always. I would not be here today without you, you inspire me every day. Un ringraziamento particolare alla mia famiglia che ha da sempre creduto in me. Non sarei qui oggi senza il vostro appoggio e amore, vi voglio bene.

Last but not least, my dearest Tariq. Thank you for taking this journey with me: you are, and you have been my sunshine in these four years. You have always been my greatest supporter and my best friend. You convinced me to go on when I wanted to give up, you made me believe in myself. Thank you for being so understanding and for always standing by my side even in the most difficult moments.

8. REFERENCES

Almagro M, Maestre FT, Martínez-López J, Valencia E, Rey A (2015) Climate change may reduce litter decomposition while enhancing the contribution of photodegradation in dry perennial Mediterranean grasslands. Soil Biology and Biochemistry 90: 214-223. doi: https://doi.org/10.1016/j.soilbio.2015.08.006.

Almagro M, Martínez-López J, Maestre FT, Rey A (2017) The Contribution of Photodegradation to Litter Decomposition in Semiarid Mediterranean Grasslands Depends on its Interaction with Local Humidity Conditions, Litter Quality and Position. Ecosystems 20: 527-542. doi: 10.1007/s10021-016-0036-5.

Aneja MK, Sharma S, Fleischmann F, Stich S, Heller W, Bahnweg G, Munch JC, Schloter M (2006) Microbial Colonization of Beech and Spruce Litter—Influence of Decomposition Site and Plant Litter Species on the Diversity of Microbial Community. Microbial Ecology 52: 127-135. doi: 10.1007/s00248-006-9006-3.

Aphalo P, Albert A, Björn L, McLeod A, Robson T, Rosenqvist E (2012) Beyond the visible. A handbook of best practice in plant UV photobiology. University of Helsinki, Division of Plant Biology, Helsinki.

Aphalo PJ (2018) Exploring temporal and latitudinal variation in the solar spectrum at ground level with the TUV model. UV4Plants Bulletin 2018 n.2: 45-56. doi: 10.19232/uv4pb.2018.2.14.

Araujo PI, Austin AT (2015) A shady business: pine afforestation alters the primary controls on litter decomposition along a precipitation gradient in Patagonia, Argentina. Journal of Ecology 103: 1408-1420. doi: 10.1111/1365-2745.12433.

Asplund J, Kauserud H, Bokhorst S, Lie MH, Ohlson M, Nybakken L (2018) Fungal communities influence decomposition rates of plant litter from two dominant tree species. Fungal Ecology 32: 1-8. doi: https://doi.org/10.1016/j.funeco.2017.11.003.

Augusto L, De Schrijver A, Vesterdal L, Smolander A, Prescott C, Ranger J (2015) Influences of evergreen gymnosperm and deciduous angiosperm tree species on the functioning of temperate and boreal forests. Biological Reviews 90: 444-466. doi: 10.1111/brv.12119.

Austin AT, Ballaré CL (2010) Dual role of lignin in plant litter decomposition in terrestrial ecosystems. Proc Natl Acad Sci U S A 107: 4618-4622. doi: 10.1073/pnas.0909396107.

Austin AT, Méndez MS, Ballaré CL (2016) Photodegradation alleviates the lignin bottleneck for carbon turnover in terrestrial ecosystems. Proceedings of the National Academy of Sciences 113: 4392. doi: 10.1073/pnas.1516157113.

Austin AT, Vivanco L (2006) Plant litter decomposition in a semi-arid ecosystem controlled by photodegradation. Nature 442: 555-558. doi: 10.1038/nature05038.

Bais AF, Lucas RM, Bornman JF, Williamson CE, Sulzberger B, Austin AT, Wilson SR, Andrady AL, Bernhard G, McKenzie RL, Aucamp PJ, Madronich S, Neale RE, Yazar S, Young AR, de Gruijl FR, Norval M, Takizawa Y, Barnes PW, Robson TM, Robinson SA, Ballare CL, Flint SD, Neale PJ, Hylander S, Rose KC, Wangberg SA, Hader DP, Worrest RC, Zepp RG, Paul ND, Cory RM, Solomon KR, Longstreth J, Pandey KK, Redhwi HH, Torikai A, Heikkila AM (2018) Environmental effects of ozone depletion, UV radiation and interactions with climate change: UNEP Environmental Effects Assessment Panel, update 2017. Photochemical & photobiological sciences : Official journal of the European Photochemistry Association and the European Society for Photobiology 17: 127-179. doi: 10.1039/c7pp90043k.

Baker NR, Allison SD (2015) Ultraviolet photodegradation facilitates microbial litter decomposition in a Mediterranean climate. Ecology 96: 1994-2003. doi: 10.1890/14-1482.1.

Ball BA, Christman MP, Hall SJ (2019) Nutrient dynamics during photodegradation of plant litter in the Sonoran Desert. Journal of Arid Environments 160: 1-10. doi: https://doi.org/10.1016/j.jaridenv.2018.09.004.

Barnes PW, Throop HL, Archer SR, Breshears DD, McCulley RL, Tobler MA (2015) Sunlight and Soil–Litter Mixing: Drivers of Litter Decomposition in Drylands. In: U Lüttge, W Beyschlag (eds) Progress in Botany: Vol 76. Springer International Publishing, Cham.

Bens O, Buczko U, Sieber S, Hüttl RF (2006) Spatial variability of O layer thickness and humus forms under different pine beech–forest transformation stages in NE Germany. Journal of Plant Nutrition and Soil Science 169: 5-15. doi: 10.1002/jpln.200521734.

Beresford GW, Selby G, Moore JC (2013) Lethal and sub-lethal effects of UV-B radiation exposure on the collembolan Folsomia candida (Willem) in the laboratory. Pedobiologia 56: 89-95. doi: https://doi.org/10.1016/j.pedobi.2012.12.001.

Best AS, Johst K, Münkemüller T, Travis JMJ (2007) Which species will succesfully track climate change? The influence of intraspecific competition and density dependent dispersal on range shifting dynamics. Oikos 116: 1531-1539. doi: 10.1111/j.0030-1299.2007.16047.x.

Bosco T, Bertiller MB, Carrera AL (2016) Combined effects of litter features, UV radiation, and soil water on litter decomposition in denuded areas of the arid Patagonian Monte. Plant and Soil 406: 71-82. doi: 10.1007/s11104-016-2864-7.

Brack D (2019) Forestsand Climate Change. UNFF14 Background Analytical Study.

Brandt LA, Bohnet C, King JY (2009) Photochemically induced carbon dioxide production as a mechanism for carbon loss from plant litter in arid ecosystems. Journal of Geophysical research 114. doi: 10.1029/2008jg000772.

Brandt LA, King JY, Hobbie SE, Milchunas DG, Sinsabaugh RL (2010) The Role of Photodegradation in Surface Litter Decomposition Across a Grassland Ecosystem Precipitation Gradient. Ecosystems 13: 765-781. doi: 10.1007/s10021-010-9353-2.

Brandt LA, King JY, Milchunas DG (2007) Effects of ultraviolet radiation on litter decomposition depend on precipitation and litter chemistry in a

shortgrass steppe ecosystem. Global Change Biology 13: 2193-2205. doi: doi:10.1111/j.1365-2486.2007.01428.x.

Bravo-Oviedo A, Ruiz-Peinado R, Onrubia R, del Río M (2017) Thinning alters the early-decomposition rate and nutrient immobilization-release pattern of foliar litter in Mediterranean oak-pine mixed stands. Forest Ecology and Management 391: 309-320. doi: https://doi.org/10.1016/j.foreco.2017.02.032.

Brelsford CC, Morales LO, Nezval J, Kotilainen TK, Hartikainen SM, Aphalo PJ, Robson TM (2019) Do UV-A radiation and blue light during growth prime leaves to cope with acute high light in photoreceptor mutants of Arabidopsis thaliana? Physiologia Plantarum 165: 537-554. doi: 10.1111/ppl.12749.

Brown MJ, Parker GG, Posner NE (1994) A survey of ultraviolet-B radiation in forests. Journal of Ecology 82: 843-854

Buitenwerf R, Rose L, Higgins SI (2015) Three decades of multi-dimensional change in global leaf phenology. Nature Climate Change 5: 364-368. doi: 10.1038/nclimate2533.

Caldwell M, Searles P, Flintl S, Barnes P (1999) Terrestrial ecosystem responses to solar UV-B radiation mediated by vegetation, microbes. Physiological Plant Ecology: 39th Symposium of the British Ecological Society. Cambridge University Press.

Caldwell MM, Camp LB, Warner CW, Flint SD (1986) Action Spectra and Their Key Role in Assessing Biological Consequences of Solar UV-B Radiation Change. In: RC Worrest, MM Caldwell (eds) Stratospheric Ozone Reduction, Solar Ultraviolet Radiation and Plant Life. Springer Berlin Heidelberg, Berlin, Heidelberg.

Caldwell MM, Flint SD (1994) Stratospheric ozone reduction, solar UV-B radiation and terrestrial ecosystems. Climatic Change 28: 375-394. doi: 10.1007/bf01104080.

Caldwell MM, Flint SD (1997) Uses of biological spectral weighting functions and the need of scaling for the ozone reduction problem. In: J Rozema, WWC Gieskes, SC Van De Geijn, C Nolan, H De Boois (eds) UV-B and Biosphere. Springer Netherlands, Dordrecht.

Chazdon RL, Pearcy RW (1991) The importance of sunflecks for forest understory plants. BioScience 41: 760-766. doi: 10.2307/1311725

Chen M, Parton WJ, Adair EC, Asao S, Hartman MD, Gao W (2016) Simulation of the effects of photodecay on long-term litter decay using DayCent. Ecosphere 7: e01631. doi: 10.1002/ecs2.1631.

Coffey A, Prinsen E, Jansen MAK, Conway J (2017) The UVB photoreceptor UVR8 mediates accumulation of UV-absorbing pigments, but not changes in plant morphology, under outdoor conditions. Plant, Cell & Environment 40: 2250-2260. doi: 10.1111/pce.13025.

Cole DW (1986) Nutrient Cycling in World Forests. In: SP Gessel (ed) Forest site and productivity. Springer Netherlands, Dordrecht.

Coleman DC, Crossley Jr D, Hendrix P (2004) Decomposition and Nutrient Cycling. In: D Coleman (ed) Fundamentals of soil ecology. Elsevier Academic press.

Conn C, Dighton J (2000) Litter quality influences on decomposition, ectomycorrhizal community structure and mycorrhizal root surface acid phosphatase activity. Soil Biology and Biochemistry 32: 489-496. doi: https://doi.org/10.1016/S0038-0717(99)00178-9.

Dainese M, Aikio S, Hulme PE, Bertolli A, Prosser F, Marini L (2017) Human disturbance and upward expansion of plants in a warming climate. Nature Climate Change 7: 577-580. doi: 10.1038/nclimate3337.

Dale VH, Joyce LA, McNulty S, Neilson RP (2000) The interplay between climate change, forests, and disturbances. Science of The Total Environment 262: 201-204. doi: https://doi.org/10.1016/S0048-9697(00)00522-2.

Dale VH, Joyce LA, McNulty S, Neilson RP, Ayres MP, Flannigan MD, Hanson PJ, Irland LC, Lugo AE, Peterson CJ, Simberloff D, Swanson FJ, Stocks BJ, Wotton BM (2001) Climate Change and Forest Disturbances: Climate change can affect forests by altering the frequency, intensity, duration, and timing of fire, drought, introduced species, insect and pathogen outbreaks, hurricanes, windstorms, ice storms, or landslides. BioScience 51: 723-734. doi: 10.1641/0006-3568(2001)051[0723:CCAFD]2.0.CO;2.

Davis RE, Hardy JP, Ni W, Woodcock C, McKenzie JC, Jordan R, Li X (1997) Variation of snow cover ablation in the boreal forest: A sensitivity study on the effects of conifer canopy. Journal of Geophysical Research: Atmospheres 102: 29389-29395. doi: 10.1029/97JD01335.

Day TA, Bliss MS, Placek SK, Tomes AR, Guénon R (2019) Thermal abiotic emission of CO2 and CH4 from leaf litter and its significance in a photodegradation assessment. Ecosphere 10: e02745. doi: 10.1002/ecs2.2745.

Day TA, Bliss MS, Tomes AR, Ruhland CT, Guénon R (2018) Desert leaf litter decay: Coupling of microbial respiration, water-soluble fractions and photodegradation. Global Change Biology 24: 5454-5470. doi: 10.1111/gcb.14438.

Day TA, Guénon R, Ruhland CT (2015) Photodegradation of plant litter in the Sonoran Desert varies by litter type and age. Soil Biology and Biochemistry 89: 109-122. doi: https://doi.org/10.1016/j.soilbio.2015.06.029.

Day TA, Vogelmann TC, DeLucia EH (1992) Are some plant life forms more effective than others in screening out ultraviolet-B radiation? Oecologia 92: 513-519. doi: 10.1007/BF00317843.

Day TA, Zhang ET, Ruhland CT (2007) Exposure to solar UV-B radiation accelerates mass and lignin loss of Larrea tridentata litter in the Sonoran Desert. Plant Ecology 193: 185-194.

Duguay KJ, Klironomos JN (2000) Direct and indirect effects of enhanced UV-B radiation on the decomposing and competitive abilities of saprobic fungi. Applied Soil Ecology 14: 157-164. doi: https://doi.org/10.1016/S0929-1393(00)00049-4.

Ensminger PA (1993) Control of development in plants and fungi by far-UV radiation. Physiologia Plantarum 88: 501-508.

FAO (2018) The State of the World's Forests 2018 – Forest pathways to sustainable development. Licence: CC BY-NC-SA 3.0 IGO., Rome.

Fay PA, Carlisle JD, Knapp AK, Blair JM, Collins SL (2003) Productivity responses to altered rainfall patterns in a C4-dominated grassland. Oecologia 137: 245-251. doi: 10.1007/s00442-003-1331-3.

Field CB, Raupach MR (2004) The global carbon cycle: integrating humans, climate, and the natural world. Island Press.

Foereid B, Bellarby J, Meier-Augenstein W, Kemp H (2010) Does light exposure make plant litter more degradable? Plant and Soil 333: 275-285. doi: 10.1007/s11104-010-0342-1.

Foereid B, Rivero MJ, Primo O, Ortiz I (2011) Modelling photodegradation in the global carbon cycle. Soil Biology and Biochemistry 43: 1383-1386. doi: https://doi.org/10.1016/j.soilbio.2011.03.004.

Fortunel C, Garnier E, Joffre R, Kazakou E, Quested H, Grigulis K, Lavorel S, Ansquer P, Castro H, Cruz P, DoleŽal J, Eriksson O, Freitas H, Golodets C, Jouany C, Kigel J, Kleyer M, Lehsten V, Lepš J, Meier T, Pakeman R, Papadimitriou M, Papanastasis VP, Quétier F, Robson M, Sternberg M, Theau J-P, Thébault A, Zarovali M (2009) Leaf traits capture the effects of land use changes and climate on litter decomposability of grasslands across Europe. Ecology 90: 598-611. doi: 10.1890/08-0418.1.

Fourtouni A, Manetas Y, Christias C (1998) Effects of UV-B radiation on growth, pigmentation, and spore production in the phytopathogenic fungus Alternaria solani. Canadian Journal of Botany 76: 2093-2099. doi: 10.1139/b98-170.

Fox GL, Coyle-Thompson CA, Bellinger PF, Cohen RW (2007) Phototactic responses to ultraviolet and white light in various species of Collembola, including the eyeless species, Folsomia candida. Journal of Insect Science 7. doi: 10.1673/031.007.2201.

Frostegård Å, Tunlid A, Bååth E (1991) Microbial biomass measured as total lipid phosphate in soils of different organic content. Journal of Microbiological Methods 14: 151-163. doi: https://doi.org/10.1016/0167-7012(91)90018-L.

Frostegård Å, Tunlid A, Bååth E (2011) Use and misuse of PLFA measurements in soils. Soil Biology and Biochemistry 43: 1621-1625. doi: https://doi.org/10.1016/j.soilbio.2010.11.021.

Gallinat AS, Primack RB, Wagner DL (2015) Autumn, the neglected season in climate change research. Trends in Ecology & Evolution 30: 169-176. doi: https://doi.org/10.1016/j.tree.2015.01.004.

Gallo ME, Porras-Alfaro A, Odenbach KJ, Sinsabaugh RL (2009) Photoacceleration of plant litter decomposition in an arid environment. Soil Biology and Biochemistry 41: 1433-1441. doi: https://doi.org/10.1016/j.soilbio.2009.03.025.

Gallo ME, Sinsabaugh RL, Cabaniss SE (2006) The role of ultraviolet radiation in litter decomposition in arid ecosystems. Applied Soil Ecology 34: 82-91. doi: https://doi.org/10.1016/j.apsoil.2005.12.006.

García-Cela E, Marin S, Sanchis V, Crespo-Sempere A, Ramos AJ (2015) Effect of ultraviolet radiation A and B on growth and mycotoxin production by Aspergillus carbonarius and Aspergillus parasiticus in grape and pistachio media. Fungal Biology 119: 67-78. doi: https://doi.org/10.1016/j.funbio.2014.11.004.

García-Palacios P, Maestre FT, Kattge J, Wall DH (2013) Climate and litter quality differently modulate the effects of soil fauna on litter decomposition across biomes. Ecology Letters 16: 1045-1053. doi: 10.1111/ele.12137.

García-Palacios P, McKie BG, Handa IT, Frainer A, Hättenschwiler S (2016) The importance of litter traits and decomposers for litter decomposition: a comparison of aquatic and terrestrial ecosystems within and across biomes. Functional Ecology 30: 819-829. doi: 10.1111/1365-2435.12589.

Gaxiola A, Armesto JJ (2015) Understanding litter decomposition in semiarid ecosystems: linking leaf traits, UV exposure and rainfall variability. Frontiers in Plant Science 6: 140.

Gehrke C, Johanson U, Callaghan TV, Chadwick D, Robinson CH (1995) The Impact of Enhanced Ultraviolet-B Radiation on Litter Quality and Decomposition Processes in Vaccinium Leaves from the Subarctic. Oikos 72: 213-222. doi: 10.2307/3546223.

Gliksman D, Rey A, Seligmann R, Dumbur R, Sperling O, Navon Y, Haenel S, De Angelis P, Arnone Iii JA, Grünzweig JM (2017) Biotic degradation at night, abiotic degradation at day: positive feedbacks on litter decomposition in drylands. Global Change Biology 23: 1564-1574. doi: 10.1111/gcb.13465.

Hamman A, Momo FR, Duhour A, Falco L, Sagario MC, Cuadrado ME (2003) Effect of UV radiation on Eisenia fetida populations: The 7th international symposium on earthworm ecology · Cardiff · Wales · 2002. Pedobiologia 47: 842-845. doi: https://doi.org/10.1078/0031-4056-00269.

Hartikainen SM, Jach A, Grané A, Robson TM (2018) Assessing scale-wise similarity of curves with a thick pen: As illustrated through comparisons of spectral irradiance. Ecology and Evolution 8: 10206-10218. doi: 10.1002/ece3.4496.

Hawes TC, Marshall CJ, Wharton DA (2012) Ultraviolet radiation tolerance of the Antarctic springtail, Gomphiocephalus hodgsoni. Antarctic Science 24: 147-153. doi: 10.1017/S0954102011000812.

Henry HAL, Brizgys K, Field CB (2008) Litter Decomposition in a California Annual Grassland: Interactions Between Photodegradation and Litter Layer Thickness. Ecosystems 11: 545-554. doi: 10.1007/s10021-008-9141-4.

Hodge A, Robinson D, Fitter A (2000) Are microorganisms more effective than plants at competing for nitrogen? Trends in Plant Science 5: 304-308. doi: https://doi.org/10.1016/S1360-1385(00)01656-3.

Hoorens B, Aerts R, Stroetenga M (2004) Elevated UV-B radiation has no effect on litter quality and decomposition of two dune grassland species: evidence from a long-term field experiment. Global Change Biology 10: 200-208. doi: 10.1111/j.1529-8817.2003.00735.x.

Huang G, Zhao H-m, Li Y (2017) Litter decomposition in hyper-arid deserts: Photodegradation is still important. Science of The Total Environment 601-602: 784-792. doi: https://doi.org/10.1016/j.scitotenv.2017.05.213.

Joly F-X, Milcu A, Scherer-Lorenzen M, Jean L-K, Bussotti F, Dawud SM, Müller S, Pollastrini M, Raulund-Rasmussen K, Vesterdal L, Hättenschwiler S (2017) Tree species diversity affects decomposition through modified micro-environmental conditions across European forests. New Phytologist 214: 1281-1293. doi: 10.1111/nph.14452.

Jones AG, Bussell J, Winters A, Scullion J, Gwynn-Jones D (2016) The functional quality of decomposing litter outputs from an Arctic plant community is affected by long-term exposure to enhanced UV-B. Ecological Indicators 60: 8-17. doi: https://doi.org/10.1016/j.ecolind.2015.05.052.

Kertész Á, Mika J (1999) Aridification — Climate change in South-Eastern Europe. Physics and Chemistry of the Earth, Part A: Solid Earth and Geodesy 24: 913-920. doi: https://doi.org/10.1016/S1464-1895(99)00135-0.

King JY, Brandt LA, Adair EC (2012) Shedding light on plant litter decomposition: advances, implications and new directions in understanding the role of photodegradation. Biogeochemistry 111: 57-81.

Kisselle KW, Zepp RG, Burke RA, de Siqueira Pinto A, Bustamante MMC, Opsahl S, Varella RF, Viana LT (2002) Seasonal soil fluxes of carbon monoxide in burned and unburned Brazilian savannas. Journal of Geophysical Research: Atmospheres 107: LBA 18-11-LBA 18-12. doi: 10.1029/2001JD000638.

Klironomos JN, Allen MF (1995) UV-B-Mediated Changes on Below-Ground Communities Associated with the Roots of Acer saccharum. Functional Ecology 9: 923-930. doi: 10.2307/2389991.

Knapp AK, Fay PA, Blair JM, Collins SL, Smith MD, Carlisle JD, Harper CW, Danner BT, Lett MS, McCarron JK (2002) Rainfall Variability, Carbon Cycling, and Plant Species Diversity in a Mesic Grassland. Science 298: 2202. doi: 10.1126/science.1076347.

Kotilainen T, Haimi J, Tegelberg R, Julkunen-Tiitto R, Vapaavuori E, Aphalo PJ (2009) Solar ultraviolet radiation alters alder and birch litter chemistry that in turn affects decomposers and soil respiration. Oecologia 161: 719-728. doi: 10.1007/s00442-009-1413-y.

Kovács B, Tinya F, Ódor P (2017) Stand structural drivers of microclimate in mature temperate mixed forests. Agricultural and Forest Meteorology 234-235: 11-21. doi: https://doi.org/10.1016/j.agrformet.2016.11.268.

Kumagai T (1988) Photocontrol of fungal development. Photochemistry and Photobiology 47: 889-896.

Landry LG, Chapple CCS, Last RL (1995) Arabidopsis Mutants Lacking Phenolic Sunscreens Exhibit Enhanced Ultraviolet-B Injury and Oxidative Damage. Plant Physiology 109: 1159. doi: 10.1104/pp.109.4.1159.

Lee H, Rahn T, Throop H (2012) An accounting of C-based trace gas release during abiotic plant litter degradation. Global Change Biology 18: 1185-1195. doi: 10.1111/j.1365-2486.2011.02579.x.

Lin Y, Karlen SD, Ralph J, King JY (2018) Short-term facilitation of microbial litter decomposition by ultraviolet radiation. Science of The Total Environment 615: 838-848. doi: https://doi.org/10.1016/j.scitotenv.2017.09.239.

Lin Y, Scarlett RD, King JY (2015) Effects of UV photodegradation on subsequent microbial decomposition of Bromus diandrus litter. Plant and Soil 395: 263-271. doi: 10.1007/s11104-015-2551-0.

Ma Z, Yang W, Wu F, Tan B (2017) Effects of light intensity on litter decomposition in a subtropical region. Ecosphere 8: e01770. doi: 10.1002/ecs2.1770.

Mao B, Zhao L, Zhao Q, Zeng D (2018) Effects of ultraviolet (UV) radiation and litter layer thickness on litter decomposition of two tree species in a semi-arid site of Northeast China. Journal of Arid Land 10: 416-428. doi: 10.1007/s40333-018-0054-6.

Melin E (1930) Biological Decomposition of Some Types of Litter From North American Forests. Ecology 11: 72-101. doi: 10.2307/1930782.

Mellander P-E, Laudon H, Bishop K (2005) Modelling variability of snow depths and soil temperatures in Scots pine stands. Agricultural and Forest Meteorology 133: 109-118. doi: https://doi.org/10.1016/j.agrformet.2005.08.008.

Méndez MS, Martinez ML, Araujo PI, Austin AT (2019) Solar radiation exposure accelerates decomposition and biotic activity in surface litter but not soil in a semiarid woodland ecosystem in Patagonia, Argentina. Plant and Soil. doi: 10.1007/s11104-019-04325-1.

Messenger DJ, Fry SC, Yamulki S, McLeod AR (2012) Effects of UV-B filtration on the chemistry and decomposition of Fraxinus excelsior leaves. Soil Biology and Biochemistry 47: 133-141. doi: https://doi.org/10.1016/j.soilbio.2011.12.010.

Miranda JD, Armas C, Padilla FM, Pugnaire FI (2011) Climatic change and rainfall patterns: Effects on semi-arid plant communities of the Iberian Southeast. Journal of Arid Environments 75: 1302-1309. doi: https://doi.org/10.1016/j.jaridenv.2011.04.022.

Møller J, Miller M, Kjøller A (1999) Fungal–bacterial interaction on beech leaves: influence on decomposition and dissolved organic carbon quality. Soil Biology and Biochemistry 31: 367-374. doi: https://doi.org/10.1016/S0038-0717(98)00138-2.

Moody SA, Newsham KK, Ayres PG, Paul ND (1999) Variation in the responses of litter and phylloplane fungi to UV-B radiation (290–315 nm). Mycological Research 103: 1469-1477. doi: 10.1017/S0953756299008783.

Moody SA, Paul ND, Björn LO, Callaghan TV, Lee JA, Manetas Y, Rozema J, Gwynn-Jones D, Johanson U, Kyparissis A, Oudejans AMC (2001) The direct effects of UV-B radiation on Betula pubescens litter decomposing at four European field sites. Plant Ecology 154: 27-36. doi: 10.1023/A:1012965610170.

Newsham KK, Greenslade PD, Kennedy VH, McLeod AR (1999) Elevated UV-B radiation incident on Quercus robur leaf canopies enhances decomposition of resulting leaf litter in soil. Global Change Biology 5: 403-409. doi: 10.1046/j.1365-2486.1999.00231.x.

Newsham KK, McLeod AR, Roberts JD, Greenslade PD, Emmett BA (1997) Direct Effects of Elevated UV-B Radiation on the Decomposition of Quercus robur Leaf Litter. Oikos 79: 592-602. doi: 10.2307/3546903.

Newsham KK, Splatt P, Coward PA, Greenslade PD, McLeod AR, Anderson JM (2001) Negligible influence of elevated UV-B radiation on leaf litter quality of Quercus robur. Soil Biology and Biochemistry 33: 659-665. doi: https://doi.org/10.1016/S0038-0717(00)00210-8.

Noce S, Collalti A, Santini M (2017) Likelihood of changes in forest species suitability, distribution, and diversity under future climate: The case of Southern Europe. Ecology and Evolution 7: 9358-9375. doi: 10.1002/ece3.3427.

Nogués-Bravo D, Araújo MB, Errea MP, Martínez-Rica JP (2007) Exposure of global mountain systems to climate warming during the 21st Century. Global Environmental Change 17: 420-428. doi: https://doi.org/10.1016/j.gloenvcha.2006.11.007.

Oliver CD, Larson BC (1996) Forest stand dynamics. Wiley New York.

Olson JS (1963) Energy Storage and the Balance of Producers and Decomposers in Ecological Systems. Ecology 44: 322-331. doi: 10.2307/1932179.

Osman M, Elsayed MA, Mohamed YAH, Abo-Zeid AM (1989) Effect of ultraviolet irradiation on germination and growth in Aspergillus flavus and Penicillium notatum. Mycological Research 92: 293-296. doi: https://doi.org/10.1016/S0953-7562(89)80068-1.

Oyarzabal M, Paruelo JM, del Pino F, Oesterheld M, Lauenroth WK (2008) Trait differences between grass species along a climatic gradient in South and North America. Journal of Vegetation Science 19: 183-192. doi: 10.3170/2007-8-18349.

Pan X, Song Y-B, Liu G-F, Hu Y-K, Ye X-H, Cornwell WK, Prinzing A, Dong M, Cornelissen JHC (2015) Functional traits drive the contribution of solar radiation to leaf litter decomposition among multiple arid-zone species. Scientific Reports 5: 13217. doi: 10.1038/srep13217.

Pancotto VA, Sala OE, Cabello M, López NI, Matthew Robson T, Ballaré CL, Caldwell MM, Scopel AL (2003) Solar UV-B decreases decomposition in herbaceous plant litter in Tierra del Fuego, Argentina: potential role of an altered decomposer community. Global Change Biology 9: 1465-1474. doi: 10.1046/j.1365-2486.2003.00667.x.

Pancotto VA, Sala OE, Robson TM, Caldwell MM, Scopel AL (2005) Direct and indirect effects of solar ultraviolet-B radiation on long-term decomposition. Global Change Biology 11: 1982-1989. doi: 10.1111/j.1365-2486.2005.1027.x.

Paul ND, Gwynn-Jones D (2003) Ecological roles of solar UV radiation: towards an integrated approach. Trends in Ecology & Evolution 18: 48-55. doi: https://doi.org/10.1016/S0169-5347(02)00014-9.

Piao S, Liu Q, Chen A, Janssens IA, Fu Y, Dai J, Liu L, Lian X, Shen M, Zhu X (2019) Plant phenology and global climate change: Current progresses and challenges. Global Change Biology 25: 1922-1940. doi: 10.1111/gcb.14619.

Pomeroy J, Goodison B (1997) Winter and Snow. In: T Oke, WR Rouse, WG Bailey (eds) The Surface Climates of Canada. McGill-Queen's University Press.

Prescott CE (2010) Litter decomposition: what controls it and how can we alter it to sequester more carbon in forest soils? Biogeochemistry 101: 133-149. doi: 10.1007/s10533-010-9439-0.

R_Core_Team (2013) R: A language and environment for statistical computing. 3.6.1 edn. R Foundation for Statistical Computing, Vienna, Austria.

Rahman M, Tsukamoto J, Rahman MM, Yoneyama A, Mostafa K (2013) Lignin and its effects on litter decomposition in forest ecosystems. Chemistry & Ecology 29: 540-553. doi: 10.1080/02757540.2013.790380.

Robson TM, Pancotto VA, Ballaré CL, Sala OE, Scopel AL, Caldwell MM (2004) Reduction of solar UV-B mediates changes in the Sphagnum capitulum microenvironment and the peatland microfungal community. Oecologia 140: 480-490. doi: 10.1007/s00442-004-1600-9.

Ross MS, Flanagan LB, Roi GHL (1986) Seasonal and successional changes in light quality and quantity in the understory of boreal forest ecosystems. Canadian Journal of Botany 64: 2792-2799. doi: 10.1139/b86-373.

Rousseaux MC, Ballaré CL, Giordano CV, Scopel AL, Zima AM, Szwarcberg-Bracchitta M, Searles PS, Caldwell MM, Díaz SB (1999) Ozone depletion and UVB radiation: Impact on plant DNA damage in southern South America. Proceedings of the National Academy of Sciences 96: 15310. doi: 10.1073/pnas.96.26.15310.

Rozema J, Kooi B, Broekman R, Kuijper L (1999) Modelling direct (photodegradation) and indirect (litter quality) effects of enhanced UV-B on litter decomposition. In: J Rozema (ed) Stratospheric ozone depletion: the effects of enhanced UV-B radiation on terrestrial ecosystems. Backhuys Publishers.

Rozema J, Tosserams M, Nelissen HJM, van Heerwaarden L, Broekman RA, Flierman N (1997) Stratospheric ozone reduction and ecosystem processes: enhanced UV-B radiation affects chemical quality and decomposition of leaves of the dune grassland species Calamagrostis epigeios. Plant Ecology 128: 285-294. doi: 10.1023/A:1009723210062.

Rutledge S, Campbell DI, Baldocchi D, Schipper LA (2010) Photodegradation leads to increased carbon dioxide losses from terrestrial organic matter. Global Change Biology 16: 3065-3074. doi: 10.1111/j.1365-2486.2009.02149.x.

Schleppi P, Conedera M, Sedivy I, Thimonier A (2007) Correcting non-linearity and slope effects in the estimation of the leaf area index of forests from hemispherical photographs. Agricultural and Forest Meteorology 144: 236-242. doi: https://doi.org/10.1016/j.agrformet.2007.02.004.

Seidl R, Thom D, Kautz M, Martin-Benito D, Peltoniemi M, Vacchiano G, Wild J, Ascoli D, Petr M, Honkaniemi J, Lexer MJ, Trotsiuk V, Mairota P, Svoboda M, Fabrika M, Nagel TA, Reyer CPO (2017) Forest disturbances under climate change. Nature Climate Change 7: 395-402. doi: 10.1038/nclimate3303.

Smith WK, Berry ZC (2013) Sunflecks? Tree physiology 33: 233-237. doi: 10.1093/treephys/tpt005 %J Tree Physiology.

Smith WK, Gao WEI, Steltzer H, Wallenstein MD, Tree R (2010) Moisture availability influences the effect of ultraviolet-B radiation on leaf litter decomposition. Global Change Biology 16: 484-495. doi: 10.1111/j.1365-2486.2009.01973.x.

Song X, Peng C, Jiang H, Zhu Q, Wang W (2013) Direct and Indirect Effects of UV-B Exposure on Litter Decomposition: A Meta-Analysis. PLOS ONE 8: e68858. doi: 10.1371/journal.pone.0068858.

Sylvain ZA, Wall DH (2011) Linking soil biodiversity and vegetation: Implications for a changing planet. American Journal of Botany 98: 517-527. doi: 10.3732/ajb.1000305.

Thimonier A, Sedivy I, Schleppi P (2010) Estimating leaf area index in different types of mature forest stands in Switzerland: a comparison of methods. European Journal of Forest Research 129: 543-562. doi: 10.1007/s10342-009-0353-8.

Uselman SM, Snyder KA, Blank RR, Jones TJ (2011) UVB exposure does not accelerate rates of litter decomposition in a semi-arid riparian ecosystem. Soil Biology and Biochemistry 43: 1254-1265. doi: https://doi.org/10.1016/j.soilbio.2011.02.016.

Vazquez-Yanes C, Orozco-Segovia A, Rincon E, Sanchez-Coronado ME, Huante P, Toledo JR, Barradas VL (1990) Light Beneath the Litter in a Tropical Forest: Effect on Seed Germination. Ecology 71: 1952-1958. doi: 10.2307/1937603.

Verhoef HA, Verspagen JMH, Zoomer HR (2000) Direct and indirect effects of ultraviolet-B radiation on soil biota, decomposition and nutrient fluxes in dune grassland soil systems. Biology and Fertility of Soils 31: 366-371. doi: 10.1007/s003749900181.

Wall DH, Bradford MA, St. John MG, Trofymow JA, Behan-Pelletier V, Bignell DE, Dangerfield JM, Parton WJ, Rusek J, Voigt W, Wolters V, Gardel HZ, Ayuke FO, Bashford R, Beljakova OI, Bohlen PJ, Brauman A, Flemming S, Henschel JR, Johnson DL, Jones TH, Kovarova M, Kranabetter JM, Kutny LES, Lin K-C, Maryati M, Masse D, Pokarzhevskii A, Rahman H, SabarÁ MG, Salamon J-A, Swift MJ, Varela A, Vasconcelos HL, White DON, Zou X (2008) Global decomposition experiment shows soil animal impacts on decomposition are climate-dependent. Global Change Biology 14: 2661-2677. doi: doi:10.1111/j.1365-2486.2008.01672.x.

Wang J, Liu L, Wang X, Chen Y (2015) The interaction between abiotic photodegradation and microbial decomposition under ultraviolet radiation. Global Change Biology 21: 2095-2104. doi: 10.1111/gcb.12812.

Wang J, Liu L, Wang X, Yang S, Zhang B, Li P, Qiao C, Deng M, Liu W (2017) High night-time humidity and dissolved organic carbon content support rapid decomposition of standing litter in a semi-arid landscape. Functional Ecology 31: 1659-1668. doi: 10.1111/1365-2435.12854.

Way DA, Pearcy RW (2012) Sunflecks in trees and forests: from photosynthetic physiology to global change biology. Tree physiology 32: 1066-1081. doi: 10.1093/treephys/tps064.

Yanni SF, Suddick EC, Six J (2015) Photodegradation effects on CO2 emissions from litter and SOM and photo-facilitation of microbial decomposition in a California grassland. Soil Biology and Biochemistry 91: 40-49. doi: https://doi.org/10.1016/j.soilbio.2015.08.021.

Zaller JG, Caldwell MM, Flint SD, BallarÉ CL, Scopel AL, Sala OE (2009) Solar UVB and warming affect decomposition and earthworms in a fen ecosystem in Tierra del Fuego, Argentina. Global Change Biology 15: 2493-2502. doi: 10.1111/j.1365-2486.2009.01970.x.

Zellweger F, Coomes D, Lenoir J, Depauw L, Maes SL, Wulf M, Kirby KJ, Brunet J, Kopecký M, Máliš F, Schmidt W, Heinrichs S, den Ouden J, Jaroszewicz B, Buyse G, Spicher F, Verheyen K, De Frenne P (2019) Seasonal drivers of understorey temperature buffering in temperate deciduous forests across Europe. Global Ecology and Biogeography 28: 1774-1786. doi: 10.1111/geb.12991.

Zepp RG, Callaghan TV, Erickson DJ (1995) Effects of increased solar ultraviolet radiation on biogeochemical cycles. Ambio 24: 181-187.

Zepp RG, Erickson Iii DJ, Paul ND, Sulzberger B (2007) Interactive effects of solar UV radiation and climate change on biogeochemical cycling. Photochemical & Photobiological Sciences 6: 286-300. doi: 10.1039/B700021A.

Zepp RG, Erickson Iii DJ, Paul ND, Sulzberger B (2011) Effects of solar UV radiation and climate change on biogeochemical cycling: interactions and feedbacks. Photochemical & Photobiological Sciences 10: 261-279. doi: 10.1039/C0PP90037K.

CHAPTER I

Solar UV-A radiation and blue light enhance tree leaf litter decomposition in a temperate forest

Marta Pieristè, Matthieu Chauvat, Titta K. Kotilainen, Alan G. Jones, Michaël Aubert, T. Matthew Robson & Estelle Forey

Oecologia

ISSN 0029-8549
Volume 191
Number 1

Oecologia (2019) 191:191-203
DOI 10.1007/s00442-019-04478-x

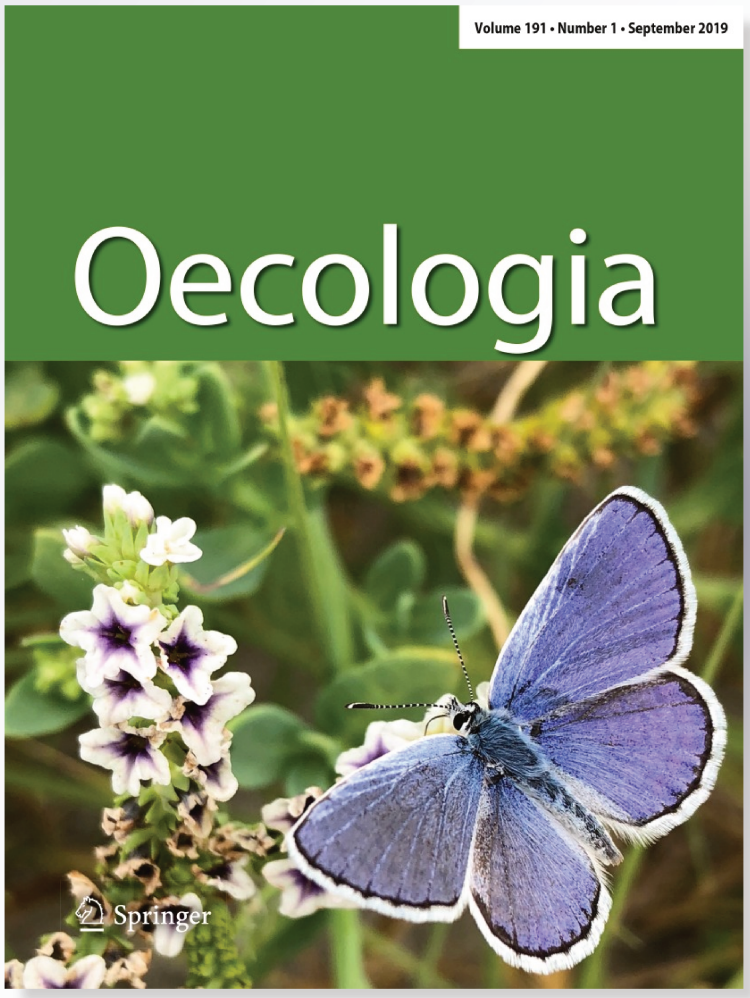

Springer

Springer

Oecologia (2019) 191:191–203
https://doi.org/10.1007/s00442-019-04478-x

ECOSYSTEM ECOLOGY – ORIGINAL RESEARCH

Solar UV-A radiation and blue light enhance tree leaf litter decomposition in a temperate forest

Marta Pieristè[1,2] · Matthieu Chauvat[2] · Titta K. Kotilainen[1,4] · Alan G. Jones[3,5] · Michaël Aubert[2] · T. Matthew Robson[1] · Estelle Forey[2]

Received: 12 June 2018 / Accepted: 23 July 2019 / Published online: 30 July 2019

Abstract

Sunlight can accelerate the decomposition process through an ensemble of direct and indirect processes known as photodegradation. Although photodegradation is widely studied in arid environments, there have been few studies in temperate regions. This experiment investigated how exposure to solar radiation, and specifically UV-B, UV-A, and blue light, affects leaf litter decomposition under a temperate forest canopy in France. For this purpose, we employed custom-made litterbags built using filters that attenuated different regions of the solar spectrum. Litter mass loss and carbon to nitrogen (C:N) ratio of three species: European ash (*Fraxinus excelsior*), European beech (*Fagus sylvatica*) and pedunculate oak (*Quercus robur*), differing in their leaf traits and decomposition rate, were analysed over a period of 7–10 months. Over the entire period, the effect of treatments attenuating blue light and solar UV radiation on leaf litter decomposition was similar to that of our dark treatment, where litter lost 20–30% less mass and had a lower C:N ratio than under the full-spectrum treatment. Moreover, decomposition was affected more by the filter treatment than mesh size, which controlled access by mesofauna. The effect of filter treatment differed among the three species and appeared to depend on litter quality (and especially C:N), producing the greatest effect in recalcitrant litter (*F. sylvatica*). Even under the reduced irradiance found in the understorey of a temperate forest, UV radiation and blue light remain important in accelerating surface litter decomposition.

Keywords Photodegradation · C:N · Sunlight · Litter bags · Mass loss

Introduction

Photodegradation involves direct (photochemical mineralization) and indirect (photofacilitation) breakdown of organic matter mediated by sunlight which, alongside warm temperatures and high humidity, can accelerate the decomposition of plant litter (Brandt et al. 2007; Gallo et al. 2006, 2009; Almagro et al. 2015; Ma et al. 2017). Factors that enhance the exposure of plant litter to sunlight, such as changes to forest structure or phenology, modulate photodegradation and are an important environmental variable controlling decomposition rate in Mediterranean forests (Bravo-Oviedo et al. 2017; Gliksman et al. 2017). Decomposition rate partly governs nutrient cycling (Austin and Vivanco 2006) and successional processes in the plant and belowground communities (Fahey et al. 1998; Bardgett et al. 2005). Therefore, the interactions between the abiotic (sunlight, soil moisture, precipitation and temperature) and biotic drivers of decomposition have the potential to impact soil decomposer assemblages and plant functional composition in the understorey

Communicated by Heather Throop.

Electronic supplementary material The online version of this article (https://doi.org/10.1007/s00442-019-04478-x) contains supplementary material, which is available to authorized users.

✉ Marta Pieristè
marta.pieriste@helsinki.fi

[1] Organismal and Evolutionary Biology (OEB), Viikki Plant Science Centre (ViPS), University of Helsinki, P.O. Box 65, Viikinkaari1, 00014 Helsinki, Finland

[2] Normandie Université, UNIROUEN, IRSTEA, ECODIV, FR Scale CNRS 3730, Rouen, France

[3] Earthwatch Institute, Mayfield House, 256 Banbury Road, Oxford OX2 7DE, UK

[4] Present Address: Natural Resources Institute Finland, Itäinen Pitkäkatu 4a, 20520 Turku, FI, Finland

[5] Present Address: Forest Systems, Scion. 49 Sala Street, Private Bag 3020, Rotorua 3046, New Zealand

(Almagro et al. 2015). These interactions make it important to quantify the relative importance of photodegradation and contribution of different spectral regions to this process.

Short wavelengths of solar radiation carry high energy and can directly break down organic matter through photochemical mineralization (Gallo et al. 2006; Austin and Ballaré 2010). Until recently, most studies have considered only UV, or specifically UV-B (280–315 nm), radiation to be the main driver of photodegradation (reviewed by Song et al. 2013). However, recent studies have revealed that UV-A radiation (315–400 nm), blue (420–490 nm) and green (500–570 nm) regions of the spectrum (Sellaro et al. 2010) are also important in this process (Brandt et al. 2009; Austin and Ballaré 2010; Austin et al. 2016). The capacity of lignin, cellulose and hemicellulose to absorb UV radiation and blue and green light (Argyropoulos 2001; Austin and Ballaré 2010; Lin and King 2015) further suggests that these wavelengths are potentially involved in the photodegradation of litter. Solar radiation also affects decomposition rate through direct effects on both the activity (Duguay and Klironomos 2000) and community composition of decomposer organisms (Pancotto et al. 2003; Robson et al. 2005). Because these multiple environmental factors interact to produce complex effects, the relative contribution of photodegradation to decomposition is difficult to quantify.

Photodegradation has mainly been studied in habitats with a low-stature vegetation, such as grasslands or scrublands, where litter is exposed to near full sunlight all year round. In these environments, especially in arid and semiarid climates, photodegradation is particularly relevant (Gallo et al. 2009) and represents a key driver of the process of litter decomposition (Austin et al. 2016, but see King et al. 2012 and Song et al. 2013). Few studies have been undertaken in temperate environments and particularly in forest ecosystems (Messenger et al. 2012; Newsham et al. 2001), where decomposition is expected to be controlled by precipitation and temperature (Adair et al. 2008; Aerts 1997; Meentemeyer 1978). However, photodegradation can play a role in peat lands (Rutledge et al. 2010; Foereid et al. 2018), aquatic systems (Måns et al. 1998) and Arctic tundra (Cory et al. 2013) by interacting with microbial activity to produce a change in decomposition rate. This suggests that the ecological relevance of sunlight is not limited to dry environments receiving high irradiances of UV radiation but extends to Arctic and alpine environments (Foereid et al. 2011). There is a need to examine the extent to which photodegradation, and its interaction with decomposer organisms, contributes to decomposition in these environments to improve our estimation of how carbon cycling might be affected by climate change (Smith et al. 2012), which will expose litter to novel combinations of temperature, precipitation, day length and solar spectral irradiance. We aimed to test how the spectral composition of received solar radiation affects the decomposition of newly fallen leaf litter from three different tree species (*Fagus sylvatica* L., *Quercus robur* L., and *Fraxinus excelsior* L.), on the floor of a temperate forest. We performed a litterbag experiment with five different sunlight attenuation filter treatments and two mesh treatments. We anticipated that the effect of photodegradation increases when the initial carbon to nitrogen (C:N) ratio is high (King et al. 2012) and expected that differences in initial litter quality according to species identity would lead to differing response in our sunlight attenuation treatments. Hence, we assessed litter decomposition of the three species over different time periods. We expected that UV radiation and blue light would enhance decomposition due to their capacity to break down organic material through photochemical mineralization (Gallo et al. 2009) and provide more nutrients for microbial activity as a result (photofacilitation, Austin et al. 2016). Consequently, we expected exposure to near-ambient UV radiation and blue light to lower the litter carbon content (Kotilainen et al. 2009; Almagro et al. 2017) and, therefore, the C:N ratio. The complexity of soil–decomposer assemblages is known to be important in the decomposition process (Hättenschwiler et al. 2005). Consequently, we expected that the exclusion of large decomposers (macrofauna and part of the mesofauna) from fine-mesh litterbags would interact with our filter treatments and produce different responses to the spectral regions of sunlight.

Materials and methods

Site description

The experiment was conducted in a mature beech forest (*Fagus sylvatica* L.) in Forêt Verte (49°31′12.6″N 1°07′00.7″E) close to Rouen University, France. The site has a relatively flat topography and the elevation is about 150 m a.s.l. The climate is "oceanic-temperate" with a mean annual air temperature of 10.5 °C and the total annual precipitation average of 851.7 mm, which is distributed relatively evenly over the year (ESM Fig. S1, climate data at the weather station "Rouen-Boos from 1981 to 2010", data from website Infoclimat: http://www.infoclimat.fr).

Spectral irradiance was measured before (February 2017) and after (May 2017) canopy closure at five locations within the study site and compared with an open area nearby. Spectral irradiance was also measured inside the litterbags for each filter treatment to test filter transmittance (Fig. 1). Measurements were taken using an array spectroradiometer (Maya2000 Pro Ocean Optics, Dunedin, FL, USA; D7-H-SMA cosine diffuser, Bentham Instruments Ltd, Reading, UK) that had been calibrated within the previous 12 months for measurements spanning the regions of solar UV radiation and photosynthetically active radiation

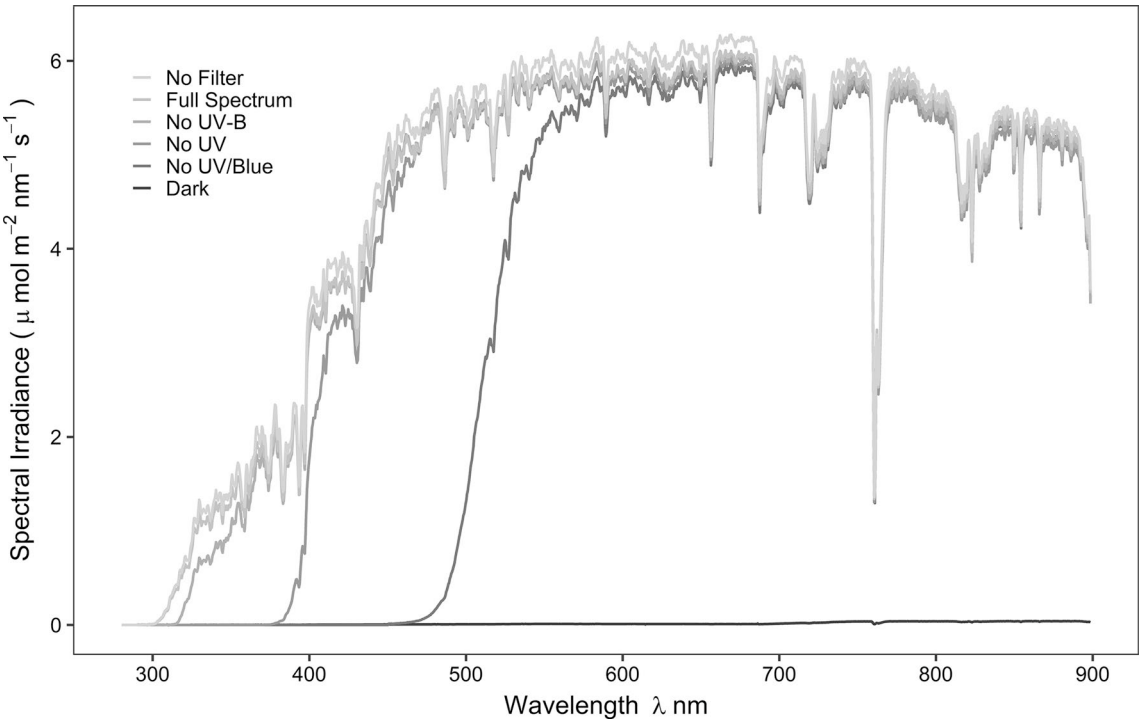

Fig. 1 Measured spectral irradiance under the five filter treatments used in the experiment compared with ambient sunlight (no filter). Spectra were recorded with spectrometer at solar noon in Helsinki in July in an open area to measure the litterbags transmittance. Figure was produced using the photobiology packages in *R* (Aphalo 2015)

(PAR) (see Hartikainen et al. 2018 for details of the calibration, Aphalo et al. 2012, 2016). Hemispherical photos were taken on multiple occasions at the same five locations as the spectral irradiance measurements. To capture the different stages of canopy development, pictures were taken on 8th February 2017 when the canopy was dormant, during canopy flushing (once a week between 25th April 2017 and 30th May 2017) and after canopy closure (10th June 2017). These photos were used to characterize canopy cover by calculation of the global light index (GLI) and the leaf area index (LAI) with the software "Hemisfer" (Schleppi et al. 2007; Thimonier et al. 2010). The LAI was estimated to be 0.895 ± 0.012 during winter (Dec 2016–Apr 2017) corresponding to a GLI of 50.5%. On 24th May 2017, when canopy leaves were completely expanded, the LAI reached 2.930 ± 0.131 while the GLI dropped to 3.8%. A time series of modelled daily PAR (Fig. 2 and ESM Fig. S3) over the whole experimental period was reconstructed with a library of radiative transfer programs, libRadtran, version 2.0.1. (Emde et al. 2016). We used the radiative transfer equation solver DISORT for the simulations to produce spectra of 280–900 nm (based on Lindfors et al. 2009). Inputs to the model were column integrated water vapour data from AERONET (https://aeronet.gsfc.nasa.gov/cgi-bin/webtool_aod_v3?stage=2&place_code=10&region=Europe&state=France&submit=Get+AERONET+Sites), total ozone column data from the Aura Validation Data Center (AVDC) (https://avdc.gsfc.nasa.gov/pub/data/satellite/Aura/OMI/V03/L2OVP/OMUVB/) and surface type as defined by the International Geosphere Biosphere Programme (IGBP). Modelled above-canopy data were cross-validated against satellite-derived irradiance data provided by SoDa Helioclim-3 and against the spectral irradiance measured with the above-mentioned spectroradiometer. Modelled understorey data (Fig. 2 and ESM Table S12) were calculated by applying the GLI to the above-canopy modelled data (Canham 1988) and were cross-validated against a subset of daily PAR irradiance measured in the understorey on the forest floor, recorded continuously from 25th May to 10th Oct 2017 as 15-min averages with two calibrated quantum sensors (QSO-S, Decagon Devices, Pullman, Washington, USA) (ESM Fig S2). Estimates of received UV-A and UV-B radiation are given (Fig. 2, ESM Table S12) according to the spectral composition of modelled incident solar radiation without adjusting for the relative enrichment of UV radiation in shade which makes a minor contribution to the daily sum.

Experimental design and litterbag design

We assigned litterbags to randomized locations within the study site (ESM Fig. S4). The experiment comprised 3 species of leaf litter × 5 filter treatments × 2 mesh sizes × 3

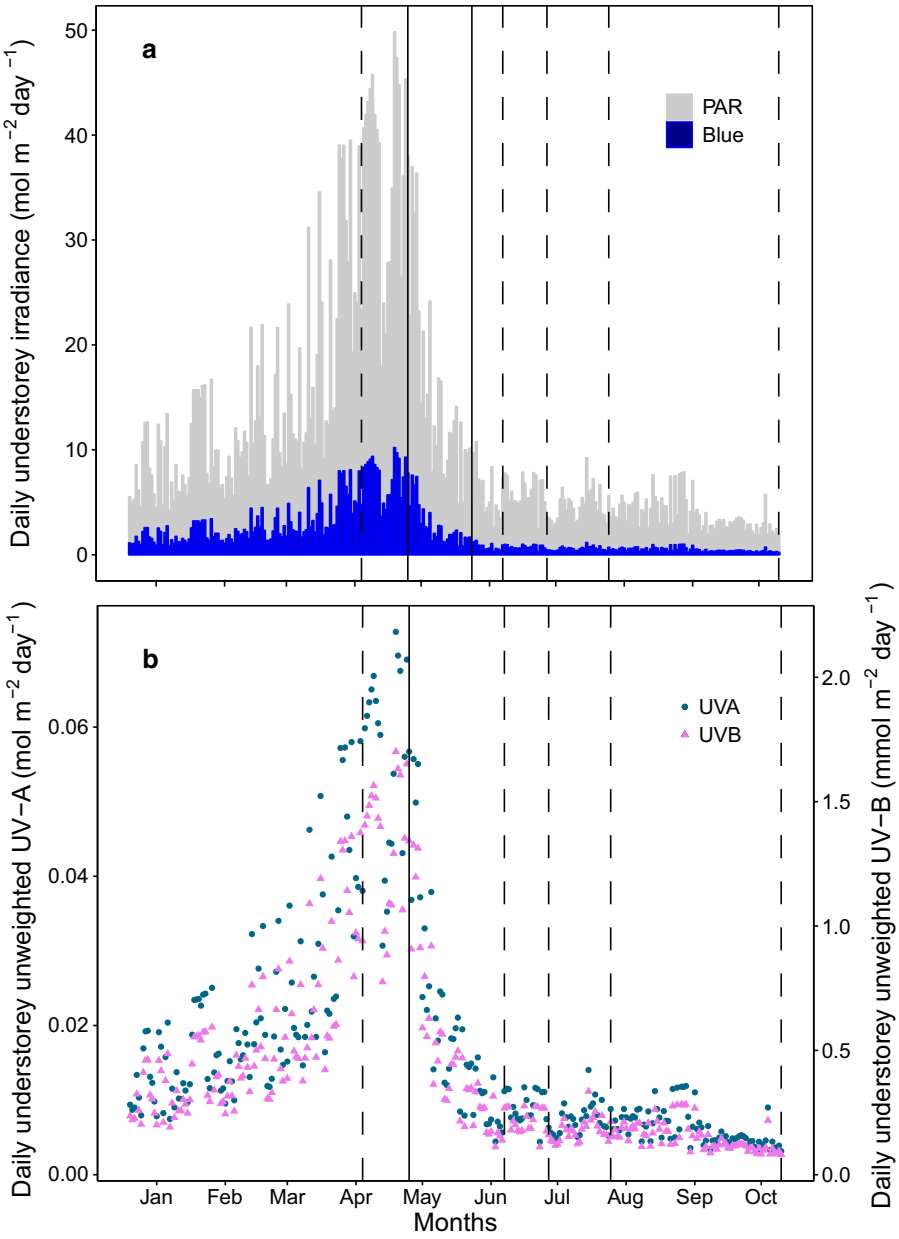

Fig. 2 **a** Daily photosynthetically active radiation and blue light in the understorey. Time series of modelled PAR reconstructed using radiative transfer modelling of solar irradiance and the global light index (GLI) calculated from hemispherical photos taken at the site over the course of the experiment. Modelled data were cross-validated against a subset of daily measured PAR irradiance at the site from 25-05-2017 to 10-10-2017 (ESM Fig. S2). Vertical dashed lines show dates of litterbag collection, and solid line show the period of spring flush from bud burst to canopy closure from a visual assessment of the buds of canopy trees. **b** Daily estimated unweighted UV-A (filled circle) and UV-B (filled triangle) radiation in the understorey. Time series of solar irradiance were reconstructed using radiative transfer modelling, validated with above-canopy irradiance data provided by SoDa Helioclim-3, and gap light index calculated from hemispherical photos taken at the site over the course of the experiment. Vertical dashed line shows dates of litterbag collection, and solid lines show the period from bud burst to canopy closure from assessment of tree flush. (This figure is available in color in the online version of the journal)

collection times × 5 replicates, giving a total number of 450 litterbags. The design of the litterbags for the experiment followed that described by Day et al. (2007). The dimensions of the litterbags were 150 × 150 mm, with the upper part made from a sheet of perforated film filter material and the bottom part made from a sterile Teflon mesh sheet of two different pore sizes: 0.1 mm allowing only microflora (fungi and bacteria) access to the litter, and 1 mm allowing microflora and part of the mesofauna (hereafter referred as mesofauna) to pass (ESM Figs. S5 and S6). The filter and the mesh sheet were not directly in contact but were held 8 mm apart by a frame made from plastic drinking straws (Ikea, Leiden, Netherlands), which helped to prevent contact between the leaves and the filter during decomposition. This separation was also important to prevent the build-up of condensation on the filter. Five different filter treatments were created (Fig. 1): a control treatment (full spectrum at near-ambient irradiance) of polyethene film (0.05 mm thick, 04 PE-LD; Etola, Jyväskylä, Finland) transmitting > 95% of incident PAR and UV radiation; no-UV-B treatment (attenuating UV-B radiation < 320 nm) using polyester (0.125 mm thick, Autostat CT5; Thermoplast, Helsinki, Finland); no-UV treatment using Rosco #226 (0.2 mm thick, West Lighting, Helsinki, Finland) attenuating UV radiation < 380 nm; no-UV/blue treatment using Rosco #312 Canary yellow (0.2 mm thick, West Lighting, Helsinki, Finland) attenuating UV radiation and blue light < 480 nm; and a dark treatment using polyethene film, solid white on the upper side

and solid black on the lower side (0.15 mm thick, Casado Sarl, France), attenuating > 95% of PAR and UV radiation.

Litterbags were deployed on 20 Dec 2016, to coincide with the end of leaf fall and follow the natural timing of decomposition as faithfully as possible. They were pinned to the soil surface through a homogeneous thin layer of the previous years' litter that remained in contact with the underside of the litterbags. Once a week, any debris that fell on the litterbags were removed, to ensure that they remained uncovered by other litter and unshaded by understorey plants. Air temperature and relative humidity (RH) inside a representative subsample of litterbags were continuously monitored with sensor ECH2O 5TM (Decagon Devices, Pullman, Washington, USA). The environment under the dark treatment was on average 0.4 °C (± 0.2) cooler (however, not statistically significant, ESM Table S14) and 1% (± 0.5) RH moister than the other treatments, while small-mesh-size (0.1 mm) bags were 0.8% (± 0.3) more moist than 1-mm mesh bags (ESM Tables S13 and S14).

Litter material

Leaf litter was used from three widespread European tree species growing within the experimental area, selected according to their different litter quality: pedunculate oak (*Quercus robur* L.); European beech (*Fagus sylvatica* L.) and European ash (*Fraxinus excelsior* L.). The latter is known to produce labile litter with low lignin:N ratio of 13.6, able to decompose completely in 6–7 months (Melillo et al. 1982), oak litter represents intermediate-quality litter with a lignin:N ratio of 17.6 (Henneron et al. 2017) and beech produces more recalcitrant litter which decomposes over longer periods (up to 3 years) due to its higher lignin content (lignin:N ratio of 36.5: Trap et al. 2013). Fully senescent "sun" leaves at the point of abscission were sampled directly from trees on the southern edge of the stands. The point of abscission was determined as the moment when the leaf would detach without any effort in pulling it away from the branch. Leaves were collected from oak and ash trees in small stands near the University in Rouen (49°27′44.2″N 1°03′48.2″E), while the equivalent beech leaves were collected in the Forêt Verte (49°30′17.0″N 1°06′44.9″E) close to the study site. The petiole was removed from the leaves before they were weighed and scanned to obtain fresh weight (FW) and leaf area was calculated with the software WinFOLIA (Image analysis for plant science, Regent Instruments Inc., Nepean, Canada). Immediately after sampling, both leaf adaxial (upper) and abaxial (lower) epidermal flavonoid content and leaf chlorophyll content were optically assessed using a Dualex Scientific + (ForceA, Paris Orsay, France) device. This allowed us to verify that there were no initial differences in pigmentation or epidermal UV transmission among the leaves of each species (ESM Table S1). The leaves were then dried at 35 °C for 1 week and reweighed (dry weight: DW) before being placed in the litterbags (ESM Table S1). Entire leaves were placed inside litterbags with the adaxial leaf epidermis facing up in a single layer of non-overlapping litter (consisting of 2–5 leaves per litterbag, weighing 300–800 mg according to the species: EMS Fig. S5).

Litter mass loss, and carbon and nitrogen content

Five replicate litterbags from each treatment combination were collected after 3, 5 and 7 months for ash litter, and 3, 6 and 10 months for oak and beech litter, as well as a zero-time sample from all species. After collection, litter was dried at 35 °C, cleaned with small brushes to eliminate any soil particles and worm casts present, and weighed on a precision balance (Entris 224i-1S, Sartorius Lab Instruments GmbH & Co. KG, Göttingen, Germany). The litter was then ground to a fine powder, and a quantity of 3–4 mg DW was used to determine the percentage of C and N content using a CN Soil Analyzer Flash 2000 (Thermo Scientific, Waltham, USA). Ash-free dry mass (AFDM) was determined by combustion of subsample of each replicate in a muffle oven at 550 °C for 12 h to allow quantification of mineral contamination, e.g. from worm casts and soil.

Data analysis

Treatment effects for mass loss, C:N ratio, C and N content were tested for each species separately, due to their differing collection dates, using a three-way ANOVA including fixed experimental factors: filter, mesh size and time and respective interactions between them. The normal distribution of the residuals and homoscedasticity of variance were checked when performing the statistical analyses. Where a significant ($p < 0.05$) interaction was given by the ANOVA, the pairwise comparisons were tested (Function glht in Package Multicomp). Holm's adjustment was used to account for multiple pairwise comparisons. All statistical analyses were performed in R version 3.3.3 (2017).

Results

Litter mass

The three species had different decomposition patterns confirming our initial hypothesis (Fig. 3). During its first 3 months, ash litter lost the largest proportion of its dry mass (60%) and by the time of its final collection (7 months) it had lost almost 70% of its initial dry mass. Oak litter decomposed much slower; only 50% mass was lost after 10 months, beech litter actually increased in mass during

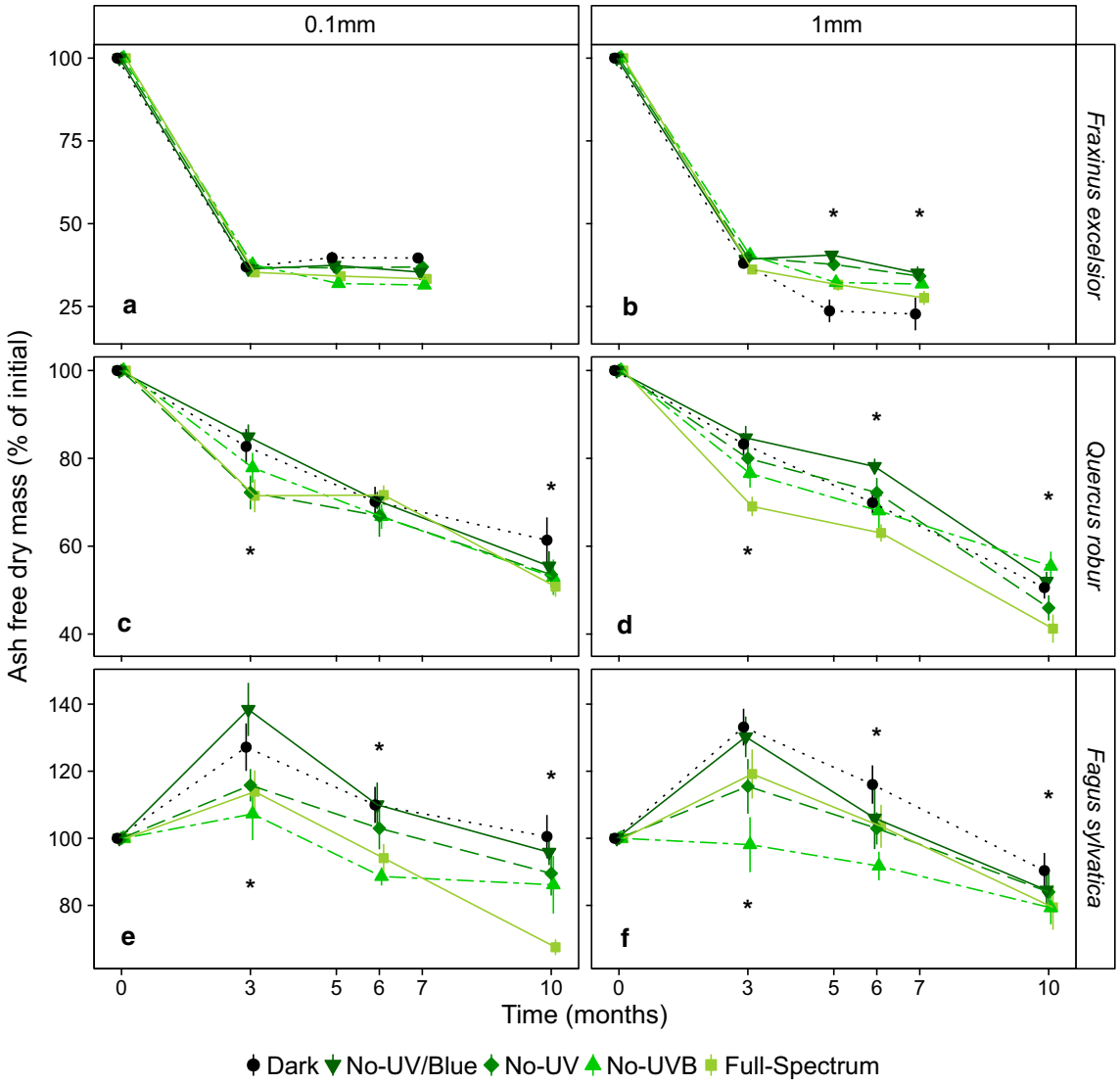

Fig. 3 Remaining ash-free dry mass as a percentage of initial weight for each species litter: *F. excelsior* (**a**), (**b**); *Q. robur* (**c**),(**d**) and *F. Sylvatica* (**e**), (**f**), mesh size (0.1 mm and 1 mm) and filter treatment, over the 10 months of the experiment. Mean ± SE are shown ($n = 5$). *Dates with significant differences between the filter treatments. Pairwise comparisons were performed with the function glht in package Multicomp applying Holm's adjustment. (This figure is available in color in the online version of the journal.)

the first 3 months; this was particularly evident in the dark (+ 25%) and in the no-UV/blue (+ 40%) treatments (Fig. 3). This initial increase was followed by a decrease during the next 7 months, resulting in a 10–20% decrease from its original mass after 10 months (Fig. 3).

The effect of filter treatments on remaining mass of ash litter changed over time and according to the mesh size (Mesh × Filter × Time interaction: $p = 0.032$, Table 1, Figs. 3 and 4), suggesting a different effect of spectral composition on different groups of decomposers (micro- and part of the mesofauna). In both mesh sizes, there was no effect of filter treatment on remaining mass in the first 3 months (Figs. 3 and 4, ESM Table S2) suggesting photodegradation did not significantly contribute to the early phase of decomposition. After longer periods of decomposition, the effect of filter treatments differed only among the litter in 1 mm mesh-size litterbags. Significantly less mass remained under the dark filters (6%–10% less) than under the other filter treatments (ESM Table S3 and Fig. 4).

The effect of filter treatment on remaining mass of oak and beech litter depended on neither "time" nor "mesh size" (Mesh × Filter × Time interaction: $p = 0.439$ for oak litter and $p = 0.960$ for beech litter, Table 1, Fig. 3). For both oak and beech, more mass remained in the dark and no-UV/blue treatments than the full-spectrum treatment (ESM Table S4, Figs. 3 and 4), suggesting that the presence of blue light accelerated mass loss in litter of these two species. Beech litter actually gained mass during the first

Table 1 ANOVA results for three fixed factors (Mesh: mesh size with two levels, Filter with five levels and Time with three levels) and their interactions on a single dependent variable: ash-free dry mass remaining for the three species' litter

Factors	*d.f.*	SS	MS	*F*	*p*
Ash (*Fraxinus excelsior* L.)					
Mesh	**1**	**140**	**140.0**	**8.242**	**0.005**
Filter	**4**	**492**	**122.9**	**7.235**	**< 0.001**
Time	**2**	**612**	**306.0**	**18.019**	**< 0.001**
Mesh × filter	**4**	**795**	**198.7**	**11.701**	**< 0.001**
Mesh × time	**2**	**340**	**170.0**	**10.007**	**< 0.001**
Filter × time	8	237	29.6	1.743	0.095
Mesh × filter × time	**8**	**299**	**37.3**	**2.198**	**0.032**
Residuals	120	2038	17.0		
Oak (*Quercus robur* L.)					
Mesh	1	61	60.7	1.158	0.284
Filter	**4**	**1786**	**446.5**	**8.517**	**< 0.001**
Time	**2**	**18,055**	**9027.5**	**172.210**	**< 0.001**
Mesh × filter	4	430	107.6	2.053	0.091
Mesh × time	**2**	**381**	**190.4**	**3.632**	**0.029**
Filter × time	8	524	65.6	1.251	0.276
Mesh × filter × time	8	419	52.4	1.001	0.439
Residuals	120	6291	52.4		
Beech (*Fagus sylvatica* L.)					
Mesh	1	31	31.4	0.163	0.687
Filter	**4**	**9881**	**2470.2**	**12.819**	**< 0.001**
Time	**2**	**29,176**	**14,588.1**	**75.705**	**< 0.001**
Mesh × filter	4	1190	297.5	1.544	0.1939
Mesh × time	2	337	168.6	0.875	0.4195
Filter × time	8	2323	290.4	1.507	0.162
Mesh × filter × time	8	484	60.4	0.314	0.960
Residuals	120	23,124	192.7		

Degrees of freedom (*d.f.*), sum of squares (SS), mean square (MS), F statistic (F) and *p* value (*p*) are presented. Significant terms are shown in bold. Non-significant terms were retained since dropping them did not significantly affect the model

phase of decomposition, and 9.9% more litter remained in the no-UV treatment than the no-UV-B treatment ($p = 0.031$, ESM Table S4 and Fig. 4), i.e. the presence of UV-A radiation contributed to mass loss. There was no significant difference in mass loss from litter between the no-UV-B and full-spectrum treatments among any of the species (ESM Tables S3 and S4 and Figs. 3 and 4).

Litter carbon and nitrogen content

The C content of the litter decreased over the decomposition period following a similar pattern to dry mass, while the N content increased in the early phases of decomposition (ESM Figs. S7 and S8); these relative changes in C and N resulted in a decrease in the C:N ratio over time (ESM Fig. S9). The effect of filter treatments on both C and N content in ash litter changed over time and according to the mesh size (Mesh × Filter × Time interaction: $p = 0.014$ and $p = 0.048$, respectively, Table 2, Fig. 4), suggesting again an effect of spectral composition on the interaction between different groups of decomposers. In both mesh sizes, there was no effect of light treatments on C and N content in the first 3 months (Fig. 4, ESM Tables S5 and S6). Following decomposition over longer time periods, the effect of filter treatments differed only for litter in litterbags with the 1 mm mesh size, with a significantly lower C content in the dark filters (−6% to −9% depending on the treatment) than the other filter treatments (ESM Table S7, Fig. 4). Considering N content, there was a significant effect of filter treatments only for litterbags with mesh size 0.1 mm. In these litterbags, the dark treatment produced litter with a higher N content (+19 to 27% depending on the treatment) than all other filter treatments (ESM Table S8, Fig. 4).

For both oak and beech litter, there was no significant change in the effect of filter treatments on C and N content over time (Table 2, Fig. 4). For both species litter, there was no significant difference in C and N content between the dark and no-UV/blue treatments (Fig. 4, ESM Tables S9 and S10). These two treatments had the highest C content (Fig. 4, ESM Table S9), suggesting blue light stimulated C loss through photodegradation. Likewise, both oak and beech litter had the highest N contents in the dark and no-UV/blue treatments (Fig. 4, ESM Table S10), a sign of greater fungal colonization. For beech litter, the no-UV treatment had higher C content than the no-UV-B treatment (+9.9%, $p = 0.031$, Fig. 4 and ESM Table S9) implying that UV-A radiation was involved in promoting C loss. No significant difference in C content between the no-UV-B and full-spectrum treatments was found in any of the species' litter (Fig. 4, ESM Tables S7, S8, S9, S10), suggesting that UV-B radiation was not involved in the process of C loss in our experiment.

Discussion

The main findings of our experiment confirmed our expectations that litter decomposition would be significantly affected by solar radiation and its spectral attenuation in a temperate woodland, but that these responses would follow a different pattern according to initial litter quality and species identity. Oak and beech litter lost the greatest mass when exposed to the full-spectrum treatment, compared with treatments excluding UV radiation and both UV radiation and blue light, but this effect was not detected in ash litter. By the end of the experiment, litter exposed to the full-spectrum treatment lost between 20% (oak) and 30% (beech) more mass than litter in the dark treatment, and around 20%

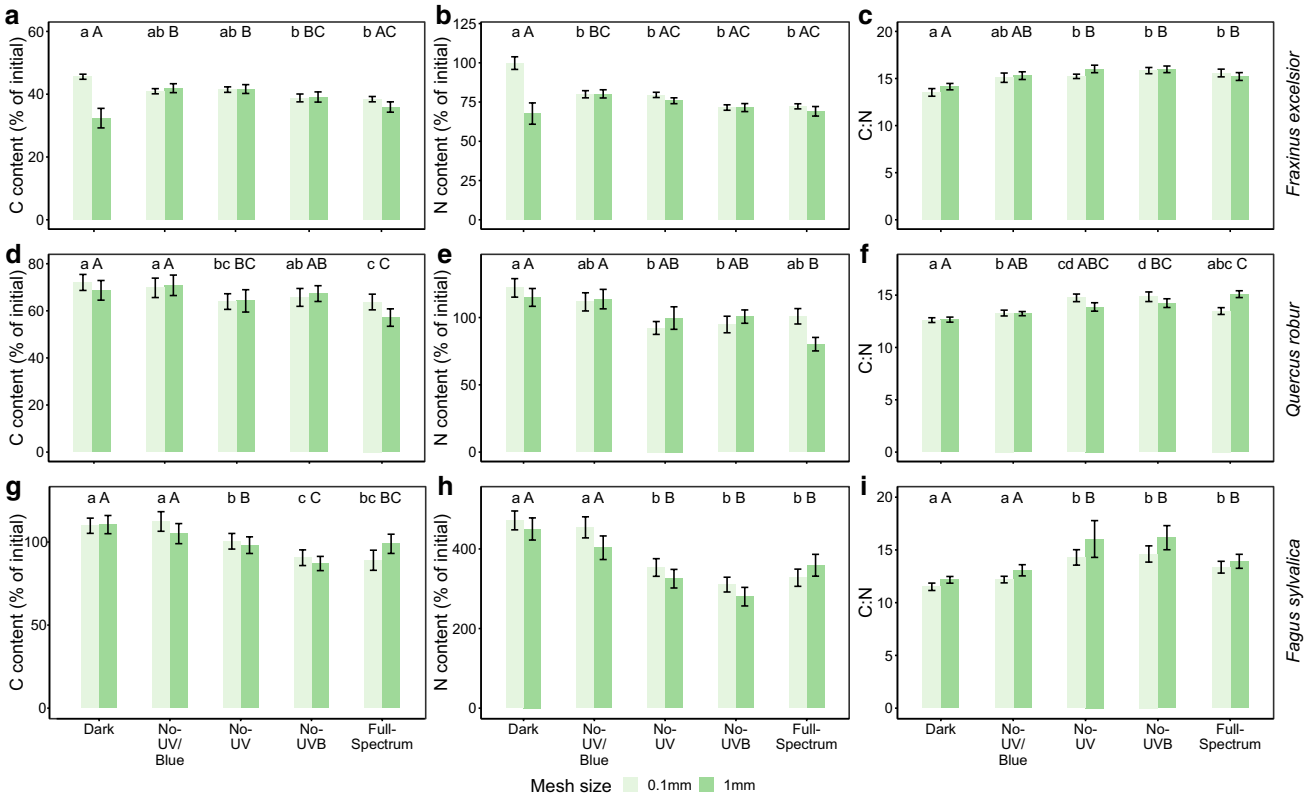

Fig. 4 C content, N content and C:N ratio for each species litter: *F. excelsior* (**a**–**c**); *Q. robur* (**d**–**f**) and *F. Sylvatica* (**g**–**i**), mesh size (0.1 mm and 1 mm) and filter treatment. Means ± SE are shown ($n = 15$). Capital letters show significant differences between light treatments for mesh size = 1 mm. Lower case letters show significant differences between light treatments for mesh size = 0.1 mm. Pairwise comparisons were performed with the function glht in package Multicomp applying Holm's adjustment. (This figure is available in color in the online version of the journal)

(both oak and beech) more mass than when both UV radiation and blue light were attenuated. These results develop further similar findings from past studies (Newsham et al. 2001; Messenger et al. 2012; King et al. 2012), showing that PAR/visible light interacts with UV-A and UV-B radiation to affect decomposition rates in temperate forests.

We are not able to infer the mechanism of response to blue light and UV-A radiation from our study. However, other experiments have found that lignin is able to absorb light in the blue and green range of the solar spectrum (Hon and Shiraishi 2001; Austin and Ballaré 2010), which may contribute to photochemical mineralization of lignin in the cell walls. For instance, Austin et al. (2016) found blue and green light to enhance litter decomposition via accelerated lignin breakdown in 23 temperate plant species. The increased bioavailability of cell-wall compounds through direct photodegradation may also prime this material for easier microbial colonization and breakdown by extracellular enzymes (Gallo et al. 2006; Baker and Allison 2015) via a so-called photofacilitation effect (Austin et al. 2016). In our experiment, exposure to blue light and UV-A radiation increased mass loss, while UV-B did not have any effect. Since microbial decomposition can be slowed by UV-B radiation (Lin et al. 2015, 2018; Wang et al. 2015), a trade-off may occur between the potential of UV-B radiation to break down organic matter and its capacity to decrease microbial activity and colonization (Verhoef et al. 2000). The importance of UV-B radiation in a forest understorey is also lessened because only approximately 2% of full sunlight is received during the period of canopy closure (Fig. 2).

The C:N ratio of litter from all three species decreased during the experiment, as a result of an overall increase in N content and a decrease in C content, which is consistent with other decomposition studies (Anderson 1973; Xuluc-Tolosa et al. 2003). This increase in N over time with declining mass has been observed in mesic environments, but it is not typical of arid environments where photodegradation plays a greater role (Parton et al. 2007). The litter C content in all those treatments receiving some portion of sunlight was lower than that of the dark treatment, which had the highest C content of all three species' litter at the end of the experiment. These results corroborate an effect of solar radiation on C mobilization in a moist temperate forest which is in line with previous studies in arid, semiarid and subtropical

Table 2 ANOVA results of three fixed factors (Mesh: mesh size with two levels, Filter with five levels and Time with three levels) and their interactions on two single dependent variables: litter C content and litter N content for the three species' litter

Species litter	Factors	Carbon content					Nitrogen content				
		df	SS	MS	*F*	*p*	*df*	SS	MS	*F*	*p*
Ash (*Fraxinus excelsior* L.)	**Mesh**	**1**	**304**	**304.2**	**15.999**	**< 0.001**	**1**	**2261.8**	**2261.8**	**18.746**	**< 0.001**
	Filter	**4**	**416**	**104.1**	**5.475**	**< 0.001**	**4**	**3755.0**	**938.5**	**7.780**	**< 0.001**
	Time	**2**	**1670**	**835.5**	**43.946**	**< 0.001**	**2**	**1036.2**	**518.1**	**4.294**	**0.016**
	Mesh × filter	**4**	**1054**	**263.7**	**13.871**	**< 0.001**	**4**	**5671.4**	**1417.9**	**11.751**	**< 0.001**
	Mesh x Time	**2**	**378**	**189.4**	**9.965**	**< 0.001**	**2**	**1962.0**	**980.9**	**8.130**	**< 0.001**
	Filter x Time	8	209	26.2	1.378	0.214	**8**	**2045.6**	**255.7**	**2.119**	**0.039**
	Mesh x filter x time	**8**	**384**	**48.1**	**2.528**	**0.014**	**8**	**1963.7**	**245.5**	**2.034**	**0.048**
	Residuals	120	2281	19.0			120	14,479.0	120.7		
Oak (*Quercus robur* L.)	Mesh	1	73	73.2	1.268	0.262	1	235	234.9	0.713	0.400
	Filter	**4**	**2159**	**539.8**	**9.355**	**< 0.001**	**4**	**16,969**	**4242.2**	**12.873**	**< 0.001**
	Time	**2**	**22,860**	**11,430.5**	**198.093**	**< 0.001**	**2**	**36,479**	**18,239.4**	**55.349**	**< 0.001**
	Mesh x filter	4	368	92.0	1.594	0.180	**4**	**4061**	**1015.3**	**3.081**	**0.019**
	Mesh x time	**2**	**434**	**217.3**	**3.767**	**0.026**	2	1557	778.7	2.363	0.099
	Filter x time	8	570	71.3	1.236	0.284	8	4365	545.6	1.656	0.116
	Mesh x filter x time	8	510	63.8	1.105	0.365	8	2690	336.3	1.021	0.424
	Residuals	120	694	57.7			120	39,544	329.5		
Beech (*Fagus sylvatica* L.)	Mesh	1	10	9.8	0.057	0.812	1	14,950	14,950	1.756	0.188
	Filter	**4**	**10,223**	**2555.7**	**14.809**	**< 0.001**	**4**	**566,543**	**141,636**	**16.635**	**< 0.001**
	Time	**2**	**35,906**	**17,953.0**	**104.032**	**< 0.001**	**2**	**93,088**	**46,544**	**5.467**	**0.005**
	Mesh x filter	4	1261	315.3	1.827	0.128	4	28,399	7100	0.834	0.506
	Mesh x time	2	171	85.5	0.496	0.611	2	10,348	5174	0.608	0.546
	Filter x time	8	1580	197.5	1.144	0.339	8	115,474	14,434	1.695	0.106
	Mesh x filter x time	8	565	70.6	0.409	0.9134	8	33,268	4158	0.488	0.862
	Residuals	120	20,709	172.6			120	1,021,697	8514		

Degrees of freedom (d.f.), sum of squares (SS), mean square (MS), F statistic (F) and *p* value (*p*) are presented. Significant terms are shown in bold. Non-significant terms were retained since dropping them did not significantly affect the model

biomes (Ma et al. 2017; Pan et al. 2015; Wang et al. 2017). Litter exposed to the full-spectrum treatment had a lower C content than litter receiving no-UV/blue light, in agreement with our hypothesis. This result suggests that blue light is involved in the breakdown of organic matter, as previously shown in a temperate grassland (Austin et al. 2016). Our results, together with previous studies, suggest that the PAR region of the spectrum is more important for photodegradation than the UV region in a temperate deciduous forest such as ours. This is not surprising given the far greater contribution of blue light than UV radiation to the received irradiance during dormancy in winter and before canopy closure in spring (Fig. 2, ESM Fig. S3, Grant et al. 2015; Hartikainen et al. 2018).

The filter treatments in our study had a smaller effect on ash litter than oak and beech litter. This reflects the importance of litter quality, and especially high initial C:N ratio, in determining the contribution of photodegradation to decomposition (reviewed by King et al. 2012), suggesting that microbial limitation due to low N content is likely to benefit most from photofacilitation. Similar trends occur in arid and semiarid environments (Gaxiola and Armesto 2015; Day et al. 2015) but are likely to be most relevant in moist environments where microbial decomposition dominates and the pool of fungal decomposers is far larger (Hodge et al. 2000). Furthermore, limiting the faunal groups able to colonize the litterbags (using a fine mesh) reduced the effect of light treatments on mass loss but increased this effect when considering litter N content. Soil fauna and microorganisms interact strongly during the decomposition process (Osler and Sommerkorn 2007); therefore, the interaction effect of our filter treatments with mesh size has implications for the relationships among these decomposers. This interaction, which is particularly evident in ash litter, suggests that functional groups of decomposers could have been differentially affected by spectral attenuation altering overall decomposition rates. However, further controlled experiments would be required to provide a mechanistic explanation for the patterns that we report here since our experiment did not consider the effect of macrofauna.

Beech litter gained mass during the first 3 months of decomposition; a similar increase in mass has been reported in studies addressing the first months of beech litter decomposition (Zeller et al. 2000; Idol et al. 2002; Brandstätter et al. 2013). Fungal colonization during the early phases of decomposition may account for this, as this is known to be particularly intense in beech litter compared to other species (Asplund et al. 2018) and fungal biomass can account for 23% of total detrital mass (Baldrian et al. 2013; Gulis et al. 2009; Gessner and Chauvet 2011). The strong correlation between change in mass and N content in beech litter over the first 3 months ($r^2 = 0.8–0.9$ according to light treatment, ESM Fig. S10) suggests fungal colonization was the overwhelming process occurring during this period (Anderson 1973; Dickinson 1974; Zeller et al. 2000; d'Annunzio et al. 2008), presumably aided by the moist environment in our litterbags even with perforated filters. The higher N content of the litter in the absence of blue light and UV radiation is likely to be due to higher fungal biomass, because these wavelengths are known to inhibit the development of some fungi (De Lucca et al. 2012; Verhoef et al. 2000).

In our study of leaf litter decomposition in a moist temperate forest, UV-A radiation and blue light were found to have a more important role in photodegradation than UV-B radiation. This finding is consistent with other studies in similar climatic regions, in a dune grassland (Hoorens et al. 2004) and in a temperate woodland (Newsham et al. 2001), but differs from most arid (Day et al. 2007, 2015) and semiarid (Austin and Vivanco 2006) environments studied where UV-B radiation typically also increases mass loss. The relative importance of direct microbial inhibition by UV-B radiation reported in the literature vs. photochemical mineralization may provide an explanation for the different net effect of UV-B radiation on decomposition in a moist temperate ecosystem where biotic decomposition processes are more dominant than in drier ecosystems. The importance of photodegradation in arid and semiarid environments as a driver of carbon loss during decomposition is well known (Austin and Ballaré 2010; Austin et al. 2016); this study allows us to extend that finding to temperate forest environments, albeit acknowledging that this study focused on decomposition of the top layer of surface leaf litter and not buried material. Compared to grassland ecosystems, forest ecosystems have greater litter thickness and litter mass, and consequently a lower ratio of exposed litter. For instance, in the area where our study site is located, the typical litter layer thickness (OL) is about 1.5 (±0.6) cm (Aubert et al. 2004), while leaf litter production is about 2.5 (±0.5) t ha^{-1} yr^{-1} (Trap et al. 2011). While the effect of photodegradation will decrease with increasing litter layer thickness (Henry et al. 2008 and Mao et al. 2018), there remains potential for it to have a priming on surface litter, which would subsequently affect decomposition of covered litter due to photopriming (Lin et al. 2018). Photodegradation is able to mineralise up to 14% of NPP in arid systems and it is responsible for up to 23% of litter mass loss (King et al. 2012; Foereid et al. 2011); however, data are lacking from temperate forest environments. Knowing the role that photodegradation plays in decomposition is crucial to understanding its consequences for the global carbon cycle in forests, especially under a scenario of climate change. Within this framework, our results clearly suggest that parameterization of models designed to integrate photodegradation in the global carbon cycle should weight the wavelength regions of the solar spectrum differently, which is not yet the case (Foereid et al. 2011).

Conclusion

This study found that even under the low solar irradiances in the understorey of a temperate forest, photodegradation, particularly by UV-A radiation and blue light, remains important in accelerating surface leaf litter decomposition (increasing mass loss by up to 30%). The extent of this effect is modulated by litter quality, which itself is known to depend on forest succession and light environment. This illustrates that sunlight is involved in mediating the rate of nutrient cycling in forest soils, not only through primary production but also through its effect on decomposition.

Acknowledgements Open access funding provided by University of Helsinki including Helsinki University Central Hospital. We thank the ONF (Office National de Forêts) for the permission to use the study site. We also thank Paul Barnes for the valuable comments on the manuscript and advice on the litterbags design, Saara Hartikainen and Santa Neimane for the hemispherical photo processing and Philippe Delporte for help in setting up the field experiment. We would like to acknowledge the FR-SCALE platform for the support. We would like to thank the weather station of Rouen Boos and Meteo France for providing the temperature and precipitation data.

Author contribution statement MP and TMR formulated the initial idea, MP EF MC AGJ and TMR designed the experiment, MP conceived and performed the experiment, MP, EF, TMR and MC collected the data including biochemical analysis, MP, MC, TMR and TKK analysed the data and all authors wrote the manuscript. Additionally, EF, MC, TMR and AGJ supervised the study.

Funding This research was funded by Academy of Finland decisions #266523 and #304519 to TMR and a grant from the Region "Haute-Normandie" through the GRR-TERA SCALE (UFOSE Project) to MP.

References

Adair EC, Parton WJ, Del Grosso SJ, Silver WL, Harmon ME, Hall SA, Burke IC, Hart SC (2008) Simple three-pool model accurately describes patterns of long-term litter decomposition in diverse climates. Glob Change Biol 14:2636–2660. https://doi.org/10.1111/j.1365-2486.2008.01674.x

Aerts R (1997) Climate, leaf litter chemistry and leaf litter decomposition in terrestrial ecosystems: a triangular relationship. Oikos 79:439–449. https://doi.org/10.2307/3546886

Almagro M, Maestre FT, Martínez-López J, Valencia E, Rey A (2015) Climate change may reduce litter decomposition while enhancing the contribution of photodegradation in dry perennial Mediterranean grasslands. Soil Biol Biochem 90:214–223. https://doi.org/10.1016/j.soilbio.2015.08.006

Almagro M, Martínez-López J, Maestre FT, Rey A (2017) The Contribution of photodegradation to litter decomposition in semiarid mediterranean grasslands depends on its interaction with local humidity conditions, litter quality and position. Ecosystems 20:527–542. https://doi.org/10.1007/s10021-016-0036-5

Anderson JM (1973) The breakdown and decomposition of sweet chestnut (*Castanea sativa* mill.) and beech (*Fagus sylvatica* L.) leaf litter in two deciduous woodland soils. Oecologia 12:275–288. https://doi.org/10.1007/BF00347567

Aphalo PJ (2015) The r4photobiology suite: spectral irradiance. UV4Plants Bull 2015:21–29. https://doi.org/10.19232/uv4pb.2015.1.14

Aphalo P, Albert A, Björn LO, McLeod A, Robson TM, Rosenqvist E (eds) (2012) Beyond the visible: A handbook of best practice in plant UV photobiology, 1st edn, COST Action FA0906 UV4growth. University of Helsinki, Division of Plant Biology, Helsinki. ISBN 978-952-10-8362-4 (paperback), ISBN 978-952-10-8363-1 (PDF)

Aphalo PJ, Robson TM, Piiparinen J (2016) How to check an array spectrometer. Int. Assoc. Plant UV Res., http://uv4plants.org/methods/how-to-check-an-array-spectrometer/, updated June 2, 2013, Accessed Nov 11 2017

Argyropoulos DS (2001) Wood and cellulosic chemistry, 2nd edn. J Am Chem Soc, New York and Basel

Asplund J, Kauserud H, Bokhorst S, Lie MH, Ohlson M, Nybakken L (2018) Fungal communities influence decomposition rates of plant litter from two dominant tree species. Fungal Ecol 32:1–8. https://doi.org/10.1016/j.funeco.2017.11.003

Aubert M, Bureau F, Alard D, Bardat J (2004) Effect of tree mixture on the humic epipedon and vegetation diversity in managed beech forests (Normandy, France). Can J For Res 34:233–248. https://doi.org/10.1139/x03-205

Austin AT, Ballaré CL (2010) Dual role of lignin in plant litter decomposition in terrestrial ecosystems. Proc Natl Acad Sci USA 107:4618–4622. https://doi.org/10.1073/pnas.0909396107

Austin AT, Vivanco L (2006) Plant litter decomposition in a semi-arid ecosystem controlled by photodegradation. Nature 442:555–558. https://doi.org/10.1038/nature05038

Austin AT, Méndez MS, Ballaré CL (2016) Photodegradation alleviates the lignin bottleneck for carbon turnover in terrestrial ecosystems. Proc Natl Acad Sci USA 113:4392–4397. https://doi.org/10.1073/pnas.1516157113

Baker NR, Allison SD (2015) Ultraviolet photodegradation facilitates microbial litter decomposition in a Mediterranean climate. Ecology 96:1994–2003. https://doi.org/10.1890/14-1482.1

Baldrian P, Větrovský T, Cajthaml T, Dobiášová P, Petránková M, Šnajdr J, Eichlerová I (2013) Estimation of fungal biomass in forest litter and soil. Fungal Ecol 6:1–11. https://doi.org/10.1016/J.FUNECO.2012.10.002

Bardgett BR, Bowman WD, Kaufmann R, Schmidt SK (2005) A temporal approach to linking aboveground and belowground ecology. Trends Ecol Evol 20:634–641. https://doi.org/10.1016/J.TREE.2005.08.005

Brandstätter C, Keiblinger K, Wanek W, Zechmeister-Boltenstern S (2013) A closeup study of early beech litter decomposition: potential drivers and microbial interactions on a changing substrate. Plant Soil 371:139–154. https://doi.org/10.1007/s11104-013-1671-7

Brandt LA, King JY, Milchunas DG (2007) Effects of ultraviolet radiation on litter decomposition depend on precipitation and litter chemistry in a shortgrass steppe ecosystem. Glob Change Biol 13:2193–2205. https://doi.org/10.1111/j.1365-2486.2007.01428.x

Brandt LA, Bohnet C, King JY (2009) Photochemically induced carbon dioxide production as a mechanism for carbon loss from plant litter in arid ecosystems. J Geophys Res 114:G02004. https://doi.org/10.1029/2008JG000772

Bravo-Oviedo A, Ruiz-Peinado R, Onrubia R, Del Río M (2017) Thinning alters the early-decomposition rate and nutrient immobilization-release pattern of foliar litter in Mediterranean oak-pine mixed stands. For Ecol Manag 391:309–320. https://doi.org/10.1016/j.foreco.2017.02.032

Canham CD (1988) An index for understory light levels in and around canopy gaps. Ecology 69:1634–1638. https://doi.org/10.2307/1941664

Cory RM, Crump BC, Dobkowski JA, Kling GW (2013) Surface exposure to sunlight stimulates CO_2 release from permafrost soil carbon in the Arctic. PNAS 110:3429–3434. https://doi.org/10.1073/pnas.1214104110

D'Annunzio R, Zeller B, Nicolas M, Dhôte JF, Saint-André L (2008) Decomposition of European beech (*Fagus sylvatica*) litter: combining quality theory and 15 N labelling experiments. Soil Biol Biochem 40:322–333. https://doi.org/10.1016/j.soilbio.2007.08.011

Day TA, Zhang ET, Ruhland CR (2007) Exposure to solar UV-B radiation accelerates mass and lignin loss of *Larrea tridentata* litter in the Sonoran Desert. Plant Ecol 193:185–194. https://doi.org/10.1007/s11258-006-9257-6

Day TA, Guénon R, Ruhland CR (2015) Photodegradation of plant litter in the Sonoran Desert varies by litter type and age. Soil Biol Biochem 89:109–122. https://doi.org/10.1016/j.soilbio.2015.06.029

De Lucca AJ, Carter-Wientjes C, Williams KA, Bhatnagar D (2012) Blue light (470 Nm) effectively inhibits bacterial and fungal growth. Lett Appl Microbiol 55:460–466. https://doi.org/10.1111/lam.12002

Dickinson CH (1974) Biology of Plant Litter Decomposition, 1st edn. Elsevier Science, New York

Duguay KJ, Klironomos JN (2000) Direct and indirect effects of enhanced UV-B radiation on the decomposing and competitive abilities of saprobic fungi. Appl Soil Ecol 14:157–164. https://doi.org/10.1016/S0929-1393(00)00049-4

Emde C, Buras-Schnell R, Kylling A, Mayer B, Gasteiger J, Hamann U et al (2016) The libRadtran software package for radiative transfer calculations (version 2.0.1). Geosci Model Dev 9(5):1647–1672

Fahey TJ, Battles JJ, Wilson GF (1998) Responses of early successional northern hardwood forests to changes in nutrient availability. Ecol Monogr 68:183–212. https://doi.org/10.1890/0012-9615(1998)068%5b0183:roesnh%5d2.0.co;2

Foereid B, Rivero MJ, Primo O, Ortiz I (2011) Modelling photodegradation in the global carbon cycle. Soil Biol Biochem 43:1383–1386. https://doi.org/10.1016/j.soilbio.2011.03.004

Foereid B, Zarov EA, Latysh IM, Filippov IV, Lapshina ED (2018) Photoexposure affects subsequent peat litter decomposition. Geoderma 315:104–110. https://doi.org/10.1016/j.geoderma.2017.10.059

Gallo ME, Sinsabaugh RL, Cabaniss SE (2006) The role of ultraviolet radiation in litter decomposition in arid ecosystems. Appl Soil Ecol 34:82–91. https://doi.org/10.1016/j.apsoil.2005.12.006

Gallo ME, Porras-Alfaro A, Odenbach KJ, Sinsabaugh RL (2009) Photoacceleration of plant litter decomposition in an arid environment. Soil Biol Biochem 41:1433–1441. https://doi.org/10.1016/j.soilbio.2009.03.025

Gaxiola A, Armesto JJ (2015) Understanding litter decomposition in semiarid ecosystems: linking leaf traits, UV exposure and rainfall variability. Front Plant Sci 6:1–9. https://doi.org/10.3389/fpls.2015.00140

Gessner MO, Chauvet E (2011) Importance of stream microfungi in controlling breakdown rates of leaf litter. Ecol Appl 75:1807–1817. https://doi.org/10.2307/1939639

Gliksman D, Haenel S, Osem Y, Yakir D, Zangy E, Preisler Y, Grünzweig JM (2017) Litter decomposition in mediterranean pine forests is enhanced by reduced canopy cover. Plant Soil 422:317–329. https://doi.org/10.1007/s11104-017-3366-y

Grant RH, Apostol K, Gao W (2015) Biologically effective UV-B exposures of an oak-hickory forest understory during leaf-out. Agric For Meteorol 132:28–43. https://doi.org/10.1016/j.agrformet.2005.06.008

Gulis V, Kuehn KA, Suberkropp K (2009) Fungi. In: Likens GE (ed) Encyclopedia of Inland Waters. Elsevier, New York, pp 233–243

Hartikainen SM, Jach A, Grané A, Robson TM (2018) Assessing scale-wise similarity of curves with a thick pen: as illustrated through comparisons of spectral irradiance. Ecol Evol 8:10206–10218. https://doi.org/10.1002/ece3.4496

Hättenschwiler S, Tiunov AV, Scheu S (2005) Biodiversity and litter decomposition in terrestrial ecosystems. Annu Rev Ecol Evol Syst 36:191–218. https://doi.org/10.1146/annurev.ecolsys.36.112904.151932

Henneron L, Chauvat M, Archaux F, Akpa-Vincesls M, Bureau F, Yann Dumas, Laurent Mignot, Ningre F, Perret S, Richter C, Balandier P, Aubert M (2017) Plant interactions as biotic drivers of plasticity in leaf litter traits and decomposability of *Quercus petraea*. Ecol Monogr 87:321–340. https://doi.org/10.1002/ecm.1252

Henry HAL, Brizgys K, Field CB (2008) Litter decomposition in a California annual grassland: interactions between photodegradation and litter layer thickness. Ecosystems 11:545–554. https://doi.org/10.1007/s10021-008-9141-4

Hodge A, Robinson D, Fitter A (2000) Are microorganisms more effective than plants at competing for nitrogen? Trends Plant Sci 5:304–308. https://doi.org/10.1016/S1360-1385(00)01656-3

Hon DNS, Shiraishi N (2001) Wood and Cellulose chemistry, Chap. 9 Color and Discoloration, Chap. 11 Weathering and photochemistry of wood. Marcel Dekker Inc, New York, Basel

Hoorens B, Aerts R, Stroetenga M (2004) Elevated UV-B radiation has no effect on litter quality and decomposition of two dune grassland species: evidence from a long-term field experiment. Glob Change Biol 10:200–208. https://doi.org/10.1111/j.1529-8817.2003.00735.x

Idol TW, Holzbaur KA, Pope PE, Ponder F (2002) Control-bag correction for forest floor litterbag contamination. Soil Sci Soc Am J 66:620–623. https://doi.org/10.2136/sssaj2002.6200

King JY, Brandt LA, Adair EC (2012) Shedding light on plant litter decomposition: advances, implications and new directions in understanding the role of photodegradation. Biogeochemistry 111:57–81. https://doi.org/10.1007/s10533-012-9737-9

Kotilainen T, Haimi J, Tegelberg R, Julkunen-Tiitto R, Vapaavuori E, Aphalo PJ (2009) Solar ultraviolet radiation alters alder and birch litter chemistry that in turn affects decomposers and soil respiration. Oecologia 161:719–728. https://doi.org/10.1007/s00442-009-1413-y

Lin Y, King JY (2015) Using 2D NMR spectroscopy to assess effects of UV radiation on cell wall chemistry during litter decomposition. Biogeochemistry 125:427–436. https://doi.org/10.1007/s10533-015-0132-1

Lin Y, Scarlett RD, King JY (2015) Effects of UV photodegradation on subsequent microbial decomposition of *Bromus diandrus* litter. Plant Soil 395:263–271. https://doi.org/10.1007/s11104-015-2551-0

Lin Y, Karlen SD, Ralph J, King JY (2018) Short-term facilitation of microbial litter decomposition by ultraviolet radiation. Sci Total Environ 615:838–848. https://doi.org/10.1016/j.scitotenv.2017.09.239

Lindfors A, Heikkilä A, Kaurola J, Koskela T, Lakkala K (2009) Reconstruction of solar spectral surface UV irradiances using radiative transfer simulations. Photochem Photobiol 85(5):1233–1239

Ma Z, Yang W, Wu F, Tan B (2017) Effects of light intensity on litter decomposition in a subtropical region. Ecosphere 8(4):e01770. https://doi.org/10.1002/ecs2.1770

Måns C, Denward T, Tranvik LJ (1998) Effects of solar radiation on aquatic macrophyte litter decomposition. Oikos 82:51–58. https://doi.org/10.2307/3546916

Mao B, Zhao L, Zhao Q, Zeng D (2018) Effects of ultraviolet (UV) radiation and litter layer thickness on litter decomposition of two tree species in a semi-arid site of Northeast China. J Arid Land 10:416–428. https://doi.org/10.1007/s40333-018-0054-6

Meentemeyer V (1978) Macroclimate and lignin control of litter decomposition rates. Ecology 59:465–472. https://doi.org/10.2307/1936576

Melillo JM, Aber JD, Muratore JF (1982) Nitrogen and lignin control of hardwood leaf litter decomposition dynamics. Ecology 63:621–626. https://doi.org/10.2307/1936780

Messenger DJ, Fry SC, Yamulki S, McLeod AR (2012) Effects of UV-B filtration on the chemistry and decomposition of *Fraxinus excelsior* leaves. Soil Biol Biochem 47:133–141. https://doi.org/10.1016/j.soilbio.2011.12.010

Newsham KK, Anderson JM, Sparks TH, Splatt P, Woods C, McLeod AR (2001) UV-B effect on *Quercus robur* leaf litter decomposition persists over 4 years. Glob Change Biol 7:479–483. https://doi.org/10.1046/j.1365-2486.2001.00423.x

Osler GH, Sommerkorn M (2007) Toward a complete soil C and N cycle: incorporating the soil fauna. Ecology 88:1611–1621. https://doi.org/10.1890/06-1357.1

Pan X, Song YB, Liu GF, Hu YK, Ye XH, Cornwell WK, Prinzing A, Dong M, Cornelissen JHC (2015) Functional traits drive the contribution of solar radiation to leaf litter decomposition among multiple arid-zone species. Sci Rep 5:13217. https://doi.org/10.1038/srep13217

Pancotto VA, Sala OE, Cabello M, López NI, Robson TM, Ballaré CL, Caldwell MM (2003) Solar UV-B decreases decomposition in herbaceous plant litter in Tierra del Fuego, Argentina: potential role of an altered decomposer community. Glob Change Biol 9:1465–1474. https://doi.org/10.1046/j.1365-2486.2003.00667.x

Parton W, Silver WL, Burke IC, Grassens L, Harmon ME, Curries WS, King JY, Adair EC, Brandt LA, Hart SC, Fasth B (2007) Global-scale similarities in nitrogen release patterns during long-term decomposition. Science 315:361–364. https://doi.org/10.1126/science.1134853

Robson TM, Pancotto VA, Scopel AL, Flint SD, Caldwell MM (2005) Solar UV-B influences microfaunal community composition in a Tierra del Fuego peatland. Soil Biol Biochem 37:2205–2215. https://doi.org/10.1016/j.soilbio.2005.04.002

Rutledge S, Campbell DI, Baldocchi D, Schipper LA (2010) Photodegradation leads to increased carbon dioxide losses from terrestrial organic matter. Glob Change Biol 16:3065–3074. https://doi.org/10.1111/j.1365-2486.2009.02149.x

Schleppi P, Conedera M, Sedivy I, Thimonier A (2007) Correcting non-linearity and slope effects in the estimation of the leaf area index of forests from hemispherical photographs. Agric Forest Meteorol 144:236–242

Sellaro R, Crepy M, Trupkin SA, Karayekov E, Buchovsky AS, Rossi C, Casal JJ (2010) Cryptochrome as a sensor of the blue/green ratio of natural radiation in *Arabidopsis*. Plant Physiol 154:401–409. https://doi.org/10.1104/pp.110.160820

Smith MJ, Vanderwel MC, Lyutsarev L, Emmott S, Purves DW (2012) The climate dependence of the terrestrial carbon cycle; including parameter and structural uncertainties. Biogeosci Discuss 9:13439–13496. https://doi.org/10.5194/bgd-9-13439-2012

Song X, Peng C, Jiang H, Zhu Q, Wang W (2013) Direct and indirect effects of UV-B exposure on litter decomposition: a meta-analysis. PLoS One 8:e68858. https://doi.org/10.1371/journal.pone.0068858

Thimonier A, Sedivy I, Schleppi P (2010) Estimating leaf area index in different types of mature forest stands in Switzerland: a comparison of methods. Eur J For Res 129:543–562

Trap J, Bureau F, Brethes A, Jabiol B, Ponge JF, Chauvat M, Decaëns T, Aubert M (2011) Does moder development along a pure beech (*Fagus sylvatica* L.) chronosequence result from changes in litter production or in decomposition rates? Soil Biol Biochem 43:1490–1497. https://doi.org/10.1016/j.soilbio.2011.03.025

Trap J, Hättenschwiler S, Gattin I, Aubert M (2013) Forest ageing: an unexpected driver of beech leaf litter quality variability in European forests with strong consequences on soil processes. For Ecol Manag 302:338–345. https://doi.org/10.1016/j.foreco.2013.03.011

Verhoef HA, Verspagen JMH, Zoomer HR (2000) Direct and indirect effects of ultraviolet-B radiation on soil biota, decomposition and nutrient fluxes in dune grassland soil systems. Biol Fertil Soils 31:366–371. https://doi.org/10.1007/s003749900181

Wang J, Liu L, Wang X, Chen Y (2015) The interaction between abiotic photodegradation and microbial decomposition under ultraviolet radiation. Glob Change Biol 21:2095–2104. https://doi.org/10.1111/gcb.12812

Wang J, Yang S, Zhang B, Liu W, Deng M, Chen S, Liu L (2017) Temporal dynamics of ultraviolet radiation impacts on litter decomposition in a semi-arid ecosystem. Plant Soil 419:71–81. https://doi.org/10.1007/s11104-017-3290-1

Xuluc-Tolosa FJ, Vester HFM, Ramírez-Marcial N, Castellanos-Albores J, Lawrence D (2003) Leaf litter decomposition of tree species in three successional phases of tropical dry secondary forest in Campeche, Mexico. For Ecol Manag 174:401–412. https://doi.org/10.1016/S0378-1127(02)00059-2

Zeller B, Colin-Belgrand M, Dambrine E, Martin F, Bottner P (2000) Decomposition of 15 N-labelled beech litter and fate of nitrogen derived from litter in a beech forest. Oecologia 123:550–559. https://doi.org/10.1007/PL00008860

ELECTRONIC SUPPLEMENTARY MATERIAL

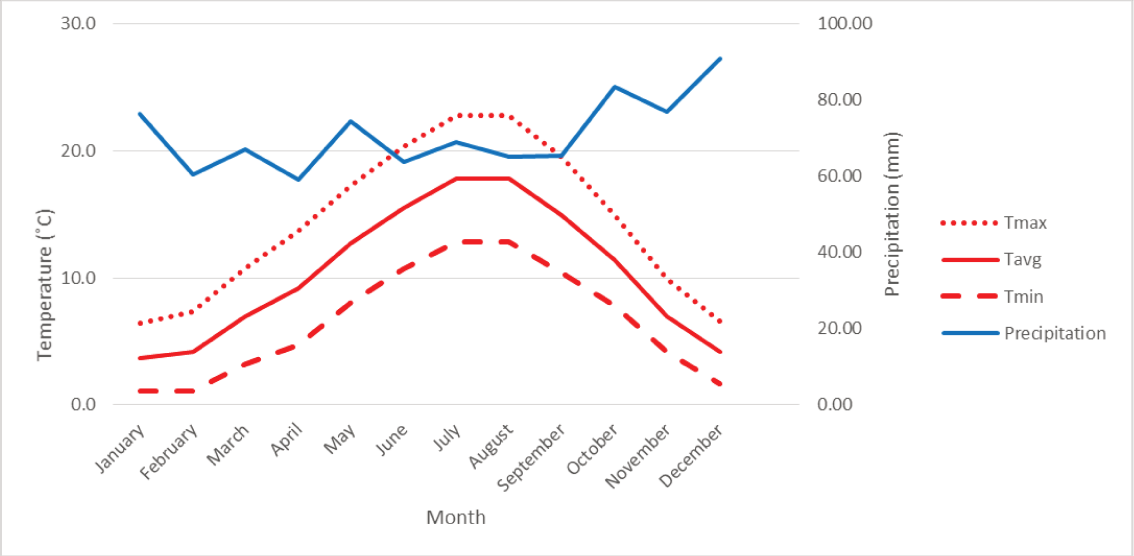

Figure S1 Climatic diagram of the study area (Rouen, France). Data from the weather station Rouen-Boos (49.38°N; 1.18°E) in Seine-Maritime, altitude 151 m.

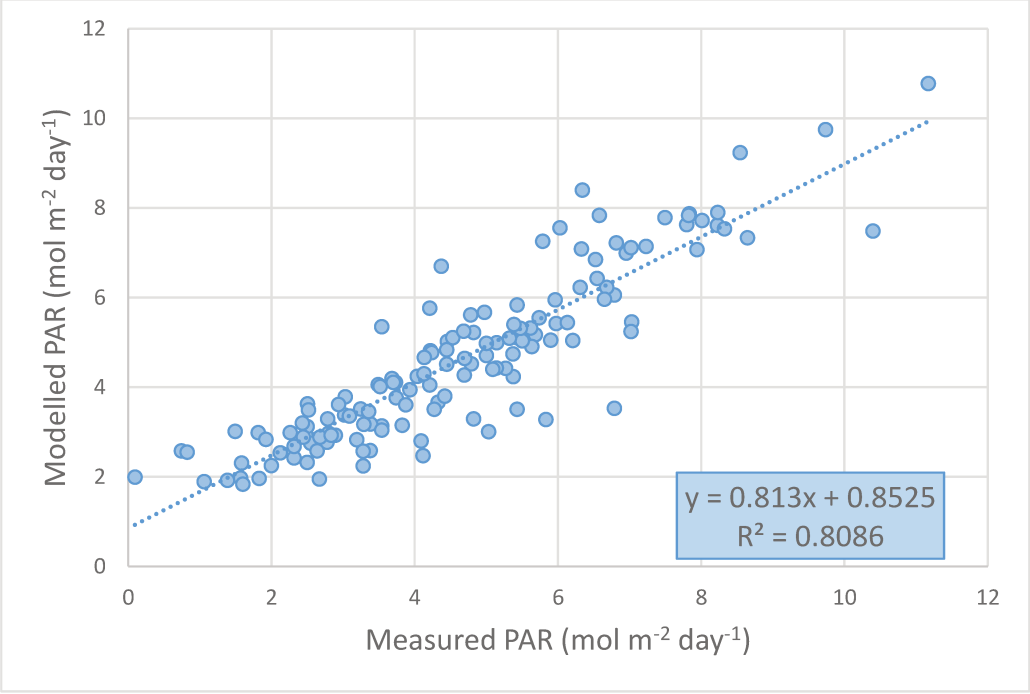

Figure S2 Cross-validation of measured understorey PAR vs. a subset of modelled understorey PAR accounting for daily weather conditions for the period 25-05-2017 to 10-10-2017.

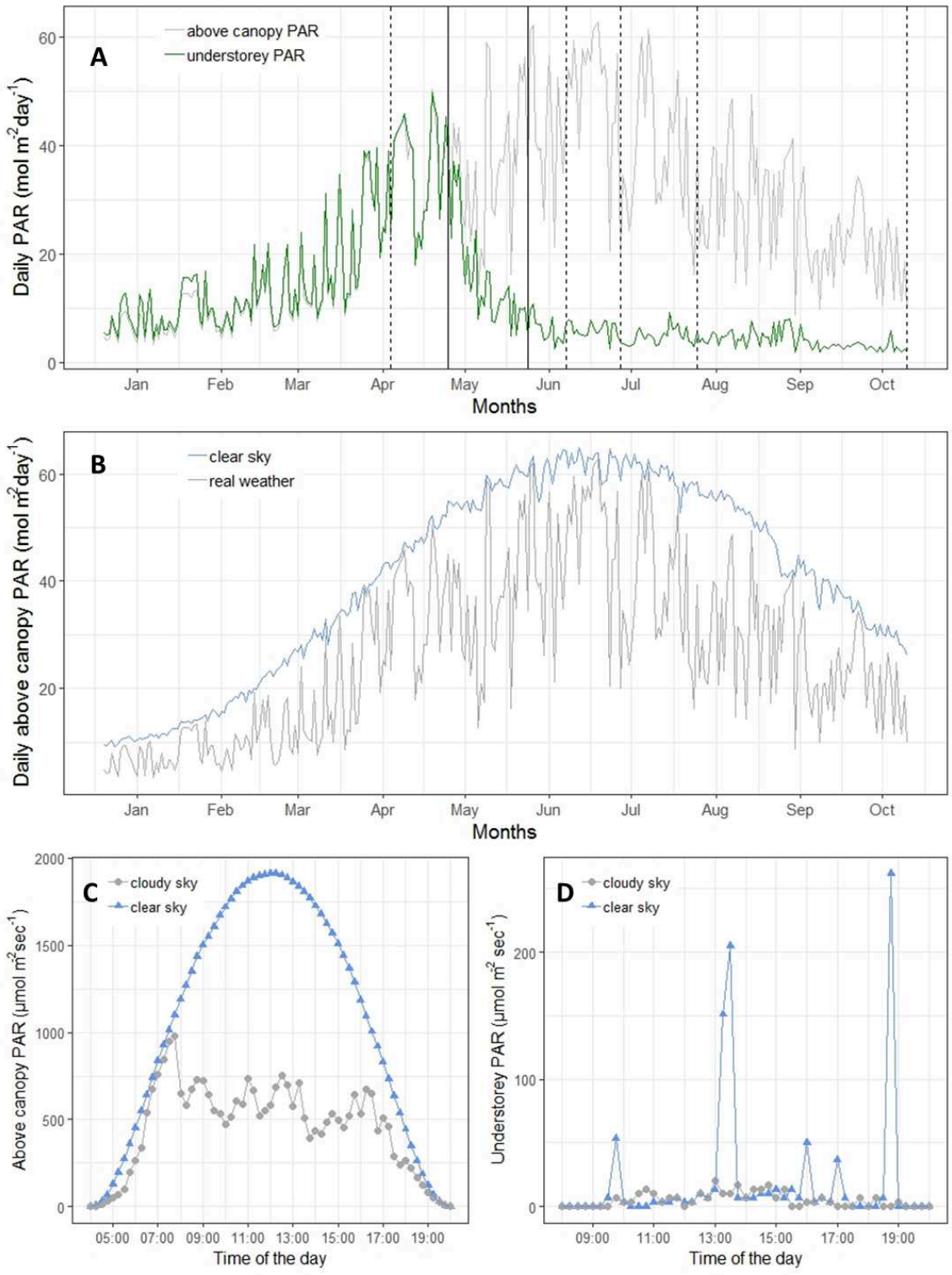

Figure S3 A) Daily photosynthetically active radiation (PAR) in the understorey (in green) and above the canopy (in grey). Time series of modelled PAR reconstructed using radiative transfer modelling of solar irradiance and global light index calculated from hemispherical photos taken

at the site over the course of the experiment. Modelled data were cross-validated against a subset of daily measured PAR irradiance at the site from 25-05-2017 to 10-10-2017. Vertical dashed lines show dates of litterbag collection, and solid lines show the period of spring flush from bud burst to canopy closure from a visual assessment of the buds of canopy trees. B) Daily PAR above the canopy modelled for clear sky conditions (light blue) and accounting for actual weather conditions (grey). Modelled data validated with satellite data from SoDa Helioclim-3. C) Diurnal pattern of PAR above the canopy under clear and cloudy sky conditions at the field site at the end of May 2017. Modelled data validated with satellite data provided by SoDa Helioclim-3. D) Diurnal pattern of PAR in the understorey under clear and cloudy sky conditions at the end of May 2017. Data measured at the field site with two calibrated quantum sensors in parallel (QSO-S, Decagon Devices, Pullman, Washington, USA).

Figure S4 Picture showing the litterbags in the study site at the beginning of the experiment.

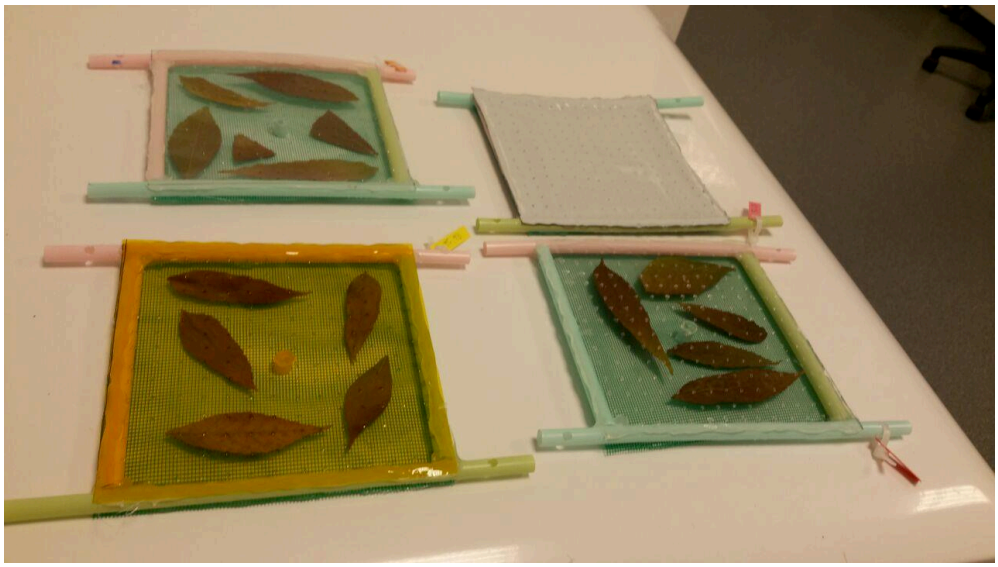

Figure S5 Picture showing some of the typical non-overlapping arrangements of leaves in the litterbags, as used in the experiment.

Figure S6 Picture showing an example of the mesh on the underside of the litterbags used in the experiment. Mesh size 0.1 mm on the left and mesh size 1 mm on the right.

Species	Light treatment	FW (g)	DW (g)	Water Content (g)	LMA	Chl	Flav	C %	N %	C : N
Ash	Dark	1.60 ± 0.02	0.60 ± 0.01	0.37 ± 0.00	0.01 ± 0.00	18.10 ± 0.20	1.34 ± 0.01	39.45 ± 0.07	1.35 ± 0.01	29.18 ± 0.29
	Full-Spectrum	1.50 ± 0.02	0.58 ± 0.01	0.39 ± 0.00	0.01 ± 0.00	17.41 ± 0.35	1.37 ± 0.01	39.45 ± 0.07	1.35 ± 0.01	29.18 ± 0.29
	No-UV	1.45 ± 0.03	0.56 ± 0.01	0.38 ± 0.00	0.01 ± 0.00	16.47 ± 0.21	1.37 ± 0.01	39.45 ± 0.07	1.35 ± 0.01	29.18 ± 0.29
	No-UV/Blue	1.51 ± 0.02	0.58 ± 0.01	0.38 ± 0.00	0.01 ± 0.00	17.21 ± 0.24	1.35 ± 0.01	39.45 ± 0.07	1.35 ± 0.01	29.18 ± 0.29
	No-UVB	1.56 ± 0.01	0.59 ± 0.01	0.38 ± 0.00	0.01 ± 0.00	17.80 ± 0.23	1.38 ± 0.01	39.45 ± 0.07	1.35 ± 0.01	29.18 ± 0.29
Beech	Dark	0.90 ± 0.02	0.33 ± 0.01	0.36 ± 0.00	0.00 ± 0.00	6.32 ± 0.35	0.84 ± 0.02	43.67 ± 0.00	0.89 ± 0.03	48.94 ± 1.84
	Full-Spectrum	0.96 ± 0.02	0.35 ± 0.01	0.37 ± 0.00	0.00 ± 0.00	6.72 ± 0.47	0.85 ± 0.02	43.67 ± 0.00	0.89 ± 0.03	48.94 ± 1.84
	No-UV	0.97 ± 0.03	0.37 ± 0.01	0.39 ± 0.00	0.00 ± 0.00	6.90 ± 0.35	0.93 ± 0.02	43.67 ± 0.00	0.89 ± 0.03	48.94 ± 1.84
	No-UV/Blue	0.90 ± 0.02	0.33 ± 0.01	0.37 ± 0.00	0.00 ± 0.00	6.23 ± 0.33	0.84 ± 0.02	43.67 ± 0.00	0.89 ± 0.03	48.94 ± 1.84
	No-UVB	0.89 ± 0.02	0.32 ± 0.01	0.36 ± 0.00	0.00 ± 0.00	6.68 ± 0.35	0.84 ± 0.02	43.67 ± 0.00	0.89 ± 0.03	48.94 ± 1.84
Oak	Dark	1.94 ± 0.03	0.80 ± 0.01	0.41 ± 0.00	0.01 ± 0.00	11.81 ± 0.49	1.28 ± 0.01	43.79 ± 0.25	2.07 ± 0.09	21.23 ± 0.79
	Full-Spectrum	1.81 ± 0.02	0.75 ± 0.01	0.41 ± 0.00	0.01 ± 0.00	12.11 ± 0.40	1.19 ± 0.01	43.79 ± 0.25	2.07 ± 0.09	21.23 ± 0.79
	No-UV	1.89 ± 0.02	0.80 ± 0.01	0.42 ± 0.00	0.01 ± 0.00	31.24 ± 0.47	1.23 ± 0.01	43.79 ± 0.25	2.07 ± 0.09	21.23 ± 0.79
	No-UV/Blue	2.04 ± 0.03	0.84 ± 0.01	0.41 ± 0.00	0.01 ± 0.00	12.25 ± 0.57	1.26 ± 0.01	43.79 ± 0.25	2.07 ± 0.09	21.23 ± 0.79
	No-UVB	1.95 ± 0.02	0.81 ± 0.01	0.41 ± 0.00	0.01 ± 0.00	12.17 ± 0.55	1.29 ± 0.01	43.79 ± 0.25	2.07 ± 0.09	21.23 ± 0.79

Table S. 1 Initial litter quality, mean and standard errors are shown (n=5)

Mesh size: 0.1mm; Collection time: 3 months

Filter	Estimate	SE	t-value	P value
Dark - No-UV/Blue	0.660	2.606	0.2532	1.000
Dark - No-UV	0.131	2.606	0.0502	1.000
Dark - No-UVB	-0.636	2.606	-0.2442	1.000
Dark - Full-Spectrum	1.723	2.606	0.6611	1.000
No-UV/Blue - No-UV	-0.529	2.606	-0.2030	1.000
No-UV/Blue - No-UVB	-1.296	2.606	-0.4973	1.000
No-UV/Blue - Full-Spectrum	1.063	2.606	0.4079	1.000
No-UV - No-UVB	-0.767	2.606	-0.2943	1.000
No-UV - Full-Spectrum	1.592	2.606	0.6109	1.000
No-UVB - Full-Spectrum	2.359	2.606	0.9052	1.000

Mesh size: 0.1mm; Collection time: 5 months

Filter	Estimate	SE	t-value	P value
Dark - No-UV/Blue	2.296	2.606	0.8810	1.000
Dark - No-UV	3.067	2.606	1.1765	1.000
Dark - No-UVB	7.806	2.606	2.9948	1.000
Dark - Full-Spectrum	5.569	2.606	2.1367	1.000
No-UV/Blue - No-UV	0.770	2.606	0.2956	1.000
No-UV/Blue - No-UVB	5.510	2.606	2.1139	1.000
No-UV/Blue - Full-Spectrum	3.273	2.606	1.2558	1.000
No-UV - No-UVB	4.739	2.606	1.8183	1.000
No-UV - Full-Spectrum	2.503	2.606	0.9602	1.000
No-UVB - Full-Spectrum	-2.237	2.606	-0.8581	1.000

Mesh size: 0.1mm; Collection time: 7 months

Filter	Estimate	SE	t-value	P value
Dark - No-UV/Blue	4.267	2.606	1.6371	1.000
Dark - No-UV	2.691	2.606	1.0326	1.000
Dark - No-UVB	8.179	2.606	3.1379	0.760
Dark - Full-Spectrum	6.312	2.606	2.4215	1.000
No-UV/Blue - No-UV	-1.576	2.606	-0.6045	1.000
No-UV/Blue - No-UVB	3.912	2.606	1.5009	1.000
No-UV/Blue - Full-Spectrum	2.045	2.606	0.7845	1.000
No-UV - No-UVB	5.488	2.606	2.1054	1.000
No-UV - Full-Spectrum	3.620	2.606	1.3890	1.000

No-UVB - Full-Spectrum	-1.867	2.606	-0.7164	1.000

Mesh size: 1mm; Collection time: 3 months

Filter	Estimate	SE	t-value	P value
Dark - No-UV/Blue	-1.223	2.606	-0.4691	1.000
Dark - No-UV	-1.759	2.606	-0.6748	1.000
Dark - No-UVB	-2.471	2.606	-0.9481	1.000
Dark - Full-Spectrum	1.880	2.606	0.7214	1.000
No-UV/Blue - No-UV	-0.536	2.606	-0.2056	1.000
No-UV/Blue - No-UVB	-1.249	2.606	-0.4790	1.000
No-UV/Blue - Full-Spectrum	3.103	2.606	1.1905	1.000
No-UV - No-UVB	-0.713	2.606	-0.2734	1.000
No-UV - Full-Spectrum	3.639	2.606	1.3962	1.000
No-UVB - Full-Spectrum	4.352	2.606	1.6695	1.000

Mesh size: 1mm; Collection time: 5 months

Filter	Estimate	SE	t-value	P value
Dark - No-UV/Blue	**-16.860**	**2.606**	**-6.4686**	**< 0.001**
Dark - No-UV	**-14.020**	**2.606**	**-5.3790**	**< 0.001**
Dark - No-UVB	-8.565	2.606	-3.2862	0.483
Dark - Full-Spectrum	-7.924	2.606	-3.0401	1.000
No-UV/Blue - No-UV	2.840	2.606	1.0896	1.000
No-UV/Blue - No-UVB	8.295	2.606	3.1824	0.670
No-UV/Blue - Full-Spectrum	8.936	2.606	3.4285	0.310
No-UV - No-UVB	5.455	2.606	2.0928	1.000
No-UV - Full-Spectrum	6.096	2.606	2.3389	1.000
No-UVB - Full-Spectrum	0.641	2.606	0.2461	1.000

Mesh size: 1mm; Collection time: 7 months

Filter	Estimate	SE	t-value	P value
Dark - No-UV/Blue	**-12.365**	**2.606**	**-4.7439**	**0.002**
Dark - No-UV	**-11.445**	**2.606**	**-4.3909**	**0.010**
Dark - No-UVB	-9.048	2.606	-3.4715	0.269
Dark - Full-Spectrum	-4.871	2.606	-1.8687	1.000
No-UV/Blue - No-UV	0.920	2.606	0.3531	1.000
No-UV/Blue - No-UVB	3.317	2.606	1.2724	1.000
No-UV/Blue - Full-Spectrum	7.494	2.606	2.8752	1.000
No-UV - No-UVB	2.396	2.606	0.9194	1.000

No-UV - Full-Spectrum	6.574	2.606	2.5221	1.000
No-UVB - Full-Spectrum	4.178	2.606	1.6028	1.000

Table S2 Pairwise comparisons for filter treatments on ash litter ash free dry mass (AFDM) according to mesh size and collection times: t- tests, with the Holm's correction for multiple comparisons, were used to calculate the *P* values. Significant contrasts are shown in bold.

Mesh size: 0.1mm				
Filter	**Estimate**	**SE**	**t-value**	**P value**
Dark - No-UV/Blue	2.408	1.505	1.6000	1.000
Dark - No-UV	1.963	1.505	1.3044	1.000
Dark - No-UVB	**5.116**	**1.505**	**3.3998**	**0.031**
Dark - Full-Spectrum	4.535	1.505	3.0134	0.095
No-UV/Blue - No-UV	-0.445	1.505	-0.2956	1.000
No-UV/Blue - No-UVB	2.708	1.505	1.7998	1.000
No-UV/Blue - Full-Spectrum	2.127	1.505	1.4134	1.000
No-UV - No-UVB	3.153	1.505	2.0954	0.918
No-UV - Full-Spectrum	2.572	1.505	1.7090	1.000
No-UVB - Full-Spectrum	-0.581	1.505	-0.3864	1.000
Mesh size: 1mm				
Filter	**Estimate**	**SE**	**t-value**	**P value**
Dark - No-UV/Blue	**-10.149**	**1.505**	**-6.7444**	**< 0.001**
Dark - No-UV	**-9.075**	**1.505**	**-6.0302**	**< 0.001**
Dark - No-UVB	**-6.695**	**1.505**	**-4.4490**	**< 0.001**
Dark - Full-Spectrum	-3.638	1.505	-2.4176	0.462
No-UV/Blue - No-UV	1.075	1.505	0.7142	1.000
No-UV/Blue - No-UVB	3.454	1.505	2.2954	0.586
No-UV/Blue - Full-Spectrum	**6.511**	**1.505**	**4.3268**	**0.001**
No-UV - No-UVB	2.380	1.505	1.5813	1.000
No-UV - Full-Spectrum	**5.436**	**1.505**	**3.6126**	**0.016**
No-UVB - Full-Spectrum	3.057	1.505	2.0314	1.000

Table S3 Pairwise comparisons for filter treatments on ash litter ash free dry mass (AFDM) according to mesh size: t- tests, with the Holm's correction for multiple comparisons, were used to calculate the *P* values. Significant contrasts are shown in bold.

Oak (*Quercus robur* L.)				
Filter	**Estimate**	**SE**	**t-value**	**P value**
Dark - No-UV/Blue	-1.267	1.883	-0.6730	1.000
Dark - No-UV	4.527	1.883	2.4041	0.088
Dark - No-UVB	3.400	1.883	1.8057	0.220
Dark - Full-Spectrum	**8.462**	**1.883**	**4.4933**	**< 0.001**
No-UV/Blue - No-UV	**5.795**	**1.883**	**3.0771**	**0.020**
No-UV/Blue - No-UVB	4.668	1.883	2.4787	0.086
No-UV/Blue - Full-Spectrum	**9.729**	**1.883**	**5.1663**	**< 0.001**
No-UV - No-UVB	-1.127	1.883	-0.5984	1.000
No-UV - Full-Spectrum	3.934	1.883	2.0892	0.154
No-UVB - Full-Spectrum	5.061	1.883	2.6876	0.057
Beech (*Fagus sylvatica* L.)				
Filter	**Estimate**	**SE**	**t-value**	**P value**
Dark - No-UV/Blue	2.028	3.580	0.5664	0.572
Dark - No-UV	**11.079**	**3.580**	**3.0950**	**0.014**
Dark - No-UVB	**21.012**	**3.580**	**5.8694**	**< 0.001**
Dark - Full-Spectrum	**16.594**	**3.580**	**4.6353**	**< 0.001**
No-UV/Blue - No-UV	**9.052**	**3.580**	**2.5285**	**0.050**
No-UV/Blue - No-UVB	**18.984**	**3.580**	**5.3030**	**< 0.001**
No-UV/Blue - Full-Spectrum	**14.566**	**3.580**	**4.0689**	**< 0.001**
No-UV - No-UVB	**9.932**	**3.580**	**2.7745**	**0.031**
No-UV - Full-Spectrum	5.514	3.580	1.5403	0.377
No-UVB - Full-Spectrum	-4.418	3.580	-1.2342	0.438

Table S4 Pairwise comparisons for filter treatments on beech and oak litter AFDM: t-tests, with the Holm's correction for multiple comparisons, were used to calculate the *P* values. Significant contrasts are shown in bold.

Mesh size: 0.1mm; Collection time: 3 months

Filter	Estimate	SE	t-value	P value
Dark - No-UV/Blue	1.188	2.758	0.4308	1.000
Dark - No-UV	1.933	2.758	0.7008	1.000
Dark - No-UVB	0.304	2.758	0.1101	1.000
Dark - Full-Spectrum	3.320	2.758	1.2039	1.000
No-UV/Blue - No-UV	0.745	2.758	0.2700	1.000
No-UV/Blue - No-UVB	-0.884	2.758	-0.3207	1.000
No-UV/Blue - Full-Spectrum	2.132	2.758	0.7730	1.000
No-UV - No-UVB	-1.629	2.758	-0.5907	1.000
No-UV - Full-Spectrum	1.387	2.758	0.5030	1.000
No-UVB - Full-Spectrum	3.016	2.758	1.0937	1.000

Mesh size: 0.1mm; Collection time: 5 months

Filter	Estimate	SE	t-value	P value
Dark - No-UV/Blue	5.298	2.758	1.9213	1.000
Dark - No-UV	5.915	2.758	2.1448	1.000
Dark - No-UVB	10.046	2.758	3.6431	0.144
Dark - Full-Spectrum	8.169	2.758	2.9623	1.000
No-UV/Blue - No-UV	0.616	2.758	0.2235	1.000
No-UV/Blue - No-UVB	4.748	2.758	1.7218	1.000
No-UV/Blue - Full-Spectrum	2.871	2.758	1.0411	1.000
No-UV - No-UVB	4.132	2.758	1.4983	1.000
No-UV - Full-Spectrum	2.254	2.758	0.8175	1.000
No-UVB - Full-Spectrum	-1.877	2.758	-0.6807	1.000

Mesh size: 0.1mm; Collection time: 7 months

Filter	Estimate	SE	t-value	P value
Dark - No-UV/Blue	7.364	2.758	2.6706	1.000
Dark - No-UV	4.453	2.758	1.6149	1.000
Dark - No-UVB	9.903	2.758	3.5913	0.169
Dark - Full-Spectrum	9.941	2.758	3.6049	0.163
No-UV/Blue - No-UV	-2.911	2.758	-1.0557	1.000
No-UV/Blue - No-UVB	2.539	2.758	0.9207	1.000
No-UV/Blue - Full-Spectrum	2.577	2.758	0.9343	1.000
No-UV - No-UVB	5.450	2.758	1.9764	1.000
No-UV - Full-Spectrum	5.488	2.758	1.9900	1.000

No-UVB - Full-Spectrum	0.038	2.758	0.0136	1.000

Mesh size: 1mm; Collection time: 3 months

Filter	Estimate	SE	t-value	P value
Dark - No-UV/Blue	-0.978	2.758	-0.3546	1.000
Dark - No-UV	-1.371	2.758	-0.4973	1.000
Dark - No-UVB	-1.849	2.758	-0.6705	1.000
Dark - Full-Spectrum	1.920	2.758	0.6962	1.000
No-UV/Blue - No-UV	-0.393	2.758	-0.1427	1.000
No-UV/Blue - No-UVB	-0.871	2.758	-0.3159	1.000
No-UV/Blue - Full-Spectrum	2.898	2.758	1.0508	1.000
No-UV - No-UVB	-0.478	2.758	-0.1732	1.000
No-UV - Full-Spectrum	3.291	2.758	1.1935	1.000
No-UVB - Full-Spectrum	3.769	2.758	1.3667	1.000

Mesh size: 1mm; Collection time: 5 months

Filter	Estimate	SE	t-value	P value
Dark - No-UV/Blue	**-16.620**	**2.758**	**-6.0271**	**< 0.001**
Dark - No-UV	**-15.123**	**2.758**	**-5.4840**	**< 0.001**
Dark - No-UVB	-9.118	2.758	-3.3065	0.415
Dark - Full-Spectrum	-7.984	2.758	-2.8954	1.000
No-UV/Blue - No-UV	1.498	2.758	0.5431	1.000
No-UV/Blue - No-UVB	7.502	2.758	2.7206	1.000
No-UV/Blue - Full-Spectrum	8.636	2.758	3.1318	< 0.001
No-UV - No-UVB	6.005	2.758	2.1775	1.000
No-UV - Full-Spectrum	7.139	2.758	2.5887	1.000
No-UVB - Full-Spectrum	1.134	2.758	0.4112	1.000

Mesh size: 1mm; Collection time: 7 months

Filter	Estimate	SE	t-value	P value
Dark - No-UV/Blue	**-11.025**	**2.758**	**-3.9980**	**0.042**
Dark - No-UV	**-11.294**	**2.758**	**-4.0957**	**0.030**
Dark - No-UVB	-9.233	2.758	-3.3482	0.370
Dark - Full-Spectrum	-4.558	2.758	-1.6528	1.000
No-UV/Blue - No-UV	-0.269	2.758	-0.0977	1.000
No-UV/Blue - No-UVB	1.792	2.758	0.6497	1.000
No-UV/Blue - Full-Spectrum	6.467	2.758	2.3452	1.000
No-UV - No-UVB	2.061	2.758	0.7474	1.000

No-UV - Full-Spectrum	6.737	2.758	2.4429	1.000
No-UVB - Full-Spectrum	4.675	2.758	1.6955	1.000

Table S5 Pairwise comparisons for filter treatments on ash litter C content per mesh and collection times: t- tests, with the Holm's correction for multiple comparisons, were used to calculate the *P* values. Significant contrasts are shown in bold.

Mesh size: 0.1mm; Collection time: 3 months

Filter	Estimate	SE	t-value	P value
Dark - No-UV/Blue	17.976	6.947	2.5875	1.000
Dark - No-UV	13.483	6.947	1.9408	1.000
Dark - No-UVB	15.502	6.947	2.2315	1.000
Dark - Full-Spectrum	20.920	6.947	3.0114	1.000
No-UV/Blue - No-UV	-4.493	6.947	-0.6468	1.000
No-UV/Blue - No-UVB	-2.474	6.947	-0.3561	1.000
No-UV/Blue - Full-Spectrum	2.944	6.947	0.4238	1.000
No-UV - No-UVB	2.020	6.947	0.2907	1.000
No-UV - Full-Spectrum	7.438	6.947	1.0706	1.000
No-UVB - Full-Spectrum	5.418	6.947	0.7799	1.000

Mesh size: 0.1mm; Collection time: 5 months

Filter	Estimate	SE	t-value	P value
Dark - No-UV/Blue	13.560	6.947	1.9518	1.000
Dark - No-UV	22.146	6.947	3.1877	0.657
Dark - No-UVB	**32.528**	**6.947**	**4.6822**	**0.003**
Dark - Full-Spectrum	24.555	6.947	3.5345	0.221
No-UV/Blue - No-UV	8.586	6.947	1.2359	1.000
No-UV/Blue - No-UVB	18.968	6.947	2.7304	1.000
No-UV/Blue - Full-Spectrum	10.995	6.947	1.5827	1.000
No-UV - No-UVB	10.382	6.947	1.4945	1.000
No-UV - Full-Spectrum	2.409	6.947	0.3468	1.000
No-UVB - Full-Spectrum	-7.973	6.947	-1.1477	1.000

Mesh size: 0.1mm; Collection time: 7 months

Filter	Estimate	SE	t-value	P value
Dark - No-UV/Blue	**28.025**	**6.947**	**4.0340**	**0.038**
Dark - No-UV	25.150	6.947	3.6202	0.166
Dark - No-UVB	**36.869**	**6.947**	**5.3071**	**< 0.001**
Dark - Full-Spectrum	**37.137**	**6.947**	**5.3456**	**< 0.001**
No-UV/Blue - No-UV	-2.874	6.947	-0.4137	1.000
No-UV/Blue - No-UVB	8.845	6.947	1.2731	1.000
No-UV/Blue - Full-Spectrum	9.112	6.947	1.3116	1.000
No-UV - No-UVB	11.719	6.947	1.6869	1.000
No-UV - Full-Spectrum	11.986	6.947	1.7254	1.000

No-UVB - Full-Spectrum	0.268	6.947	0.0385	1.000

Mesh size: 1mm; Collection time: 3 months

Filter	Estimate	SE	t-value	P value
Dark - No-UV/Blue	12.422	6.947	1.7880	1.000
Dark - No-UV	10.072	6.947	1.4498	1.000
Dark - No-UVB	8.623	6.947	1.2412	1.000
Dark - Full-Spectrum	12.356	6.947	1.7786	1.000
No-UV/Blue - No-UV	-2.350	6.947	-0.3383	1.000
No-UV/Blue - No-UVB	-3.799	6.947	-0.5468	1.000
No-UV/Blue - Full-Spectrum	-0.065	6.947	-0.0094	1.000
No-UV - No-UVB	-1.449	6.947	-0.2085	1.000
No-UV - Full-Spectrum	2.285	6.947	0.3289	1.000
No-UVB - Full-Spectrum	3.733	6.947	0.5374	1.000

Mesh size: 1mm; Collection time: 5 months

Filter	Estimate	SE	t-value	P value
Dark - No-UV/Blue	**-30.889**	**6.947**	**-4.4462**	**0.008**
Dark - No-UV	-17.603	6.947	-2.5338	1.000
Dark - No-UVB	-8.029	6.947	-1.1557	1.000
Dark - Full-Spectrum	-9.503	6.947	-1.3678	1.000
No-UV/Blue - No-UV	13.286	6.947	1.9124	1.000
No-UV/Blue - No-UVB	22.860	6.947	3.2905	0.485
No-UV/Blue - Full-Spectrum	21.386	6.947	3.0784	0.913
No-UV - No-UVB	9.574	6.947	1.3781	1.000
No-UV - Full-Spectrum	8.100	6.947	1.1659	1.000
No-UVB - Full-Spectrum	-1.474	6.947	-0.2122	1.000

Mesh size: 1mm; Collection time: 7 months

Filter	Estimate	SE	t-value	P value
Dark - No-UV/Blue	-19.189	6.947	-2.7622	1.000
Dark - No-UV	-16.977	6.947	-2.4437	1.000
Dark - No-UVB	-12.035	6.947	-1.7323	1.000
Dark - Full-Spectrum	-7.194	6.947	-1.0355	1.000
No-UV/Blue - No-UV	2.212	6.947	0.3184	1.000
No-UV/Blue - No-UVB	7.155	6.947	1.0299	1.000
No-UV/Blue - Full-Spectrum	11.995	6.947	1.7266	1.000
No-UV - No-UVB	4.943	6.947	0.7114	1.000

No-UV - Full-Spectrum	9.783	6.947	1.4082	1.000
No-UVB - Full-Spectrum	4.841	6.947	0.6968	1.000

Table S6 Pairwise comparisons for filter treatments on ash litter N content per mesh and collection times: t- tests, with the Holm's correction for multiple comparisons, were used to calculate the *P* values. Significant contrasts are shown in bold.

Mesh size: 0.1mm				
Filter	**Estimate**	**SE**	**t-value**	**P value**
Dark - No-UV/Blue	4.617	1.592	2.8999	0.129
Dark - No-UV	4.100	1.592	2.5753	0.314
Dark - No-UVB	**6.751**	**1.592**	**4.2403**	**0.002**
Dark - Full-Spectrum	**7.143**	**1.592**	**4.4867**	**< 0.001**
No-UV/Blue - No-UV	-0.517	1.592	-0.3245	1.000
No-UV/Blue - No-UVB	2.134	1.592	1.3405	1.000
No-UV/Blue - Full-Spectrum	2.526	1.592	1.5868	1.000
No-UV - No-UVB	2.651	1.592	1.6650	0.918
No-UV - Full-Spectrum	3.043	1.592	1.9113	1.000
No-UVB - Full-Spectrum	0.392	1.592	0.2463	1.000
Mesh size: 1mm				
Filter	**Estimate**	**SE**	**t-value**	**P value**
Dark - No-UV/Blue	**-9.541**	**1.592**	**-5.9928**	**< 0.001**
Dark - No-UV	**-9.263**	**1.592**	**-5.8180**	**< 0.001**
Dark - No-UVB	**-6.733**	**1.592**	**-4.2293**	**0.002**
Dark - Full-Spectrum	-3.541	1.592	-2.2239	0.701
No-UV/Blue - No-UV	0.278	1.592	0.1748	1.000
No-UV/Blue - No-UVB	2.808	1.592	1.7635	1.000
No-UV/Blue - Full-Spectrum	**6.000**	**1.592**	**3.7688**	**0.008**
No-UV - No-UVB	2.529	1.592	1.5887	1.000
No-UV - Full-Spectrum	**5.722**	**1.592**	**3.5940**	**0.015**
No-UVB - Full-Spectrum	3.193	1.592	2.0053	1.000

Table S7 Pairwise comparisons for filter treatments on ash litter C content per mesh treatment: t- tests, with the Holm's correction for multiple comparisons, were used to calculate the *P* values. Significant contrasts are shown in bold.

Mesh size: 0.1mm				
Filter	**Estimate**	**SE**	**t-value**	**P value**
Dark - No-UV/Blue	**19.853**	**4.011**	**4.9498**	**< 0.001**
Dark - No-UV	**20.260**	**4.011**	**5.0511**	**< 0.001**
Dark - No-UVB	**28.300**	**4.011**	**7.0557**	**< 0.001**
Dark - Full-Spectrum	**27.537**	**4.011**	**6.8656**	**< 0.001**
No-UV/Blue - No-UV	0.406	4.011	0.1013	1.000
No-UV/Blue - No-UVB	8.446	4.011	2.1058	1.000
No-UV/Blue - Full-Spectrum	7.684	4.011	1.9157	1.000
No-UV - No-UVB	8.040	4.011	2.0046	0.918
No-UV - Full-Spectrum	7.278	4.011	1.8145	1.000
No-UVB - Full-Spectrum	-0.762	4.011	-0.1901	1.000
Mesh size: 1mm				
Filter	**Estimate**	**SE**	**t-value**	**P value**
Dark - No-UV/Blue	-12.552	4.011	-3.1294	0.079
Dark - No-UV	-8.169	4.011	-2.0368	1.000
Dark - No-UVB	-3.813	4.011	-0.9508	1.000
Dark - Full-Spectrum	-1.447	4.011	-0.3607	1.000
No-UV/Blue - No-UV	4.383	4.011	1.0927	1.000
No-UV/Blue - No-UVB	8.739	4.011	2.1787	0.939
No-UV/Blue - Full-Spectrum	11.105	4.011	2.7687	0.215
No-UV - No-UVB	4.356	4.011	1.0860	1.000
No-UV - Full-Spectrum	6.723	4.011	1.6761	1.000
No-UVB - Full-Spectrum	2.367	4.011	0.5900	1.000

Table S8 Pairwise comparisons for filter treatments on ash litter N content per mesh treatment: t- tests, with the Holm's correction for multiple comparisons, were used to calculate the *P* values. Significant contrasts are shown in bold.

Oak (*Quercus robur* L.)				
Filter	**Estimate**	**SE**	**t-value**	**P value**
Dark - No-UV/Blue	0.082	1.997	0.0413	0.967
Dark - No-UV	**6.305**	**1.997**	**3.1574**	**0.016**
Dark - No-UVB	3.873	1.997	1.9397	0.272
Dark - Full-Spectrum	**9.942**	**1.997**	**4.9791**	**< 0.001**
No-UV/Blue - No-UV	**6.222**	**1.997**	**3.1161**	**0.016**
No-UV/Blue - No-UVB	3.791	1.997	1.8985	0.272
No-UV/Blue - Full-Spectrum	**9.860**	**1.997**	**4.9378**	**< 0.001**
No-UV - No-UVB	-2.431	1.997	-1.2177	0.451
No-UV - Full-Spectrum	3.637	1.997	1.8217	0.272
No-UVB - Full-Spectrum	**6.069**	**1.997**	**3.0394**	**0.017**
Beech (*Fagus sylvatica* L.)				
Filter	**Estimate**	**SE**	**t-value**	**P value**
Dark - No-UV/Blue	1.432	3.365	0.4256	0.67
Dark - No-UV	**10.860**	**3.365**	**3.2269**	**0.009**
Dark - No-UVB	**21.335**	**3.365**	**6.3393**	**< 0.001**
Dark - Full-Spectrum	**16.176**	**3.365**	**4.8064**	**< 0.001**
No-UV/Blue - No-UV	**9.428**	**3.365**	**2.8013**	**0.023**
No-UV/Blue - No-UVB	**19.902**	**3.365**	**5.9137**	**< 0.001**
No-UV/Blue - Full-Spectrum	**14.743**	**3.365**	**4.3808**	**< 0.001**
No-UV - No-UVB	**10.475**	**3.365**	**3.1124**	**0.011**
No-UV - Full-Spectrum	5.316	3.365	1.5795	0.349308
No-UVB - Full-Spectrum	-5.159	3.365	-1.5329	0.349308

Table S9 Pairwise comparisons for filter treatments on beech and oak litter C content: t-tests, with the Holm's correction for multiple comparisons, were used to calculate the *P* values. Significant contrasts are shown in bold.

Oak (*Quercus robur* L.)				
Filter	**Estimate**	**SE**	**t-value**	**P value**
Dark - No-UV/Blue	5.823	4.779	1.2184	0.676
Dark - No-UV	**22.564**	**4.779**	**4.7210**	**< 0.001**
Dark - No-UVB	**20.736**	**4.779**	**4.3386**	**< 0.001**
Dark - Full-Spectrum	**27.929**	**4.779**	**5.8435**	**< 0.001**
No-UV/Blue - No-UV	**16.741**	**4.779**	**3.5026**	**0.004**
No-UV/Blue - No-UVB	**14.913**	**4.779**	**3.1202**	**0.011**
No-UV/Blue - Full-Spectrum	**22.105**	**4.779**	**4.6251**	**< 0.001**
No-UV - No-UVB	-1.828	4.779	-0.3824	0.703
No-UV - Full-Spectrum	5.365	4.779	1.1225	0.676
No-UVB - Full-Spectrum	7.192	4.779	1.5049	0.539
Beech (*Fagus sylvatica* L.)				
Filter	**Estimate**	**SE**	**t-value**	**P value**
Dark - No-UV/Blue	32.311	23.889	1.3525	0.357
Dark - No-UV	**121.617**	**23.889**	**5.0909**	**< 0.001**
Dark - No-UVB	**165.686**	**23.889**	**6.9356**	**< 0.001**
Dark - Full-Spectrum	**117.593**	**23.889**	**4.9224**	**< 0.001**
No-UV/Blue - No-UV	**89.307**	**23.889**	**3.7384**	**0.002**
No-UV/Blue - No-UVB	**133.376**	**23.889**	**5.5831**	**< 0.001**
No-UV/Blue - Full-Spectrum	**85.282**	**23.889**	**3.5699**	**0.002**
No-UV - No-UVB	44.069	23.889	1.8447	0.201
No-UV - Full-Spectrum	-4.025	23.889	-0.1685	0.866
No-UVB - Full-Spectrum	-48.094	23.889	-2.0132	0.184

Table S10 Pairwise comparisons for filter treatments on beech and oak litter N content: t- tests, with the Holm's correction for multiple comparisons, were used to calculate the *P* values. Significant contrasts are shown in bold.

Ash (*Fraxinus excelsior* L.)					
Factors	**d.f.**	**SS**	**MS**	**F**	***p***
Mesh	1	2.857	2.857	1.7595	0.187
Filter	**4**	**77.735**	**19.434**	**11.9698**	**< 0.001**
Time	**2**	**88.268**	**44.134**	**27.1832**	**< 0.001**
Mesh x Filter	4	6.148	1.537	0.9467	0.440
Mesh x Time	2	1.899	0.950	0.5849	0.559
Filter x Time	8	21.541	2.693	1.6584	0.116
Mesh x Filter x Time	8	4.650	0.581	0.3580	0.941
Residuals	120	194.828	1.624		
Oak (*Quecus robur* L.)					
Factors	**d.f.**	**SS**	**MS**	**F**	***p***
Mesh	1	0.023	0.0235	0.0180	0.894
Filter	**4**	**80.622**	**20.1556**	**15.4383**	**< 0.001**
Time	**2**	**51.577**	**25.7885**	**19.7529**	**< 0.001**
Mesh x Filter	**4**	**28.015**	**7.0038**	**5.3646**	**< 0.001**
Mesh x Time	2	0.982	0.4909	0.3760	0.687
Filter x Time	8	20.432	2.5539	1.9562	0.058
Mesh x Filter x Time	8	5.852	0.7315	0.5603	0.808
Residuals	120	156.667	1.3056		
Beech (*Fagus sylvatica* L.)					
Factors	**d.f.**	**SS**	**MS**	**F**	***p***
Mesh	**1**	**43.56**	**43.556**	**5.8811**	**0.017**
Filter	**4**	**288.45**	**72.113**	**9.7371**	**< 0.001**
Time	**2**	**359.53**	**179.766**	**24.2731**	**< 0.001**
Mesh x Filter	4	8.60	2.151	0.2905	0.884
Mesh x Time	2	8.88	4.441	0.5997	0.551
Filter x Time	**8**	**142.10**	**17.763**	**2.3984**	**0.020**
Mesh x Filter x Time	8	36.76	4.595	0.6204	0.759
Residuals	120	888.72	7.406		

Table S11 ANOVAs' results of three categorical factors (Mesh: mesh size with 2 levels, Filter with 5 levels and Time with 3 levels) and their interactions on a single dependent variable: C:N for the three species. Degrees of freedom (d.f.), sum of squares (SS), mean square (MS), F statistic (F) and p-value (p) are presented. Significant terms are shown in

bold. Since dropping non-significant terms didn’t change the model, we decided to keep them.

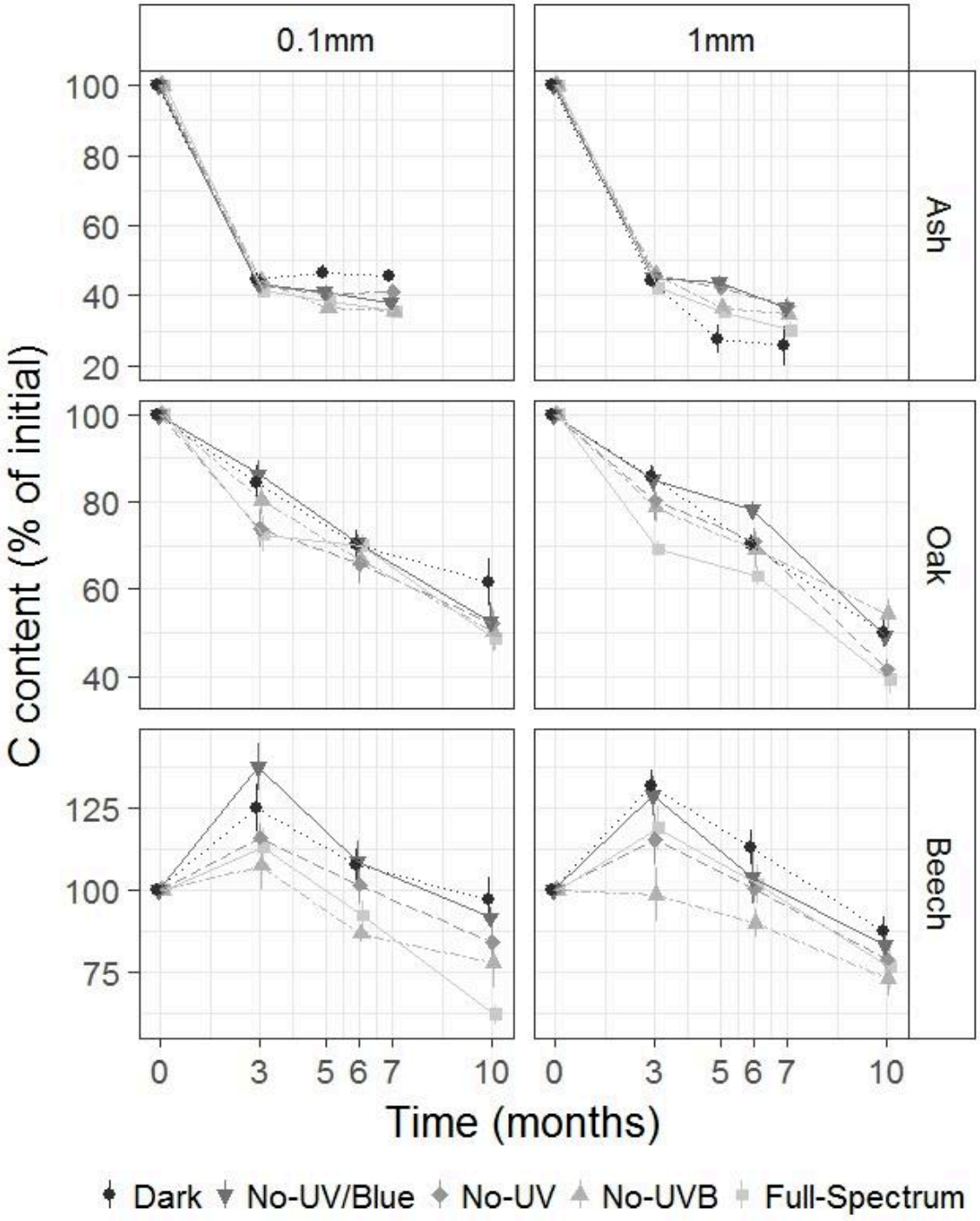

Figure S7 Carbon content in percentage of initial weight for each species litter, mesh size and filter treatment. Means ± SE are shown (n = 5)

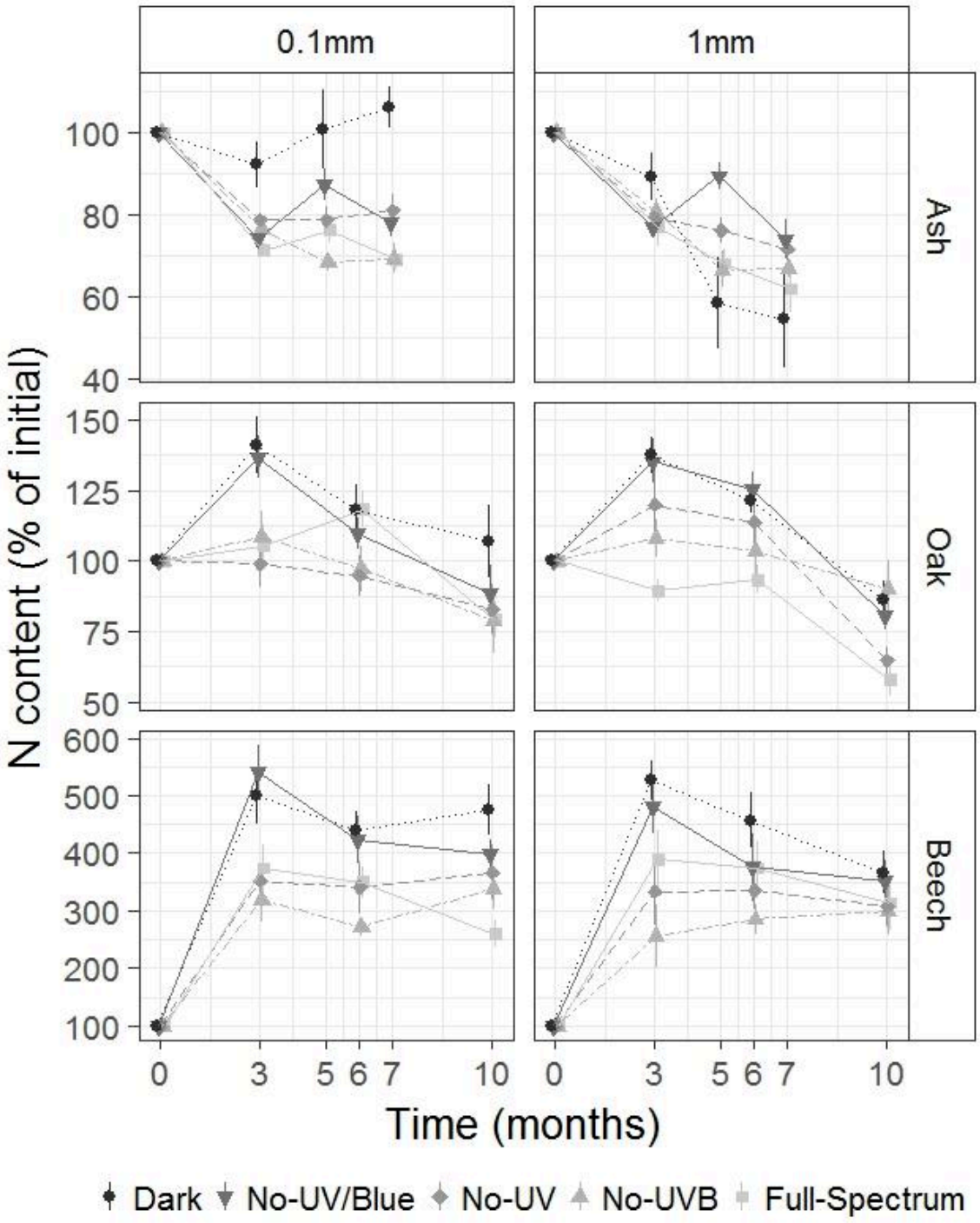

Figure S8 Nitrogen content in percentage of initial weight for each species litter, mesh size and filter treatment. Means ± SE are shown (n = 5)

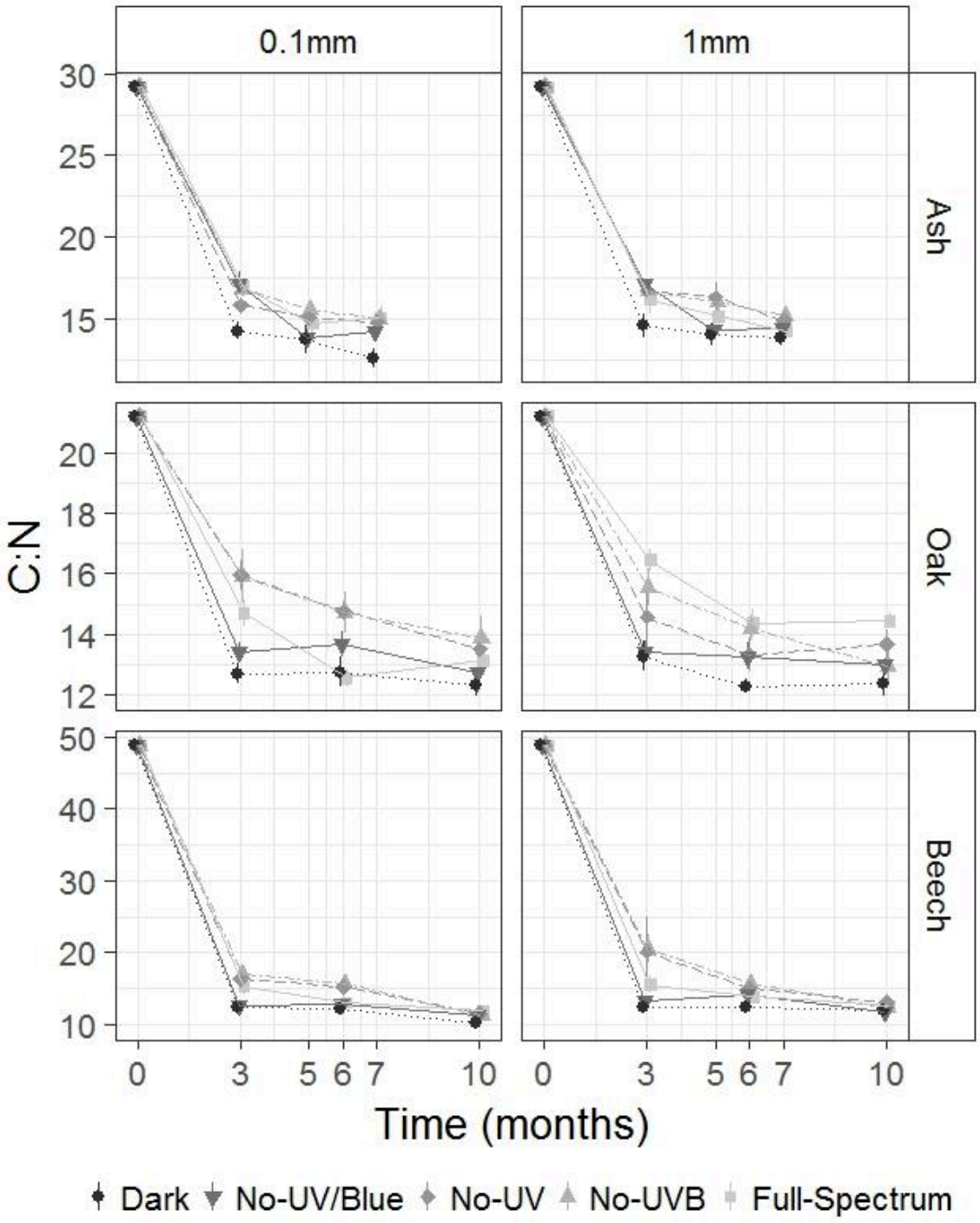

Figure S9 C:N ratio for each species litter, mesh size and filter treatment. Means ± SE are shown (n = 5).

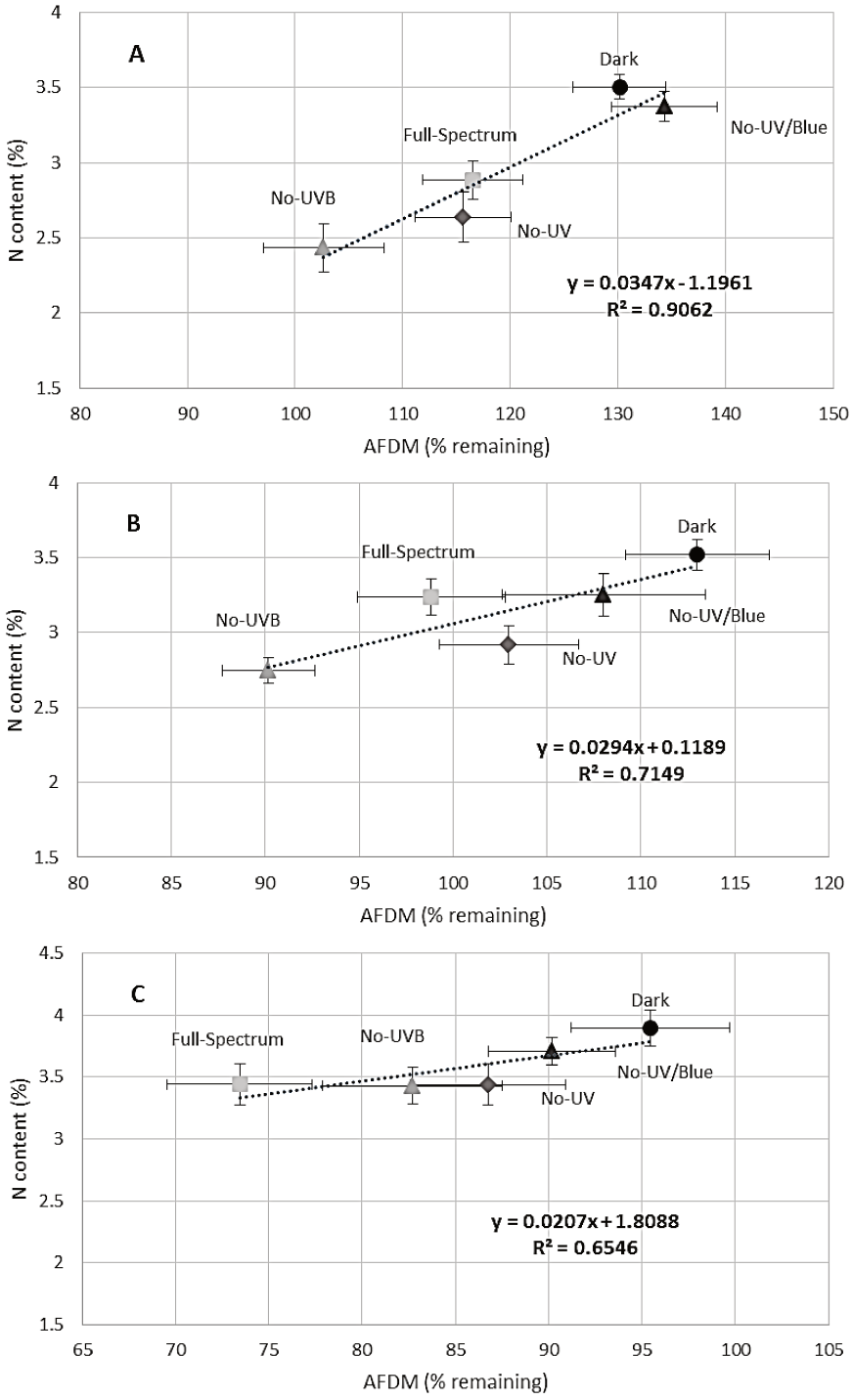

Figure S10 Scatterplot showing the linear regression and the coefficient of determination (R2) between remaining mass and N content in beech litter at the three collection dates, (A) 3 months, (B) 6 months and (C) 10 months after deployment. Means and standard errors are shown for each treatment (n=10).

Collection time (months)	Filter treatment /unfiltered	UV-B (mmol m-2 day-1)	UV-A (mol m-2 day-1)	Blue light (mol m-2 day-1)	PAR (mol m-2 day-1)
3	Dark	-5.1668	0.0282	0.4469	2.9607
	No-UV/blue	-5.5027	0.1222	5.6734	1324.7577
	No-UV	28.4433	16.0595	408.0265	2010.1689
	No-UVB	22.8178	34.2465	413.7614	2024.6098
	Full-Spectrum	820.0680	40.6450	411.3940	2023.8637
	Unfiltered	***924.3216***	***43.9426***	***429.5084***	***2094.3745***
5	Dark	-8.6741	0.0477	0.7508	5.0862
	No-UV/blue	-9.2380	0.2068	9.5318	2275.8206
	No-UV	47.7509	27.1667	685.5224	3453.2986
	No-UVB	38.3067	57.9323	695.1576	3478.1068
	Full-Spectrum	1376.7378	68.7562	691.1802	3476.8251
	Unfiltered	***1551.7595***	***74.3347***	***721.6139***	***3597.9567***
6	Dark	-8.9349	0.0491	0.7659	5.2476
	No-UV/blue	-9.5157	0.2131	9.7237	2348.0531
	No-UV	49.1863	27.9985	699.3250	3562.9032
	No-UVB	39.4582	59.7062	709.1542	3588.4988
	Full-Spectrum	1418.1227	70.8615	705.0966	3587.1764
	Unfiltered	***1598.4056***	***76.6108***	***736.1431***	***3712.1525***
7	Dark	-9.2452	0.0508	0.7830	5.4303
	No-UV/blue	-9.8462	0.2205	9.9409	2429.7929
	No-UV	50.8945	28.9716	714.9442	3686.9341
	No-UVB	40.8285	61.7813	724.9929	3713.4207
	Full-Spectrum	1467.3717	73.3244	720.8448	3712.0522
	Unfiltered	***1653.9156***	***79.2734***	***752.5847***	***3841.3791***
10	Dark	-10.0205	0.0551	0.8250	5.8786
	No-UV/blue	-10.6719	0.2389	10.4739	2630.3926
	No-UV	55.1626	31.3887	753.2758	3991.3213
	No-UVB	44.2526	66.9357	763.8633	4019.9946
	Full-Spectrum	1590.4300	79.4417	759.4927	4018.5131
	Unfiltered	***1792.6180***	***85.8871***	***792.9344***	***4158.5170***

Table S12 Estimated cumulated doses of UV-B and UV-A radiation, blue light and total PAR received by the litter under different filter treatments at each collection time, compared with unfiltered conditions. Estimates obtained by applying transmittance parameter of the filters measured using an array spectroradiometer (Maya2000 Pro Ocean Optics, Dunedin, FL, USA; D7-H-SMA cosine diffuser, Bentham Instruments Ltd, Reading, UK) that had been calibrated for measurements in the solar UV and visible radiation within the previous 12 months.

Variable	Factors	d.f.	SS	MS	F	*p*
Temperature	Mesh	1	6.5	6.46	0.9663	0.325
	Filter	**3**	**84.5**	**28.17**	**4.2137**	**0.006**
	Mesh x Filter	3	6.3	2.11	0.3158	0.814
	Residuals	1144	7646.8	6.68		
Moisture	**Mesh**	**1**	**198**	**197.55**	**5.9319**	**0.02**
	Filter	**3**	**1476**	**491.99**	**14.7729**	**< 0.001**
	Mesh x Filter	3	252	84.16	2.5269	0.06
	Residuals	1144	38100	33.30		

Table S. 13 ANOVAs' results of two categorical factors (Mesh: mesh size with 2 levels, Filter with 5 levels) and their interactions on a single dependent variable: temperature (above) and moisture (below) measured inside the different treatments during the decomposition study. Degrees of freedom (d.f.), sum of squares (SS), mean square (MS), F statistic (F) and p-value (p) are presented.

Temperature				
Filter	**Estimate**	**SE**	**t-value**	**P value**
Dark - No-UV/Blue	0.149266	0.21545	0.228666	0.819169
Dark - No-UVB	**-0.50544**	**0.21545**	**-2.81014**	**0.025182**
Dark - Full-Spectrum	-0.22852	0.21545	-1.06068	0.578119
No-UV/Blue - No-UVB	**-0.52471**	**0.21545**	**-3.0388**	**0.014575**
Full-Spectrum – No-UV/Blue	-0.42619	0.21545	-1.97812	0.192618
Full-Spectrum – No-UVB	-0.37692	0.21545	-1.74946	0.241441
Moisture				
Filter	**Estimate**	**SE**	**t-value**	**P value**
Dark - No-UV/Blue	0.021253	0.480912	0.044193	0.965
Dark - No-UVB	**2.689758**	**0.480912**	**5.593037**	**< 0.001**
Dark - Full-Spectrum	**1.57651**	**0.480912**	**3.278167**	**0.004**
No-UV/Blue - No-UVB	**2.668505**	**0.480912**	**5.548844**	**< 0.001**
Full-Spectrum – No-UV/Blue	**-1.55526**	**0.480912**	**-3.23397**	**0.004**
Full-Spectrum – No-UVB	**1.113249**	**0.480912**	**2.31487**	**0.042**
Mesh	**Estimate**	**SE**	**t-value**	**P value**
0.1 mm – 1 mm	**0.828223**	**0.340056**	**2.435547**	**0.015**

Table S. 14 Pairwise comparisons for filter treatments and mesh size on temperature and moisture: t- tests, with the Holm's correction for multiple comparisons, were used to calculate the *P* values. Significant contrasts are shown in bold.

CHAPTER II

Plant Physiology and Biochemistry 146 (2020) 42–54

Contents lists available at ScienceDirect

Plant Physiology and Biochemistry

journal homepage: www.elsevier.com/locate/plaphy

Research article

Ultraviolet radiation accelerates photodegradation under controlled conditions but slows the decomposition of senescent leaves from forest stands in southern Finland

Marta Pieristè[a,b,1], Santa Neimane[a,c,d,1], Twinkle Solanki[a], Line Nybakken[e], Alan G. Jones[f], Estelle Forey[b], Matthieu Chauvat[b], Jevgenija Ņečajeva[c], T. Matthew Robson[a,*]

[a] Organismal and Evolutionary Biology (OEB), Viikki Plant Science Centre (ViPS), Faculty of Biological and Environmental Science, P.O. Box 65, 00014, University of Helsinki, Finland
[b] Normandie Université, UNIROUEN, Ecodiv URA/EA1293, IRSTEA, FR Scale CNRS 3730, Rouen, France
[c] Department of Plant Physiology, University of Latvia, Jelgavas Street 1, LV-1004, Riga, Latvia
[d] Latvian State Forest Research Institute (Silava), Rigas Iela 111, Salaspils, Salaspils Pilsēta, LV-2169, Latvia
[e] Faculty of Environmental Sciences and Natural Resource Management, CERAD, Norwegian University of Life Sciences, 1432, Ås, Norway
[f] Forest Systems, Scion. 49 Sala Street, Private Bag 3020, Rotorua, 3046, New Zealand

ARTICLE INFO

Keywords:
Photodegradation
Phenolic compounds
UV radiation
Flavonoids
Understorey light environment

ABSTRACT

Depending on the environment, sunlight can positively or negatively affect litter decomposition, through the ensemble of direct and indirect processes constituting photodegradation. Which of these processes predominate depends on the ecosystem studied and on the spectral composition of sunlight received. To examine the relevance of photodegradation for litter decomposition in forest understoreys, we filtered ultraviolet radiation (UV) and blue light from leaves of *Fagus sylvatica* and *Betula pendula* at two different stages of senescence in both a controlled-environment experiment and outdoors in four different forest stands (*Picea abies, Fagus sylvatica, Acer platanoides, Betula pendula*). Controlling for leaf orientation and initial differences in leaf chlorophyll and flavonol concentrations; we measured mass loss at the end of each experiment and characterised the phenolic profile of the leaf litter following photodegradation. In most forest stands, less mass was lost from decomposing leaves that received solar UV radiation compared with those under UV-attenuating filters, while in the controlled environment UV-A radiation either slightly accelerated or had no significant effect on photodegradation, according to species identity. Only a few individual phenolic compounds were affected by our different filter treatments, but photodegradation did affect the phenolic profile. We can conclude that photodegradation has a small stand- and species-specific effect on the decomposition of surface leaf litter in forest understoreys during the winter following leaf fall in southern Finland. Photodegradation was wavelength-dependent and modulated by the canopy species filtering sunlight and likely creating different combinations of spectral composition, moisture, temperature and snowpack characteristics.

1. Introduction

Decomposition is a key ecological process in nutrient cycling, during which organic compounds are broken down and thus become available for primary producers. In temperate and boreal forests, decomposition is controlled by many biotic and abiotic factors, such as temperature, moisture, frost, freeze-thaw cycles, soil pH, sunlight, microbial communities, soil fauna and fertility, etc. (Swift et al., 1979; Sulkava and Huhta, 2003; Chapin et al., 2002; Liski et al., 2003; Zhu et al., 2013; Paudel et al., 2015). Litter traits, together with climatic variables, explain up to 70% of the decomposition rates in terrestrial ecosystems on a global scale (Parton et al., 2007). However, at a continental scale, the rate of decomposition is mainly controlled by litter chemistry (Perry et al., 2008). Moreover, canopy trees may impact decomposition directly through their leaf litter traits or indirectly by altering the microenvironment including solar radiation in the understorey; this effect at the local level may have a bigger impact on decomposition than large-scale climatic gradients (Joly et al., 2017).

* Corresponding author.
E-mail address: matthew.robson@helsinki.fi (T.M. Robson).
[1] Joint first author contribution.

https://doi.org/10.1016/j.plaphy.2019.11.005
Received 3 June 2019; Received in revised form 4 November 2019; Accepted 5 November 2019
Available online 06 November 2019
0981-9428/

Abbreviations

UV	Ultraviolet radiation (280–400 nm)
UV-B	Ultraviolet-B radiation (280–320 nm)
UV-A	Ultraviolet-A radiation (320–400 nm)
PAR	Photosynthetically Active Radiation (400–700 nm)
FW	Fresh weight
DW	Dry weight
C	Carbon
N	Nitrogen
C:N	Carbon to nitrogen ratio
[C]	Concentration of carbon
[N]	Concentration of nitrogen
Lig:N	Lignin to nitrogen ratio
LAI	Leaf Area Index
GLI	Global Light Index
HPLC	High-performance liquid chromatography
MeOH	Methanol

Solar radiation impacts decomposition, both directly and indirectly - through photochemical mineralization, photopriming, and microbial photoinhibition (Predick et al., 2018), together these processes are known as photodegradation. In arid and semi-arid environments, photodegradation has been shown to play a key role in the control of litter decomposition rate and to be effected by UV radiation and the short-wavelength region of the visible spectrum (such as blue and green light) (Austin and Vivanco, 2006; Austin et al., 2016). However, worldwide studies have presented conflicting results regarding factors that enhance the photodegradation of plant litter (King et al., 2012; Barnes et al., 2015). The variability of climatic conditions (cloud cover, rainfall, Ozone Layer thickness, pollutants concentration, etc.), impacting the total amount of incoming radiation, makes it hard to assess the role of photodegradation in global nutrient fluxes and how they might respond to climate change (Madronich et al., 1998; Bornman et al., 2015; Sercu et al., 2017; Erdenebileg et al., 2018). At mid-high latitudes, large seasonal differences in sunlight hours mean that, when overstorey canopies are open and there is no snow cover during the autumn and early spring, high solar irradiances can transiently reach the understorey. Nevertheless, the total irradiance received annually at the forest floor is still quite small compared with areas with no canopy cover (Hartikainen et al., 2018).

While solar UV radiation can on balance enhance the rate of decomposition (Bornman et al., 2019a), its positive and negative effects may even out because UV-B and UV-A radiation differ in their effect on decomposition according to environmental conditions and litter chemistry (Austin et al., 2016). Typically, traits associated with litter chemistry such as its concentration of lignin and phenolics (such as tannins), carbon to nitrogen ratio (C:N), lignin to nitrogen ratio (lig:N), etc., were thought to determine the rate of decomposition (Hoorens et al., 2003). However, recent studies have found traditional indices of litter quality to poorly explain litter mass loss due to photodegradation in arid environments (Day et al., 2018; Liu et al., 2018).

The morphology and biochemistry of living leaves determine their optical properties, but once senescent the continued capacity of these leaf traits to interact with sunlight, and potentially influence photodegradation, has not been widely studied. Some of the phenolic compounds in the leaf epidermis, absorb UV radiation and consequently screen the interior of the leaf potentially interfering with photodegradation (Kotilainen et al., 2009). During leaf senescence, when plants remobilise the nutrients held in chlorophyll, the content of epidermal UV-screening phenolics is also known to change (Mattila et al., 2018; Hoch et al., 2001). Green leaves are rich in chlorophyll and photosynthetic enzymes which have a high nitrogen content, making them more palatable to decomposers and faster to decompose (Cornelissen, 1996) than yellow leaves.

To test how spectral composition affects photodegradation and identify its role in the initial phase of leaf litter decomposition in forest understoreys, we performed two parallel experiments using filters to create different light treatments. We tested the effect of the blue and UV portions of the spectrum on photodegradation of senescent leaves (1) in a controlled experiment in a growth room, and (2) whether these effects remained evident in equivalent leaves under the same set of filters in a decomposition experiment in forest stands. We employed senescent leaves from two species with contrasting leaf morphological traits; *Betula pendula* which is light-demanding and produces leaves with an exploitative strategy, and *Fagus sylvatica* which grows in shadier stands and produces leaves with a conservative strategy expected to be more recalcitrant. We deployed these leaves in adjacent forest stands dominated by different canopy species designed to create continuum of understorey shade (from dark to light stands - *Picea abies, Fagus sylvatica, Acer platanoides, Betula pendula*). In order to test whether differences in pigment contents affecting leaf optical properties can affect photodegradation, we employed leaf litter at two different stages of senescence (green and yellow leaves). We expected green leaves to both photodegrade and decompose faster than yellow leaves because they contain more labile compounds. We also placed leaves under our filters in two different orientations (adaxial leaf epidermis facing upwards or downwards): while leaf orientation has no ecological significance in itself, the penetration of UV radiation through the adaxial and abaxial epidermis differs due to UV-screening by epidermal flavonols. Moreover, the abaxial side of the leaf is richer in stomata which favour light penetration (Day et al., 1993). Hence, leaf orientation will affect UV penetration into the leaf and may serve as a control for exposure of the targets of photodegradation in the mesophyll to UV radiation in otherwise similar leaves. We expected mass lost from decomposing leaves to be affected by the spectrum of radiation received during photodegradation, with greater mass loss from leaves exposed to UV radiation than those under dark or partially-attenuated spectra. We hypothesize that leaves with the abaxial epidermis facing upwards would decompose faster than leaves with the adaxial epidermis facing upwards, since the higher phenolic content of the adaxial epidermis provides more effective screening of the mesophyll from UV-radiation; and that this interaction between filter treatments and epidermal phenolics would be visible in the phenolic profile of litter following photodegradation.

2. Materials and methods

2.1. Sampling and preparation of leaves for controlled and forest experiments

Leaves were harvested from six-year-old stands of *Betula pendula* and *Fagus sylvatica*, planted in Viikki experimental plots at the University of Helsinki in southern Finland (60°13′39.7′N, 25°01′09.5′E). This vegetation zone is where the hemi-boreal borders the southern boreal region (Ahti et al., 1968).

Leaves that received full sun in the canopy ("sun leaves") of approximately the same size (c 20 cm^2) were harvested in a systematic fashion, directly from the south-side and upper third of each tree, avoiding the leaves at the tip of the branch and those closest to the trunk. Only leaves with no visible signs of herbivory or pathogens were collected and not more than four leaves per tree. Green leaves of *B. pendula* and *F. sylvatica* were harvested on 29-09-2016 during autumn leaf senescence; fully senescent yellow leaves of the same size and at the same location on the trees as the green leaves, were harvested 8–14 days later.

Directly after leaf collection the petiole was removed, leaves were

numbered and put into plastic bags to restrict moisture loss and keep them fresh. Within 1 h of collection, the leaves were scanned for leaf area, which was calculated using imageJ (Schneider et al., 2012) following the protocol from (Wang, 2017). Leaves were then immediately weighed for fresh weight (FW) and optical measurements of leaf pigments taken with a Dualex Scientific$^+$ device (Force-A, Paris, France) on both sides of the leaves. These measurements give an index of epidermal flavonol content and leaf chlorophyll contents based on chlorophyll fluorescence and absorbance at various wavelengths of the spectrum, described by (Pfündel et al., 2007) and (Cerovic et al., 2012). Since some chlorophyll is required as a reference for the flavonol and anthocyanin measurements, those values where chlorophyll was very low (Dualex Index < 3.0) were not considered reliable and were removed from the analyses. The same place on the lamina of all leaves was measured, two-thirds down from the tip to the side of the midrib.

For the experiment in controlled conditions, for maximum realism in leaf traits and microbial communities, fresh leaves were deployed immediately after their harvest, whereas oven dried leaves were used for the field experiment as it was impractical to install the two experiments simultaneously. For this field experiment, 576 leaves were dried at 37 °C until they achieved a constant weight, which took 3 days for yellow leaves and 7 days for green leaves. Following the measurement of their dry mass, leaf area was remeasured and Dualex Scientific$^+$ measurements repeated as mentioned above, to test whether the epidermal flavonol values for both sides of the leaf, as well as leaf chlorophyll content, were affected by drying (the relationships between these values for fresh and dried leaves are given in Fig. S1).

The very tight relationship between the FW and dry weight (DW) for green and yellow leaves of each species was used to obtain a conversion factor for calculations of mass loss involving fresh leaves used in the controlled experiment (Fig. S2).

2.2. Filter treatments attenuating light and UV radiation

In the controlled and forest experiments, four different plastic films were used to create the different filter treatments. These were: a solid black/white polyester (0.07 mm thick, Siemenliike Siren, Helsinki, Finland) attenuating the full spectrum ("Dark"); transparent polyethene (0.05 mm thick, 04 PE-LD; Etola, Jyväskylä, Finland) transmitting > 95% of radiation throughout the spectrum ("Full-Spectrum"); Rosco #226 (0.2 mm thick, Supergel; Foiltek Oy, Vantaa, Finland) attenuating UV-A and UV-B radiation ("No-UVA" in controlled experiment and "No-UV" in field experiment), and Rosco #312 Canary Yellow (0.2 mm thick, Supergel; Foiltek Oy, Vantaa, Finland) attenuating UV-A and UV-B radiation and blue light ("No-UV/Blue"). Each filter was cut into 8- × -8-cm squares and attached to a leaf by a staple through the base of the midrib and to a Teflon mosquito net (mesh size 1.5 mm). Half of the leaves were arranged with their adaxial epidermis facing upwards and the other half with the abaxial epidermis facing upwards, in 16 randomised complete blocks in the controlled environment (Figs. S3A and B). A similar arrangement with 16 blocks per stand was employed in the forest stands (Figs. S3C and D). The spectral transmittance of all filter materials was found not to differ between before and after a period of exposure in the field exceeding the duration of the experiments (data from Qing-Wei Wang - not shown).

2.3. Controlled photodegradation experiment

The controlled experiment tested the effects of photodegradation on senescent leaves with and without UV-A radiation and blue light under a broad LED spectrum (Fig. 1) containing those spectral regions present in a forest understorey (Brelsford et al., 2018, 2019). A total of 256 fresh leaves were divided among the treatments: 2 species × 2 leaf

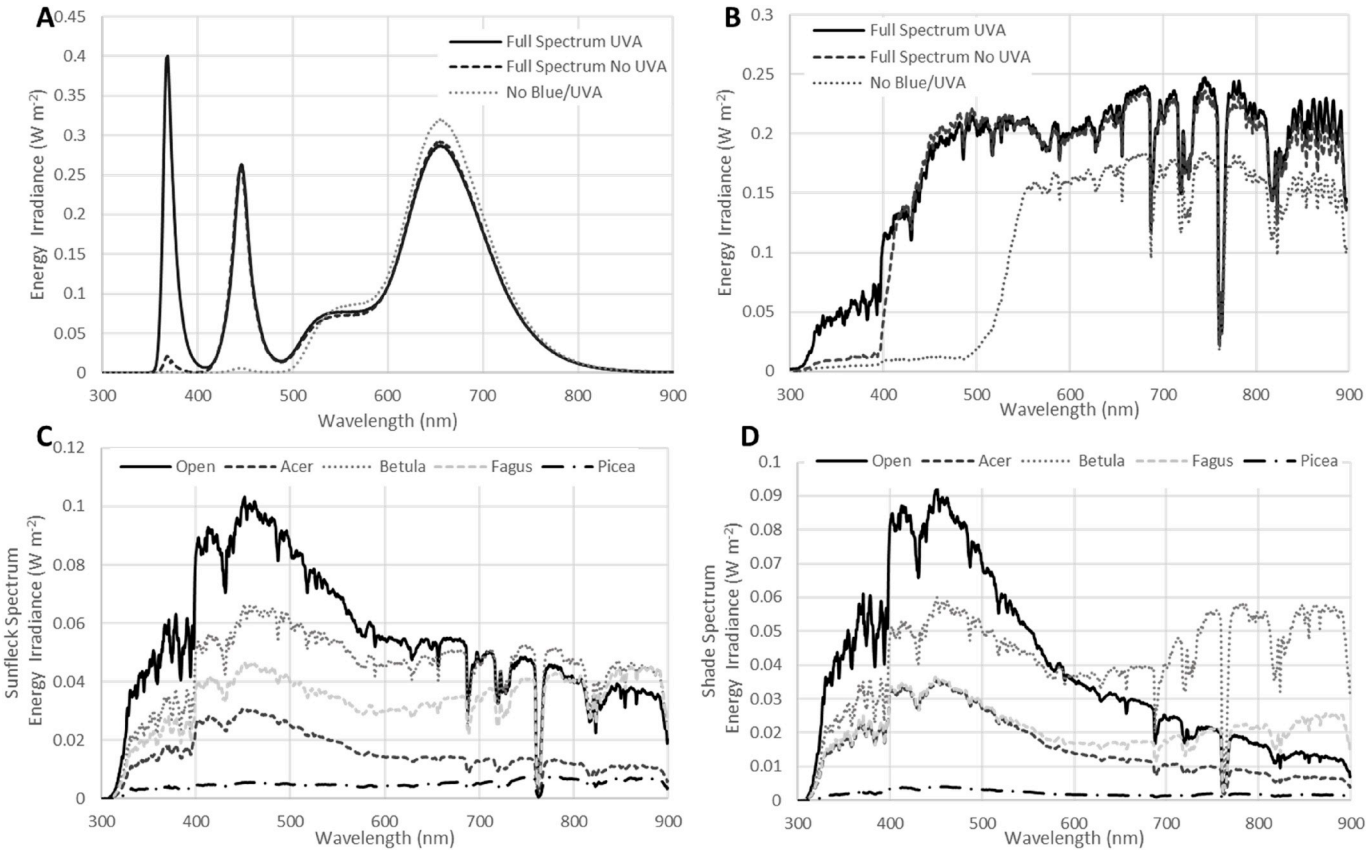

Fig. 1. Spectral treatments created by selective attenuation of radiation by plastic filters in experiments under (A) controlled and (B) sunlight conditions. Measurements (B) in full sun between 9:00–9:25 a.m. on October 4th, 2016 in Viikki field site. Measurements of (C) sunfleck and (D) shade spectra from each of the forest stands.

colours × 4 filter types × 16 replicate leaves with either the adaxial or abaxial side facing upwards. Leaves were positioned on mosquito netting on a metal shelf 40 cm beneath the light sources: UV-A LEDs (Z1-00UV00 365 nm GEN2 emittor, LED Engin, San Jose, CA, USA, 15 μmol m^{-2} s^{-1}) and broad-spectrum visible LED light (AP67, Valoya, Helsinki, Finland). Leaves received 168 μmol m^{-2} s^{-1} (6.04 mol m^{-2} d^{-1}) of photosynthetically active radiation (400–750 nm, PAR) plus 32 μmol m^{-2} s^{-1} (1.15 mol m^{-2} d^{-1}) of far red radiation; a similar exposure to those in the forest understoreys between October and February (Fig. S4). The lamps were illuminated in a cycle on for 10 h from 08:00–18:00 and off for 14 h. The irradiance under each lamp treatment and filter combination was measured with a Maya 2000 Pro array spectrometer (Ocean Optics Inc., Florida, USA), which had been calibrated for measurements of the UV–visible spectrum following (Aphalo and Jordan, 2017) and (Hartikainen et al., 2018) (Fig. 1). The temperature in the chamber was thermostatically controlled to 20 °C day/18 °C night and monitored in each compartment with i-button sensors (Maxim Integrated, San Jose, United States) (Fig. S5). Leaf temperature was monitored with a micro-epsilon high-precision infrared thermometer (Optris, Berlin, Germany) and was about 5 °C above the ambient daytime temperature when illuminated (Fig. S6). These data showed that temperature was on average 0.8 °C lower under the dark filter than the other filter treatments, and that the green *B. pendula* leaves were 1.0 °C cooler than the other leaves on average, but otherwise there were no differences among leaves.

To account for any uncontrolled gradients in temperature and irradiance in the controlled environment, leaves were rotated under each set of lamps every 2 weeks throughout the experiment. After 6 weeks (44–50 days) of filter treatments the first half of the leaves were removed (average daily mass loss 0.540%) and after 10 weeks (75–77 days) the remaining leaves were collected (average daily mass loss 0.534%). The two harvest dates were normalised to mean daily relative mass loss as there was no significant different (or interaction with other factors) between the two harvested cohorts (data not shown).

2.4. Forest decomposition experiment

Senescing leaves were arranged in four different forest stands in Viikki, Helsinki (60°13′39.7′N, 25°01′09.5′E), as described above, on 07-10-2016 for *F. sylvatica* leaves and 19-10-2016 for *B. pendula* leaves, and collected on 11-04-2017 (6 months after the beginning of the experiment) for both species. The canopy trees in the four different stands of differing leaf area index (LAI) were 10-year-old *B. pendula* and 6-year-old *F. sylvatica*, and mature (> 60 years old) *A. platanoides* and *P. abies* trees. Before starting the experiment, any ground vegetation (minimal) was removed from directly under and surrounding the leaves, and a thin litter layer consisting only of the surrounding leaf litter at each stand was placed between the ground and the mosquito net holding the leaves and filters to ensure conditions were natural and homogeneous (Figs. S2C and D). The mosquito net was anchored to the ground using nails. A fine bird net, minimally affecting the irradiance received by the experiment, was placed like a wigwam over the leaves to deflect any falling or blown leaves, which might otherwise build-up on the filters obscuring the sunlight. Any leaves stuck on the net were cleaned away every few days but any snow that was not intercepted by the canopy was allowed to accumulate and melt naturally on the filters over winter.

The spectral irradiance was measured in all the forest stands using an array spectroradiometer (Maya2000 Pro Ocean Optics, Dunedin, FL, USA; D7-H-SMA cosine diffuser, Bentham Instruments Ltd, Reading, UK) that had been calibrated within the previous 12 months for measurements spanning the regions of solar UV radiation and PAR (see Hartikainen et al., 2018 for details of the calibration), (Aphalo et al., 2012, 2013) (Tables S1 and S2). Hemispherical photos were taken at the same locations as spectral irradiance, to characterize canopy cover by calculation of the global light index (GLI) and the leaf area index (LAI) with the software Hemisfer (Schleppi et al., 2007; Thimonier et al., 2010) following the protocol from Hartikainen et al. (2018). Above-canopy PAR was obtained from the Viikki Fields Weather Station of the University of Helsinki located within the experimental site (60°13′39.7′N, 25°01′09.5′E). UV radiation was obtained from the Finnish Meteorological Institute (FMI) weather station located in the adjacent suburb of Kumpula (60°12′00.0″N, 24°57′36.0″E), Helsinki (Mäkelä et al., 2016; Heikkilä et al., 2016). Below-canopy irradiance was modelled from above-canopy irradiance data, whereby GLI and LAI estimated from hemispherical photos were used to model selective filtration by the different canopies, validated against understorey spectroradiometer measurements following the protocol in (Pieristè et al., 2019).

2.5. Mass loss, HPLC and C:N analyses of leaf litter

Following collection of the experimental leaf litter at the end of their decomposition and photodegradation periods, leaves were separated from their filters taking care not to lose any fragments of leaf. They were placed in paper bags and dried at 37 °C in a ventilated desiccating oven until reaching a constant weight (after 13 days) to obtain their DW. Worm casts and dirt were carefully removed from leaves that had decomposed outdoors using a small paintbrush, in order to reduce the error due to contamination from inorganic particles.

Biochemical analyses were done on litter samples from the controlled environment. To prepare leaves for biochemical analyses, first the midrib was cut out of the leaf, as was the small mark on the lamina used to number the leaf prior to decomposition. The remaining leaf lamina material was placed into a 1.5-ml Eppendorf tube. To grind the leaf material, 25 glass beads of 1 mm diameter (#22.222.0005, Retsch GmbH, Haan, Germay) were added to each tube, and tubes were shaken for 1.5–2 min in a Silamat S6 mixer (Ivoclar Vivadent, Amherst, USA) at rotation speed of 4500 rpm. Dry powdered samples were stored in the dark at room temperature between grinding and analysis.

For the elemental analysis, 5–6 mg of ground leaf material was used. The total nitrogen (N) and carbon (C), and the C:N ratio per leaf dry-mass were determined using a Vario Micro Cube (Elemental Analysis Systems GmbH, Hanau, Germany). For the analysis of phenolic compounds by HPLC (high-performance liquid chromatography), 10 mg of leaf material was used. Leaf extraction and HPLC analysis was performed as in (Kolstad et al., 2016). Compounds were identified by comparing the absorbance spectrum (270–320 nm) to commercially available standards. Flavonoid glycosides were identified down to their respective aglycones, and numbered (e.g. quercetin glyc1, quercetin glyc2) if we were not able to identify the type and position of glycosylation.

The same samples run for the HPLC analysis were used two-days later to determine the condensed tannin content by acid-butanol assay following the protocol of (Hagerman, 2002). The content of MeOH-insoluble condensed-tannin residues from phenolic compound extraction were mixed with methanol to give a total sample volume of 0.5 ml. Afterwards 3 ml of butyric acid (95% butanol, 5% hydrochloric acid) and 100 μl Fe reagent (2 M HCL with 2% ferric ammonium sulphate) were added and mixed. The sealed sample tubes were placed in boiling water for 50 min and once cooled their absorbance at 550 nm was measured with an UV-1800 spectrophotometer (Shimadzu Corp., Kyoto, Japan).

2.6. Data analysis

We first tested the effect of species (*Betula pendula* and *Fagus sylvatica*) and phase of senescence (green and yellow coloured leaves) on the rate of mass loss and on the biochemistry of leaf litter from the controlled experiments with a mixed-model ANOVA using the function lmer from package lme4 (Pinheiro et al., 2019).

The effects of our different filter treatments (Dark, No-UVA/Blue,

No-UVA, Full-Spectrum) and leaf orientation were tested separately for each species and leaf colour, using a split-plot mixed-model ANOVA. Filter treatment was the main fixed effect, while orientation (adaxial or abaxial epidermis up) was the split-plot effect, and harvest cohort was a random factor. Function glht from Multcomp package was used to obtain individual pair-wise comparisons, and Holm's adjustment was applied between treatments to account for multiple comparisons.

For the forest experiment, a three-way mixed model ANOVA was used, with stand an additional fixed effects factor in the models, otherwise the model was described above for mass loss in the controlled experiment. To better visualise the effects of filter treatments on mass loss and leaf chemistry in both experiments against a fixed baseline that is normalised for differences due to species and leaf colour, these data were plotted as response ratios for each filter type compared with the results under the dark filter.

When analysing HPLC data for birch leaves, because of insufficient leaf mass remaining from all levels of treatments at both leaf orientations, orientation could not be included as a fixed factor in the ANOVA model. As well as the ANOVA, patterns in the composition of the phenolic profile were mapped against explanatory variables for each species' litter by nonmetric multidimensional scaling using function metaMDS from community ecology package, vegan (Oksanen et al., 2019).

Relationships between abaxial and adaxial flavonols and anthocyanins, chlorophyll content and nitrogen balance index, as well as fresh weight and leaf area, were examined by determining correlation coefficients. Linear regression models were tested using R function lm. To plot non-linear relationships, i.e. between leaf nitrogen content and leaf carbon/nitrogen ratio, we used ggplot2 package (Wickham, 2009) and package ggpmisc version 0.2.15 (Aphalo, 2016) fitting a GAM smoother (stat_smooth). Irradiance spectra measured with the Maya 2000 Pro spectrometer were pre-processed using the R packages Ooacquire and Photobiology (Aphalo, 2015). All data were analysed in R core version 3.3.3 (R-Core-Team, 2018).

3. Results

3.1. Spectral irradiance in the forest experiment

The spectral irradiance differed among the forest stands (Fig. 1C and D, Fig. S4). The leaf litter in the *B. pendula* stand received the highest PAR and UV radiation over the study period (Table S3 Fig. S4) since this stand transmitted about 69% and 66% of above-canopy PAR and UV, respectively. The *Acer platanoides* stand transmitted 46% of above-canopy PAR, 51% of UV radiation and 52% of blue light, followed by the *Fagus sylvatica* stand (19% of PAR, 16% of UV, 13% blue) and the *Picea abies* stand (13% of PAR and UV, 14% blue: Fig. S4 and Table S3).

3.2. Effect of species, senescence stage and leaf orientation on harvested leaf traits

The traits of sampled green and yellow leaves from *F. sylvatica* and *B. pendula* are given in Table S4. In both species, epidermal flavonol content, as measured by Dualex, decreased during leaf senescence (from green to yellow leaves), in addition to the expected drop in chlorophyll and water contents (Table S4). Epidermal flavonols were higher for *B. pendula* than *F. sylvatica* leaves at the equivalent stage of senescence.

The relationship between upper epidermal and lower epidermal flavonols differed, similarly in both species, between green and yellow senescent leaves (Fig. S7). In green leaves, there was no correlation between the adaxial and abaxial flavonol content in *F. sylvatica*

Table 1
Mean (± 1 SE) values and ANOVA table for average daily mass loss, C and N content and C:N in yellow and green leaves of *F. sylvatica* and *B. pendula* in the controlled photodegradation experiment (up to 77 days). $p < 0.05$ are in bold face, and $0.05 < p < 0.10$ underlined.

Species	*F. sylvatica*		*B. pendula*		ANOVA		
Leaf colour	Green	Yellow	Green	Yellow	Colour (C)	Species (S)	C × S
Mass Loss (% day^{-1})	0.62 ± 0.02	0.47 ± 0.02	0.66 ± 0.02	0.41 ± 0.02	F = 224 **$p = 0.003$**	F = 1.04 $p = 0.370$	F = 17.7 $p = 0.052$
C content (% g g^{-1})	45.45 ± 0.12	45.41 ± 0.15	48.32 ± 0.11	49.47 ± 0.15	F = 15.8 $p = 0.058$	F = 665 **$p = 0.001$**	F = 19.5 **$p = 0.048$**
N content (% g g^{-1})	2.26 ± 0.03	1.40 ± 0.02	3.01 ± 0.04	1.18 ± 0.03	F = 1581 **$p < 0.001$**	F = 55.7 **$p = 0.017$**	F = 204 **$p = 0.005$**
C:N Ratio	20.38 ± 0.31	32.47 ± 0.41	16.29 ± 0.26	43.61 ± 1.37	F = 882 **$p = 0.001$**	F = 31.9 **$p = 0.030$**	F = 135 **$p = 0.007$**

Species	*F. sylvatica*				ANOVA	*B. pendula*				ANOVA
Filter Treatment	Dark	No UVA/Blue	No UVA	Full Spectrum	Filter Treatment	Dark	No UVA/Blue	No UVA	Full Spectrum	Filter Treatments
Green leaves										
Mass Loss (% day^{-1})	0.58 ± 0.03	0.60 ± 0.02	0.62 ± 0.02	0.68 ± 0.02	F = 2.59 $p = 0.062$	0.64 ± 0.02	0.65 ± 0.02	0.67 ± 0.02	0.68 ± 0.01	F = 1.49 $p = 0.226$
C content (% g g^{-1})	45.34 ± 0.41	44.95 ± 0.27	45.36 ± 0.16	45.54 ± 0.20	F = 0.08 $p = 0.777$	48.58 ± 0.23	47.99 ± 0.27	47.99 ± 0.23	48.24 ± 0.33	F = 0.38 $p = 0.541$
N content (% g g^{-1})	2.21 ± 0.06	2.25 ± 0.06	2.30 ± 0.06	2.28 ± 0.07	F = 0.19 $p = 0.828$	3.00 ± 0.10	3.09 ± 0.09	2.96 ± 0.07	2.91 ± 0.10	F = 0.72 $p = 0.484$
C:N Ratio	20.77 ± 0.59	20.28 ± 0.59	19.96 ± 0.61	20.34 ± 0.70	F = 0.10 $p = 0.903$	16.47 ± 0.61	15.67 ± 0.44	16.30 ± 0.39	16.87 ± 0.65	F = 0.87 $p = 0.359$
Yellow leaves										
Mass Loss (% day^{-1})	0.46 ± 0.02	0.46 ± 0.03	0.47 ± 0.02	0.47 ± 0.02	F = 0.09 $p = 0.965$	0.39 ± 0.03	0.40 ± 0.03	0.39 ± 0.02	0.45 ± 0.03	F = 2.31 $\underline{p = 0.085}$
C content (% g g^{-1})	45.57 ± 0.32	45.43 ± 0.36	45.54 ± 0.28	44.91 ± 0.26	F = 1.13 $p = 0.332$	49.41 ± 0.30	49.94 ± 0.34	49.34 ± 0.35	48.99 ± 0.24	F = 1.67 $p = 0.424$
N content (% g g^{-1})	1.41 ± 0.04	1.41 ± 0.04	1.43 ± 0.04	1.39 ± 0.03	F = 0.33 $p = 0.719$	1.27 ± 0.08	1.16 ± 0.04	1.18 ± 0.07	1.13 ± 0.08	F = 4.71 **$p = 0.048$**
C:N Ratio	32.64 ± 0.89	32.54 ± 0.85	31.95 ± 0.77	32.45 ± 0.84	F = 0.15 $p = 0.869$	41.9 ± 2.82	44.74 ± 2.08	43.87 ± 2.13	46.09 ± 2.61	F = 4.15 $\underline{p = 0.061}$

(R^2_{adj} = 0.01, p = 0.101) or *B. pendula* (R^2_{adj} < 0.01, p = 0.339), whereas in yellow leaves there was a strong positive correlation between flavonols measured on either side of the leaves in both species (*F. sylvatica* R^2_{adj} = 0.40, p < 0.001 and *B. pendula* R^2_{adj} = 0.54, p < 0.001; Fig. S7). This appears primarily to be due to a decrease in adaxial epidermal flavonols during leaf senescence which brought them down to similar levels as the abaxial flavonols (Fig. S7).

3.3. Mass loss from litter in the controlled experiment

During incubation, green leaves of both *B. pendula* and *F. sylvatica* lost more mass than yellow leaves (49% vs. 34%, F = 225, p = 0.003, Table 1). When response ratios to the dark treatments were compared for each species and leaf colour there was an overall effect of filter treatment on mass loss (Fig. 2, Table 2), but when compared separately the filter treatment only had a marginally non-significant effect on mass loss of green leaves of *F. sylvatica* (F = 2.6, p = 0.062, Table 1). In this case, leaves receiving the full spectrum in the chambers lost mass faster than those in the dark or under treatments where UV-A radiation and blue light were attenuated (Fig. 2, Table 1). Yellow leaves of *B. pendula* followed a similar pattern even though the effect was marginally non-significant (F = 2.3, p = 0.085, Fig. 2, Table 1).

Only yellow *B. pendula* leaves differed in mass loss according to leaf orientation (F = 11.05, p = 0.002, Fig. 2): leaves orientated with their abaxial epidermis facing the light source lost mass faster (0.05–0.10% higher daily mass loss depending on the filter treatment) than leaves with their adaxial epidermis facing the light source (Fig. 2).

3.4. Mass loss from litter in the forest experiment

During decomposition in the forest stands green leaves of both *B. pendula* and *F. sylvatica* lost more mass than yellow leaves (65.0% against 34.2% and 35.2% against 16.2% respectively, F = 702, p = 0.001, Table 3), as was consistent with green and yellow leaves in the controlled experiment. The rate of mass loss was also slower in *F. sylvatica* than *B. pendula* (Fig. 3, species-by-colour interaction, F = 114, p = 0.009, Table 3). There were no differences in mass loss according to leaf orientation for either of the species and there was no interaction between the effects of filter treatments and leaf orientation (not shown). The filter treatment affected mass loss of (green-and-yellow) leaves of *F. sylvatica* and of green leaves of *B. pendula,* and this effect differed according to the stand (significant Filter treatment-by-stand interactions; Fig. 3, Table 3).

The effects of filter treatment were small and inconsistent among the stands. In green leaves of *F. sylvatica,* an effect of the filter treatment was found only in the *F. sylvatica* stand; where the No-UV treatment had a higher mass loss than the Full-spectrum treatment (pairwise comparison: No-UV – Full-spectrum p = 0.031, Table S5). For yellow leaf litter of *F. sylvatica,* there was no effect of filter treatment in the *A. platanoides* stand (Fig. 3, Table S5), while the other three stands presented contrasting results. In the *P. abies* and *F. sylvatica* stands, leaves exposed to Dark and No-UV/Blue treatments had higher daily mass loss than *F. sylvatica* litter exposed to the Full-spectrum and No-UV treatments (Fig. 3, Table S5), whereas in the *B. pendula* stand, the *F. sylvatica* litter exposed to the No-UV/Blue treatment had the highest mass loss (Fig. 3, Table S5).

For green leaf litter of *B. pendula* there was no effect of filter treatment in the *A. platanoides* stand (Fig. 3, Table S5). In the *F. sylvatica* stand, *B. pendula* litter exposed to the Dark treatment had higher daily mass loss than litter exposed to the Full-spectrum and No-UV treatments (Fig. 3, Table S5). In the *P. abies* stand, *B. pendula* litter exposed to Dark and Full-spectrum treatments had higher daily mass loss than litter exposed to the No-UV/Blue and No-UV treatments (Fig. 3, Table S5). In the *B. pendula* stand, the *B. pendula* litter exposed to the Full-Spectrum treatment had higher daily mass loss than litter exposed to the No-UV treatment (Fig. 3, Table S5).

3.5. Carbon and nitrogen content of litter in the controlled experiment

Leaf C:N ratio as well as C and N concentration (henceforth [C] and [N]) significantly differed between species at the end of the photodegradation experiment (Table 2). There was a significant interaction effect (Species x Leaf Colour) for [C], [N], and C:N ratio, meaning that the response of yellow and green leaves varied with species (Table 2). At the end of our photodegradation experiment, [C] was higher in yellow than green leaves of *B. pendula*, as was the C:N ratio in leaves of both species. The difference between [N] of green and yellow *B. pendula* leaves was much larger than that of *F. sylvatica* (Table 2). However, there was no general response of leaf [N] to our filter treatments (Table 1), an effect was only apparent in yellow leaves (F = 4.71,

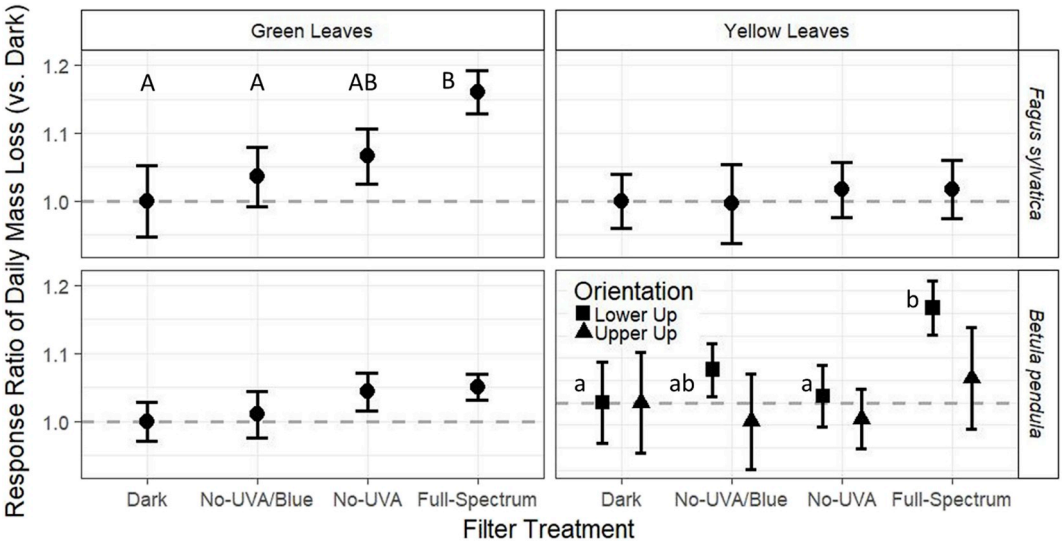

Fig. 2. The response ratio of average daily % mass loss from leaves under each filter treatment over the duration of the controlled environment. Panels separate for green and yellow leaves of *B. pendula* and *F. sylvatica.* Table 2 gives ANOVA results and means values. Leaf orientation, (adaxial [▲] or abaxial [■] epidermis facing upwards toward the lamps) had no significant effect apart from in Yellow Leaves of *Betula pendula* (F = 11.05, p = 0.002), for which significant pair-wise interactions between filters for "lower up" leaves are distinguished with lower case letters. Upper case letters denote significant pairwise interactions among filter treatments for green leaves of *F. sylvatica.*

Table 2
Mixed model ANOVA giving overall effects of filter treatments on mass loss, [C], [N], and C:N ratio from the controlled photodegradation experiment.

Response	Dark	No UVA/Blue	No UVA	Full Spectrum	ANOVA Filter Treatments
Controlled Mass Loss (% day^{-1})	0.52 ± 0.02	0.53 ± 0.02	0.54 ± 0.02	0.57 ± 0.02	F = 4.28 **p = 0.028**
C content (% g g^{-1})	47.22 ± 0.31	47.08 ± 0.31	47.06 ± 0.25	46.92 ± 0.26	F = 0.55 p = 0.657
N content (% g g^{-1})	1.97 ± 0.07	1.98 ± 0.06	1.97 ± 0.06	1.93 ± 0.07	F = 0.32 p = 0.812
C:N Ratio	27.9 ± 1.2	28.3 ± 1.0	28.0 ± 1.0	28.9 ± 1.2	F = 0.42 p = 0.739

$p = 0.048$), where leaf orientation was also a significant factor ($F = 3.41$, $p = 0.027$, Fig. 4). Here, [N] was higher in yellow leaves of *B. pendula* with the adaxial epidermis facing up (N = 1.25% of dry weight, Fig. 4) than those leaves with the abaxial epidermis facing up (N = 1.13% of dry weight, Fig. 4). Considering pairwise interactions for this effect, the [N] under the Full-Spectrum treatment was lower in those yellow leaves of *B. pendula* with the abaxial epidermis facing up than those under the dark treatment (Table 2, Fig. 4, $p = 0.012$).

3.6. Phenolic compounds from leaf litter after the controlled experiment

We identified 29 phenolic compounds from green and yellow leaves of *Fagus sylvatica* and 16 from green and yellow leaves of *Betula pendula*. A comprehensive comparison of the phenolic concentration and composition is given in Table S6 in the supplementary material, while those compounds which responded to our treatments are illustrated in Fig. 5. At the end of the experiment under controlled-irradiance treatments, the phenolic concentration varied most with leaf colour and orientation (Table S7). Likewise, MDS mapping showed that the composition of the phenolics profile of both species segregated primarily according to leaf colour and then with leaf orientation, but not with filter treatment (Fig. 6).

In *F. sylvatica* leaves, only three compounds were affected by our filter treatments: kaempferol 3-rhamnoside ($F = 2.88$, $p = 0.046$); neochlorogenic acid ($F = 3.40$, $p = 0.025$) and methanol (MeOH)-soluble condensed tannins in yellow leaves ($F = 5.52$, $p = 0.002$) (Table S7). The effect of filter treatment on the concentration of MeOH-soluble condensed tannins varied with the leaf colour (filter treatment x leaf colour interaction: $F = 2.81$, $p = 0.049$), being evident only in yellow leaves (Fig. 5). In this case, yellow leaves exposed to the Full-spectrum treatment had a lower content of MeOH-soluble condensed tannins than leaves expose to No-UVA/Blue treatment (pairwise comparison No-UVA/Blue - Full-Spectrum $p = 0.009$, Fig. 5, Table S8). Kaempferol 3-rhamnoside was lower in leaves of *F. sylvatica* exposed to treatments excluding UV-A radiation and blue light than in leaves exposed to the full spectrum or under filters only excluding UV-A (pairwise comparisons: No-UVA/Blue - Full-Spectrum $p = 0.037$, No-UVA/Blue – No-UVA $p = 0.042$, Fig. 5, Table S8). Neochlorogenic acid was lower in leaves of *F. sylvatica* exposed to the Dark treatment than those exposed to the Full-spectrum treatment (pairwise comparisons: Dark – Full-spectrum $p = 0.042$, Fig. 5, Table S8).

In *B. pendula* leaves, only chlorogenic acid was affected by our filter treatments ($F = 2.80$, $p = 0.050$, Table S7), being lower in leaves exposed to the Dark and No-UVA/Blue treatments than treatments excluding only UV-A radiation (pairwise comparisons: Dark – No-UVA $p = 0.029$; No-UVA/Blue - No-UVA $p = 0.035$, Fig. 5, Table S9).

4. Discussion

In our study, species and stage of senescence were the main factors affecting litter decomposition. Compared to these factors, filter treatments had a minor effect both on mass loss and litter chemistry. The

Table 3
Mean (± 1 SE) rate of mass loss from leaf litter in each stand (up to 186 days). Baseline differences between the stands are exemplified by value from the dark litter bags, and filter treatment effects shown in Fig. 3 as response ratios. ANOVA table for daily mass loss in the forest decomposition experiment for each filter treatment and stand and the interaction between them. $p < 0.05$ are in bold face.

Mass Loss (% day^{-1}) Forest Stands (mean ± 1 SE under dark filter treatment)				
Species	*F. sylvatica* litter		*B. pendula* litter	
Leaf colour	Green	Yellow	Green	Yellow
Picea abies stand	0.16 ± 0.01	0.10 ± 0.01	0.48 ± 0.01	0.23 ± 0.03
Fagus sylvatica stand	0.16 ± 0.01	0.11 ± 0.01	0.36 ± 0.04	0.17 ± 0.02
Acer platanoides stand	0.14 ± 0.01	0.10 ± 0.01	0.27 ± 0.02	0.18 ± 0.01
Betula pendula stand	0.13 ± 0.01	0.10 ± 0.01	0.29 ± 0.01	0.17 ± 0.01
ANOVA (Forest stands)				
Filter Treatment (F)	F = 1.91 **$p < 0.001$**	F = 4.79 **$p < 0.001$**	F = 4.07 **$p < 0.001$**	F = 0.32 p = 0.807
Stand (St)	F = 23.14 **$p < 0.001$**	F = 2.97 **$p < 0.001$**	F = 22.45 **$p < 0.001$**	F = 13.77 **$p < 0.001$**
F x St	F = 0.51 **$p < 0.001$**	F = 1.23 **$p < 0.001$**	F = 2.02 **$p < 0.001$**	F = 1.25 p = 0.258

ANOVA		
Colour (C)	**Species (S)**	**C × S**
F = 317 **p = 0.003**	F = 702 **p = 0.001**	F = 114 **p = 0.009**

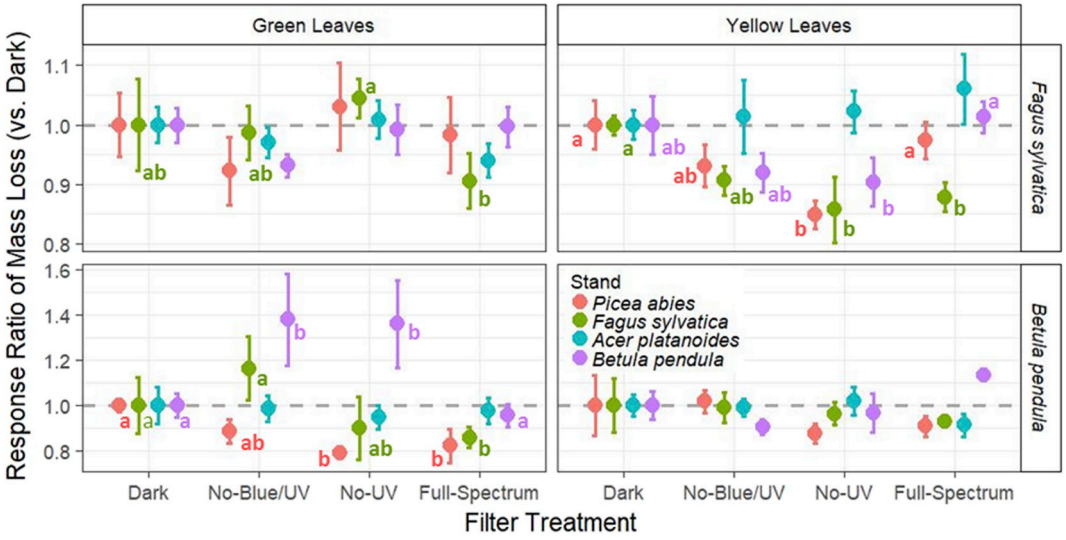

Fig. 3. The response ratio of average daily mass loss of leaf litter under each filter treatment, decomposing in different forest stands. Table 3 gives ANOVA results and means values. Lower case letters denote significant differences between filter treatments within the same stand for those three species-by-leaf-colour combinations where there was a significant effect of filter treatment. (For interpretation of the references to colour in this figure legend, the reader is referred to the Web version of this article.)

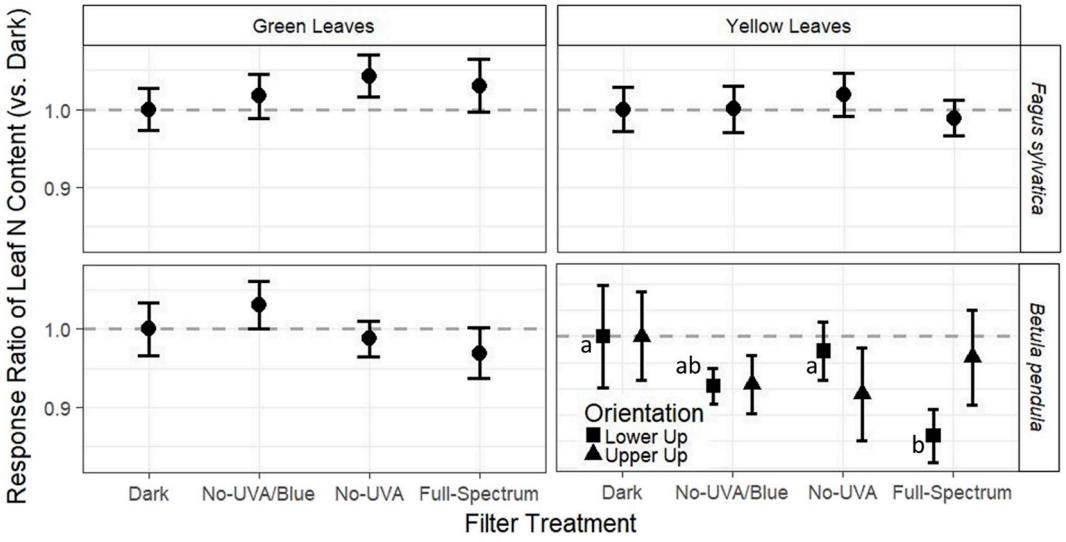

Fig. 4. The response ratio of N content of leaf litter under each filter treatment at the end of the controlled conditions photodegradation experiment. Table 2 gives ANOVA results and means values. Leaf orientation, (adaxial [▲] or abaxial [■] epidermis facing upwards toward the lamps) had no significant effect apart from in Yellow Leaves of *Betula pendula* ($F = 4.71$, $p = 0.048$), for which significant differences between pairs of filters for "lower up" leaves are distinguished with lower case letters. The equivalent response ratios of C content and C:N ratio are given in Fig. S8.

effects of our filter treatments on photodegradation in the controlled environments differed from their effects on decomposition in forest stands. While the exclusion of solar UV radiation enhanced mass loss from leaf litter decomposing in the forest stands, the presence of UV-A radiation in the controlled environment tended to accelerate photodegradation. An increase in mass loss due to photodegradation in controlled environments has also been reported for rice and wheat straws exposed to enhanced UV-A (Li et al., 2016) and UV-B radiation (Zhou et al., 2015). The effect of UV radiation did not transfer to decomposition under equivalent filters in forest stands, a distinction that would be consistent with any effect of sunlight photoinhibition on decomposers predominating over photochemical mineralization during the initial 6 months of decomposition following leaf fall. An inhibitory effect of sunlight on litter decomposition has also been reported for grass-litter decomposition in sub-arctic environments (Pancotto et al., 2003). However, in that environment when equivalent litter was monitored in the same field site over a longer period of time (12–17 months), the effect of UV-B radiation on litter mass loss changed from negative to positive (Pancotto et al., 2005). Such a transition, attributed to a shift in the relative importance of different antagonistic processes affected by UV radiation (Zhou et al., 2015), may also occur in our forest stands over a longer period of decomposition, but this remains untested. However, in a filter experiment in a temperate forest, solar UV radiation accelerated decomposition of leaf litter from *Quercus robur* and *F. sylvatica* over a 10-month period, but not of litter from *Fraxinus excelsior* over 7 months, under similar experimental treatments to ours but implemented later after leaf senescence (Pieristè et al., 2019). The treatment effects in our study may have differed over a longer period, not only due to a changing role of photodegradation during different phases of decomposition (Pancotto et al., 2003, 2005), but also because of seasonal environmental changes including canopy closure which reduces irradiance in the understorey and alters its spectral

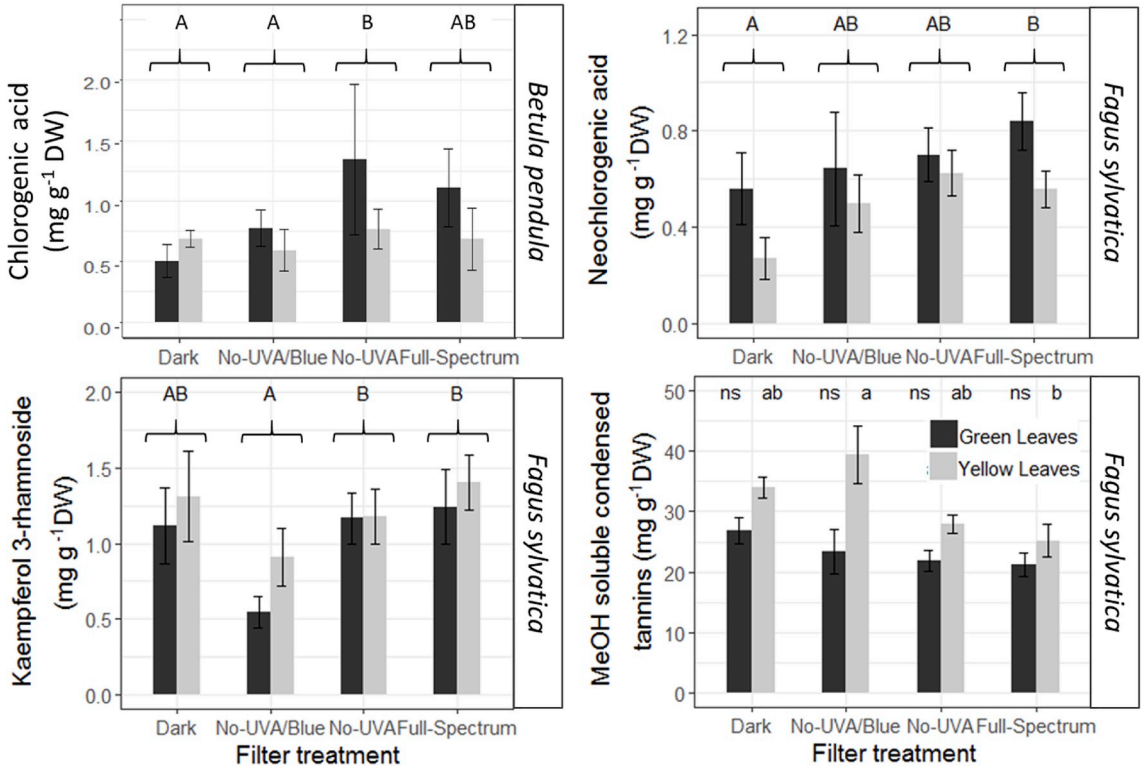

Fig. 5. Phenolic compounds in senescent yellow and green leaves of *Fagus sylvatica* and *Betula pendula* following 10 weeks of photdegradation under our filter treatments. Mean and SE are shown. Upper case letters show significant difference between pairs of filter treatments, "ns" stands for "non-significant, lower case letters indicate significant differences between pairs of filter treatments in yellow leaves (filter treatment x leaf colour interaction). Only compounds which responded to our treatment are displayed here, the complete leaf phenolic profiles are given in Table S7.

composition. In forest environments, where decomposers principally determine the rate of decomposition, the effect of direct photo-mineralization might be overridden by the capability of UV-B radiation to inhibit microbial activity (photoinhibition) (Bais et al., 2017; Bornman et al., 2019a). In general, micro- and meso-fauna tend to prefer darker environments (Lin et al., 2018; Wang et al., 2015); this is one likely reason for the high mass loss under our dark treatment. This effect of filter treatments is consistent with that reported for *F. excelsior* leaf litter under a similar combination of spectral-attenuation treatments in a moist-temperate *F. sylvatica* forest (Pieristè et al., 2019). The higher decomposition rates with increasing canopy cover among our four stands, also supports this assertion (Table 3). On the other hand, the lack of a UV-B radiation treatment in our controlled experiment could explain why we didn't find an inhibitory effect of UV radiation on litter mass loss as reported elsewhere, e.g. with *Pinus radiata* litter exposed to UV-B radiation (Kirschbaum et al., 2011). While the radiation exposures in the two experiments were largely well matched, there were greater fluctuations in temperature and PAR in the forest environment due to sunflecks, especially during March and April. Sunlight is relatively enriched in the green region (500–570 nm) in forest understoreys compared with open environments (Fig. 1C and D), which may have stimulated photomineralization or photopriming while having few consequences on photoinhibition (Austin et al., 2016). These differences in exposure and the lack of interactive effects between different wavelengths might partially explain the different results obtained in the two experiments. Moreover, temperature conditions in the forest stands and in the controlled experiment differed, with the forest environment presenting a higher temperature fluctuation daily, and over the 6 months of the experiment (Fig. S9), while in the controlled environment the temperature was kept constant during the experiment with only small day-night variations (Fig, S5).

4.1. Leaf biochemistry and photodegradation

The results of both experiments confirmed our expectations that green leaves would decompose faster than yellow leaves in both species. The higher content of N-rich Rubisco, chlorophyll and other photosynthetic pigments in green leaf litter makes it more palatable (Schädler et al., 2003) for decomposers than fully senesced leaves, allowing faster decomposition (Cornelissen, 1996). Senescent and green leaves differ in their nutrients content due to the process of nutrient reabsorption, which takes place during leaf senescence (Simon et al., 2018; Wright and Westoby, 2003). This results in fewer low molecular phenolics and accumulation of tannins in senescent leaves (Hättenschwiler and Vitousek, 2000; Koricheva et al., 2012). A result consistent with the higher concentration of condensed tannins and fewer low-molecular phenolics in senescent leaves than leaves that were harvested when still green in our study. Tannins reduce the rate of litter decomposition in various woody species, by binding proteins and simple polymers making them unavailable for microbial decomposition (Hättenschwiler and Jørgensen, 2010; Schimel et al., 1996; Schweitzer et al., 2004). It is worth noting, however, that flavonoids isolated through HPLC after photodegradation, were higher in *F. sylvatica* leaves harvested when yellow than those harvested when green. This might suggest an increase in flavonoid concentration during leaf senescence, as recently reported for several tree species by (Mattila et al., 2018). However, it contradicts the decrease in upper epidermal flavonols measured with the Dualex before the experiment in yellow leaves compared with green leaves of *F. sylvatica* (Fig. S7). This change, specific to the adaxial epidermis, might suggest that flavonols are translocated from the vacuoles of epidermal cells elsewhere in the leaf rather than broken down during senescence.

The exposure of leaves to UV radiation during the growing season causes the accumulation of photoprotective pigments, mainly flavonoids, in leaf adaxial epidermis which reduces the penetration of

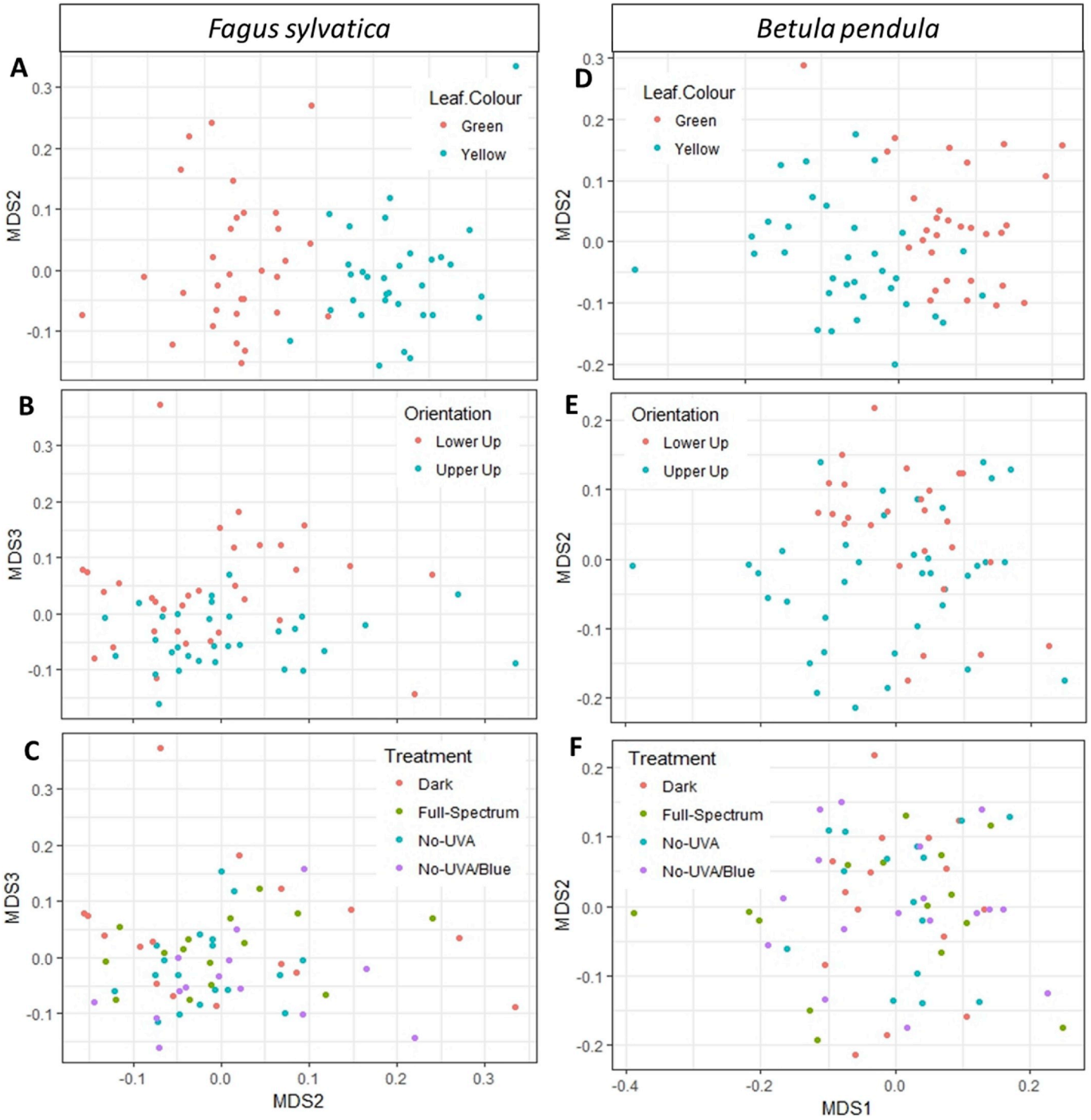

Fig. 6. Patterns of leaf phenolics compound composition following the controlled photodegradation experiment, mapped against explanatory variables for each species using nonmetric multidimensional scaling (MDS). *Fagus sylvatica* MDS had a stress of 0.125 and clear segregation according to (A) leaf colour along MDS1 (vs MDS2) and (B) leaf orientation along MDS2 (vs MDS3), but not according to (C) filter treatment. *Betula pendula* MDS had a stress of 0.219, and similar patterns of segregation according to the explanatory variables, (D) leaf colour along MDS1 (vs MDS2) and (E) leaf orientation along MDS2 (vs MDS1). (For interpretation of the references to colour in this figure legend, the reader is referred to the Web version of this article.)

sunlight and particularly UV radiation into leaf tissues (Landry et al., 1995; Day and Vogelmann, 1995; Jansen et al., 1998), potentially protecting the mesophyll from photodegradation effects (Barnes et al., 2015). The accumulation of these photoprotective pigments, as a consequence of UV exposure, has been reported to alter litter chemistry of *Alnus* sp. and *Betula* sp. and consequently impact decomposition through an effect on microbial communities and soil respiration (Kotilainen et al., 2009). By taking Dualex measurements of the same leaves before and after drying, we confirmed that differences in optical properties attributed to epidermal flavonols were conserved in dried leaves (Fig. S1), meaning that the differences between upper and lower epidermal screening are likely to alter the penetration of UV within the leaf during photodegradation. However, we only found an effect of leaf orientation on mass loss and [N] in yellow leaves of *B. pendula* in the controlled environment experiment. This effect would be consistent with reduced microbial colonisation on these leaves, which we also considered a viable explanation for the filter effect found in the forest stands. However, lack of association between effects on [N] and mass

loss in the controlled experiment would imply that direct photodegradation is the dominant process. Nevertheless, the phenolic profile of leaves recorded after the photodegradation experiment segregated clearly with leaf orientation, and orientation had an effect on the content of some of the flavonoids isolated with the HPLC analysis in *F. sylvatica* leaves (Figs. 5 and 6). Taken together, these results suggest that the spatial distribution of flavonoids within the leaves, affecting their optical properties and the penetration of UV radiation, can have an effect on photodegradation. However, these effects were too small, or the duration of exposure to our irradiance treatments was insufficient, to produce an effect of orientation that could be quantified in terms of mass loss, [N] or [C]. Such a test might be more informative with clonal leaf material from plants grown under fully standardised conditions, where comparable initial phenolic profiles would provide a consistent baseline prior to decomposition.

4.2. The role of photodegradation in initial decomposition in the forest understorey

After 6 months of decomposition in the forest, the mass loss was about 35.2% and 16.2% for green and yellow leaves of *Fagus sylvatica*, and 65.0% and 34.2% for green and yellow leaves of *Betula pendula* respectively. This scale of mass loss from senescent leaves was reasonable, compared with that reported in other studies in similar environments after 6 months of decomposition: 15–20% for *F. sylvatica* litter and 40–45% for *B. pendula* litter (Portillo-Estrada et al., 2016; Silfver et al., 2007). In our forest decomposition experiment, where adjacent stands were selected to form a gradient of LAI, litter mass loss was affected by stand type. This might suggest that even in southern Finland, where winter irradiances are low, the light environment created by different canopies can affect litter decomposition. Mass loss was highest from the *Picea abies* stand in our experiment (Table S10). But since the understorey in this stand received both the lowest irradiance and the highest amount of blue light (Table S3) over the 6 months of the experiment, either spectral composition or total irradiance or both, could be responsible for this result. This would be in agreement with previous studies that proved the importance of blue light in the process of photodegradation (Austin et al., 2016; Pieristè et al., 2019). Stands with high canopy density also intercept more precipitation in the form of snow, leading to smaller snow depths and consequently modifying soil temperature and moisture (Mellander et al., 2005; Pomeroy et al., 1997; Davis et al., 1997). Since forest canopies also affect a variety of micro-environmental conditions such as temperature, water availability, soil characteristics and decomposer assemblages, any effect of light environment on decomposition will operate in combination with these factors (Augusto et al., 2014; Kovács et al., 2017; Zellweger et al., 2019). We found no evidence for home-field advantage; the theory that litter from a particular forest decomposes fastest in its own stand irrespective of conditions because of its specialised decomposer assemblage (Ayres et al., 2009; Asplund et al., 2017), e.g. *Betula pendula* litter in the *Betula pendula* stand. However, further investigation is needed, both in controlled and forest environments, to assess the relative importance of photodegradation compared with other environmental factors in litter decomposition at high latitudes and over longer experimental periods.

5. Conclusions

This study revealed that photodegradation can play a role in surface leaf litter decomposition in forest ecosystems at high latitudes, but this role was not consistent with photodegradation produced by UV-A radiation and blue light under controlled conditions. There, UV-A radiation and blue light accelerated mass loss, while in forest stands decomposition was generally slightly slower under filters transmitting UV radiation and blue light. The contribution of photodegradation to decomposition was relatively small, and varied according to the canopy tree species, the leaf litter species and leaf traits related to stage of leaf senescence.

Contribution

The study was conceived and designed in Helsinki by Marta Pieristè and Santa Neimane (who are joint first authors of the paper) with the help of T. Matthew Robson. In addition to supervision by T. Matthew Robson in Helsinki, Marta Pieristè's research was supervised by Estelle Forey, Matthieu Chauvat and Alan G. Jones, and Santa Neimane's research was supervised by Jevgenija Ņečajeva, at their respective home universities. Santa Neimane, Twinkle Solanki and T. Matthew Robson performed the experiments. Santa Neimane, Marta Pieristè, and T. Matthew Robson analysed the data. Line Nybakken performed the HPLC analysis at CERAD Norway, and interpreted their outcome together with Santa Neimane and Marta Pieristè. Santa Neimane and Marta Pieristè wrote the first draft of the manuscript, and T. Matthew Robson and Marta Pieristè revised the manuscript after review. All co-authors commented on these edits to manuscript as it was finalised.

Declaration of cpmpeting interest

The authors have no direct or indirect conflicting interests to declare.

Acknowledgements

We are grateful to Anu Heikkilä (for the UV data) and FMI for diffuse direct irradiance/cloudiness data, and Viikki Arboretum and Experiment Plots of the University of Helsinki managed by Daniel Richterich, for allowing use of the experimental sites, and provision of meteorological station data from their *in situ* weather station and Pedro José Aphalo's weather station. This research was funded by Academy of Finland decisions #266523 and #304519 to TMR, and a grant from the Region Haute-Normandie through the GRR-TERA SCALE (UFOSE Project) to MP.

Appendix A. Supplementary data

Supplementary data to this article can be found online at https://doi.org/10.1016/j.plaphy.2019.11.005.

References

Ahti, T., Hämet-Ahti, L., Jalas, J., 1968. Vegetation zones and their sections in northwestern Europe. Ann. Bot. Fenn. 5, 169–211.
Aphalo, P.J., 2015. The R4photobiology suite: spectral irradiance. UV4Plants Bull. 21–29 No 1 (2015).
Aphalo, P.J., 2016. Learn R… as You Learnt Your Mother Tongue. Leanpub, Helsinki, Finland.
Aphalo, P.J., 2017. Quantification of UV radiation. In: Jordan, B.R. (Ed.), UV-B Radiation and Plant Life: Molecular Biology to Ecology. CAB International, Oxford, UK, pp. 10–22.
Aphalo, P.J., Albert, A., McLeod, A., Heikkilä, A., Gómez, I., López Figueroa, F., Robson, T.M., Strid, Å., 2012. Beyond the Visible: a Handbook of Best Practice in Plant UV Photobiology, first ed. University of Helsinki, Division of Plant Biology, Helsinki, pp. 1–176.
Aphalo, P.J., Robson, T.M., Piiparinen, J., 2013. How to check an array spectrometer. updated June 2. Int. Assoc. Plant UV Res 2016. https://www.uv4plants.org/methods/how-to-check-an-array-spectrometer/, Accessed date: 11 November 2017.
Asplund, J., Kauserud, H., Bokhorst, S., Lie, M.H., Ohlson, M., Nybakken, L., 2017. Fungal communities influence decomposition rates of plant litter from two dominant tree species. Fungal Ecol. 32, 1–8.
Augusto, L., De Schrijver, A., Vesterdal, L., Smolander, A., Prescott, C., Ranger, J., 2014. Influences of evergreen gymnosperm and deciduous angiosperm tree species on the functioning of temperate and boreal forests. Biol. Rev. 90, 444–466.
Austin, A.T., Vivanco, L., 2006. Plant litter decomposition in a semi-arid ecosystem controlled by photodegradation. Nature 442, 555.
Austin, A.T., Méndez, M.S., Ballaré, C.L., 2016. Photodegradation alleviates the lignin bottleneck for carbon turnover in terrestrial ecosystems. Proc. Natl. Acad. Sci. 113, 4392.
Ayres, E., Steltzer, H., Simmons, B.L., Simpson, R.T., Steinweg, J.M., Wallenstein, M.D., Mellor, N., Parton, W.J., Moore, J.C., Wall, D.H.J.S.B., 2009. Home-field advantage

accelerates leaf litter decomposition in forests. Soil Biol. Biochem. 41, 606–610.
Bais, A.F., Lucas, R.M., Bornman, J.F., Williamson, C.E., Sulzberger, B., Austin, A.T., Wilson, S.R., Andrady, A.L., Bernhard, G., McKenzie, R.L., 2017. Environmental effects of ozone depletion, UV radiation and interactions with climate change: UNEP Environmental Effects Assessment Panel, update. Photochem. Photobiol. Sci. 17, 127–179 2018.
Barnes, P.W., Throop, H.L., Archer, S.R., Breshears, D.D., McCulley, R.L., Tobler, M.A., 2015. Sunlight and soil–litter mixing: drivers of litter decomposition in drylands. In: In: Lüttge, U., Beyschlag, W. (Eds.), Progress in Botany, vol. 76. Springer International Publishing, Cham, pp. 273–302.
Bornman, J.F., Barnes, P.W., Robinson, S.A., Ballare, C.L., Flint, S., Caldwell, M.M.J.P., Sciences, P., 2015. Solar ultraviolet radiation and ozone depletion-driven climate change: effects on terrestrial ecosystems. Photochem. Photobiol. Sci. 14, 88–107.
Bornman, J.F., Barnes, P.W., Robson, T.M., Robinson, S.A., Jansen, M.A., Ballaré, C.L., Flint, S.D., 2019a. Linkages between stratospheric ozone, UV radiation and climate change and their implications for terrestrial ecosystems. Photochem. Photobiol. Sci. 18, 681–716.
Brelsford, C.C., Morales, L.O., Nezval, J., Kotilainen, T.K., Hartikainen, S.M., Aphalo, P.J., Robson, T.M., 2018. Do UV-A radiation and blue light during growth prime leaves to cope with acute high light in photoreceptor mutants of Arabidopsis thaliana? Physiol. Plant. 165, 537–554.
Brelsford, C.C., Morales, L.O., Nezval, J., Kotilainen, T.K., Hartikainen, S.M., Aphalo, P.J., Robson, T.M., 2019. Do UV-A radiation and blue light during growth prime leaves to cope with acute high light in photoreceptor mutants of Arabidopsis thaliana? Physiol. Plant. 165, 537–554.
Cerovic, Z.G., Masdoumier, G., Ghozlen, N.B., Latouche, G., 2012. A new optical leaf-clip meter for simultaneous non-destructive assessment of leaf chlorophyll and epidermal flavonoids. Physiol. Plant. 146, 251–260.
Chapin III, F.S., Matson, P.A., Mooney, H.A., 2002. Principles of Terrestrial Ecosystem Ecology. Springer-Verlag., New York, pp. 1–447.
Cornelissen, J.H.C., 1996. An experimental comparison of leaf decomposition rates in a wide range of temperate plant species and types. J. Ecol. 84, 573–582.
Davis, R., Hardy, J., Ni, W., Woodcock, C., McKenzie, J., Jordan, R., Li, X., 1997. Variation of snow cover ablation in the boreal forest: a sensitivity study on the effects of conifer canopy. J. Geophys. Res.: Atmos. 102, 29389–29395.
Day, T.A., Martin, G., Vogelmann, T.C., 1993. Penetration of UV-B radiation in foliage: evidence that the epidermis behaves as a non-uniform filter. Plant Cell Environ. 16, 735–741.
Day, T.A., Vogelmann, T.C., 1995. Alterations in photosynthesis and pigment distributions in pea leaves following UV-B exposure. Photobiophys. photosynth. 94, 433–440.
Day, T.A., Bliss, M.S., Tomes, A.R., Ruhland, C.T., Guénon, R., 2018. Desert leaf litter decay: coupling of microbial respiration, water-soluble fractions and photodegradation. Glob. Chang. Biol. 24, 5454–5470.
Erdenebileg, E., Ye, X., Wang, C., Huang, Z., Liu, G., Cornelissen, J.H.C., 2018. Positive and negative effects of UV irradiance explain interaction of litter position and UV exposure on litter decomposition and nutrient dynamics in a semi-arid dune ecosystem. Soil Biol. Biochem. 124, 245–254.
Hagerman, A.E., 2002. Tanin Chemistry Handbook. Miami University, Oxford, Ohio, USA. www.users.muohio.edu/hagermae/.
Hartikainen, S.M., Jach, A., Grané, A., Robson, T.M., 2018. Assessing scale-wise similarity of curves with a thick pen: as illustrated through comparisons of spectral irradiance. Ecol. Evol. 8, 10206–10218.
Hättenschwiler, S., Jørgensen, H.B., 2010. Carbon quality rather than stoichiometry controls litter decomposition in a tropical rain forest. J. Ecol. 98, 754–763.
Hättenschwiler, S., Vitousek, P.M., 2000. The role of polyphenols in terrestrial ecosystem nutrient cycling. Trends Ecol. Evol. 15, 238–243.
Heikkilä, A., Mäkelä, J.S., Lakkala, K., Meinander, O., Kaurola, J., Koskela, T., Karhu, J.M., Karppinen, T., Kyrö, E., Leeuw, G.d., 2016. In search of traceability: two decades of calibrated Brewer UV measurements in Sodankylä and Jokioinen. Geosci. Instrum. Method Data Syst. 5, 531–540.
Hoch, W.A., Zeldin, E.L., McCown, B.H., 2001. Physiological significance of anthocyanins during autumnal leaf senescence. Tree Physiol. 21, 1–8.
Hoorens, B., Aerts, R., Stroetenga, M.J.O., 2003. Does initial litter chemistry explain litter mixture effects on decomposition? Ecosyst. Ecol. 137, 578–586.
Jansen, M.A.K., Gaba, V., Greenberg, B.M., 1998. Higher plants and UV-B radiation: balancing damage, repair and acclimation. Trends Plant Sci. 3, 131–135.
Joly, F.-X., Milcu, A., Scherer-Lorenzen, M., Jean, L.-K., Bussotti, F., Dawud, S.M., Müller, S., Pollastrini, M., Raulund-Rasmussen, K., Vesterdal, L., Hättenschwiler, S., 2017. Tree species diversity affects decomposition through modified micro-environmental conditions across European forests. New Phytol. 214, 1281–1293.
King, J.Y., Brandt, L.A., Adair, E.C.J.B., 2012. Shedding light on plant litter decomposition: advances, implications and new directions in understanding the role of photodegradation. Biogeochemistry 111, 57–81.
Kirschbaum, M.U.F., Lambie, S.M., Zhou, H., 2011. No UV enhancement of litter decomposition observed on dry samples under controlled laboratory conditions. Soil Biol. Biochem. 43, 1300–1307.
Kolstad, A.L., Asplund, J., Nilsson, M.-C., Ohlson, M., Nybakken, L., 2016. Soil fertility and charcoal as determinants of growth and allocation of secondary plant metabolites in seedlings of European beech and Norway spruce. Environ. Exp. Bot. 131, 39–46.
Koricheva, J., Barton, K.E., 2012. Temporal changes in plant secondary metabolite production: patterns, causes and consequences. In: Iason GR, D.M., Hartley, S.E. (Eds.), The Ecology of Plant Secondary Metabolites. Cambridge University Press, Cambridge, pp. 10–33.
Kotilainen, T., Haimi, J., Tegelberg, R., Julkunen-Tiitto, R., Vapaavuori, E., Aphalo, P.J., 2009. Solar ultraviolet radiation alters alder and birch litter chemistry that in turn affects decomposers and soil respiration. Oecologia 161, 719–728.
Kovács, B., Tinya, F., Ódor, P., 2017. Stand structural drivers of microclimate in mature temperate mixed forests. Agric. For. Meteorol. 234, 11–21.
Landry, L.G., Chapple, C.C.S., Last, R.L., 1995. Arabidopsis mutants lacking phenolic sunscreens exhibit enhanced ultraviolet-B injury and oxidative damage. Plant Physiol. 109, 1159.
Li, Y., Huang, H., Wu, G., Yan, S., Chang, Z., Bi, J., Chen, L., 2016. The effects of UV-a on dry rice straw decomposition under controlled laboratory conditions. BioResources 11, 2568–2582. https://doi.org/10.15376/biores.11.1.2568-2582.
Lin, Y., Karlen, S.D., Ralph, J., King, J.Y., 2018. Short-term facilitation of microbial litter decomposition by ultraviolet radiation. Sci. Total Environ. 615, 838–848.
Liski, J., Nissinen, A., Erhard, M., Taskinen, O., 2003. Climatic effects on litter decomposition from arctic tundra to tropical rainforest. Glob. Chang. Biol. 9, 575–584.
Liu, G., Wang, L., Jiang, L., Pan, X., Huang, Z., Dong, M., Cornelissen, J.H.C., 2018. Specific leaf area predicts dryland litter decomposition via two mechanisms. J. Ecol. 106, 218–229.
Madronich, S., McKenzie, R.L., Björn, L.O., Caldwell, M.M., 1998. Changes in biologically active ultraviolet radiation reaching the Earth's surface. J. Photochem. Photobiol. B Biol. 46, 5–19.
Mäkelä, J.S., Lakkala, K., Koskela, T., Karppinen, T., Karhu, J.M., Savastiouk, V., Suokanerva, H., Kaurola, J., Arola, A., Lindfors, A.V., Meinander, O., de Leeuw, G., Heikkilä, A., 2016. Data flow of spectral UV measurements at Sodankylä and Jokioinen. Geosci. Instrum. Method Data Syst. 5, 193–203.
Mattila, H., Valev, D., Antinluoma, M., Virtanen, O., Khorobrykh, S., Havurinne, V., Tyystjärvi, E., Mishra, K.B., 2018. Degradation of chlorophyll and synthesis of flavonols during autumn senescence—the story told by individual leaves. AoB Plants 10 (3), ply028. https://doi.org/10.1093/aobpla/ply028.
Mellander, P.-E., Laudon, H., Bishop, K., 2005. Modelling variability of snow depths and soil temperatures in Scots pine stands. Agric. For. Meteorol. 133, 109–118.
Oksanen, J., Blanchet, F.G., Kindt, R., Legendre, P., Minchin, P.R., O'hara, R., Simpson, G.L., Solymos, P., Stevens, M.H.H., Wagner, H., 2019. Vegan: Community Ecology Package - Version 2.5-4.
Pancotto, V.A., Sala, O.E., Cabello, M., López, N.I., Matthew Robson, T., Ballaré, C.L., Caldwell, M.M., Scopel, A.L., 2003. Solar UV-B decreases decomposition in herbaceous plant litter in Tierra del Fuego, Argentina: potential role of an altered decomposer community. Glob. Chang. Biol. 9, 1465–1474.
Pancotto, V.A., Sala, O.E., Robson, T.M., Caldwell, M.M., Scopel, A.L., 2005. Direct and indirect effects of solar ultraviolet-B radiation on long-term decomposition. Glob. Chang. Biol. 11, 1982–1989.
Parton, W., Silver, W.L., Burke, I.C., Grassens, L., Harmon, M.E., Currie, W.S., King, J.Y., Adair, E.C., Brandt, L.A., Hart, S.C., Fasth, B., 2007. Global-scale similarities in nitrogen release patterns during long-term decomposition. Science 315, 361.
Paudel, E., Dossa, G.G.O., de Blécourt, M., Beckschäfer, P., Xu, J., Harrison, R.D., 2015. Quantifying the factors affecting leaf litter decomposition across a tropical forest disturbance gradient. Ecosphere 6, 1–20.
Perry, D.A., Oren, R., Hart, S.C., 2008. Forest Ecosystems, second ed. The Johns Hopkins University Press, Baltimore.
Pfündel, E.E., Ben Ghozlen, N., Meyer, S., Cerovic, Z.G.J.P.R., 2007. Investigating UV screening in leaves by two different types of portable UV fluorimeters reveals in vivo screening by anthocyanins and carotenoids. Photosynth. Res. 93, 205–221.
Pieristè, M., Chauvat, M., Kotilainen, T.K., Jones, A.G., Aubert, M., Robson, T.M., Forey, E., 2019. Solar UV-A radiation and blue light enhance tree leaf litter decomposition in a temperate forest. Oecologia 191, 191–203.
Pinheiro, J., Bates, D., DebRoy, S., Sarkar, D., R Core Team, 2019. In: nlme: Linear and Nonlinear Mixed Effects Models. R Package Version 3.1-141. . https://CRAN.R-project.org/package=nlme, Accessed date: 17 September 2019.
Pomeroy, J., Goodison, B., 1997. Winter and snow. In: Oke, T., Rouse, W.R., Bailey, W.G. (Eds.), The Surface Climates of Canada. McGill-Queen's University Press, pp. 68–100.
Portillo-Estrada, M., Pihlatie, M., Korhonen, J.F., Levula, J., Frumau, A.K., Ibrom, A., Lembrechts, J.J., Morillas, L., Horváth, L., Jones, S.K., 2016. Climatic controls on leaf litter decomposition across European forests and grasslands revealed by reciprocal litter transplantation experiments. Biogeosciences 13, 1621–1633.
Predick, K.I., Archer, S.R., Aguillon, S.M., Keller, D.A., Throop, H.L., Barnes, P.W., 2018. UV-B radiation and shrub canopy effects on surface litter decomposition in a shrub-invaded dry grassland. J. Arid Environ. 157, 13–21.
R-Core-Team, R., 2018. In: A Language and Environment for Statistical Computing. R Foundation for Statistical Computing, Vienna, Austria.
Schädler, M., Jung, G., Auge, H., Brandl, R., 2003. Palatability, decomposition and insect herbivory: patterns in a successional old-field plant community. Oikos 103, 121–132.
Schimel, J.P., Cleve, K.V., Cates, R.G., Clausen, T.P., Reichardt, P.B., 1996. Effects of balsam poplar (Populus balsamifera) tannins and low molecular weight phenolics on microbial activity in taiga floodplain soil: implications for changes in N cycling during succession. Can. J. Bot. 74, 84–90.
Schleppi, P., Conedera, M., Sedivy, I., Thimonier, A., 2007. Correcting non-linearity and slope effects in the estimation of the leaf area index of forests from hemispherical photographs. Agric. For. Meteorol. 144, 236–242.
Schneider, C.A., Rasband, W.S., Eliceiri, K.W.J.N., 2012. NIH Image to ImageJ: 25 years of image analysis. Nat. Methods 9, 671–675.
Schweitzer, J.A., Bailey, J.K., Rehill, B.J., Martinsen, G.D., Hart, S.C., Lindroth, R.L., Keim, P., Whitham, T.G., 2004. Genetically based trait in a dominant tree affects ecosystem processes. Ecol. Lett. 7, 127–134.
Sercu, B.K., Baeten, L., van Coillie, F., Martel, A., Lens, L., Verheyen, K., Bonte, D., 2017. How tree species identity and diversity affect light transmittance to the understory in mature temperate forests. Ecol. Evol. 7, 10861–10870.
Silfver, T., Mikola, J., Rousi, M., Roininen, H., Oksanen, E., 2007. Leaf litter decomposition differs among genotypes in a local Betula pendula population. Oecologia 152, 707–714.

Simon, J., Dörken, V.M., Arnold, A.L.-M., Adamczyk, B., 2018. Environmental conditions and species identity drive metabolite levels in green leaves and leaf litter of 14 temperate woody species. Forests 9, 775. https://doi.org/10.3390/f9120775.
Sulkava, P., Huhta, V., 2003. Effects of hard frost and freeze-thaw cycles on decomposer communities and N mineralisation in boreal forest soil. Appl. Soil Ecol. 22, 225–239.
Swift, M.J., Heal, O.W., Anderson, J.M., Anderson, J., 1979. Decomposition in Terrestrial Ecosystems. Univ of California Press.
Thimonier, A., Sedivy, I., Schleppi, P., 2010. Estimating leaf area index in different types of mature forest stands in Switzerland: a comparison of methods. Eur. J. For. Res. 129, 543–562.
Wang, F., 2017. SIOX plugin in ImageJ: area measurement made easy. UV4Plants Bull. 2, 37–44.
Wang, J., Liu, L., Wang, X., Chen, Y., 2015. The interaction between abiotic photodegradation and microbial decomposition under ultraviolet radiation. Glob. Chang. Biol. 21, 2095–2104.
Wickham, H., 2009. ggplot2: Elegant Graphics for Data Analysis. Springer-Verlag, New York Version.
Wright, I.J., Westoby, M., 2003. Nutrient concentration, resorption and lifespan: leaf traits of Australian sclerophyll species. Funct. Ecol. 17, 10–19.
Zellweger, F., Coomes, D., Lenoir, J., Depauw, L., Maes, S.L., Wulf, M., Kirby, K.J., Brunet, J., Kopecký, M., Máliš, F., 2019. Seasonal drivers of understorey temperature buffering in temperate deciduous forests across Europe. Glob. Ecol. Biogeogr. 0, 1–13. https://doi.org/10.1111/geb.12991.
Zhou, G., Zhang, J., Mao, J., Zhang, C., Chen, L., Xin, X., Zhao, B., 2015. Mass loss and chemical structures of wheat and maize straws in response to ultraviolet-B radiation and soil contact. Sci. Rep. 5, 14851.
Zhu, J., Yang, W., He, X.J.P.o., 2013. Temporal dynamics of abiotic and biotic factors on leaf litter of three plant species in relation to decomposition rate along a subalpine elevation gradient. PLoS One 8, e62073.

Supplemental Information

Supplemental Figures

Figure S1 The relationship between (A) chlorophyll content and (B & C) epidermal flavonoids for individual fresh vs. dried leaves of each species. The same leaf was measured with Dualex before and after drying. The Dualex measurements of chlorophyll content of fresh and air-dried green leaves of both species were strongly positively correlated (*F. sylvatica* R^2adj =0.70 or *B. pendula* R^2adj = 0.45; Fig. S1), whereas in yellow leaves the relationship was weaker (F. sylvatica R2adj =0.15 or B. pendula R2adj = 0.02 NS; Fig. S1), possibly due in part to less-even pigmentation across the leaf lamina during senescence. Similarly, leaf flavonol readings were consistent between fresh and dry green leaves and to some extent yellow F. sylvatica leaves, but highly variable in yellow B. pendula leaves (Fig. S1). Since the flavonol index is dependent on chlorophyll as a reference, higher variability in the two indices at low values of chlorophyll would be expected.

*FW Lower Epidermal Flavonoid data were not collected from *Betula pendula* green leaves.

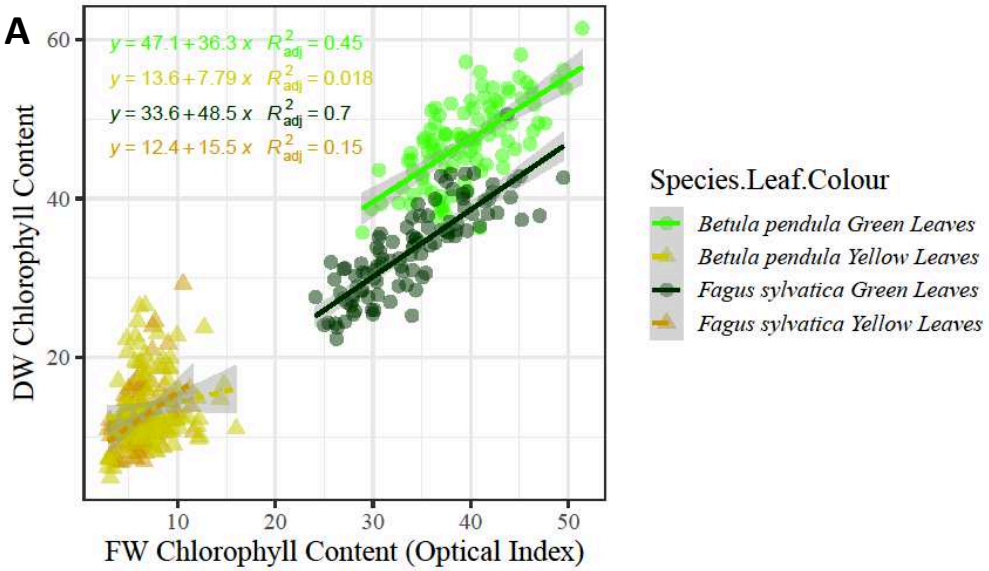

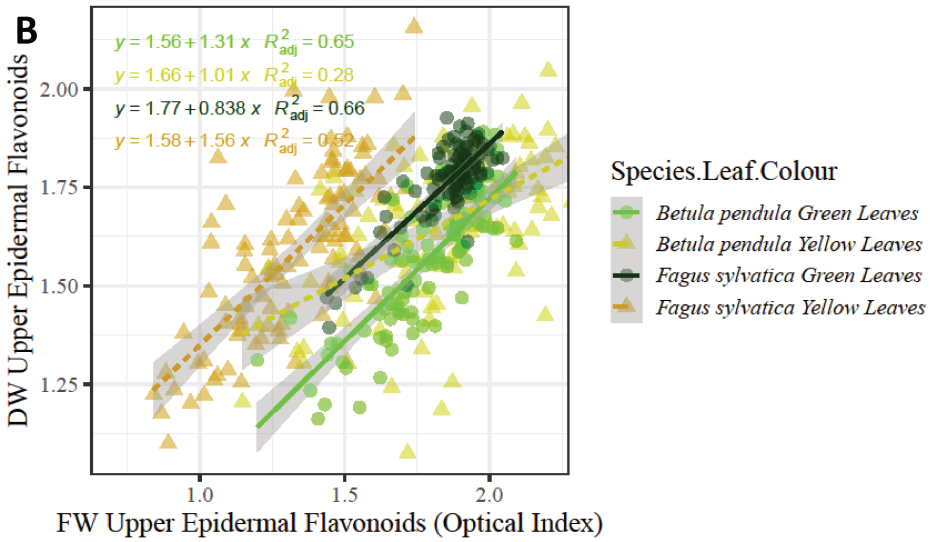
B
y = 1.56 + 1.31 x R²adj = 0.65
y = 1.66 + 1.01 x R²adj = 0.28
y = 1.77 + 0.838 x R²adj = 0.66
y = 1.58 + 1.56 x R²adj = 0.52
DW Upper Epidermal Flavonoids
2.00
1.75
1.50
1.25
1.0
1.5
2.0
FW Upper Epidermal Flavonoids (Optical Index)
Species.Leaf.Colour
Betula pendula Green Leaves
Betula pendula Yellow Leaves
Fagus sylvatica Green Leaves
Fagus sylvatica Yellow Leaves

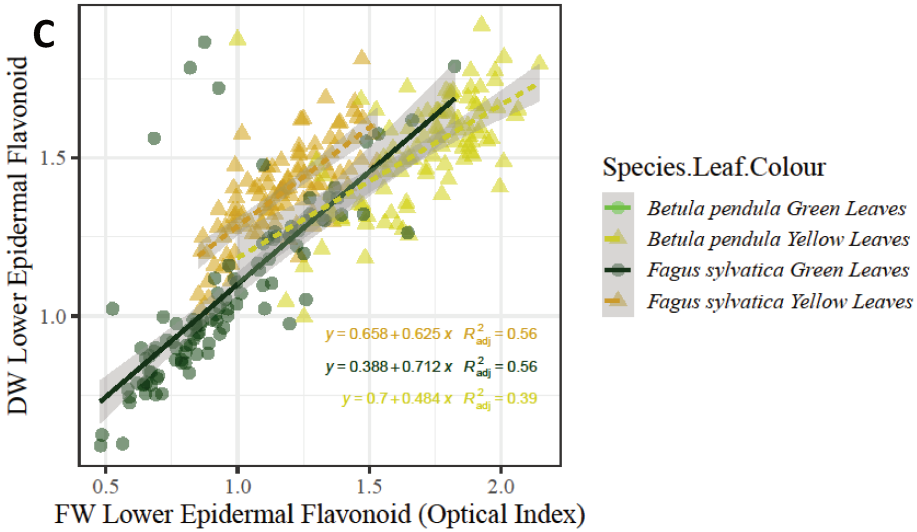
C
y = 0.658 + 0.625 x R²adj = 0.56
y = 0.388 + 0.712 x R²adj = 0.56
y = 0.7 + 0.484 x R²adj = 0.39
DW Lower Epidermal Flavonoid
1.5
1.0
0.5
1.0
1.5
2.0
FW Lower Epidermal Flavonoid (Optical Index)
Species.Leaf.Colour
Betula pendula Green Leaves
Betula pendula Yellow Leaves
Fagus sylvatica Green Leaves
Fagus sylvatica Yellow Leaves

Figure S2 Scatterplot and linear regressions of the relationship between fresh weight and dry weight of *B. pendula* and *F. sylvatica*, green and yellow leaves. Leaves were weighed before and after drying.

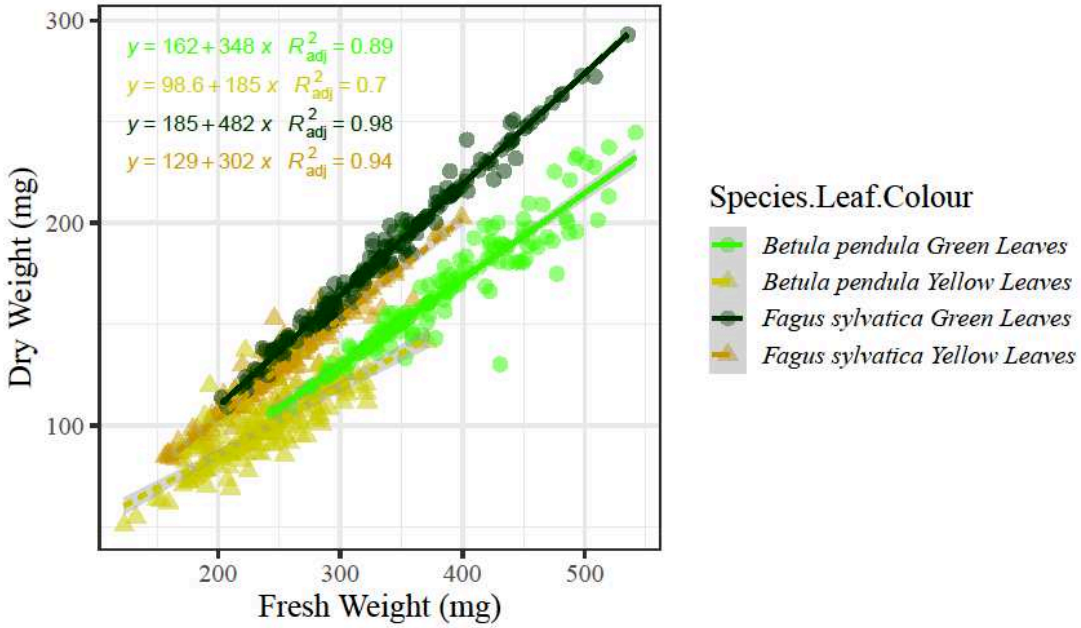

Figure S3 A & B. Arrangement of leaves in the controlled environment experiment, C. in the forest decomposition experiment (*Acer* stand), and D. during installation to show a thin layer of leaf litter from the stand between the net and the soil (*Betula* stand).

Figure S4 Time series of (A) photosynthetically active radiation (PAR), (B) blue light and (C) UV radiation in the stands at Viikki (Helsinki) during the experiment.

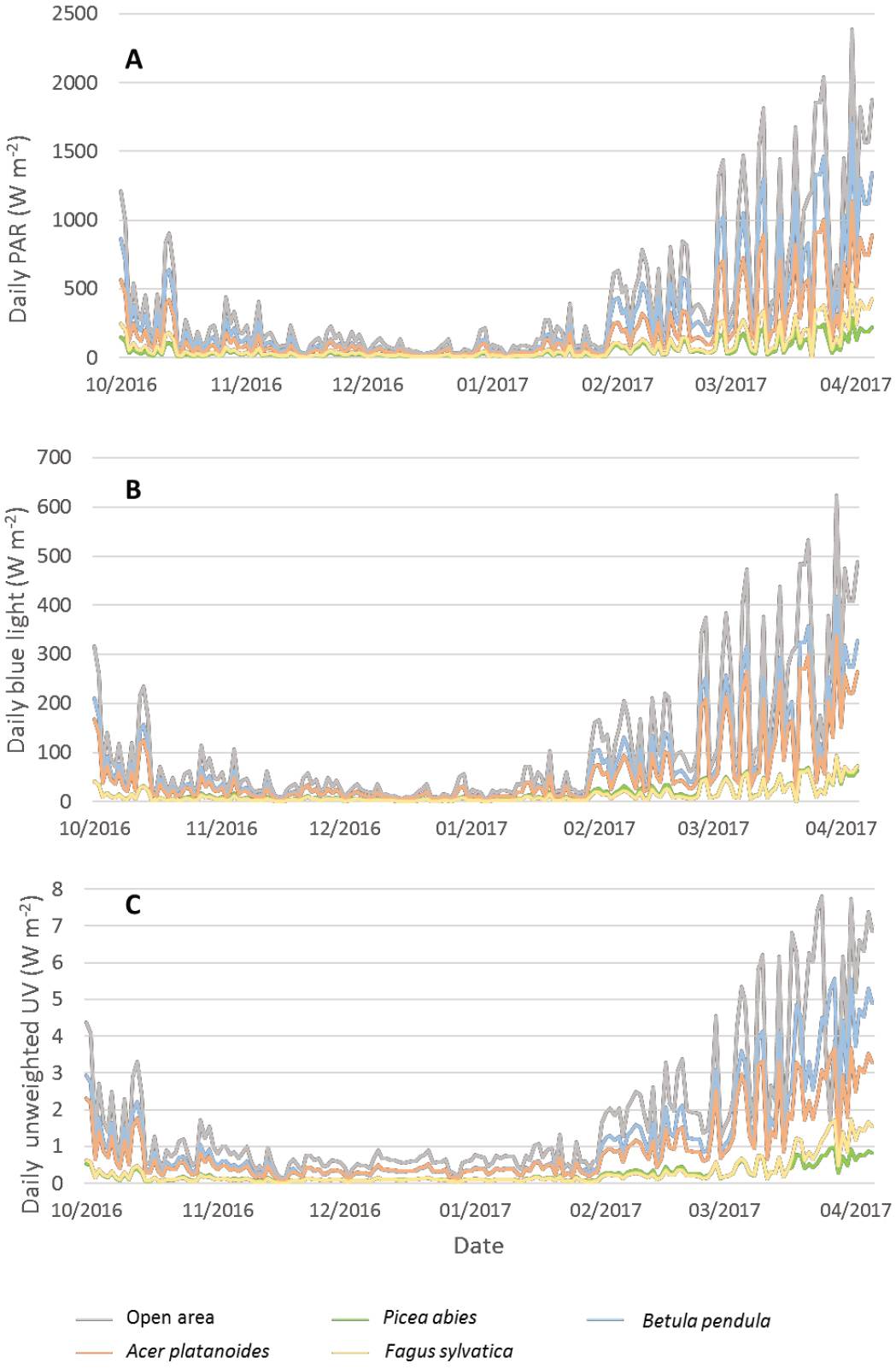

Figure S5 Plot showing average diurnal time courses of (A) leaf surface temperature (red) and relative humidity (blue) in the experimental chamber, and (B) air temperature in different parts of the chamber (centre - orange , side - red, and edge - yellow).

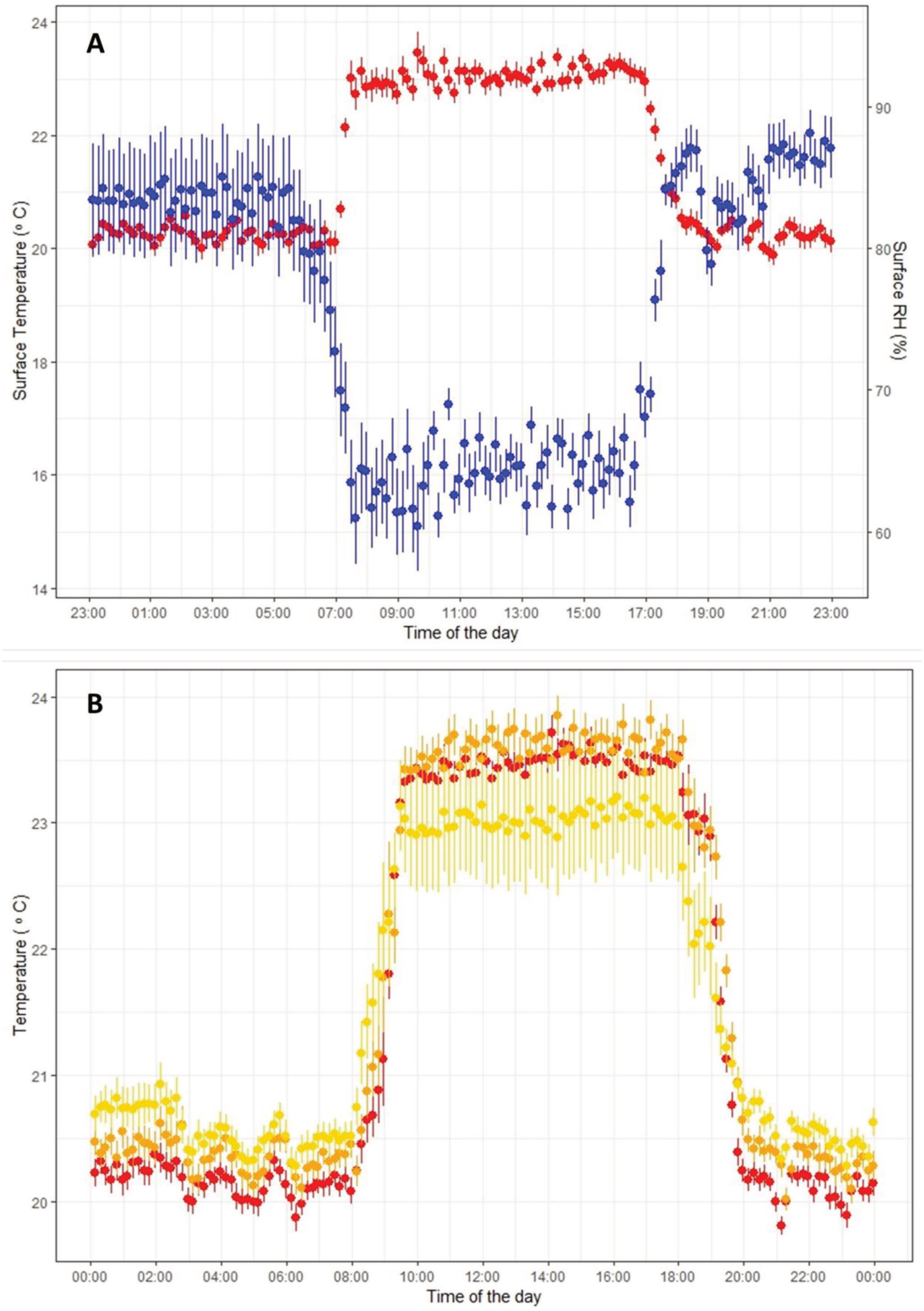

Figure S6 Leaf temperature under controlled conditions according to leaf colour and light exposure treatment. Data measured in the growth room compartments under controlled conditions on 13th October 2016. Leaves under the dark filter are 0.8 °C cooler on average than under the other filters (Effect of Filter $p < 0.001$). Green leaves of silver birch are also 1.0°C cooler on average than the yellow leaves of silver birch and both coloured leaves of beech (Effect of Leaf Colour, $p = 0.001$; Colour x Species $p = 0.005$).

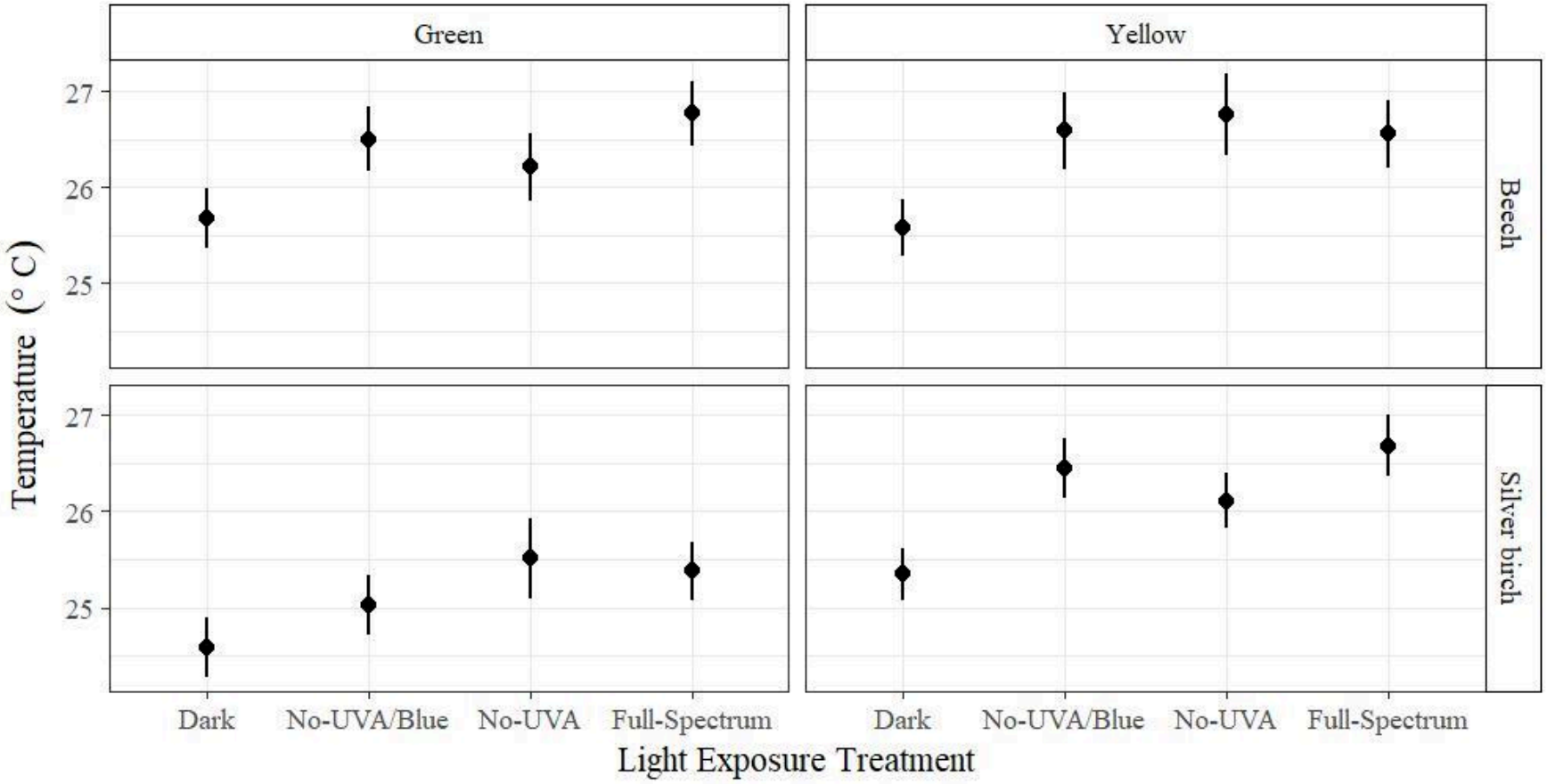

Figure S7 The relationship between epidermal flavonoids for the upper (adaxial) vs. lower (abaxial) epidermis of each species. The same leaf was measured with Dualex on either side.

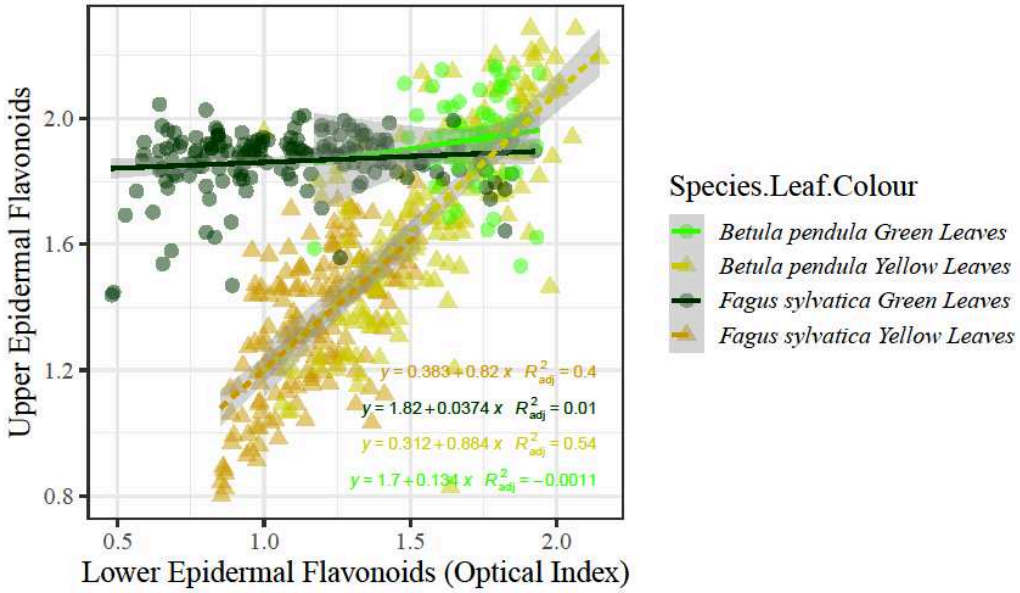

Figure S8 The response ratio of (A) C content and (B) C:N ratio of leaf litter under each filter treatment at the end of the controlled conditions photodegradation experiment. Table 1 gives ANOVA results and means values. Scatterplots of C:N ratio against [N] for leaf from (C) the controlled experiment, and (D) forest stands.

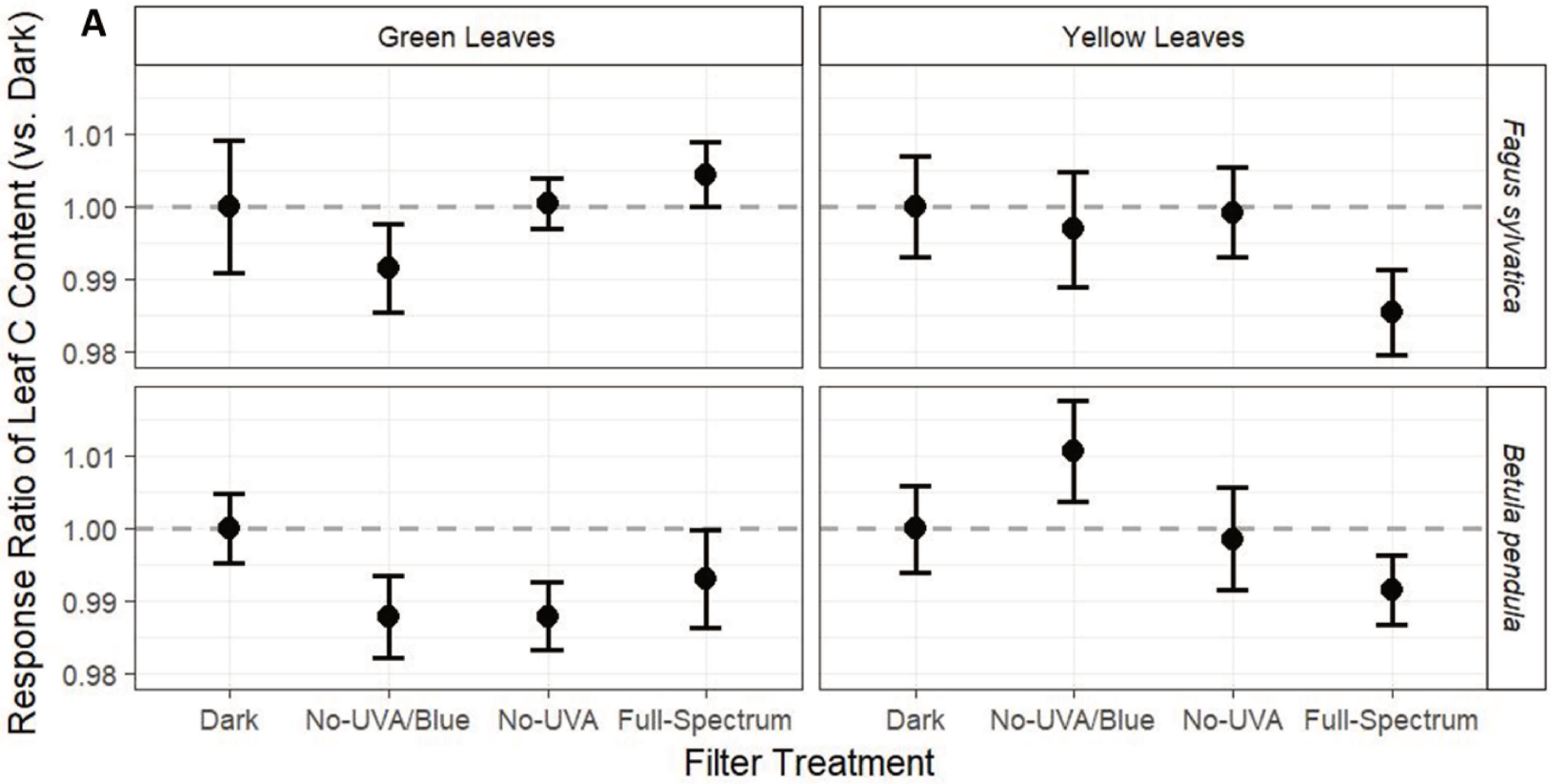

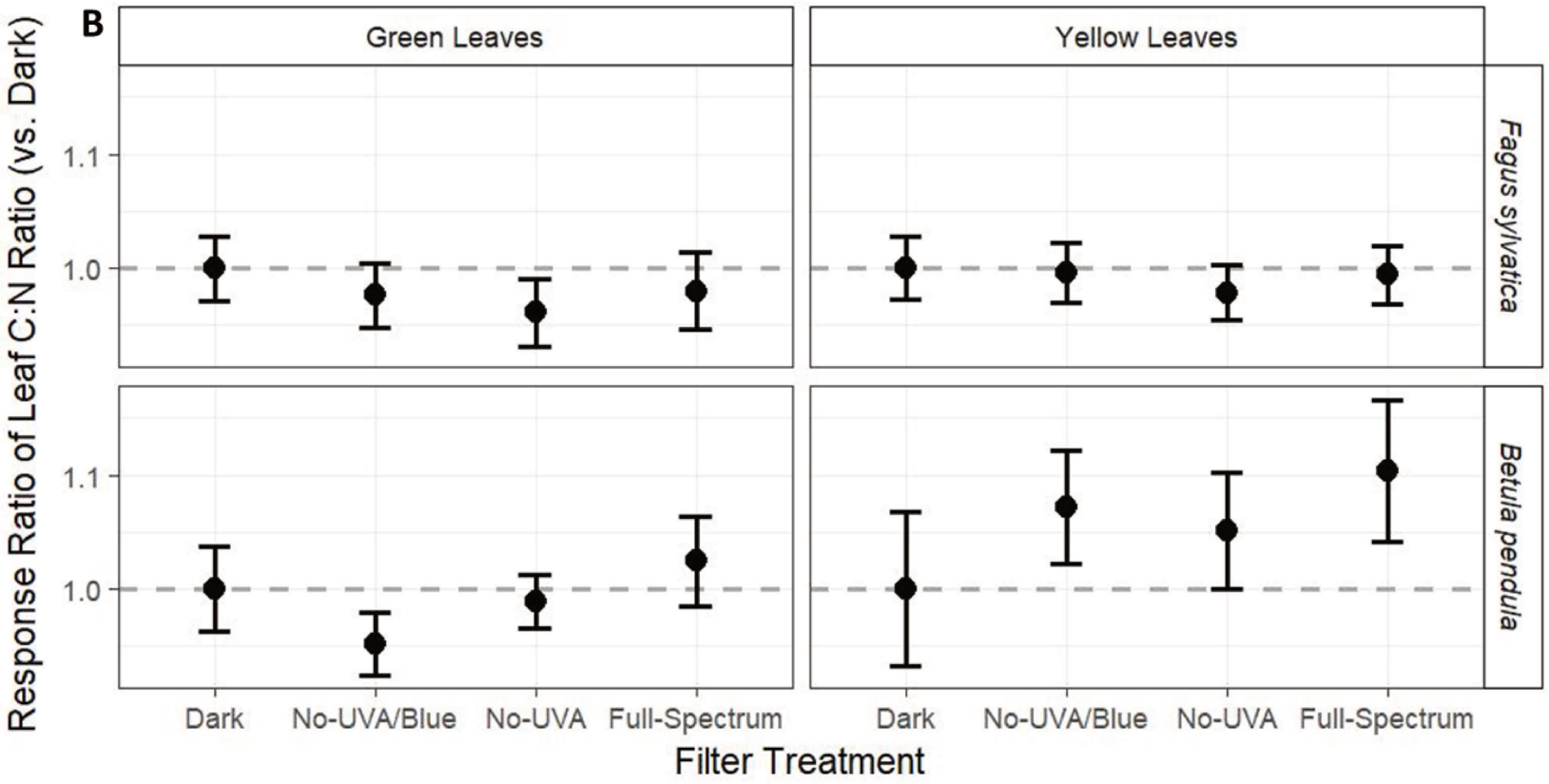
B
Green Leaves
Yellow Leaves
Fagus sylvatica
Betula pendula
Response Ratio of Leaf C:N Ratio (vs. Dark)
1.1
1.0
1.1
1.0
Dark
No-UVA/Blue
No-UVA
Full-Spectrum
Dark
No-UVA/Blue
No-UVA
Full-Spectrum
Filter Treatment

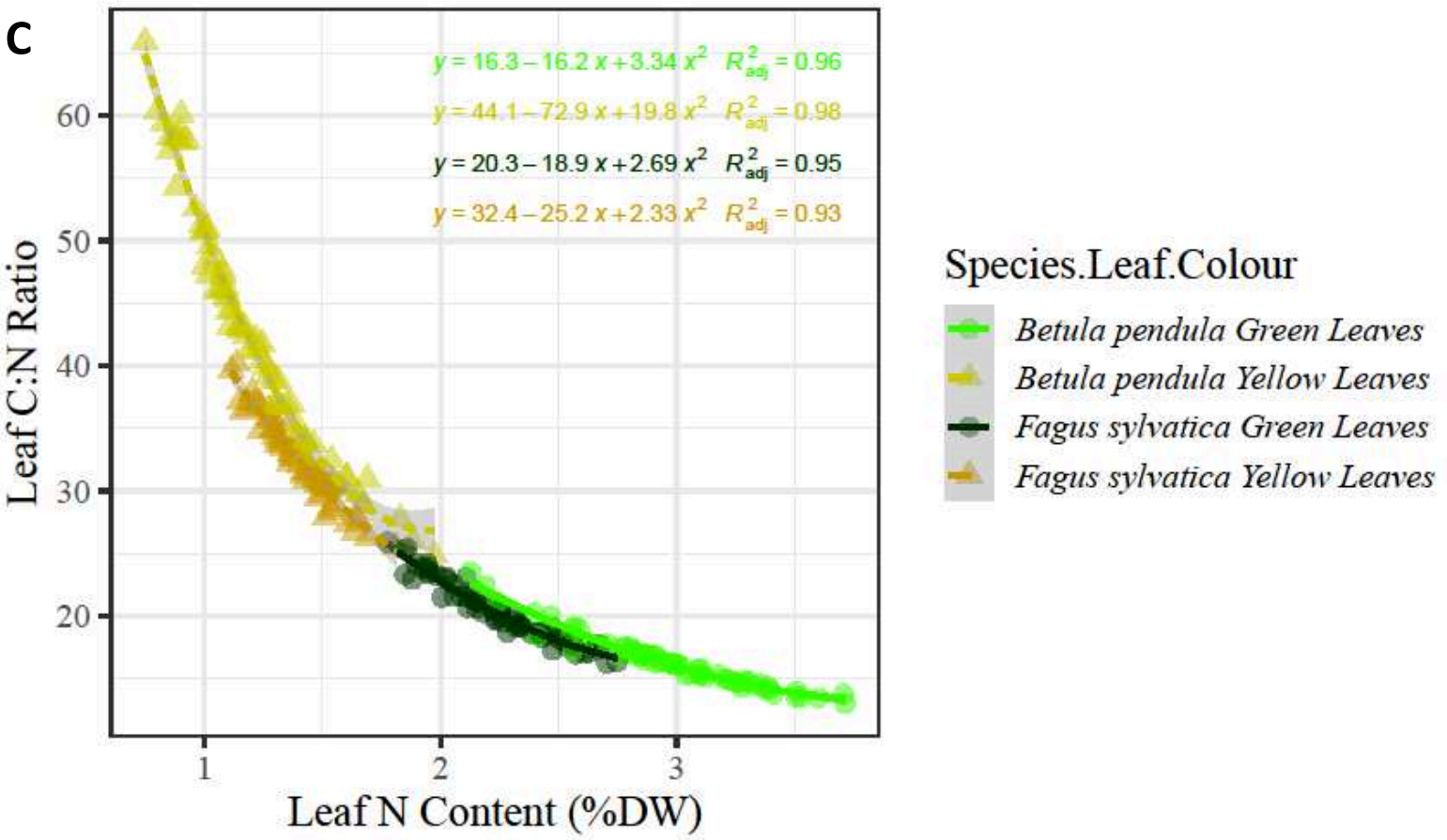

Scatterplot and fitted function of the relationship between leaf nitrogen content (as percentage of dry weight) and leaf carbon/nitrogen ratio of *B. pendula* and *F. sylvatica*, green and yellow leaves after light exposure treatments in controlled conditions for total time of six weeks. Each coloured equation shows corresponding groups' fit and adjusted R^2 value. Leaf phase of senescence is represented either with circle and continuous line (green leaves) or triangle and dotted line (yellow leaves).

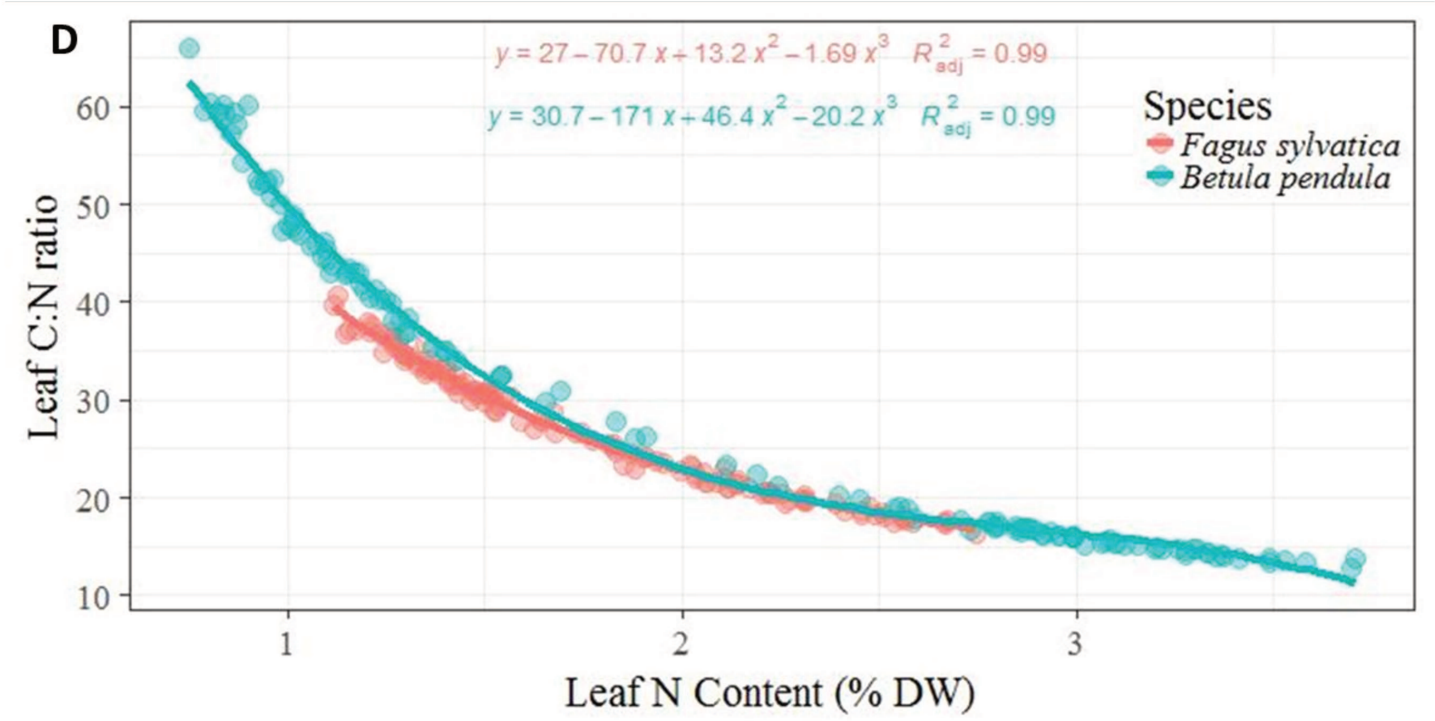

Scatterplot and fitted function of the relationship between leaf nitrogen content (as percentage of dry weight) and leaf carbon/nitrogen ratio of *B. pendula* and *F. sylvatica* leaves that senesced in the stand (collected in December). Each coloured equation shows the fitted function and adjusted R^2 value for the corresponding species. The best fit in each case was to a 3rd order polynomial function. DW- dry weight.

Figure S9 Plot showing daily average temperature (red) ± 1 SE (grey) at the experimental study site in Viikki (Helsinki).

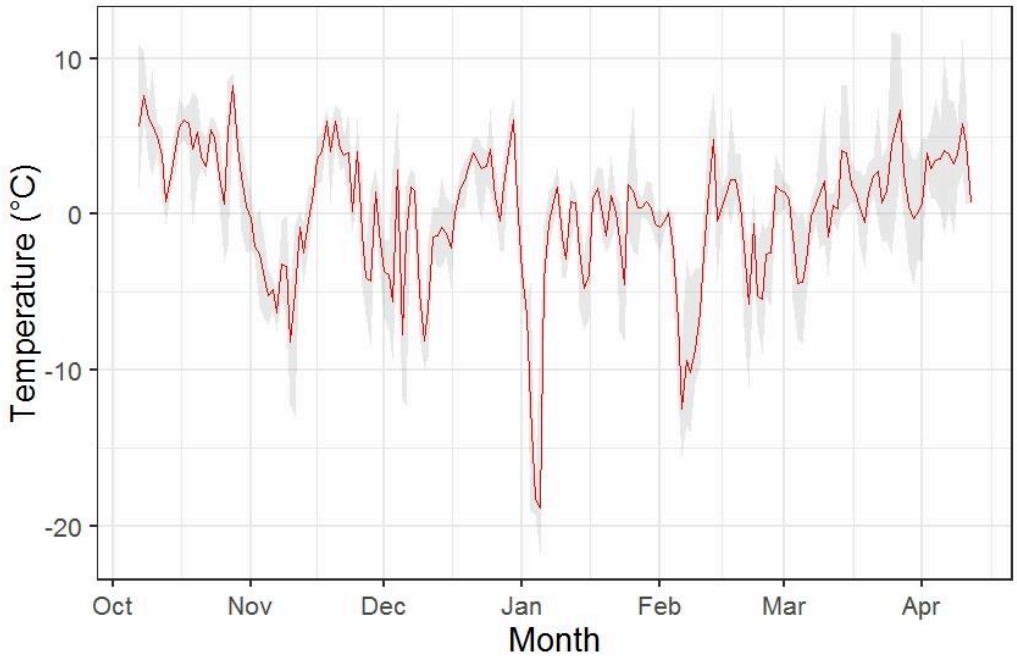

Supplemental Tables

Table S1 The spectral energy irradiance in the controlled experiment growth room under each treatment combination (mean ± SE of measurements from four blocks).

Treatment	PAR	Blue	UV-A
Full Spectrum and UV-A	76.3 ± 1.2 W m^{-2}	13.3 ± 0.2 W m^{-2}	10.19 ± 2.47 W m^{-2}
Full Spectrum No UV-A	74.7 ± 1.2 W m^{-2}	13.0 ± 0.2 W m^{-2}	0.02 ± <0.001 W m^{-2}
No Blue and UV-A	51.8 ± 1.2 W m^{-2}	0.09 ± 0.008 W m^{-2}	12.14 ± 2.49 W m^{-2}
No Blue No UV-A	48.9 ± 1.0 W m^{-2}	0.11 ± W m^{-2}	0.02 ± 0.003 W m^{-2}

Table S2 Examples of the light environment in the forest stands compared with a nearby open area. The mean photon irradiance (µmol m^{-2} s^{-1}) and standard error are shown. Measurements were done using an array spectroradiometer (Maya2000 Pro Ocean Optics, Dunedin, FL, USA; D7-H-SMA cosine diffuser, Bentham Instruments Ltd, Reading, UK) in clear sky conditions on 5th December 2016 at four measuring points in each stand where the leaf litter was placed. R:FR ratio is defined according to Sellaro. Only one measurements was taken in the open where direct sunlight was occluded from the cosine diffusor to create the shade measurement.

Treatment Stand	Position	PAR (PPFD)	Blue	UV-A	UV-B	UV:PAR	B:G	R:FR
Open	Sun	93.9± 0.4	24.6 ± 0.1	11.1 ± 0.1	0.032 ± 0.002	0.119 ± 0.027	1.08 ± 0.01	1.19 ± 0.01
	Shade	69.9	21.9	10.9	0.029	0.156	1.27	1.46
Betula	Sunfleck	64.0 ± 10.3	15.0 ± 1.3	6.4 ± 0.10	0.012 ± 0.001	0.101 ± 0.029	0.99 ± 0.07	1.13 ± 0.01
	Shade	59.6 ± 2.2	14.3 ± 0.1	6.4 ± 0.11	0.017 ± 0.004	0.107 ± 0.011	1.02 ± 0.03	0.89 ± 0.01
Acer	Sunfleck	28.1 ± 0.2	7.5 ± 0.1	3.4 ± 0.10	0.009 ± 0.002	0.122 ± 0.013	1.11 ± 0.01	1.19 ± 0.01
	Shade	25.7 ± 0.9	8.3 ± 0.1	4.2 ± 0.11	0.012 ± 0.003	0.164 ± 0.004	1.30 ± 0.02	1.46 ± 0.03
Fagus	Sunfleck	50.8 ± 11.3	11.4 ± 1.5	5.0 ± 0.10	0.013 ± 0.001	0.099 ± 0.027	0.98 ± 0.08	1.02 ± 0.02
	Shade	31.2 ± 0.8	8.7 ± 0.0	4.5 ± 0.02	0.017 ± 0.001	0.145 ± 0.004	1.20 ± 0.01	1.00 ± 0.01
Picea	Sunfleck	5.4 ± 1.4	1.4 ± 0.2	0.84 ± 0.06	0.061 ± 0.052	0.166 ± 0.080	1.16 ± 0.26	0.94 ± 0.11
	Shade	3.3 ± 0.3	1.0 ± 0.0	0.46 ± 0.03	0.001 ± 0.001	0.141 ± 0.008	1.19 ± 0.01	1.04 ± 0.09

Table S3 Cumulative daily irradiance doses received by the litter at the end of the experiment (6 months) in the forest stands and a nearby open area, under different filter treatments and in unfiltered conditions.

Stand	Cumulative mean daily Irradiance	Photon Irradiance (mol m^{-2})			Energy Irradiance (W m^{-2})		
	Filter treatment /unfiltered	UV	Blue light	PAR	UV	Blue light	PAR
Open	Dark	0.06	0.39	2.02	0.21	20.62	107.47
	No-UV/blue	0.24	4.92	903.21	0.91	261.84	48087.31
	No-UV	32.17	353.70	1370.51	120.11	18831.32	72967.01
	Full-Spectrum	81.91	356.62	1379.85	306.23	18986.74	73464.12
	Unfiltered	*88.58*	*372.32*	*1427.92*	331.18	*19822.76*	*76023.59*
Betula pendula	Dark	0.04	0.25	1.40	0.14	13.08	74.31
	No-UV/blue	0.16	3.18	624.55	0.61	166.03	33251.60
	No-UV	21.34	229.04	947.69	79.68	11940.77	50455.51
	Full-Spectrum	54.31	230.93	954.14	203.02	12039.32	50799.25
	Unfiltered	*58.73*	*241.10*	*987.38*	219.56	*12569.43*	*52569.08*
Acer platanoides	Dark	0.03	0.20	0.93	0.11	10.59	49.69
	No-UV/blue	0.12	2.58	417.64	0.46	134.48	22235.49
	No-UV	16.25	185.58	633.72	60.69	9671.98	33739.83
	Full-Spectrum	41.37	187.11	638.04	154.66	9751.81	33969.69
	Unfiltered	*44.74*	*195.35*	*660.27*	167.26	*10181.20*	*35153.18*
Fagus sylvatica	Dark	0.01	0.05	0.39	0.03	2.60	20.88
	No-UV/blue	0.04	0.63	175.45	0.14	32.96	9341.11
	No-UV	5.05	45.37	266.23	18.86	2370.21	14174.07
	Full-Spectrum	12.87	45.75	268.04	48.12	2389.77	14270.63
	Unfiltered	*13.92*	*47.76*	*277.38*	52.05	*2495.00*	*14767.81*
Picea abies	Dark	0.01	0.05	0.26	0.03	2.86	13.79
	No-UV/blue	0.03	0.69	115.88	0.12	36.29	6169.54
	No-UV	4.20	49.93	175.83	15.67	2610.16	9361.57
	Full-Spectrum	10.61	50.35	177.03	39.90	2631.70	9425.35
	Unfiltered	*11.54*	*52.56*	*183.20*	43.15	*2747.58*	*9753.73*

Table S4 The leaf traits between species and phase of senescence measured prior to the experiment. Irradiance and temperature in each treatment combination (mean ± SE of four compartments). LMA is estimated for leaves used in the experiment from the calibration with the pool of dried leaves. Adaxial Epi refers to the upper epidermis, and abaxial epi the lower epidermis.

Species	***Fagus sylvatica***	***Fagus sylvatica***	***Betula pendula***	***Betula pendula***	ANOVA		
Senescence	**Green**	**Yellow**	**Green**	**Yellow**	**Colour**	**Species**	**Interaction**
Leaf Area (LA cm^2)	21.12 ± 0.33	18.35 ± 0.32	18.36 ± 0.24	16.26 ± 0.32	**F = 375** ***P* = 0.015**	**F = 378** ***P* = 0.015**	F = 1.3 *P* = 0.372
Leaf Fresh Mass Area (LFMA mg cm^{-2})	17.71 ± 0.54	14.85 ± 0.51	18.54 ± 0.43	14.12 ± 0.41	**F = 172** ***P* = 0.006**	F = 0.03 *P* = 0.886	F = 7.93 *P* =0.106
Leaf Mass Area (LMA mg cm^{-2})	9.82 ± 0.26	7.20 ± 0.31	7.44 ± 0.23	5.94 ± 0.21			
Leaf Water Content (g g^{-1})	0.278 ± 0.008	0.132 ± 0.003	0.149 ± 0.008	0.123 ± 0.005	**F = 175** ***P* = 0.006**	**F = 109** ***P* = 0.009**	**F = 85** ***P* = 0.012**
Adaxial Epi Flavonoids (OI)	1.87 ± 0.01	1.38 ± 0.03	1.93 ± 0.02	1.54 ± 0.03	**F = 12.0** ***P* = 0.003**	**F = 22.1** ***P* = 0.042**	F = 4.21 *P* = 0.176
Abaxial Epi Flavonoids (OI)	1.31 ± 0.04	1.19 ± 0.02	1.74 ± 0.01	1.45 ± 0.03	**F = 49.3** ***P* = 0.020**	**F = 162** ***P* = 0.006**	F = 6.44 *P* = 0.126
Chlorophyll Contents (OI)	31.48 ± 0.66	5.64 ± 0.20	35.37 ± 0.53	8.01 ± 0.44	**F = 3238** ***P* < 0.001**	**F = 40.7** ***P* = 0.024**	F = 2.9 *P* = 0.230

Table S5 List of relevant pairwise comparisons for daily mass loss of green and yellow leaves of *Fagus sylvatica* and *Betula pendula* in the forest experiment: t-tests, with the Holm's correction for multiple comparisons, were used to calculate the P values. Significant contrasts are shown in bold.

Fagus sylvatica – green leaves

Stand x Filter treatment (t-value, p-value)

Dark,Picea abies - No-Blue/UV,Picea abies	1.24930529	2.152424e-01
Dark,Picea abies - No-UV,Picea abies	-0.49398333	6.226887e-01
Dark,Picea abies - Full-Spectrum,Picea abies	0.26791392	7.894639e-01
No-Blue/UV,Picea abies - No-UV,Picea abies	-1.74328862	8.517377e-02
No-Blue/UV,Picea abies - Full-Spectrum,Picea abies	-0.98139137	3.293958e-01
No-UV,Picea abies - Full-Spectrum,Picea abies	0.76189724	4.483900e-01
Dark,Fagus sylvatica - No-Blue/UV,Fagus sylvatica	0.21259091	8.321937e-01
Dark,Fagus sylvatica - No-UV,Fagus sylvatica	-0.69640809	4.882173e-01
Dark,Fagus sylvatica - Full-Spectrum,Fagus sylvatica	1.49555538	1.387538e-01
No-Blue/UV,Fagus sylvatica - No-UV,Fagus sylvatica	-0.90899900	3.661155e-01
No-Blue/UV,Fagus sylvatica - Full-Spectrum,Fagus sylvatica	1.28296447	2.032557e-01
No-UV,Fagus sylvatica - Full-Spectrum,Fagus sylvatica	**2.19196347**	**3.132651e-02**
Dark,Acer platanoides - No-Blue/UV,Acer platanoides	0.41194061	6.814986e-01
Dark,Acer platanoides - No-UV,Acer platanoides	-0.12324782	9.022239e-01
Dark,Acer platanoides - Full-Spectrum,Acer platanoides	0.81294549	4.186925e-01
No-Blue/UV,Acer platanoides - No-UV,Acer platanoides	-0.53518843	5.940229e-01
No-Blue/UV,Acer platanoides - Full-Spectrum,Acer platanoides	0.40100488	6.894991e-01
No-UV,Acer platanoides - Full-Spectrum,Acer platanoides	0.93619331	3.520268e-01
Dark,Betula pendula - No-Blue/UV,Betula pendula	0.86312693	3.906805e-01
Dark,Betula pendula - No-UV,Betula pendula	0.09855178	9.217438e-01
Dark,Betula pendula - Full-Spectrum,Betula pendula	0.03605694	9.713279e-01
No-Blue/UV,Betula pendula - No-UV,Betula pendula	-0.76457515	4.468024e-01
No-Blue/UV,Betula pendula - Full-Spectrum,Betula pendula	-0.82706999	4.106886e-01
No-UV,Betula pendula - Full-Spectrum,Betula pendula	-0.06249485	9.503266e-01

Fagus sylvatica – yellow leaves

Stand x Filter treatment (t-value, p-value)

Dark,Picea abies - No-Blue/UV,Picea abies	1.26264965	2.104770e-01
Dark,Picea abies - No-UV,Picea abies	**2.75920256**	**7.217062e-03**
Dark,Picea abies - Full-Spectrum,Picea abies	0.47660336	6.349771e-01
No-Blue/UV,Picea abies - No-UV,Picea abies	1.49655291	1.385452e-01
No-Blue/UV,Picea abies - Full-Spectrum,Picea abies	-0.78604629	4.342218e-01
No-UV,Picea abies - Full-Spectrum,Picea abies	**-2.28259919**	**2.517847e-02**
Dark,Fagus sylvatica - No-Blue/UV,Fagus sylvatica	1.86078307	6.654329e-02
Dark,Fagus sylvatica - No-UV,Fagus sylvatica	**2.82017952**	**6.083044e-03**
Dark,Fagus sylvatica - Full-Spectrum,Fagus sylvatica	**2.40656798**	**1.846848e-02**
No-Blue/UV,Fagus sylvatica - No-UV,Fagus sylvatica	0.95939645	3.403236e-01
No-Blue/UV,Fagus sylvatica - Full-Spectrum,Fagus sylvatica	0.54578491	5.867714e-01
No-UV,Fagus sylvatica - Full-Spectrum,Fagus sylvatica	-0.41361154	6.802936e-01
Dark,Acer platanoides - No-Blue/UV,Acer platanoides	-0.24813209	8.046843e-01

Dark,Acer platanoides - No-UV,Acer platanoides	-0.31972135	7.500344e-01
Dark,Acer platanoides - Full-Spectrum,Acer platanoides	-1.09820665	2.754928e-01
No-Blue/UV,Acer platanoides - No-UV,Acer platanoides	-0.08324621	9.338690e-01
No-Blue/UV,Acer platanoides - Full-Spectrum,Acer platanoides	-0.85007457	3.978855e-01
No-UV,Acer platanoides - Full-Spectrum,Acer platanoides	-0.72689288	4.694676e-01
Dark,Betula pendula - No-Blue/UV,Betula pendula	1.54454363	1.265044e-01
Dark,Betula pendula - No-UV,Betula pendula	1.82655375	7.159287e-02
Dark,Betula pendula - Full-Spectrum,Betula pendula	-0.25172631	8.019147e-01
No-Blue/UV,Betula pendula - No-UV,Betula pendula	0.28201011	7.786827e-01
No-Blue/UV,Betula pendula - Full-Spectrum,Betula pendula	-1.79626994	7.632351e-02
No-UV,Betula pendula - Full-Spectrum,Betula pendula	**-2.07828006**	**4.097235e-02**

Betula pendula – green leaves

Stand x Filter treatment (t-value, p-value)

Dark,Picea abies - No-Blue/UV,Picea abies	1.67299895	9.879132e-02
Dark,Picea abies - No-UV,Picea abies	**2.91698599**	**4.746742e-03**
Dark,Picea abies - Full-Spectrum,Picea abies	**2.49144685**	**1.509522e-02**
No-Blue/UV,Picea abies - No-UV,Picea abies	1.24398704	2.176540e-01
No-Blue/UV,Picea abies - Full-Spectrum,Picea abies	0.81844790	4.158790e-01
No-UV,Picea abies - Full-Spectrum,Picea abies	-0.42553914	6.717492e-01
Dark,Fagus sylvatica - No-Blue/UV,Fagus sylvatica	-0.56665471	5.727613e-01
Dark,Fagus sylvatica - No-UV,Fagus sylvatica	**2.22376770**	**2.939263e-02**
Dark,Fagus sylvatica - Full-Spectrum,Fagus sylvatica	1.40955961	1.630972e-01
No-Blue/UV,Fagus sylvatica - No-UV,Fagus sylvatica	**2.55256242**	**1.287703e-02**
No-Blue/UV,Fagus sylvatica - Full-Spectrum,Fagus sylvatica	1.82740315	7.190158e-02
No-UV,Fagus sylvatica - Full-Spectrum,Fagus sylvatica	-0.88039355	3.816588e-01
Dark,Acer platanoides - No-Blue/UV,Acer platanoides	0.11758821	9.067307e-01
Dark,Acer platanoides - No-UV,Acer platanoides	0.37922330	7.056700e-01
Dark,Acer platanoides - Full-Spectrum,Acer platanoides	0.18980308	8.500128e-01
No-Blue/UV,Acer platanoides - No-UV,Acer platanoides	0.26163508	7.943711e-01
No-Blue/UV,Acer platanoides - Full-Spectrum,Acer platanoides	0.07221486	9.426369e-01
No-UV,Acer platanoides - Full-Spectrum,Acer platanoides	-0.18942022	8.503116e-01
Dark,Betula pendula - No-Blue/UV,Betula pendula	**-2.55463288**	**1.280733e-02**
Dark,Betula pendula - No-UV,Betula pendula	-1.46579052	1.471831e-01
Dark,Betula pendula - Full-Spectrum,Betula pendula	0.27198974	7.864305e-01
No-Blue/UV,Betula pendula - No-UV,Betula pendula	1.15426290	2.523179e-01
No-Blue/UV,Betula pendula - Full-Spectrum,Betula pendula	**2.86922806**	**5.435928e-03**
No-UV,Betula pendula - Full-Spectrum,Betula pendula	1.77909839	7.956495e-02

Table S6 Phenolic compounds isolated from leaf litter of *B. pendula* and *F. sylvatica* by HLPC follow the controlled-conditions experiment. Each point shows mean ± SE expressed in mg g^{-1} DW.

Fagus sylvatica	Green leaves								Yellow leaves							
	Adaxial up				Abaxial up				Adaxial up				Abaxial up			
	Dark	No-UVA/ Blue	No-UVA	Full-spectrum	Dark	No-UVA/ Blue	No-UVA	Full-spectrum	Dark	No-UVA/ Blue	No-UVA	Full-spectrum	Dark	No-UVA/ Blue	No-UVA	Full-spectrum
STILBENES																
Taxifolin xyloside	0.94 ± 0.04	0.85 ± 0.19	0.98 ± 0.26	0.90 ± 0.15	1.28 ± 0.31	1.21 ± 1.05	1.13 ± 0.33	1.16 ± 0.25	0.99 ± 0.28	0.54 ± 0.14	0.81 ± 0.42	1.66 ± 0.58	0.56 ± 0.08	0.92 ± 0.19	0.60 ± 0.03	0.58 ± 0.13
Taxifolin glucoside	1.17 ± 0.35	0.95 ± 0.21	0.90 ± 0.20	0.62 ± 0.32	0.91 ± 0.16	0.61 ± 0.41	0.96 ± 0.26	0.99 ± 0.31	0.88 ± 0.20	0.88 ± 0.20	1.23 ± 0.42	1.35 ± 0.42	1.19 ± 0.04	1.37 ± 0.29	1.47 ± 0.14	1.30 ± 0.24
Taxifolin aglycon	1.83 ± 0.88	0.75 ± 0.16	0.96 ± 0.37	0.59 ± 0.17	0.68 ± 0.09	0.46 ± 0.46	0.18 ± 0.22	0.46 ± 0.23	0.80 ± 0.06	0.71 ± 0.24	1.11 ± 0.22	0.97 ± 0.13	0.90 ± 0.05	1.12 ± 0.37	1.09 ± 0.08	1.12 ± 0.16
Sum, stilbenes	*3.94 ± 1.20*	*2.56 ± 0.37*	*2.85 ± 0.74*	*2.11 ± 0.07*	*2.88 ± 0.37*	*2.28 ± 1.93*	*3.26 ± 0.71*	*3.57 ± 0.95*	*2.67 ± 0.38*	*2.47 ± 0.75*	*3.27 ± 0.97*	*3.86 ± 0.66*	*2.64 ± 0.13*	*3.40 ± 0.76*	*3.16 ± 0.10*	*3.00 ± 0.48*
FLAVONOIDS																
Myricetin 3-rhamnoside	0.72 ± 0.19	0.53 ± 0.31	1.29 ± 0.40	1.12 ± 0.21	0.59 ± 0.24	0.56 ± 0.08	0.79 ± 0.19	1.14 ± 0.17	1.08 ± 0.15	0.80 ± 0.41	1.32 ± 0.40	1.40 ± 0.34	1.66 ± 0.08	1.76 ± 0.32	1.51 ± 0.08	1.59 ± 0.31
Quercetin 3-rhamnoside	12.38 ± 2.23	13.40 ± 2.31	14.79 ± 1.87	15.76 ± 0.64	10.46 ± 2.80	7.72 ± 0.52	9.88 ± 2.19	7.54 ± 0.60	20.61 ± 3.68	14.68 ± 4.63	16.90 ± 3.49	21.63 ± 4.44	22.37 ± 5.03	15.07 ± 1.26	18.25 ± 5.39	17.80 ± 5.53
Quercetin 3-galactoside	10.54 ± 3.47	11.84 ± 2.69	12.37 ± 2.24	13.04 ± 2.05	9.34 ± 1.53	7.76 ± 5.30	9.23 ± 2.31	8.56 ± 1.30	14.44 ± 3.43	11.00 ± 1.92	11.23 ± 2.03	15.03 ± 4.97	19.62 ± 3.24	11.40 ± 0.85	20.03 ± 6.47	15.17 ± 3.54
Quercetin 3-glucoside	4.70 ± 1.70	4.98 ± 1.34	5.16 ± 1.10	5.59 ± 1.25	2.73 ± 0.46	1.65 ± 0.74	4.19 ± 0.94	1.81 ± 0.42	6.52 ± 1.06	5.60 ± 0.64	4.51 ± 0.61	8.16 ± 2.26	7.28 ± 2.04	4.21 ± 0.43	5.08 ± 0.72	6.31 ± 1.14
Quercetin 7-glycoside	0.35 ± 0.35	0.10 ± 0.10	0.25 ± 0.15	0.24 ± 0.24	0.72 ± 0.11	0.27 ± 0.01	0.53 ± 0.21	0.59 ± 0.28	0.82 ± 0.25	0.82 ± 0.18	0.23 ± 0.15	0.91 ± 0.46	0.96 ± 0.22	0.45 ± 0.26	1.01 ± 0.35	1.15 ± 0.49
Kaempferol 3-galactoside	4.57 ± 1.24	3.72 ± 0.63	4.09 ± 0.28	4.10 ± 0.64	3.23 ± 0.43	1.78 ± 0.99	3.46 ± 0.59	2.76 ± 0.44	3.85 ± 0.90	3.78 ± 0.56	3.63 ± 0.18	4.67 ± 1.73	4.50 ± 1.42	3.70 ± 0.52	4.56 ± 0.63	4.91 ± 1.13
Kaempferol 3-glucoside	11.49 ± 4.24	9.25 ± 1.43	10.42 ± 1.76	10.80 ± 2.98	14.87 ± 1.97	15.86 ± 3.05	11.03 ± 2.12	12.57 ± 3.87	9.72 ± 1.40	9.61 ± 1.64	9.09 ± 1.95	12.49 ± 0.47	18.15 ± 3.00	9.58 ± 2.05	11.38 ± 2.78	12.16 ± 1.10
Kaempferol 3-arabinoside	3.62 ± 0.47	3.47 ± 0.47	3.64 ± 0.13	4.49 ± 1.54	2.92 ± 0.76	1.80 ± 1.31	2.89 ± 0.54	2.47 ± 0.34	4.53 ± 0.39	4.38 ± 0.30	3.50 ± 0.55	5.51 ± 0.58	4.33 ± 1.00	3.33 ± 0.37	4.02 ± 0.18	4.67 ± 0.45
Kaempferol 3-rhamnoside	1.26 ± 0.62	0.65 ± 0.12	0.97 ± 0.22	1.23 ± 0.44	1.07 ± 0.30	0.32 ± 0.09	1.36 ± 0.25	1.25 ± 0.34	0.77 ± 0.18	0.86 ± 0.41	0.89 ± 0.17	1.17 ± 0.32	2.22 ± 0.25	0.96 ± 0.05	1.66 ± 0.15	1.55 ± 0.21
Monocoumaroyl-astragallin 1	0.28 ± 0.28	0.35 ± 0.21	0.53 ± 0.27	0.30 ± 0.15	-	0.33 ± 0.33	0.11 ± 0.11	0.06 ± 0.06	-	-	-	-	-	-	-	-
Monocoumaroyl-astragallin 2	0.65 ± 0.18	0.51 ± 0.27	0.77 ± 0.28	0.47 ± 0.07	0.41 ± 0.25	0.17 ± 0.17	0.23 ± 0.10	0.45 ± 0.28	1.03 ± 0.41	0.87 ± 0.15	0.83 ± 0.55	2.31 ± 0.57	1.19 ± 0.04	0.87 ± 0.10	1.05 ± 0.33	0.83 ± 0.34

Fagus sylvatica	Green leaves								Yellow leaves							
	Adaxial up				Abaxial up				Adaxial up				Abaxial up			
	Dark	**No-UVA/ Blue**	**No-UVA**	**Full-spectrum**	**Dark**	**No-UVA/ Blue**	**No-UVA**	**Full-spectrum**	**Dark**	**No-UVA/ Blue**	**No-UVA**	**Full-spectrum**	**Dark**	**No-UVA/ Blue**	**No-UVA**	**Full-spectrum**
Monocoumaroyl-astragallin 3	0.40 ± 0.03	0.15 ± 0.09	0.53 ± 0.32	0.28 ± 0.05	0.29 ± 0.18	0.46 ± 0.46	0.19 ± 0.13	0.37 ± 0.16	1.38 ± 0.22	1.28 ± 0.30	0.80 ± 0.22	1.34 ± 0.12	1.04 ± 0.06	1.07 ± 0.16	1.14 ± 0.30	0.84 ± 0.20
Monocoumaroyl-astragallin 4	0.11 ± 0.11	0.29 ± 0.15	0.65 ± 0.23	0.46 ± 0.23	0.31 ± 0.16	0.21 ± 0.11	0.39 ± 0.12	0.41 ± 0.17	1.08 ± 0.23	0.93 ± 0.20	0.64 ± 0.21	2.08 ± 0.01	0.64 ± 0.64	0.50 ± 0.17	1.62 ± 0.38	0.52 ± 0.26
Dicoumaroyl-astragallin 1	0.10 ± 0.10	0.18 ± 0.13	0.23 ± 0.10	0.19 ± 0.10	0.21 ± 0.13	0.20 ± 0.12	0.34 ± 0.05	0.17 ± 0.14	0.57 ± 0.12	0.67 ± 0.16	0.41 ± 0.18	0.96 ± 0.25	0.93 ± 0.22	0.39 ± 0.30	0.69 ± 0.27	0.44 ± 0.29
Dicoumaroyl-astragallin 2	0.20 ± 0.20	0.06 ± 0.06	0.21 ± 0.14	0.17 ± 0.17	0.11 ± 0.08	0.26 ± 0.26	0.14 ± 0.14	0.14 ± 0.14	0.44 ± 0.11	0.44 ± 0.14	0.14 ± 0.04	0.76 ± 0.36	0.92 ± 0.10	0.23 ± 0.08	0.69 ± 0.35	0.59 ± 0.22
Sum, flavonoids	*51.40 ± 0.74*	*49.51 ± 6.95*	*55.92 ± 5.71*	*58.24 ± 8.31*	*47.28 ± 4.17*	*39.37 ± 13.37*	*44.76 ± 6.68*	*40.32 ± 7.57*	*66.86 ± 8.55*	*55.73 ± 8.10*	*54.15 ± 6.38*	*78.43 ± 13.19*	*85.83 ± 10.63*	*53.55 ± 3.68*	*73.41 ± 18.12*	*68.53 ± 12.50*
PHENOLIC ACIDS																
Hydroxycinnamic acid (HCA)	0.86 ± 0.21	0.51 ± 0.26	0.51 ± 0.11	0.57 ± 0.22	1.15 ± 0.25	0.96 ± 0.77	0.63 ± 0.23	1.39 ± 0.43	0.68 ± 0.22	0.53 ± 0.20	1.03 ± 0.30	0.49 ± 0.20	0.49 ± 0.18	0.41 ± 0.11	0.84 ± 0.19	0.95 ± 0.22
Neochlorogenic acid	0.38 ± 0.13	0.83 ± 0.31	0.89 ± 0.14	0.75 ± 0.07	0.62 ± 0.19	0.27 ± 0.22	0.50 ± 0.13	0.90 ± 0.21	0.31 ± 0.14	0.52 ± 0.21	0.72 ± 0.13	0.48 ± 0.15	0.21 ± 0.04	0.47 ± 0.15	0.47 ± 0.05	0.61 ± 0.09
Chlorogenic acid	3.25 ± 3.00	1.42 ± 0.46	1.26 ± 0.42	1.32 ± 0.43	11.24 ± 3.45	12.39 ± 11.42	7.82 ± 3.87	10.46 ± 3.87	1.97 ± 0.32	1.87 ± 0.62	1.90 ± 0.40	2.50 ± 0.36	1.72 ± 0.33	2.58 ± 0.92	3.99 ± 0.80	2.66 ± 0.72
Chlorogenic acid derivative 1	3.57 ± 0.22	4.28 ± 1.48	2.98 ± 0.94	4.89 ± 2.57	1.73 ± 0.40	1.25 ± 1.25	1.39 ± 0.64	2.01 ± 1.04	0.30 ± 0.05	0.21 ± 0.07	0.51 ± 0.15	0.71 ± 0.43	1.97 ± 0.26	0.27 ± 0.11	0.62 ± 0.39	0.46 ± 0.19
Chlorogenic acid derivative 2	0.12 ± 0.12	0.18 ± 0.08	0.37 ± 0.07	0.34 ± 0.03	0.22 ± 0.04	0.21 ± 0.10	0.22 ± 0.07	0.23 ± 0.08	0.54 ± 0.02	0.47 ± 0.13	0.52 ± 0.13	0.59 ± 0.05	0.55 ± 0.04	0.61 ± 0.02	0.63 ± 0.05	0.54 ± 0.12
Chlorogenic acid derivative 3	0.45 ± 0.12	0.36 ± 0.12	0.44 ± 0.10	0.47 ± 0.14	0.28 ± 0.07	0.23 ± 0.10	0.39 ± 0.08	0.44 ± 0.06	0.62 ± 0.78	0.78 ± 0.17	0.58 ± 0.07	0.61 ± 0.18	0.87 ± 0.03	0.74 ± 0.01	0.89 ± 0.13	0.64 ± 0.13
Chlorogenic acid derivative 4	0.43 ± 0.04	0.37 ± 0.13	0.46 ± 0.08	0.48 ± 0.08	0.27 ± 0.06	0.25 ± 0.05	0.26 ± 0.05	0.36 ± 0.11	0.47 ± 0.11	0.23 ± 0.08	0.43 ± 0.17	0.68 ± 0.14	-	0.38 ± 0.22	0.19 ± 0.19	0.28 ± 0.20
Chlorogenic acid derivative 5	0.41 ± 0.11	0.28 ± 0.05	0.27 ± 0.03	0.11 ± 0.06	0.39 ± 0.06	0.15 ± 0.15	0.30 ± 0.06	0.37 ± 0.06	0.32 ± 0.09	0.43 ± 0.11	0.35 ± 0.02	0.29 ± 0.16	0.48 ± 0.14	0.38 ± 0.04	0.38 ± 0.05	0.30 ± 0.02
Chlorogenic acid derivative 6	-	-	-	-	-	-	-	-	0.04 ± 0.04	0.29 ± 0.29	0.12 ± 0.09	-	0.44 ± 0.04	0.36 ± 0.05	0.51 ± 0.02	0.52 ± 0.13
Sum, phenolic acids	*9.48 ± 2.85*	*8.24 ± 1.95*	*7.20 ± 1.39*	*8.95 ± 2.93*	*15.89 ± 3.67*	*15.71 ± 14.06*	*11.52 ± 4.62*	*16.17 ± 4.19*	*5.25 ± 0.45*	*5.34 ± 1.70*	*6.17 ± 0.81*	*6.35 ± 1.18*	*6.74 ± 0.62*	*6.21 ± 1.12*	*8.53 ± 1.19*	*6.98 ± 1.07*
OTHERS																
Sum, low molecular phenolics	*64.83 ± 3.31*	*60.31 ± 7.92*	*65.96 ± 7.44*	*69.31 ± 11.09*	*66.05 ± 4.79*	*57.37 ± 29.37*	*59.54 ± 9.67*	*60.06 ± 21.61*	*74.78 ± 8.51*	*63.54 ± 10.51*	*63.59 ± 8.03*	*88.63 ± 14.98*	*95.21 ± 10.15*	*63.17 ± 4.62*	*85.11 ± 18.96*	*78.51 ± 13.55*

Fagus sylvatica	Green leaves								Yellow leaves							
	Adaxial up				Abaxial up				Adaxial up				Abaxial up			
	Dark	No-UVA/ Blue	No-UVA	Full-spectrum	Dark	No-UVA/ Blue	No-UVA	Full-spectrum	Dark	No-UVA/ Blue	No-UVA	Full-spectrum	Dark	No-UVA/ Blue	No-UVA	Full-spectrum
CONDENSED TANNINS																
MeOH soluble	32.89 ± 0.25	28.74 ± 2.07	24.33 ± 1.82	19.65 ± 1.83	24.84 ± 2.39	12.67 ± 3.79	19.41 ± 2.47	22.50 ± 3.30	35.64 ± 2.16	35.53 ± 8.91	27.76 ± 2.49	22.46 ± 0.82	31.32 ± 1.93	43.29 ± 4.40	28.00 ± 0.61	26.84 ± 4.31
MeOH insoluble	100.72 ± 70.20	50.76 ± 14.80	35.60 ± 4.67	23.57 ± 1.92	30.22 ± 7.34	39.37 ± 12.41	22.77 ± 2.51	56.57 ± 16.09	203.37 ± 179.01	31.71 ± 11.49	39.07 ± 6.59	32.31 ± 6.34	13.40 ± 4.69	20.76 ± 2.66	19.87 ± 4.26	28.24 ± 6.33
Sum, condensed tannins	*133.61 ± 70.45*	*79.50 ± 12.73*	*59.93 ± 5.86*	*43.22 ± 2.68*	*55.06 ± 8.78*	*52.04 ± 16.21*	*42.18 ± 1.59*	*79.07 ± 15.30*	*239.02 ± 178.50*	*67.25 ± 20.16*	*66.82 ± 7.24*	*54.76 ± 5.55*	*44.72 ± 4.52*	*64.05 ± 6.39*	*47.88 ± 3.71*	*55.08 ± 9.35*

Betula pendula	Green leaves				Yellow leaves			
	Dark	No-UVA/Blue	No-UVA	Full-spectrum	Dark	No-UVA/Blue	No-UVA	Full-spectrum
FLAVONOIDS								
Quercetin glycoside 1	9.71 ± 0.99	13.30 ± 1.87	7.87 ± 0.94	13.28 ± 3.21	7.04 ± 0.92	7.80 ± 1.25	7.75 ± 0.83	5.23 ± 0.84
Quercetin glycoside 2	1.92 ± 0.80	3.18 ± 0.72	0.85 ± 0.40	1.74 ± 0.63	2.11 ± 0.43	3.01 ± 0.45	2.29 ± 0.56	1.51 ± 0.35
Quercetin glycoside 3	1.07 ± 0.19	0.83 ± 0.16	0.81 ± 0.15	0.79 ± 0.24	0.49 ± 0.10	0.53 ± 0.14	0.57 ± 0.11	0.70 ± 0.12
Quercetin glycoside 4	0.22 ± 0.17	0.87 ± 0.30	0.18 ± 0.14	0.93 ± 0.45	1.69 ± 0.34	1.37 ± 0.20	1.20 ± 0.13	1.02 ± 0.20
Quercetin glycoside 5	3.22 ± 1.11	4.94 ± 0.90	2.93 ± 1.11	4.08 ± 1.33	2.43 ± 0.95	2.19 ± 0.96	1.34 ± 0.47	1.47 ± 0.27
Quercetin glycoside 6	26.03 ± 1.83	28.09 ± 2.44	25.01 ± 2.58	25.93 ± 3.57	21.40 ± 1.52	21.64 ± 2.57	24.05 ± 3.06	23.03 ± 3.53
Quercetin glycoside 7	8.46 ± 1.44	9.19 ± 1.09	6.33 ± 1.71	7.01 ± 1.44	7.53 ± 0.71	8.36 ± 0.80	8.58 ± 0.92	7.54 ± 1.46
Quercetin glycoside 8	0.64 ± 0.12	0.76 ± 0.24	0.58 ± 0.14	0.64 ± 0.21	1.96 ± 0.65	2.78 ± 0.83	1.02 ± 0.26	2.45 ± 0.64
Quercetin glycoside 9	6.04 ± 0.47	6.94 ± 0.73	6.02 ± 0.72	6.30 ± 0.87	4.62 ± 0.62	3.23 ± 0.77	5.44 ± 0.56	4.50 ± 1.24
Quercetin aglycon	1.09 ± 0.36	0.76 ± 0.14	0.72 ± 0.06	0.77 ± 0.05	0.85 ± 0.20	0.83 ± 0.20	0.61 ± 0.14	0.53 ± 0.13
Apigenin glycoside 1	2.14 ± 0.56	2.41 ± 0.35	2.18 ± 0.42	1.88 ± 0.27	1.22 ± 0.37	1.28 ± 0.30	1.14 ± 0.51	1.59 ± 0.25
Apigenin glycoside 2	0.72 ± 0.16	0.87 ± 0.12	0.92 ± 0.33	0.73 ± 0.16	0.67 ± 0.23	1.01 ± 0.37	0.66 ± 0.21	0.86 ± 0.40
Sum, flavonoids	*61.10 ± 4.34*	*72.30 ± 5.24*	*54.40 ± 3.33*	*63.98 ± 8.56*	*51.71 ± 2.28*	*53.83 ± 4.76*	*54.67 ± 5.33*	*50.77 ± 6.45*

Betula pendula	**Green leaves**				**Yellow leaves**			
	Dark	**No-UVA/Blue**	**Dark**	**No-UVA/Blue**	**Dark**	**No-UVA/Blue**	**Dark**	**No-UVA/Blue**
PHENOLIC ACIDS								
Hydroxycinnamic acid (HCA)	0.57 ± 0.16	0.59 ± 0.14	0.53 ± 0.13	0.39 ± 0.14	0.40 ± 0.09	0.61 ± 0.12	0.42 ± 0.09	0.64 ± 0.13
Neochlorogenic acid	12.86 ± 4.18	10.99 ± 3.10	9.38 ± 2.01	8.68 ± 0.94	14.68 ± 3.01	19.57 ± 4.36	17.21 ± 4.31	16.13 ± 2.12
Chlorogenic acid	0.50 ± 0.13	0.77 ± 0.15	1.34 ± 0.62	1.11 ± 0.32	0.69 ± 0.07	0.59 ± 0.17	0.77 ± 0.16	0.68 ± 0.26
Sum, phenolic acids	*13.80 ± 4.28*	*12.30 ± 3.00*	*10.95 ± 1.84*	*10.78 ± 0.99*	*15.94 ± 2.96*	*20.67 ± 4.37*	*18.54 ± 4.22*	*17.12 ± 2.13*
OTHERS								
Sum, low molecular phenolics	*74.91 ± 4.66*	*84.60 ± 6.08*	*65.35 ± 3.72*	*74.76 ± 8.10*	*67.65 ± 3.73*	*74.50 ± 8.24*	*73.21 ± 8.32*	*67.88 ± 6.15*
CONDENSED TANNINS								
MeOH soluble	2.42 ± 0.42	2.42 ± 0.36	3.22 ± 1.08	2.75 ± 0.47	7.33 ± 1.02	11.54 ± 2.40	6.13 ± 1.45	9.98 ± 2.94
MeOH insoluble	17.95 ± 1.92	19.02 ± 2.74	21.64 ± 3.52	22.16 ± 2.69	18.26 ± 3.40	14.61 ± 1.08	19.45 ± 1.46	15.39 ± 2.37
Sum, condensed tannins	*20.37 ± 2.32*	*21.44 ± 2.74*	*24.87 ± 4.57*	*24.91 ± 2.91*	*25.60 ± 3.51*	*26.15 ± 2.73*	*25.58 ± 2.58*	*25.37 ± 4.76*

Table S7 ANOVA table for the phenolic compounds isolated from leaf litter of *B. pendula* and *F. sylvatica* by HLPC follow the controlled-conditions experiment.

Fagus sylvatica	**Colour (C)**	**Orientation (O)**	**Filter treatment (F)**	**C x O x F**	**C x O**	**C x F**	**O x F**
	$F_{1,47}$ **(*p*)**	$F_{1,47}$ **(*p*)**	$F_{3,47}$ **(*p*)**	$F_{3,47}$ **(*p*)**	$F_{3,47}$ **(*p*)**	$F_{1,47}$ **(*p*)**	$F_{1,47}$ **(*p*)**
STILBENES							
Taxifolin xyloside	3.53 (0.066)	0.02 (0.880)	0.38 (0.766)	1.10 (0.358)	1.72 (0.196)	0.20 (0.897)	0.87 (0.464)
Taxifolin glucoside	**4.61 (0.037)**	0.06 (0.805)	0.16 (0.926)	0.21 (0.888)	1.13 (0.292)	0.59 (0.626)	0.10 (0.959)
Taxifolin aglycon	0.17 (0.682)	1.64 (0.207)	0.81 (0.492)	2.24 (0.097)	0.02 (0.898)	0.29 (0.830)	1.81 (0.159)
Sum, stilbenes	*0.26 (0.613)*	*0.28 (0.601)*	*0.36 (0.780)*	*1.39 (0.257)*	*0.003 (0.954)*	*0.48 (0.699)*	*0.08 (0.969)*
FLAVONOIDS							
Myricetin 3-rhamnoside	**12.38 (< 0.001)**	0.67 (0.418)	2.32 (0.087)	0.24 (0.869)	2.88 (0.096)	0.74 (0.533)	1.69 (0.183)
Quercetin 3-rhamnoside	**13.47 (< 0.001)**	**4.41 (0.041)**	0.46 (0.714)	0.04 (0.988)	3.69 (0.06)	0.42 (0.737)	0.44 (0.726)
Quercetin 3-galactoside	**6.99 (0.011)**	0.17 (0.683)	0.40 (0.756)	0.21 (0.891)	**6.37 (0.015)**	0.29 (0.830)	0.41 (0.743)
Quercetin 3-glucoside	**18.87 (< 0.001)**	**9.78 (0.003)**	0.57 (0.636)	0.03 (0.994)	**8.97 (0.004)**	1.81 (0.159)	2.04 (0.122)
Quercetin 7-glycoside	**5.50 (0.023)**	**5.59 (0.022)**	1.33 (0.275)	1.04 (0.383)	0.55 (0.461)	0.36 (0.781)	1.07 (0.370)
Kaempferol 3-galactoside	2.65 (0.110)	0.78 (0.381)	0.49 (0.693)	0.04 (0.988)	**5.77 (0.020)**	0.43 (0.731)	0.30 (0.822)
Kaemperfol 3-glucoside	0.23 (0.629)	**5.53 (0.023)**	1.32 (0.279)	1.01 (0.395)	0.01 (0.936)	0.43 (0.729)	0.84 (0.481)
Kaempferol 3-arabinoside	**12.86 (< 0.001)**	**7.62 (0.008)**	1.69 (0.182)	0.08 (0.972)	**4.21 (0.046)**	0.77 (0.519)	1.05 (0.381)
Kaempferol 3-rhamnoside	2.31 (0.135)	**6.80 (0.012)**	**2.88 (0.046)**	0.94 (0.426)	**6.03 (0.018)**	0.43 (0.734)	0.97 (0.416)
Monocoumaroylastragallin 1	**18.24 (< 0.001)**	**4.75 (0.034)**	0.76 (0.524)	0.37 (0.772)	**5.14 (0.028)**	0.40 (0.753)	0.43 (0.735)
Monocoumaroylastragallin 2	**10.27 (0.002)**	2.77 (0.102)	0.54 (0.657)	1.80 (0.159)	2.02 (0.161)	0.37 (0.772)	0.57 (0.636)
Monocoumaroylastragallin 3	**50.66 (< 0.001)**	2.76 (0.103)	0.76 (0.512)	1.40 (0.258)	0.03 (0.856)	0.52 (0.672)	0.51 (0.678)
Monocoumaroylastragallin 4	**11.93 (0.001)**	**5.07 (0.029)**	1.03 (0.388)	3.77 (0.017)	1.84 (0.181)	0.05 (0.986)	1.40 (0.255)
Dicoumaroylastragallin 1	**4.14 (0.049)**	0.07 (0.797)	0.86 (0.472)	0.64 (0.592)	0.02 (0.879)	0.23 (0.877)	1.81 (0.165)
Dicoumaroylastragallin 2	**31.47 (< 0.001)**	0.07 (0.800)	0.81 (0.495)	2.45 (0.076)	2.25 (0.141)	0.37 (0.776)	0.49 (0.687)
Sum, flavonoids	***14.61 (< 0.001)***	*0.86 (0.359)*	*1.22 (0.313)*	*0.28 (0.840)*	***5.41 (0.024)***	*0.57 (0.636)*	*0.83 (0.482)*

Fagus sylvatica	**Colour (C)** $F_{1,47}$ **(*p*)**	**Orientation (O)** $F_{1,47}$ **(*p*)**	**Filter treatment (F)** $F_{3,47}$ **(*p*)**	**C x O x F** $F_{3,47}$ **(*p*)**	**C x O** $F_{3,47}$ **(*p*)**	**C x F** $F_{1,47}$ **(*p*)**	**O x F** $F_{1,47}$ **(*p*)**
PHENOLIC ACIDS							
Hydroxycinnamic acid (HCA)	0.31 (0.578)	2.48 (0.122)	1.25 (0.302)	0.06 (0.982)	1.92 (0.172)	1.79 (0.161)	1.11 (0.355)
Neochlorogenic acid	**5.34 (0.025)**	0.96 (0.332)	**3.40 (0.025)**	0.86 (0.469)	0.21 (0.650)	0.62 (0.602)	1.86 (0.149)
Chlorogenic acid	**5.19 (0.027)**	**17.17 (< 0.001)**	0.40 (0.750)	0.31 (0.818)	**9.32 (0.004)**	0.55 (0.652)	0.01 (0.998)
Chlorogenic acid derivative 1	**52.34 (< 0.001)**	2.74 (0.105)	0.28 (0.842)	0.58 (0.628)	**15.12 (< 0.001)**	2.49 (0.072)	0.90 (0.447)
Chlorogenic acid derivative 2	**41.32 (< 0.001)**	0.59 (0.448)	0.46 (0.709)	0.38 (0.765)	1.77 (0.190)	0.47 (0.705)	0.51 (0.675)
Chlorogenic acid derivative 3	**32.02 (< 0.001)**	0.06 (0.809)	0.16 (0.923)	0.56 (0.641)	3.44 (0.070)	1.66 (0.188)	0.26 (0.853)
Chlorogenic acid derivative 4	1.39 (0.255)	3.60 (0.066)	0.75 (0.530)	2.33 (0.111)	3.44 (0.071)	0.15 (0.997)	0.83 (0.485)
Chlorogenic acid derivative 5	**5.74 (0.021)**	0.47 (0.497)	2.07 (0.117)	1.93 (0.139)	1.65 (0.206)	0.14 (0.936)	0.06 (0.980)
Chlorogenic acid derivative 6	**80.11 (< 0.001)**	**25.22 (< 0.001)**	1.21 (0.317)	0.64 (0.595)	**29.83 (< 0.001)**	0.26 (0.850)	0.78 (0.513)
Sum, phenolic acids	***9.78 (0.003)***	***6.69 (0.013)***	*0.42 (0.740)*	*0.16 (0.923)*	*1.21 (0.276)*	*0.64 (0.592)*	*0.08 (0.969)*
OTHERS							
Sum, low molecular phenolics	***4.79 (0.034)***	*0.01 (0.912)*	*1.21 (0.317)*	*0.30 (0.824)*	*2.00 (0.164)*	*0.20 (0.892)*	*0.55 (0.647)*
CONDENSED TANNINS							
MeOH soluble	**20.39 (< 0.001)**	2.20 (0.144)	**5.52 (0.002)**	2.41 (0.078)	**4.54 (0.038)**	**2.81 (0.049)**	0.92 (0.489)
MeOH insoluble	0.29 (0.595)	2.60 (0.113)	0.92 (0.439)	0.15 (0.928)	0.73 (0.397)	0.12 (0.945)	1.68 (0.185)
Sum, condensed tannins	*0.22 (0.643)*	*3.97 (0.052)*	*1.01 (0.398)*	*0.30 (0.825)*	*0.11 (0.743)*	*0.05 (0.983)*	*2.36 (0.084)*

Betula pendula	**Colour (C)** $F_{1,55}$ **(*p*)**	**Filter treatment (F)** $F_{3,55}$ **(*p*)**	**C x F** $F_{1,55}$ **(*p*)**
FLAVONOIDS			
Quercetin glycoside 1	**16.71 (< 0.001)**	1.60 (0.199)	2.48 (0.070)
Quercetin glycoside 2	2.98 (0.092)	2.68 (0.060)	2.43 (0.079)
Quercetin glycoside 3	**4.68 (0.035)**	0.15 (0.929)	0.44 (0.721)

Quercetin glycoside 4	0.88 (0.353)	0.41 (0.745)	1.85 (0.154)
Betula pendula	**Colour (C)** $F_{1,55}$ **(*p*)**	**Filter treatment (F)** $F_{3,55}$ **(*p*)**	**C x F** $F_{1,55}$ **(*p*)**
Quercetin glycoside 5	**10.98 (0.002)**	0.88 (0.458)	0.83 (0.483)
Quercetin glycoside 6	**4.17 (0.046)**	0.10 (0.957)	0.28 (0.837)
Quercetin glycoside 7	0.27 (0.608)	0.79 (0.504)	0.74 (0.529)
Quercetin glycoside 8	**23.69 (< 0.001)**	1.56 (0.209)	0.89 (0.454)
Quercetin glycoside 9	**13.24 (< 0.001)**	0.32 (0.808)	1.50 (0.224)
Quercetin aglycon	0.27 (0.608)	1.27 (0.294)	0.15 (0.923)
Apigenin glycoside 1	**11.30 (0.001)**	0.80 (0.500)	0.69 (0.561)
Apigenin glycoside 2	0.37 (0.542)	0.47 (0.705)	0.36 (0.779)
Sum, flavonoids	***7.18 (0.010)***	*1.19 (0.322)*	*0.85 (0.473)*
PHENOLIC ACIDS			
Hydroxycinnamic acid (HCA)	0.01 (0.929)	0.28 (0.837)	0.72 (0.544)
Neochlorogenic acid	**8.37 (0.005)**	0.03 (0.992)	0.36 (0.779)
Chlorogenic acid	2.78 (0.102)	**2.80 (0.050)**	1.88 (0.147)
Sum, phenolic acids	***7.61 (0.008)***	*0.02 (0.995)*	*0.25 (0.862)*
OTHERS			
Sum, low molecular phenolics	*1.03 (0.315)*	*1.01 (0.394)*	*0.61 (0.611)*
CONDENSED TANNINS			
MeOH soluble	**48.88 (< 0.001)**	0.44 (0.721)	1.59 (0.203)
MeOH insoluble	3.59 (0.063)	0.67 (0.573)	0.35 (0.790)
Sum, condensed tannins	***6.05 (0.017)***	*0.29 (0.830)*	*0.32 (0.810)*

Table S8 Pairwise comparisons for HPLC phenolics responding to filter treatments in *Fagus sylvatica* leaves in the controlled experiment: t- tests, with the Holm's correction for multiple comparisons, were used to calculate the P values. Significant contrasts are shown in bold.

Kaempferol 3-rhamnoside				
Filter	**Estimate**	**SE**	**t-value**	**P value**
Dark - No-UVA/Blue	0.237	0.098	2.426	0.074
Dark - No-UVA	-0.019	0.091	-0.211	1.000
Dark - Full-Spectrum	-0.041	0.095	-0.432	1.000
No-UVA/Blue - No-UVA	**-0.256**	**0.094**	**-2.729**	**0.042**
No-UVA/Blue - Full-Spectrum	**-0.278**	**0.098**	**-2.843**	**0.037**
No-UVA - Full-Spectrum	-0.022	0.092	-0.237	1.000
Neochlorogenic acid				
Filter	**Estimate**	**SE**	**t-value**	**P value**
Dark - No-UVA/Blue	-0.102	0.079	-1.291	0.617
Dark - No-UVA	-0.185	0.074	-2.509	0.076
Dark - Full-Spectrum	**-0.218**	**0.078**	**-2.806**	**0.042**
No-UVA/Blue - No-UVA	-0.084	0.078	-1.087	0.617
No-UVA/Blue - Full-Spectrum	-0.116	0.080	-1.445	0.617
No-UVA - Full-Spectrum	-0.033	0.076	-0.431	0.668
MeOH soluble condensed tannins				
Green leaves				
Filter	**Estimate**	**SE**	**t-value**	**P value**
Dark - No-UVA/Blue	0.912	0.387	2.354	0.411
Dark - No-UVA	0.702	0.336	2.088	0.633
Dark - Full-Spectrum	0.783	0.364	2.152	0.585
No-UVA/Blue - No-UVA	-0.210	0.349	-0.601	1.000
No-UVA/Blue - Full-Spectrum	-0.129	0.376	-0.343	1.000
No-UVA - Full-Spectrum	0.081	0.323	0.251	1.000
Yellow leaves				
Filter	**Estimate**	**SE**	**t-value**	**P value**
Dark - No-UVA/Blue	-0.421	0.331	-1.272	1.000
Dark - No-UVA	0.506	0.336	1.505	1.000
Dark - Full-Spectrum	0.855	0.336	2.544	0.286
No-UVA/Blue - No-UVA	0.926	0.331	2.801	0.155
No-UVA/Blue - Full-Spectrum	**1.276**	**0.331**	**3.857**	**0.009**
No-UVA - Full-Spectrum	0.349	0.336	1.039	1.000

Table S9 Pairwise comparisons for HPLC phenolics responding to filter treatments in *Betula pendula* leaves in the controlled experiment: t- tests, with the Holm's correction for multiple comparisons, were used to calculate the P values. Significant contrasts are shown in bold.

Chlorogenic acid				
Filter	**Estimate**	**SE**	**t-value**	**P value**
Dark - No-UVA/Blue	-0.028	0.104	-0.265	0.792
Dark - No-UVA	**-0.345**	**0.117**	**-2.956**	**0.029**
Dark - Full-Spectrum	-0.212	0.113	-1.875	0.268
No-UVA/Blue - No-UVA	**-0.317**	**0.112**	**-2.823**	**0.035**
No-UVA/Blue - Full-Spectrum	-0.184	0.108	-1.697	0.289
No-UVA - Full-Spectrum	0.133	0.120	1.106	0.549

Table S10 List of pairwise comparisons between forest stands for daily mass loss of green and yellow leaves of *Fagus sylvatica* and *Betula pendula* in the forest experiment: t- tests, with the Holm's correction for multiple comparisons, were used to calculate the P values. Significant contrasts are shown in bold.

Fagus sylvatica – green leaves

	Estimate	Sigma	t-value	p-value
Picea abies - Fagus sylvatica	0.002953929	0.005056817	0.5841479	5.607852e-01
Picea abies - Acer platanoides	**0.025573700**	**0.005056817**	**5.0572721**	**2.697791e-06**
Picea abies - Betula pendula	**0.035232408**	**0.005056817**	**6.9673092**	**8.629000e-10**
Fagus sylvatica - Acer platanoides	**0.022619771**	**0.005056817**	**4.4731242**	**2.552844e-05**
Fagus sylvatica - Betula pendula	**0.032278479**	**0.005056817**	**6.3831613**	**1.099344e-08**
Acer platanoides - Betula pendula	0.009658708	0.005056817	1.9100371	5.975779e-02

Fagus sylvatica – yellow leaves

	Estimate	Sigma	t-value	p-value
Picea abies - Fagus sylvatica	-0.004850646	0.002870346	-1.6899166	0.095037167
Picea abies - Acer platanoides	**-0.008397483**	**0.002906365**	**-2.8893419**	**0.004996198**
Picea abies - Betula pendula	**-0.005945492**	**0.002870346**	**-2.0713500**	**0.041632619**
Fagus sylvatica - Acer platanoides	-0.003546837	0.002906365	-1.2203687	0.226001819
Fagus sylvatica - Betula pendula	-0.001094846	0.002870346	-0.3814334	0.703918777
Acer platanoides - Betula pendula	0.002451991	0.002906365	0.8436625	0.401437997

Betula pendula – green leaves

	Estimate	Sigma	t-value	p-value
Picea abies - Fagus sylvatica	**0.083368627**	**0.01927312**	**4.3256428**	**4.951291e-05**
Picea abies - Acer platanoides	**0.150936050**	**0.01847946**	**8.1677740**	**8.967271e-12**
Picea abies - Betula pendula	**0.089233679**	**0.02036276**	**4.3821992**	**4.042020e-05**
Fagus sylvatica - Acer platanoides	**0.067567423**	**0.01927312**	**3.5057857**	**7.989121e-04**
Fagus sylvatica - Betula pendula	0.005865052	0.02109605	0.2780166	7.818192e-01
Acer platanoides - Betula pendula	**-0.061702371**	**0.02036276**	**-3.0301572**	**3.423368e-03**

Betula pendula – yellow leaves

	Estimate	Sigma	t-value	p-value
Picea abies - Fagus sylvatica	**0.0497523513**	**0.009251949**	**5.37749939**	**8.036199e-07**
Picea abies - Acer platanoides	**0.0426155583**	**0.009024600**	**4.72215487**	**1.044825e-05**
Picea abies - Betula pendula	**0.0504409127**	**0.009137846**	**5.52000008**	**4.519126e-07**
Fagus sylvatica - Acer platanoides	-0.0071367930	0.009251949	-0.77138264	4.428719e-01
Fagus sylvatica - Betula pendula	0.0006885613	0.009366877	0.07351023	9.415932e-01
Acer platanoides - Betula pendula	0.0078253543	0.009137846	0.85636747	3.944867e-01

Description of understorey light estimation

Above canopy PAR

Above canopy PAR was obtained from the Viikki Fields Weather Station of the University of Helsinki located within the experimental site (60°13'39.7'N, 25°01'09.5'E). Additionally, PAR was measured at regular intervals during the experiments in all the forest stands and in a nearby open area using an array spectroradiometer (Maya2000 Pro Ocean Optics, Dunedin, FL, USA; D7-H-SMA cosine diffuser, Bentham Instruments Ltd, Reading, UK) that had been calibrated within the previous 12 months (see Hartikainen et al 2018 for details of the calibration), [39, 40] (Table S1 and S2).

Above canopy UV radiation

Above canopy UV radiation was obtained from the Finnish Meteorological Institute (FMI) weather station located in the adjacent suburb of Kumpula (60°12'00.0"N, 24°57'36.0"E), Helsinki [43, 44]. Additionally, UV radiation was measured at regular intervals during the experiments in all the forest stands and in a nearby open area using an array spectroradiometer (Maya2000 Pro Ocean Optics, Dunedin, FL, USA; D7-H-SMA cosine diffuser, Bentham Instruments Ltd, Reading, UK) that had been calibrated within the previous 12 months (see Hartikainen et al 2018 for details of the calibration), [39, 40] (Table S1 and S2).

Understorey PAR

Transmission percentages of different PAR wavelengths were calculated through comparisons of measurements made in the understorey of each forest stand with measurements in the open area nearby as mentioned above. Hemispherical photos were taken at the same locations as spectral irradiance, to characterize canopy cover of each stand by calculation of the global light index (GLI) through the software Hemisfer, as defined by [41, 42]. The GLI was calculated over several dates during the experiment (once every 15 days) in order to account for sun elevation angle and sunrise and sunset time. GLI were estimated for both clear sky and totally overcast conditions. Several GLI indexes have been used to calculate the amount of the above canopy PAR transmitted through the understorey over the study period taking into account the cloudiness per each day. Days have been considered cloudy when the diffuse radiation was higher than 30% of direct radiation. An average GLI has been employed for partially cloudy days. The understorey PAR was then corrected per wavelength using the transmission percentages

calculated from the measurements taken with the Maya spectroradiometer. This allowed us to also estimate the amount of blue light in the understorey.

Understorey UV radiation

Transmission percentages of different biological spectral weighting functions for UV exposure and unweighted UV radiation were calculated through comparisons of measurements made in the understorey of each forest stand with measurements in the open area nearby as mentioned above, as well as UV:PAR ratios. These percentages and the UV:PAR ratio in the understorey were used to correct the estimated percentage of transmitted PAR, in order to obtain an index of UV transmittance (GLI_{UV}) for clear and overcast conditions through the period of the experiment, accounting for sun elevation angle and sunrise and sunset time. The several estimated GLI_{uv} for each period of the experiment where used to calculate the understorey UV as a percentage of the above canopy UV obtained from the Kumpula weather station.

CHAPTER III

Plant Soil
https://doi.org/10.1007/s11104-020-04557-6

REGULAR ARTICLE

Spectral Composition of Sunlight Affects the Microbial Functional Structure of Beech Leaf Litter During the Initial Phase of Decomposition

Marta Pieristè · Estelle Forey · Anissa Lounès-Hadj Sahraoui · Hacène Meglouli · Frédéric Laruelle · Philippe Delporte · T. Matthew Robson · Matthieu Chauvat

Received: 28 October 2019 / Accepted: 30 April 2020

Abstract
Aims This study tests whether different spectral regions of sunlight affect the microbial decomposer assemblage in surface leaf litter in a beech understorey over the first 6 months following leaf senescence.
Methods We performed a litterbag experiment employing filters attenuating combinations of UV-B, UV-A, blue, and green light as well as the whole spectrum of sunlight. We measured changes in microbial biomass and community structure, litter mass loss and litter chemistry during the first 6 months of decomposition.
Results Fungal and total microbial biomass were highest in the treatment excluding UV radiation, blue and green light. Exclusion of UV-B radiation decreased the fungal:bacterial biomass ratio and litter nitrogen content. Bacterial biomass was lower in the dark treatment compared to treatments receiving at least part of the solar spectrum. Our filter treatments affected microbial functional structure from the beginning of the experiment, whereas mass loss was only significantly affected after 6 months of decomposition and no effect was found on litter carbon content.
Conclusions This study proves that sunlight, in a spectrally dependent manner, affects both microbial functional structure and biomass in temperate deciduous forests early in the decomposition process, with bacteria tending to dominate in sunlight and fungi in dark conditions. We found sunlight to be important in the decomposition in temperate forest understoreys despite the low irradiance characterizing these environments. However, long-term studies are required to estimate the relative contribution of sunlight among factors affecting the eventual incorporation of decomposing leaf litter into forest soils.

Keywords Photodegradation · UV · Blue light · Green light · Microbial communities · PLFA

Abbreviations

AFDM	Ash-Free Dry Mass
AMF	Arbuscular Mycorrhizal Fungi
[C]	Carbon content
C:N	carbon-to-nitrogen ratio

T Matthew Robson and Matthieu Chauvat Joint last author contribution

Responsible Editor: Feike A. Dijkstra .

Electronic supplementary material The online version of this article (https://doi.org/10.1007/s11104-020-04557-6) contains supplementary material, which is available to authorized users.

M. Pieristè (✉) · T. M. Robson
Organismal and Evolutionary Biology (OEB), Viikki Plant Science Centre (ViPS), University of Helsinki, P.O. Box 65 (Viikinkaari1), 00014 Helsinki, Finland
e-mail: marta.pieriste@helsinki.fi

M. Pieristè · E. Forey · P. Delporte · M. Chauvat
UNIROUEN, IRSTEA, ECODIV, Normandie Université, FR Scale CNRS 3730, Rouen, France

A. Lounès-Hadj Sahraoui · H. Meglouli · F. Laruelle
Unité de Chimie Environnementale et Interactions sur le Vivant (UCEIV), EA 4492, Université du Littoral Côte d'Opale, SFR Condorcet FR CNRS 3417, 50 rue Ferdinand Buisson, 62228 Calais, France

Published online: 15 May 2020

F:B	fungal-to-bacterial biomass ratio
FAMEs	Fatty-Acid Methyl Esters
DW	Dry Weight
GLI	Global Light Index
Gram-N	Gram-negative bacteria
Gram-P	Gram-positive bacteria
Gram-P:Gram-N	Gram-P bacteria to Gram-N bacteria biomass ratio
LAI	Leaf Area Index
[N]	Nitrogen content
NLFA	Neutral Lipid Fatty Acids
PAR	Photosynthetically Active Radiation
PLFA	Phospholipid Fatty Acid
UV	Ultraviolet radiation

Introduction

In most terrestrial ecosystems, sunlight is prominent among the suite of biotic and abiotic factors driving the litter decomposition process. This is true for arid (Day et al. 2015; Day et al. 2007) to mesic (Brandt et al. 2010) ecosystems, grasslands (Almagro et al. 2017; Brandt et al. 2007) to woodlands (Pieristè et al. 2019a; Pieristè et al. 2019b), and low (Ma et al. 2017) to high latitudes (Pancotto et al. 2003). The mechanism through which sunlight interacts with litter decomposition is known as photodegradation (Bais et al. 2018), and it is driven by UV-B (280–315 nm) and UV-A (315–400 nm) radiation and the short-wavelength regions of visible light (blue 420–490 nm and green 500–570 nm) (Austin et al. 2016). Photodegradation encompasses different processes, i.e. direct (photomineralization, photoinhibition) and indirect (photofacilitation, also known as photopriming) (King et al. 2012), interacting with the other biotic and abiotic drivers of decomposition. As a consequence, sunlight can increase (Day et al. 2007) or decrease (Pancotto et al. 2003) the decomposition rate and potentially affect nutrient cycling (Foereid et al. 2011). The question of whether direct or indirect and positive or negative effects dominate, depends on the climate and the type of ecosystem considered (Almagro et al. 2017). For instance, in mesic environments, where microbial decomposition is the predominant process, direct photoinhibition appears more important than direct photomineralization; which plays a greater role in arid environments at lower latitudes were UV radiation is higher (Bais et al. 2018).

At present, two contrasting effects of sunlight on microbial decomposition are known: photofacilitation and photoinhibition. The first involves the facilitation of microbial decomposition as a result of direct photomineralization of litter typically increasing its bioavailability (Baker and Allison 2015, but see Austin et al. 2016 for a counter-example), while the second refers to direct inhibition of microbial decomposition by sunlight, reducing respiration and altering the structure of microbial assemblages (Duguay and Klironomos 2000; Verhoef et al. 2000). Both these processes are thought to be dependent on the spectral composition of sunlight to which litter and decomposers are exposed (Lin et al. 2018), and thereby may occur concomitantly. For instance, Austin et al. (2016) found that microbial decomposition was inhibited as a consequence of pre-exposure of litter to UV radiation, while photofacilitation occurred when litter was exposed to blue and green light. Furthermore, the relative importance of photofacilitation and photoinhibition seems to depend on the duration of exposure (King et al. 2012; Lin et al. 2018). Most studies into the effect of sunlight on microbial decomposition and decomposer communities focus on UV radiation, more specifically the UV-B region: often trying to simulate potential effects of ozone depletion in arid environments, consequently applying very high UV-B doses, which are not necessarily interpretable for most environments receiving ambient sunlight (Duguay and Klironomos 2000; Lin et al. 2018; Moody et al. 1999). High UV doses such as these can reduce spore germination and fungal hyphal length in fungi colonizing leaf litter (Moody et al. 1999; Verhoef et al. 2000), but evidence is lacking on whether these effects also occur under ambient UV doses.

Only a few recent studies in arid and semiarid environments have analysed photofacilitation and photoinhibition processes in natural conditions (Baker and Allison 2015; Ball et al. 2019; Day et al. 2018; Pancotto et al. 2003). Exposure to ambient UV radiation and blue light enhanced microbial respiration in an arid environment (Day et al. 2018), while bacterial biomass seemed to be reduced (Ball et al. 2019), suggesting a higher metabolic quotient (Anderson and Domsch 1990, 1993). The opposite effect was found in a Mediterranean climate, where microbial respiration was reduced by exposure of *Bromus diandrus* litter to UV radiation (Lin et al. 2015). These contrasting results from different

ecosystems make it hard to generalize about the effects of UV radiation on litter decomposer organisms. Moreover, to be able to scale photodegradation effects across ecosystems and biomes, it would be necessary to separate the direct and indirect effects of sunlight on litter and decomposer organisms in ecological studies.

Those arid and semiarid ecosystems are characterized by low canopy cover, while there are only a few studies under forest canopies (Newsham et al. 2001; Pieristè et al. 2019a; Pieristè et al. 2019b). Deciduous forest understoreys are very-dynamic light environments, in which irradiance and its spectral composition vary over the year as the canopy flushes in spring and opens in autumn (Hartikainen et al. 2018). Although irradiance can be low in the understorey, sunlight can enhance the decomposition of leaf litter in temperate forests and the effect is dependent on initial litter quality, as found for three tree species of differing litter quality in a beech forest in France (Pieristè et al. 2019a). However, this effect seems to vary according to the canopy species and latitude: whereby irradiance interacts with different environmental conditions in winter at high- and mid-latitudes (Pieristè et al. 2019a; Pieristè et al. 2019b). Moreover, during autumn and winter, when the canopy is dormant in deciduous forests, the direct exposure of litter to sunlight has the potential to enhance mass loss and, as a consequence, we could expect to see a priming effect that would facilitate subsequent microbial decomposition (photofacilitation) at later stages (Hättenschwiler et al. 2005; Swift et al. 1979), similar to the processes observed in arid environments.

In forest environments, microbial decomposition drives nutrient cycling and determines nutrient availability to plants (Asplund et al. 2018). Saprophytic and ectomycorrhizal fungi play a decisive role in litter decomposition in these ecosystems and are considered as primary decomposers, due to their capacity to break-down recalcitrant components of leaf litter inaccessible to other organisms (Baldrian 2016; Kubartová et al. 2009). Fungal decomposers colonize litter in the early stages of decomposition, while bacteria appear relatively late and take advantage of the fragmentation of litter and nutrients released by fungi and invertebrates during the initial phase of decomposition (Purahong et al. 2014). Recently, however, several studies have suggested that many bacterial taxa are better adapted to decompose complex C-compounds than previously thought (Sauvadet et al. 2019). Enhanced UV, and its constituent UV-B, radiation reportedly reduce spore germination and fungal hyphal length in fungi colonizing leaf litter (Moody et al. 1999; Verhoef et al. 2000). On the other hand, UV-A radiation has been found to enhance sporulation in some fungal phytopathogens (Paul and Gwynn-Jones 2003), but inhibit sporulation and delay germination of the conidia of some saprophytic fungi (García-Cela et al. 2016; Osman et al. 1989). However, this effect seems to depend on the dose of UV-A radiation, the length of the exposure, the interaction with UV-B radiation and the fungal species considered (Fourtouni et al. 1998; Kumagai 1988; Osman et al. 1989; Paul and Gwynn-Jones 2003). In the same way, the photosensitivity of bacteria is species specific and depends on traits such as pigmentation (Paul and Gwynn-Jones 2003). Since microbes have a crucial role in carbon and nutrient cycles in forest ecosystems (Johnson 2003), it is important to know how they respond to UV radiation and visible light, to better understand the potential effects of changes in spectral composition due to changing canopy phenology.

This study aims to test whether sunlight has an impact on the initial phase of microbial decomposition in the understorey of a temperate forest, and to distinguish the effects that different regions of the solar spectrum can have on microbial decomposition. Hence, we performed a 6-months litterbag experiment employing filters over *Fagus sylvatica* litter to successively attenuate more of the short-wavelength spectral regions of solar radiation from UV-B to green light (Table S1; Fig. S1). We determined mass loss, carbon content [C], nitrogen content [N] and microbial biomass and community structure through PLFA analysis. We expected the attenuation of different spectral regions to lead to dissimilar microbial assemblages with different decomposition rates compared to full sunlight exposure. In particular, we expected treatments excluding UV radiation and blue light to have the highest fungal and bacterial biomass due to removal of the inhibitory effect of these spectral regions, producing a higher photodegradation rate. We expected litter exposed to the full spectrum of sunlight to have higher mass loss and [C] loss than the other treatments due to the presence of shortwave radiation (UV radiation and blue and green light) promoting photomineralization and photofacilitation. Moreover, we expected the dark treatment to have the lowest decomposition rate due to the absence of photodegradation.

Material and Methods

Site Description

The experiment was conducted in a mature pure beech forest (*Fagus sylvatica* L.) in Forêt Verte (49°31′12.6”N 1°07′00.7″E), close to Rouen University, France. The topography at the site is flat and the elevation is about 150 m a.s.l. The understorey at the site of deployment of the litterbags was absent and removed where present (see Fig. S5). The climate of the field site is oceanic temperate, the mean annual air temperature is 10.5 °C and the total annual precipitation average 851.7 mm, distributed relatively evenly over the year. During the study period, the average temperature in the understorey was 8.7 °C (see Fig. S4 for more details). At the end of the 6 months of the study the understorey received about 1160 mol m^{-2} of PAR and about 90 mol m^{-2} of UV (see Table S1 for details about light doses).

Spectral irradiance of sunlight was measured outdoors, inside the litterbags for each filter treatment and without any filter in the forest understorey (Fig. S1). Measurements were taken using an array spectroradiometer (Maya2000 Pro Ocean Optics, Dunedin, FL, USA; D7-H-SMA cosine diffuser, Bentham Instruments Ltd., Reading, UK) that had been calibrated within the previous 12 months for highest precision over the regions of solar UV radiation and photosynthetically active radiation (PAR) (see Hartikainen et al. (2018) for details of the calibration, Aphalo et al. (2012), Aphalo et al. (2016)). Hemispherical photos were taken on multiple occasions to capture the different stages of canopy development. These photos were used to characterize canopy cover by calculation of the global light index (GLI) and the leaf area index (LAI) with the software Hemispher (Schleppi et al. 2007, Thimonier et al. 2010). The LAI was estimated to be 0.74 ± 0.06 during winter (Dec 2017 – mid Apr 2018) corresponding to a GLI of 41.69% ± 1.00%. On 14th May 2018, when canopy leaves were completely expanded, the LAI reached 2.96 ± 0.40 while the GLI dropped to 11.62% ± 3.05%. Above-canopy irradiance data were obtained from SoDa Helioclim-3 (Blanc et al. 2011; Gschwind et al. 2006; Udo and Aro 1999). Modelled understorey irradiance data were calculated by applying the GLI to the above-canopy irradiance data (Canham 1988) following the protocol from Pieristè et al. (2019b) and Hartikainen et al. (2018). Estimates of received PAR, UV-A and UV-B radiation are given (Fig. S2, Fig. S3, Table S1) according to the spectral composition of modelled incident solar radiation; adjusting for the relative enrichment of UV radiation in shade (Hartikainen et al. 2018) by comparison with the understorey spectral irradiance measured as described above.

Temperature inside a representative sub-sample of litterbags was continuously monitored with ECH2O 5TM sensors (Decagon devices, Pullman, Washington, USA). These data showed no significant differences in temperature between litterbags from the six different filter treatments ($p = 0.814$, ESM Fig. S4).

Experimental Design and Litterbags Design

We assigned litterbags to randomised locations within the study site (Fig. S5). The experiment comprised 273 litterbags in total: 105 used for analysis of C and N and for the determination of mass loss (6 filter treatments × 5 replicates × 3 collection times +5 replicate conventional litterbags × 3 collection times) and 168 for PLFA analysis (6 filter treatments × 6 replicates × 4 collection times +5 replicate conventional litterbags × 4 collection times). The design of the litterbags for the experiment followed that described by Pieristè et al. (2019a). The dimensions of the litterbags were 150-x-150 mm, with the upper part made from a sheet of perforated film filter material and the bottom part made from a sterile Teflon mesh sheet of pore sizes 0.1 mm allowing only microflora (fungi and bacteria) access to the litter (Fig. S6). Six different filter treatments were created (Fig. S1): a “Full-spectrum” treatment (full-spectrum at near-ambient sunlight) of polyethene film (0.05 mm thick, 04 PE-LD; Etola, Jyväskylä, Finland) transmitting >95% of incident PAR and UV radiation; a “No-UV-B” treatment (attenuating UV-B radiation <320 nm) using polyester (0.125 mm thick, Autostat CT5; Thermoplast, Helsinki, Finland); a “No-UV” treatment using Rosco #226 (0.2 mm thick, Westlighting, Helsinki, Finland) attenuating UV radiation <380 nm; a “No-UV/Blue” treatment using Rosco #312 Canary yellow (0.2 mm thick, Westlighting, Helsinki, Finland) attenuating UV radiation and blue light <480 nm; a “No-UV/Blue/Green” treatment using Rosco #135 deep golden amber (0.2 mm thick, Westlighting, Helsinki, Finland) attenuating UV radiation and blue and green light <580 nm; and a “Dark” treatment using solid polyethene film, white on the upper-side and solid black on the lower-side (0.15 mm thick, Casado sarl, France), attenuating >95% of PAR and UV radiation. In addition, a treatment

(henceforth "mesh") made from classic litterbags with mesh size 0.1 mm was included to test differences between our litterbags and classical litterbag used in decomposition studies. There were no significant differences in mass loss ($p = 0.541$), [C] ($p = 0.888$) and [N] ($p = 0.123$) between the full-spectrum treatment and the mesh treatment (Table S17, Fig. S13). However, the full-spectrum treatment had a lower C:N (20.5) than the mesh treatment (21.9) ($p = 0.024$, Table S17, Fig. S13).

Litterbags were deployed on 05-Dec-2017, to coincide with the end of leaf fall and follow the natural timing of decomposition as faithfully as possible. They were pinned to the soil surface with small tent pegs, through a homogeneous thin layer of the previous years' litter that remained in contact with the underside of the litterbags. Once a week, any debris that fell on the litterbags was removed, to assure that they remained uncovered in order to avoid any confounding effects.

Litter Material

Fully senescent "sun" leaves from European beech (*Fagus sylvatica* L.) trees were collected directly from trees on the southern border of the stand in the Forêt Verte, Rouen, France (49°30′17.0"N 1°06′44.9″E). The petiole was removed from the leaves before they were scanned to obtain leaf area calculated with the software WinFOLIA (Image analysis for plant science, Regent Instruments Inc., Nepean, Canada). Immediately after sampling, both the adaxial (upper) and abaxial (lower) epidermal flavonoid content and leaf chlorophyll content were optically assessed using a Dualex Scientific + (ForceA, Paris Orsay, France) device in order to verify that there were no initial differences in their pigmentation or epidermal UV transmittance (Table S2). The leaves were then oven-dried at 37 °C for one week and reweighed to obtain their dry weight (DW) (Table S2). Entire leaves were placed inside litterbags with the adaxial leaf epidermis facing up in a single layer (consisting of 4–5 leaves per litterbag, weighing 300–400 mg, Table S2).

Litter Mass Remaining, Carbon and Nitrogen Content

Five replicate litterbags from each treatment combination were collected after 1, 3 and 6 months. After collection, litter was dried at 37 °C, cleaned with small brushes to eliminate any soil particles and worm casts present in most samples, and weighed on a precision balance (Entris 224i-1S, Sartorius Lab Instruments GmbH & Co. KG, Göttingen, Germany). The litter was then ground to a fine powder, and 3–4 mg DW was used to determine the percentage [C] and [N] content using a CN Soil Analyzer Flash 2000 (Thermo Scientific, Waltham, USA), and calculate the carbon to nitrogen ratio (C:N). Ash free dry mass (AFDM) was determined by combustion of a subsample of each replicate in a muffle oven at 550 °C for 12 h to allow quantification of mineral contamination.

PLFA and NLFA Analysis

Six replicate litterbags from each treatment combination were collected after 1, 2, 3 and 6 months. An extra collection time was included for these analyses as we expected the microbial biomass to vary more within the first 3 months than the amount mass loss or C. After collection, litter was freeze-dried, to conserve the samples until PLFA (phospholipid-derived fatty acids) and NLFA (neutral lipid fatty acids) analyses could be performed. Freeze-dried litter was ground and a subsample 0.15 g (from each litterbag) was used to determine the fatty acid content. Lipid extraction was performed according to Frostegård et al. (1991). The extracted lipids were fractionated into neutral lipids, glycolipids and polar lipids on a SPE silica- column (Solid Phase Extraction, Hypersep SILICA 500 mg from Thermo Scientific) by successive elution with chloroform, acetone and methanol. NLFA and PLFA were then concentrated under a nitrogen stream, re-dissolved in toluene/methanol (1:1) and subjected to a trans-esterification using a base solution (0.2 M KOH prepared in methanol) at 37 °C for 15 min to release free fatty acid methyl esters from the PLFA and the NLFA. Fatty-acid methyl esters (FAMEs) were compared to nonadecanoic acid methyl ester (C19:0-Me) as an internal standard: identified by comparing retention times against those of a range of standards (fatty acid methyl ester mixtures C4-C24:1, Sigma– Aldrich) and quantified according to their mass (vs known mass of an internal standard). The final extracts were analysed and FAMEs were characterised by Fast GC–MS. Samples were injected in split mode (ratio 100.0) at 280 °C. The separation was performed on a Zebron ZB-1 MS capillary column (10 m length × 0.1 mm i.d., 0.1 μm film thickness (Phenomenex, USA). The system was operated at constant linear velocity (40 cm s^{-1}) using helium as the carrier gas and the oven was programmed as follow:

heated from 175 °C to 275 °C (at 25 °C min^{-1}) and subsequently maintained at this temperature for 30 s in a Gas Chromatograph (Shimadzu 2010 Plus System, Shimadzu Corporation, Kyoto, Japan). This GC was equipped with a Shimadzu QP 2010 Ultra mass spectrometer detector (Shimadzu Corporation) and a Flam Ionization Detector (300 °C) used alternately. Fatty acids were identified by comparing their mass spectra with the standard mass spectra in the NIST MS library. The amounts of the NLFA 16:1ω5 and the PLFA 16:1ω5 in the litter were determined and the ratio used as an indicator of AMF (arbuscular mycorrhizal fungi) biomass. The PLFA c18:2ω6,9 was used as an indicator of saprotrophic fungal biomass (Frostegård et al., 1991). The biomass of Gram-positive bacteria (Gram-P) was estimated by the quantification of the PLFA: i15:0, a15:0, i16:0, i17:0, a17:0 and Gram-negative bacteria (Gram-N) by the quantification of the PLFA: cy17:0, c18:1ω7 and cy19:0 in the litter (Frostegård et al. 2011). The Gram-P biomass to Gram-N biomass ratio (Gram-P:Gram-N) was also calculated. The fungal-to-bacterial biomass ratio (F:B) was calculated, and the total amount of PLFA was used as an indicator of total microbial biomass in each sample.

Data Analysis

Treatment effects on AFDM, [C], [N], C:N, fungal and bacterial biomass, total microbial biomass, F:B, Gram-P biomass, Gram-N biomass and Gram-P:Gram-N, were tested using a two-way ANOVA with fixed experimental factors: filter and time and the interaction between them. The normal distribution of the residuals and homoscedasticity of variance were checked when performing the statistical analyses. Where a significant ($p < 0.05$) interaction was given by the ANOVA, the pairwise comparisons were tested (Function glht in Package Multicomp). Holm's adjustment was used to account for multiple pairwise comparisons. Abundances of individual PLFA biomarkers were used as input values for the non-metric multidimensional scaling analysis (NMDS), to check for differences among the microbial communities in the different filter treatments, using the package 'vegan' (Oksanen et al. 2019). The Bray-Curtis similarity index was employed in the analysis. PERMANOVA with function adonis() in the package 'vegan' (Oksanen et al. 2019) with filter treatment and time as fixed factor was performed and followed by post-hoc test pairwise.adonis() with Holm's correction to allow us to evaluate differences between treatments (Martinez Arbizu 2019). Additionally, SIMPER test was applied to estimate the contribution of the individual PLFA biomarkers to dissimilarity between the different treatments. Correlations between litter quality (C and N content) and decomposer assemblages (PLFAs) were inspected with the functions cor() and cor_pmat() in package 'ggcorrplot' (Kassambara 2019). All statistical analyses were performed in R version 3.3.3 (2017).

Results

Litter Mass Remaining, Carbon and Nitrogen Content

The effect of our filter treatments on remaining AFDM of leaf litter varied according to the time of exposure (interaction filter-treatment-by-time: $p = 0.009$, Table 1) and became significant only at the end of the experiment (Fig. 1), with the Dark treatment having higher AFDM remaining than the No-UV (+15.2%) and No-UVB (+14.9%) treatments (pairwise comparison Dark – No-UV: $p = 0.012$, Dark – No-UVB: $p = 0.016$, Table S3). Over the 6 months of the experiment, mass loss was about 20% (Fig. 1).

Filter treatment did not have a significant effect on litter [C] ($p = 0.800$, Table 1, Fig. 2), but did impact [N] ($p = 0.034$, Table 1, Fig. 2) and consequently the C:N ($p = 0.031$, Table 1, Fig. 2). This resulted in litter in the Dark treatment having a higher [N] (pairwise comparisons Dark – No-UVB: $p < 0.001$, Dark – No-UV $p = 0.029$, Table S4) than litter in the No-UVB (+155.9%) and No-UV (+120.9%) treatments, and a lower C:N (pairwise comparison Dark – No-UVB: $p = 0.014$) than litter in the No-UVB treatment, at the end of the experiment (Fig. 2, Table S5).

Microbial Biomass

Total PLFA, a surrogate for microbial biomass on the litter samples, increased with time ($p < 0.001$, Table 2, Fig. S7) and was affected by our filter treatments ($p = 0.022$, Table 2, Fig. 3) consistently over time (interaction filter-treatment-by-time: $p = 0.370$, Table 2). Litter under the No-UV/Blue/Green treatment had higher microbial biomass than litter in the No-UVB (+221.4 μg g^{-1}) treatment (pairwise comparison No-UV/Blue/Green – No-UVB: $p = 0.006$, Fig. 3, Table S6).

Table 1 Anova results for two fixed factors (filter treatment: with 6 levels and time with 3 levels) and their interactions on single dependent variables: Ash Free Dry Mass (AFDM) remaining, carbon content, nitrogen content and C:N ratio. Degrees of freedom (d.f.), sum of squares (SS), mean square (MS), F statistic (f) and p value (p). Significant terms are shown in bold. Non-significant terms were retained since dropping them did not significantly affect the model. One sample was unusable for AFDM and [C] analyses so these residual d.f. are 71 rather than 72

	d.f.	SS	MS	F	p
Variable: AFDM					
Filter treatment	5	216.94	43.39	1.318	0.266
Time	**2**	**552.17**	**276.08**	**8.388**	**< 0.001**
Filter treatment x Time	**10**	**860.97**	**86.097**	**2.616**	**0.009**
Residuals	71	2336.81	32.913		
Variable: Carbon content					
Filter treatment	5	70.92	14.18	0.467	0.800
Time	**2**	**1008.40**	**504.20**	**16.593**	**< 0.001**
Filter treatment x Time	10	536.33	53.63	1.765	0.083
Residuals	71	2157.46	30.39		
Variable: Nitrogen content					
Filter treatment	**5**	**30,654**	**6131**	**2.5632**	**0.034**
Time	**2**	**88,652**	**44,326**	**18.526**	**< 0.001**
Filter treatment x Time	**10**	**50,776**	**5078**	**2.122**	**0.033**
Residuals	72	172,270	2393		
Variable: C:N ratio					
Filter treatment	**5**	**416.67**	**83.33**	**2.620**	**0.031**
Time	**2**	**2674.62**	**1337.31**	**42.037**	**< 0.001**
Filter treatment x Time	10	245.75	24.58	0.773	0.655
Residuals	72	2290.52	31.81		

The biomass of both bacteria and fungi followed the same temporal pattern as total microbial biomass, increasing over the course of the experiment ($p < 0.001$ in both cases, Table 2, Fig. S7, Fig. S8) and both were also affected by our filter treatments ($p = 0.001$ and $p = 0.021$ respectively, Table 2, Fig. 3); an effect that remained constant through time (filter treatment-by-time interaction: $p = 0.270$ and $p = 0.390$ respectively, Table 2). Fungal biomass was higher in the No-UV/Blue/Green treatment than the No-UVB (+209.6 μg g^{-1}) treatment (pairwise comparison: No-UV/Blue/Green – No-UVB: $p = 0.006$, Fig. 3, Table S7). On the other hand, bacterial biomass was lower in the Dark treatment than the other treatments (Fig.3, Table S8), and consequently, the F:B ratio of the Dark treatment was highest (Fig. 3, Table S9). The filter treatments had an effect on the biomass of both Gram-P ($p = 0.001$, Table 2) and Gram-N bacteria ($p = 0.029$, Table 2). The biomass of Gram-P was lower in the Dark treatment than the other treatments (Fig. 3, Table S10), while the biomass of Gram-N was higher in the No-UV/Blue/Green treatment than the No-UVB (+4.4 μg g^{-1}) treatment (pairwise comparison: No-UV/Blue/Green – No-UVB: $p = 0.034$, Fig. 3, Table S11).

The ratio NLFA 16:1ω5:PLFA 16.1ω5 was less than 1 in all the samples (Fig. S9), therefore we concluded that no AMF were present in our samples.

Microbial Assemblages

The greatest change in composition of PLFA biomarkers occurred over time ($p = 0.001$, Table 3, Fig.

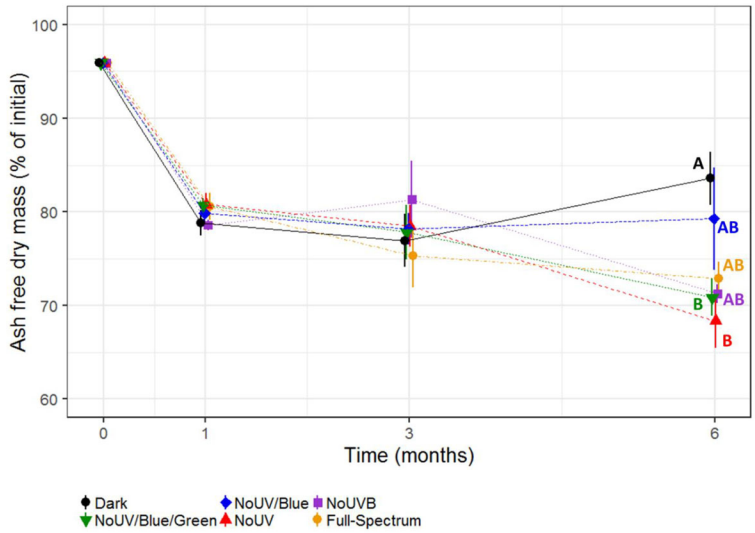

Fig. 1 Remaining ash free dry mass (AFDM) as a percentage of initial weight for each filter treatment after each sampling period over the 6 months of the experiment. Means ± SE are shown (n = 5). Letters indicate significant differences between filter treatments at the end of the experiment. Symbols represent the following filter treatments: ● black = "Dark" (attenuating >95% of PAR and UV radiation); ▼ green = "No-UV/Blue/Green" (attenuating UV radiation and blue and green light <580 nm); ♦ blue = "No-UV/Blue" (attenuating UV radiation and blue light <480 nm); ▲ red = "No-UV" (attenuating UV radiation <380 nm); ■ purple = "No-UV-B" (attenuating UV-B radiation <320 nm); ○ yellow = "Full-spectrum" (transmitting >95% of incident PAR and UV radiation). Pairwise comparisons between filter treatments are given in Table S3

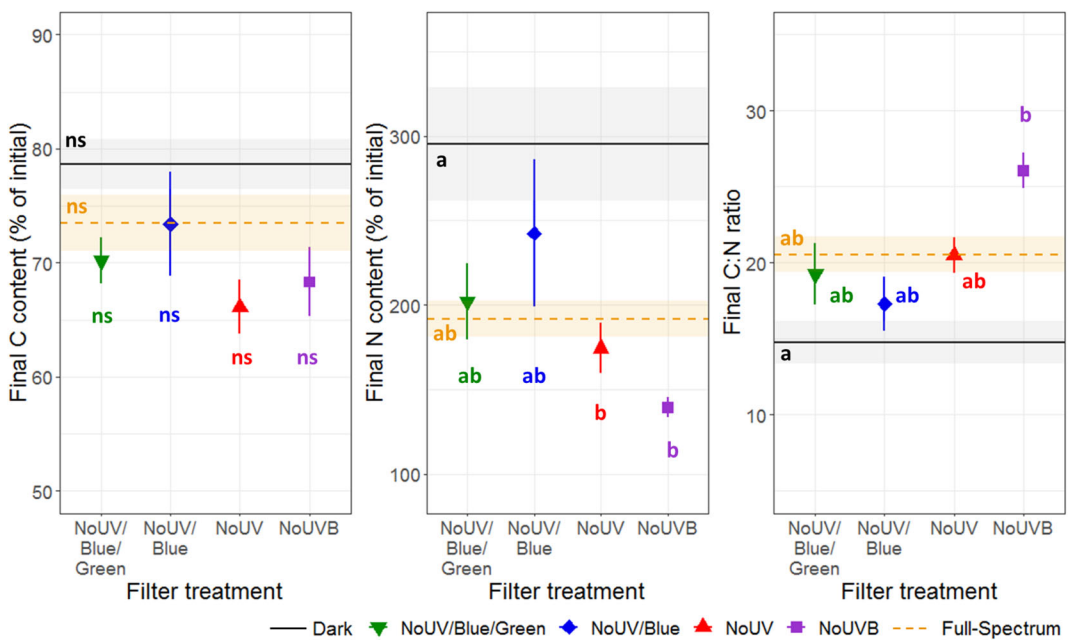

Fig. 2 Final C content, N content and C:N ratio for each filter treatment. Means ± SE are shown ($n = 5$). Letters show significant differences between filter treatments, while "ns" stands for "non-significant". Symbols represent the following filter treatments: ▼ green = "No-UV/Blue/Green" (attenuating UV radiation and blue and green light <580 nm); ♦ blue = "No-UV/Blue" (attenuating UV radiation and blue light <480 nm); ▲ red = "No-UV" (attenuating UV radiation <380 nm); ■ purple = "No-UV-B" (attenuating UV-B radiation <320 nm). The solid black line represents the mean of the "Dark" treatment (attenuating >95% of PAR and UV radiation) and the shaded areas around it represent the SE. The dashed yellow line represents the mean of the "Full-spectrum" treatment (transmitting >95% of incident PAR and UV radiation) and the shaded areas around it represent the SE. Pairwise comparisons between time and filter treatment are given in Tables S4 and S5

Table 2 Anova results for two fixed factors (filter treatment: with 6 levels and time with 4 levels) and their interactions on single dependent variables: microbial biomass, bacterial biomass, fungal biomass, F:B ratio, Gram-P bacteria biomass, Gram-N bacteria biomass, Gram-P:Gram-N. Degrees of freedom (d.f.), sum of squares (SS), mean square (MS), f statistic (f) and *p* value (*p*). Significant terms are shown in bold. Non-significant terms were retained since dropping them did not significantly affect the model. One sample was unusable for PLFA analyses so these residual d.f. are 119 rather than 120

	d.f.	SS	MS	F	*p*
Variable: Microbial biomass					
Filter treatment	**5**	**606,246**	**121,249**	**2.749**	**0.022**
Time	**3**	**2,972,335**	**990,778**	**22.462**	**< 0.001**
Filter treatment x Time	15	723,027	48,202	1.093	0.370
Residuals	119	5,248,886	44,108		
Variable: Bacterial biomass					
Filter treatment	**5**	7149	**1430**	**4.285**	**0.001**
Time	**3**	**126,353**	**42,118**	**126.216**	**< 0.001**
Filter treatment x Time	15	6085	406	1.216	0.270
Residuals	119	39,710	334		
Variable: Fungal biomass					
Filter treatment	**5**	**548,902**	**109,780**	**2.774**	**0.021**
Time	**3**	**1,956,270**	**652,090**	**16.480**	**< 0.001**
Filter treatment x Time	15	635,744	42,383	1.071	0.390
Residuals	119	4,708,723	39,569		
Variable: F:B ratio					
Filter treatment	**5**	**152**	**30**	**5.574**	**< 0.001**
Time	**3**	**385**	**128**	**23.493**	**< 0.001**
Filter treatment x Time	15	58	4	0.713	0.767
Residuals	119	645	5		
Variable: Gram-P biomass					
Filter treatment	**5**	**5403**	**1081**	**4.405**	**0.001**
Time	**3**	**114,443**	**38,148**	**155.488**	**< 0.001**
Filter treatment x Time	15	4964	311	1.349	0.184
Residuals	119	29,196	145		
Variable: Gram-N biomass					
Filter treatment	**5**	**307**	**61**	**2.593**	**0.029**
Time	**3**	**519**	**173**	**7.306**	**< 0.001**
Filter treatment x Time	15	418	28	1.177	0.299
Residuals	119	2815	24		
Variable: Gram-P: Gram-N ratio					
Filter treatment	**5**	**15**	**3**	**5.079**	**< 0.001**
Time	**3**	**200**	**67**	**112.275**	**< 0.001**
Filter treatment x Time	**15**	**16**	**1**	**1.785**	**0.045**
Residuals	119	71	1		

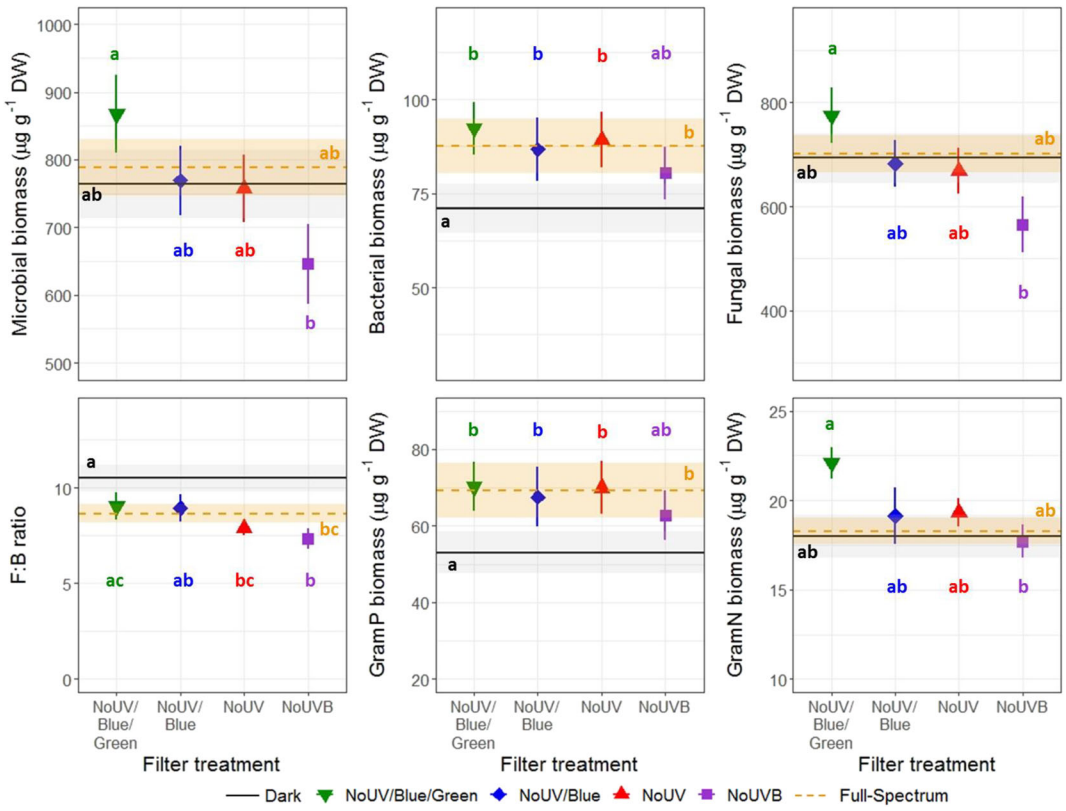

Fig. 3 Microbial biomass, bacterial biomass, fungal biomass, F:B ratio, Gram-P biomass and Gram-N biomass for each filter treatment pooled over the entire 6 months of the experiment. Means ± SE are shown ($n = 24$). Letters show significant differences between filter treatments. Symbols represent the following filter treatments: ▼ green = "No-UV/Blue/Green" (attenuating UV radiation and blue and green light <580 nm); ♦ blue = "No-UV/Blue" (attenuating UV radiation and blue light <480 nm); ▲ red = "No-UV" (attenuating UV radiation <380 nm); ■ purple = "No-UV-B" (attenuating UV-B radiation <320 nm). The solid black line represents the mean of the "Dark" treatment (attenuating >95% of PAR and UV radiation) and the shaded areas around it represent the SE. The dashed yellow line represents the mean of the "Full-spectrum" treatment (transmitting >95% of incident PAR and UV radiation) and the shaded areas around it represent the SE. Pairwise comparisons between time and filter treatment are given in Tables S6-S11 and details on separate collection times are given in Fig. S7

S11) which explained 31.9% of the variation, while the filter treatment ($p = 0.001$, Table 3, Fig. 4, Fig. S11) accounted only for 10.9%. There was no interaction between time and filter treatment ($p = 0.185$, Table 3). The No-UV/Blue/Green and the No-UVB treatments were the two most different treatments (pairwise comparison: $p = 0.015$, Table S13) with an overall dissimilarity of 27.1%. The fungal PLFA biomarker C18:2ω6,9 alone accounted for 84.4% of this difference (Table S14). However, when separating the four collection times, an effect of the filter treatment was found only after one month ($p = 0.004$, Table 3, Fig. 4), and, individually, the Dark treatment and the No-UV/Blue/Green treatments each differed from the No-UV treatment (pairwise comparisons respectively: $p = 0.030$ and $p = 0.042$, Table S15). The fungal PLFA biomarker C18:2ω6,9 alone accounted for most of the difference between these two treatments (87.7% and 87.4% respectively with dissimilarity 20.6% and 20.5% respectively, Table S16).

Litter Quality and Microbial Assemblages

Generally, the different microbial variables were only weakly correlated with litter quality (Fig. S12). For instance, [C] was positively correlated with F:B ($R^2 = 0.4$, $p < 0.001$), while it was negatively correlated with Gram-P biomass ($R^2 = -0.5$, $p < 0.001$); bacterial biomass ($R^2 = -0.4$, $p < 0.001$); microbial biomass ($R^2 = -0.2$, $p = 0.050$) and Gram-P:Gram-N ($R^2 = -0.4$, $p < 0.001$). In contrast, [N] was positively correlated with Gram-P biomass ($R^2 = 0.4$, $p < 0.001$); bacterial

Table 3 Permanova results for two fixed factors (filter treatment: with 6 levels and time with 4 levels) and for one fixed factor (filter treatment) at the four collection times, after NMDS on PLFA markers. Degrees of freedom (d.f.), sum of squares (SS), mean square (MS), F model (F mod), R^2 and *p* value (*p*). Significant terms are shown in bold. Non-significant terms were retained since dropping them did not significantly affect the model

	Df	SS	MS	F mod	R^2	*p*
Filter treatment	**5**	**0.503**	**0.101**	**5.319**	**0.115**	**0.001**
Time	**3**	**1.297**	**0.432**	**22.880**	**0.296**	**0.001**
Filter treatment x Time	15	0.367	0.024	1.295	0.838	0.185
Residuals	117	2.212	0.019		0.505	
Total	140	4.379			1.000	
1 month						
Filter treatment	**5**	**0.288**	**0.058**	**3.494**	**0.368**	**0.004**
Residuals	30	0.495	0.017		0.632	
Total	35	0.784			1.000	
2 months						
Filter treatment	5	0.124	0.025	1.110	0.161	0.379
Residuals	29	0.649	0.022		0.839	
Total	34	0.774			1.000	
3 months						
Filter treatment	5	0.167	0.033	2.016	0.265	0.083
Residuals	28	0.464	0.017		0.735	
Total	33	0.631			1.000	
6 months						
Filter treatment	*5*	*0.158*	*0.032*	*2.034*	*0.260*	*0.056*
Residuals	29	0.450	0.016		0.740	
Total	34	0.608			1.000	

biomass ($R^2 = 0.4$, $p = 0.001$); microbial biomass ($R^2 = 0.3$, $p = 0.016$) and fungal biomass ($R^2 = 0.2$, $p = 0.030$), but negatively correlated with F:B ($R^2 = -0.2$, $p = 0.030$). Moreover, C:N was positively correlated with F:B ($R^2 = 0.4$, $p < 0.001$), but negatively correlated with Gram-P biomass ($R^2 = -0.5$, $p < 0.001$); bacterial biomass ($R^2 = -0.5$, $p < 0.001$); fungal biomass ($R^2 = -0.3$, $p = 0.006$); microbial biomass ($R^2 = -0.3$, $p = 0.001$) and Gram-P:Gram-N ($R^2 = -0.5$, $p < 0.001$).

Discussion

In our study, leaf litter lost about 20–25% of its initial mass during the first 6 months of decomposition. This mass loss was strongly affected by the interaction between filter treatments and time. This became evident after 6 months, whereby exclusion of the full spectrum, and likewise exclusion of both UV and blue light, caused slower decomposition than the other filter treatments (Fig. 1). This result is consistent with trends among filter treatments from the previous year (2016–2017) at the same site (Pieristè et al. 2019a). The previous study examined decomposition of leaf litter from three tree species, including European beech, and together these studies confirm that sunlight plays a role in litter decomposition in temperate forests. The effect of sunlight on mass loss in 2017–2018 (+15% of mass lost) was lower than in 2016–2017 (+30%) (Pieristè et al. 2019a), despite the LAI being the same during the two years (data not shown). This might be explained by the higher rainfall during the 2017–2018 study: 622.9 mm, accumulated between

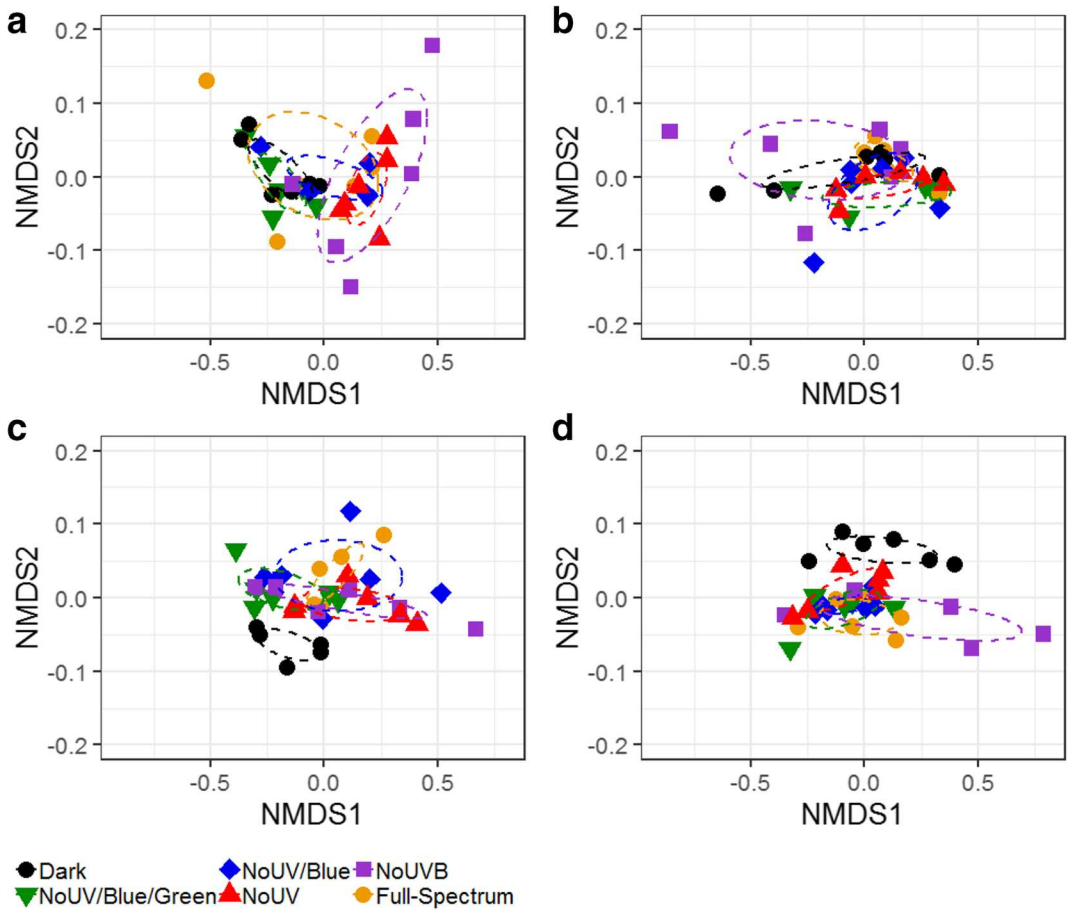

Fig. 4 Patterns of PLFA-biomarker composition mapped against the explanatory variable Filter at different collection times: a) 1 month (stress = 0.027); b) 2 months (stress = 0.018); c) 3 months (stress = 0.024) and d) 6 months (stress = 0.021), using non-metric multidimensional scaling (NMDS). Symbols represent the following filter treatments: ● black = "Dark" (attenuating >95% of PAR and UV radiation); ▼ green = "No-UV/Blue/Green" (attenuating UV radiation and blue and green light <580 nm); ♦ blue = "No-UV/Blue" (attenuating UV radiation and blue light <480 nm); ▲ red = "No-UV" (attenuating UV radiation <380 nm); ■ purple = "No-UV-B" (attenuating UV-B radiation <320 nm); ○ yellow = "Full-spectrum" (transmitting >95% of incident PAR and UV radiation). The No-UV/Blue/Green (▼ green) and the No-UVB (■ purple) treatments were the two most different treatments. When separating the four collection times, an effect of the filter treatment was found only after one month ($p = 0.004$, Table 3). More details are given in Tables S13-S16 and Fig. S11

Dec 2017 and June 2018, compared with 314.8 mm during the same period in 2017 ("Rouen-Boos" weather station: http://www.infoclimat.fr). Differences in precipitation elsewhere have been found to produce large variations in photodegradation: for instance in a semi-arid environment, where the effect of photodegradation also decreased with increased precipitation (Brandt et al. 2007). In a temperate mesic forest, high precipitation and relative humidity can create a more-favourable environment for microbial development (Salamanca et al. 2003; Zhou et al. 2018), thus the relative benefit to microbial decomposition from photofacilitation is likely to be smaller than in arid environments.

In our study the effect of photodegradation on microbial biomass was small. Across different filter treatments, this modest impact tallied with the modest effect on mass loss associated with successive spectral regions (Figs. 1 & 3). Moreover, previous studies showed the effects of UV radiation on microbial biomass and activity to be dependent on their interaction with other factors that can affect microbial activity, such as temperature, moisture and nutrient availability (Belnap et al. 2008; Gunasekera and Paul 2007; Rangel et al. 2004). In general, time was the most determinant factor affecting not only litter mass, but also microbial biomass. Indeed, the inhibitory effect of UV-B radiation in wet

environments is small and variable across different timescales depending on the phase of decomposition considered (Barnes et al. 2015).

In our study, the F:B ratio was higher in treatments that excluded UV radiation and the blue-green region of the visible spectrum, due to a higher fungal biomass, suggesting that fungi are favoured by the exclusion of the short-wavelength regions of the solar spectrum (e.g. UV radiation, blue and green light). These results are in agreement with earlier findings that fungal growth and litter colonization are inhibited by supplemental UV radiation (Gehrke et al. 1995; Moody et al. 2001; Newsham et al. 1997; Verhoef et al. 2000) and ambient UV radiation in the leaf litter of some plant species (Pancotto et al. 2003). Moreover, green and blue light decreased hyphal length and the biomass of several fungi species in controlled conditions on a synthetic growing medium; suggesting fungi to prefer darker environments for their development (Velmurugan et al. 2010).

In our study, bacterial biomass was higher on litter receiving some sunlight rather than in darkness, suggesting that bacteria are facilitated in light compared to dark environments. This might be due to the greater nutrient availability for bacteria in these treatments as a consequence of photofacilitation (direct photomineralization). Several studies have found the process of photofacilitation of microbial decomposition to occur in arid and semi-arid ecosystems (Austin et al. 2016; Baker and Allison 2015; Lin et al. 2018). This might produce a divergence between microbial assemblages, with a tendency for photofacilitation of bacteria in sunlight where more simple nutrients are available, and fungi dominating in the dark where bacteria are unable to consume the complex substrates present. However, we cannot test this hypothesis with our study as further analysis of carbon quality would be required. Another factor possibly helping to segregate light and dark microbial assemblages, is the competitive relationship between bacteria and fungi previously observed in beech litter in a microcosm study (Møller et al. 1999), which may limit bacterial colonisation in the dark. In our study, it was not possible to distinguish the effect of photofacilitation from the direct effect of sunlight on microbial assemblages.

Our treatment excluding UV-B radiation tended to segregate from the other filter treatments, even though its effect on microbial community structure was not significantly different from the full-spectrum treatment. The No-UVB treatment had lower microbial and fungal biomass, and lower F:B, corresponding to lower [N] and C:N. UV-B radiation carries more energy than UV-A radiation and visible light, implying higher potential for photochemical mineralization and consequent photofacilitation, but also for photoinhibition (Lin et al. 2015; Song et al. 2013). Hence, even at the low irradiances found in temperate forest understoreys UV-B radiation can be important in shaping microbial communities, confirming previous findings from studies with supplemental lamps and high UV-B irradiances (Gehrke et al. 1995; Johnson 2003; Verhoef et al. 2000).

The structure of microbial assemblages, interpreted through the change in composition of PLFA biomarkers, varied during the course of the decomposition experiment in a manner that depended on the spectral composition, confirming the importance of sunlight in shaping microbial communities. The effect of sunlight on microbial decomposer communities has previously been found to change depending on the stage of decomposition (Pancotto et al. 2003; Pancotto et al. 2005). Our experiment examines only the initial 6-months of decomposition of beech leaf litter, when we expected effects of photodegradation on microbial biomass and assemblage structure to be most pronounced, and a longer study would be required to determine how microbial communities evolve later in the decomposition process. As decomposition proceeds, the potential role of interactions with other litter or soil biota in shaping microbial assemblages is also likely to become increasingly important (Coulibaly et al. 2019), adding further complexity to this process.

Conclusion

Our study shows that sunlight affects the microbial assemblages involved in the decomposition of leaf litter in temperate forests. Similar responses were previously recorded in arid environments and confirm the potential of photodegradation to affect microbes in a wavelength-dependent manner. Different regions of the solar spectrum affect microbial-assemblage structure and microbial biomass during the early stages of decomposition in a temperate forest understorey. UV radiation, and blue and green light, had a photoinhibitory effect on fungal decomposers; and are the key mediators of decomposition processes in temperate forest ecosystems, even at the very low irradiances occurring during winter and spring prior to canopy closure.

Acknowledgments We thank the ONF (Office National de Forêts) for the permission to use the study site. We would like to

acknowledge the support of the PRESEN platform (FR SCALE 3730 CNRS; Normandie Université), and SoDa HelioClim-3 for the satellite data (Transvalor S.A., 694 avenue du Dr. Maurice Donat, 06255 Mougins, France).

Funding information Open access funding provided by University of Helsinki including Helsinki University Central Hospital. This research was funded by Academy of Finland decisions #266523, #304519 and #324555 to TMR, personal EF project and a grant from the Region "Haute-Normandie" through the GRR-TERA SCALE (UFOSE Project) to MP.

References

Almagro M, Martínez-López J, Maestre FT, Rey A (2017) The contribution of Photodegradation to litter decomposition in semiarid Mediterranean grasslands depends on its interaction with local humidity conditions, litter quality and position. Ecosystems 20:527–542. https://doi.org/10.1007/s10021-016-0036-5

Anderson T-H, Domsch KH (1990) Application of eco-physiological quotients (qCO2 and qD) on microbial biomasses from soils of different cropping histories. Soil Biol Biochem 22:251–255. https://doi.org/10.1016/0038-0717(90)90094-G

Anderson T-H, Domsch KH (1993) The metabolic quotient for CO2 (qCO2) as a specific activity parameter to assess the effects of environmental conditions, such as ph, on the microbial biomass of forest soils. Soil Biol Biochem 25:393–395. https://doi.org/10.1016/0038-0717(93)90140-7

Aphalo P, Albert A, Björn L, McLeod A, Robson TM, Rosenqvist E (2012) Beyond the visible: a handbook of best practice in plant UV photobiology. COST action FA0906 UV4growth, Helsinki

Aphalo P, Robson TM, Piiparinen J (2016) How to check an array spectrometer. Int Assoc Plant UV Res

Asplund J, Kauserud H, Bokhorst S, Lie MH, Ohlson M, Nybakken L (2018) Fungal communities influence decomposition rates of plant litter from two dominant tree species. Fungal Ecol 32:1–8. https://doi.org/10.1016/j.funeco.2017.11.003

Austin AT, Méndez MS, Ballaré CL (2016) Photodegradation alleviates the lignin bottleneck for carbon turnover in terrestrial ecosystems. Proc Natl Acad Sci 113:4392–4397. https://doi.org/10.1073/pnas.1516157113

Bais AF, Lucas RM, Bornman JF, Williamson CE, Sulzberger B, Austin AT, Wilson SR, Andrady AL, Bernhard G, McKenzie RLJP (2018) Environmental effects of ozone depletion, UV radiation and interactions with climate change: UNEP environmental effects assessment panel, update 2017. Photochemical & Photobiological Sciences 17:127–179. https://doi.org/10.1039/C7PP90043K

Baker NR, Allison SD (2015) Ultraviolet photodegradation facilitates microbial litter decomposition in a Mediterranean climate. Ecology 96:1994–2003. https://doi.org/10.1890/14-1482.1

Baldrian P (2016) Forest microbiome: diversity, complexity and dynamics. FEMS Microbiol Rev 41:109–130. https://doi.org/10.1093/femsre/fuw040

Ball BA, Christman MP, Hall SJ (2019) Nutrient dynamics during photodegradation of plant litter in the Sonoran Desert. J Arid Environ 160:1–10. https://doi.org/10.1016/j.jaridenv.2018.09.004

Barnes PW, Throop HL, Archer SR, Breshears DD, McCulley RL, Tobler MA (2015) Sunlight and soil–litter mixing: drivers of litter decomposition in Drylands. In: U Lüttge, W Beyschlag (eds) Progress in botany: Vol 76. Springer International Publishing, Cham

Belnap J, Phillips SL, Flint S, Money J, Caldwell M (2008) Global change and biological soil crusts: effects of ultraviolet augmentation under altered precipitation regimes and nitrogen additions. Glob Chang Biol 14:670–686. https://doi.org/10.1111/j.1365-2486.2007.01509.x

Blanc P, Gschwind B, Lefèvre M, Wald L (2011) The HelioClim project: surface solar irradiance data for climate applications. Remote Sens 3:343–361. https://doi.org/10.3390/rs3020343

Brandt LA, King JY, Hobbie SE, Milchunas DG, Sinsabaugh RL (2010) The role of Photodegradation in surface litter decomposition across a grassland ecosystem precipitation gradient. Ecosystems 13:765–781. https://doi.org/10.1007/s10021-010-9353-2

Brandt LA, King JY, Milchunas DG (2007) Effects of ultraviolet radiation on litter decomposition depend on precipitation and litter chemistry in a shortgrass steppe ecosystem. Glob Chang Biol 13:2193–2205. https://doi.org/10.1111/j.1365-2486.2007.01428.x

Coulibaly SFM, Winck BR, Akpa-Vinceslas M, Mignot L, Legras M, Forey E, Chauvat M (2019) Functional Assemblages of Collembola Determine Soil Microbial Communities and Associated Functions Frontiers in Environmental Science 7. doi: https://doi.org/10.3389/fenvs.2019.00052

Day TA, Bliss MS, Tomes AR, Ruhland CT, Guénon R (2018) Desert leaf litter decay: coupling of microbial respiration, water-soluble fractions and photodegradation. Glob Chang Biol 24:5454–5470. https://doi.org/10.1111/gcb.14438

Day TA, Guénon R, Ruhland CT (2015) Photodegradation of plant litter in the Sonoran Desert varies by litter type and age. Soil Biol Biochem 89:109–122. https://doi.org/10.1016/j.soilbio.2015.06.029

Day TA, Zhang ET, Ruhland CT (2007) Exposure to solar UV-B radiation accelerates mass and lignin loss of Larrea tridentata litter in the Sonoran Desert. Plant Ecol 193:185–194. https://doi.org/10.1007/s11258-006-9257-6

Duguay KJ, Klironomos JN (2000) Direct and indirect effects of enhanced UV-B radiation on the decomposing and competitive abilities of saprobic fungi. Appl Soil Ecol 14:157–164. https://doi.org/10.1016/S0929-1393(00)00049-4

Foereid B, Rivero MJ, Primo O, Ortiz I (2011) Modelling photodegradation in the global carbon cycle. Soil Biol Biochem 43:1383–1386. https://doi.org/10.1016/j.soilbio.2011.03.004

Fourtouni A, Manetas Y, Christias C (1998) Effects of UV-B radiation on growth, pigmentation, and spore production in the phytopathogenic fungus Alternaria solani. Can J Bot 76:2093–2099. https://doi.org/10.1139/b98-170

Frostegård Å, Tunlid A, Bååth E (1991) Microbial biomass measured as total lipid phosphate in soils of different organic content. J Microbiol Methods 14:151–163

Frostegård Å, Tunlid A, Bååth E (2011) Use and misuse of PLFA measurements in soils. Soil Biol Biochem 43:1621–1625. https://doi.org/10.1016/j.soilbio.2010.11.021

García-Cela ME, Marín S, Reyes M, Sanchis V, Ramos AJ (2016) Conidia survival of Aspergillus section Nigri, Flavi and Circumdati under UV-A and UV-B radiation with cycling temperature/light regime. J Sci Food Agric 96:2249–2256. https://doi.org/10.1002/jsfa.7343

Gehrke C, Johanson U, Callaghan TV, Chadwick D, Robinson CH (1995) The impact of enhanced ultraviolet-B radiation on litter quality and decomposition processes in Vaccinium leaves from the subarctic. Oikos 72:213–222. https://doi.org/10.2307/3546223

Gschwind B, Ménard L, Albuisson M, Wald L (2006) Converting a successful research project into a sustainable service: the case of the SoDa web service. Environ Model Softw 21:1555–1561. https://doi.org/10.1016/j.envsoft.2006.05.002

Gunasekera TS, Paul ND (2007) Ecological impact of solar ultraviolet-B (UV-B: 320–290nm) radiation on Corynebacterium aquaticum and Xanthomonas sp. colonization on tea phyllosphere in relation to blister blight disease incidence in the field. Lett Appl Microbiol 44:513–519. https://doi.org/10.1111/j.1472-765X.2006.02102.x

Hartikainen SM, Jach A, Grané A, Robson TM (2018) Assessing scale-wise similarity of curves with a thick pen: as illustrated through comparisons of spectral irradiance. Ecol Evol 8:10206–10218. https://doi.org/10.1002/ece3.4496

Hättenschwiler S, Tiunov AV, Scheu S (2005) Biodiversity and litter decomposition in terrestrial ecosystems. Annu Rev Ecol Evol Syst 36:191–218. https://doi.org/10.1146/annurev.ecolsys.36.112904.151932

Johnson D (2003) Response of terrestrial microorganisms to ultraviolet-B radiation in ecosystems. Res Microbiol 154:315–320. https://doi.org/10.1016/S0923-2508(03)00078-0

Kassambara A (2019) Package 'ggcorrplot' - visualization of a correlation matrix using 'ggplot2'. 0.1.3 edn

King JY, Brandt LA, Adair EC (2012) Shedding light on plant litter decomposition: advances, implications and new directions in understanding the role of photodegradation. Biogeochemistry 111:57–81. https://doi.org/10.1007/s10533-012-9737-9

Kubartová A, Ranger J, Berthelin J, Beguiristain T (2009) Diversity and decomposing ability of saprophytic Fungi from temperate Forest litter. Microb Ecol 58:98–107. https://doi.org/10.1007/s00248-008-9458-8

Kumagai T (1988) PHOTOCONTROL OF FUNGAL DEVELOPMENT. Photochem Photobiol 47:889–896. https://doi.org/10.1111/j.1751-1097.1988.tb01672.x

Lin Y, Karlen SD, Ralph J, King JY (2018) Short-term facilitation of microbial litter decomposition by ultraviolet radiation. Sci Total Environ 615:838–848. https://doi.org/10.1016/j.scitotenv.2017.09.239

Lin Y, Scarlett RD, King JY (2015) Effects of UV photodegradation on subsequent microbial decomposition of Bromus diandrus litter. Plant Soil 395:263–271. https://doi.org/10.1007/s11104-015-2551-0

Ma Z, Yang W, Wu F, Tan B (2017) Effects of light intensity on litter decomposition in a subtropical region. Ecosphere 8. https://doi.org/10.1002/ecs2.1770

Martinez Arbizu P (2019) pairwiseAdonis: pairwise multilevel comparison using Adonis. R package version 0.3

Møller J, Miller M, Kjøller A (1999) Fungal–bacterial interaction on beech leaves: influence on decomposition and dissolved organic carbon quality. Soil Biol Biochem 31:367–374. https://doi.org/10.1016/S0038-0717(98)00138-2

Moody SA, Newsham KK, Ayres PG, Paul ND (1999) Variation in the responses of litter and phylloplane fungi to UV-B radiation (290–315 nm). Mycol Res 103:1469–1477. https://doi.org/10.1017/S0953756299008783

Moody SA, Paul ND, Björn LO, Callaghan TV, Lee JA, Manetas Y, Rozema J, Gwynn-Jones D, Johanson U, Kyparissis A, Oudejans AMC (2001) The direct effects of UV-B radiation on Betula pubescens litter decomposing at four European field sites. Plant Ecol 154:27–36. https://doi.org/10.1023/A:1012965610170

Newsham KK, Anderson JM, Sparks TH, Splatt P, Woods C, Mcleod AR (2001) UV-B effect on Quercus robur leaf litter decomposition persists over four years. Glob Chang Biol 7:479–483. https://doi.org/10.1046/j.1365-2486.2001.00423.x

Newsham KK, Low MNR, McLeod AR, Greenslade PD, Emmett BA (1997) Ultraviolet-B radiation influences the abundance and distribution of phylloplane fungi on pedunculate oak (Quercus rohur). New Phytol 136:287–297. https://doi.org/10.1046/j.1469-8137.1997.00740.x

Oksanen J, Blanchet FG, Kindt R, Legendre P, Minchin PR, O'hara R, Simpson GL, Solymos P, Stevens MHH, Wagner H (2019) Vegan: community ecology package - version 2.5-4

Osman M, Elsayed MA, Mohamed YAH, Abo-Zeid AM (1989) Effect of ultraviolet irradiation on germination and growth in Aspergillus flavus and Penicillium notatum. Mycol Res 92:293–296. https://doi.org/10.1016/S0953-7562(89)80068-1

Pancotto VA, Sala OE, Cabello M, López NI, Matthew Robson T, Ballaré CL, Caldwell MM, Scopel AL (2003) Solar UV-B decreases decomposition in herbaceous plant litter in Tierra del Fuego, Argentina: potential role of an altered decomposer community. Glob Chang Biol 9:1465–1474. https://doi.org/10.1046/j.1365-2486.2003.00667.x

Pancotto VA, Sala OE, Robson TM, Caldwell MM, Scopel AL (2005) Direct and indirect effects of solar ultraviolet-B radiation on long-term decomposition. Glob Chang Biol 11:1982–1989. https://doi.org/10.1111/j.1365-2486.2005.1027.x

Paul ND, Gwynn-Jones D (2003) Ecological roles of solar UV radiation: towards an integrated approach. Trends Ecol Evol 18:48–55. https://doi.org/10.1016/S0169-5347(02)00014-9

Pieristè M, Chauvat M, Kotilainen TK, Jones AG, Aubert M, Robson TM, Forey E (2019a) Solar UV-A radiation and blue light enhance tree leaf litter decomposition in a temperate forest. Oecologia 191:191–203. https://doi.org/10.1007/s00442-019-04478-x

Pieristè M, Neimane S, Nybakken L, Solanki T, Jones AG, Forey E, Chauvat M, Ņečajeva J, Robson TM (2019b) Ultraviolet radiation accelerates photodegradation under controlled conditions but slows the decomposition of leaf litter from forest stands in southern Finland. Plant Physiology and Biochemistry Under review

Purahong W, Schloter M, Pecyna MJ, Kapturska D, Däumlich V, Mital S, Buscot F, Hofrichter M, Gutknecht JLM, Krüger D (2014) Uncoupling of microbial community structure and function in decomposing litter across beech forest ecosystems in Central Europe. Sci Rep 4:7014. https://doi.org/10.1038/srep07014 https://www.nature.com/articles/srep07014#supplementary-information

Rangel DEN, Braga GUL, Flint SD, Anderson AJ, Roberts DW (2004) Variations in UV-B tolerance and germination speed of Metarhizium anisopliae conidia produced on insects and artificial substrates. J Invertebr Pathol 87:77–83. https://doi.org/10.1016/j.jip.2004.06.007

Salamanca EF, Kaneko N, Katagiri S (2003) Rainfall manipulation effects on litter decomposition and the microbial biomass of the forest floor. Appl Soil Ecol 22:271–281. https://doi.org/10.1016/S0929-1393(02)00153-1

Sauvadet M, Fanin N, Chauvat M, Bertrand I (2019) Can the comparison of above- and below-ground litter decomposition improve our understanding of bacterial and fungal successions? Soil Biol Biochem 132:24–27. https://doi.org/10.1016/j.soilbio.2019.01.022

Song X, Peng C, Jiang H, Zhu Q, Wang W (2013) Direct and indirect effects of UV-B exposure on litter decomposition: a meta-analysis. PLoS One 8:e68858–e68858. https://doi.org/10.1371/journal.pone.0068858

Swift MJ, Heal OW, Anderson JM (1979) Decomposition in terrestrial ecosystems. Univ of California Press, Berkeley & Los Angeles

Udo S, Aro T (1999) Global PAR related to global solar radiation for Central Nigeria. Agric For Meteorol 97:21–31. https://doi.org/10.1016/S0168-1923(99)00055-6

Velmurugan P, Lee YH, Venil CK, Lakshmanaperumalsamy P, Chae J-C, Oh B-T (2010) Effect of light on growth, intracellular and extracellular pigment production by five pigment-producing filamentous fungi in synthetic medium. J Biosci Bioeng 109:346–350. https://doi.org/10.1016/j.jbiosc.2009.10.003

Verhoef HA, Verspagen JMH, Zoomer HR (2000) Direct and indirect effects of ultraviolet-B radiation on soil biota, decomposition and nutrient fluxes in dune grassland soil systems. Biol Fertil Soils 31:366–371. https://doi.org/10.1007/s003749900181

Zhou S, Huang C, Xiang Y, Tie L, Han B, Scheu S (2018) Effects of reduced precipitation on litter decomposition in an evergreen broad-leaved forest in western China. For Ecol Manag 430:219–227. https://doi.org/10.1016/j.foreco.2018.08.022

ELECTRONIC SUPPLEMENTARY MATERIAL

TABLES

Table S1

Cumulative daily irradiance doses received by the litter under different filter treatments and in unfiltered conditions at each collection time.

Collection time (months)	Filter treatment	UV-B (mol m^{-2} day^{-1})	UV-A (mol m^{-2} day^{-1})	Blue light (mol m^{-2} day^{-1})	Green light (mol m^{-2} day^{-1})	PAR (mol m^{-2} day^{-1})
1	Dark	0.00	0.01	0.18	0.29	1.34
	No-UV/Blue/Green	0.00	0.07	0.17	0.39	23.30
	No-UV/Blue	0.00	0.09	0.37	11.97	41.57
	No-UV	0.00	0.35	11.41	13.60	54.91
	No-UVB	0.00	4.20	11.64	13.75	56.00
	Full-Spectrum	0.10	4.81	12.08	14.30	58.30
	Unfiltered	*0.12*	*5.50*	*13.61*	*16.24*	*66.32*
2	Dark	0.00	0.03	0.38	0.63	2.93
	No-UV/Blue/Green	0.00	0.15	0.37	0.84	50.79
	No-UV/Blue	0.00	0.20	0.80	26.09	90.61
	No-UV	0.02	0.76	24.87	29.64	119.68
	No-UVB	0.01	9.14	25.37	29.97	122.06
	Full-Spectrum	0.22	10.49	26.33	31.17	127.06
	Unfiltered	*0.26*	*11.99*	*29.67*	*35.40*	*144.56*
3	Dark	0.00	0.08	0.96	1.58	7.32
	No-UV/Blue/Green	0.00	0.37	0.91	2.10	126.80
	No-UV/Blue	0.00	0.50	2.01	65.13	226.19
	No-UV	0.00	1.90	62.09	73.98	298.77
	No-UVB	0.02	22.83	63.34	74.82	304.72
	Full-Spectrum	0.55	26.20	65.72	77.81	317.19
	Unfiltered	*0.65*	*29.92*	*74.06*	*88.36*	*360.88*
6	Dark	0.00	0.23	2.58	5.66	23.53
	No-UV/Blue/Green	0.01	0.00	2.45	7.56	407.75
	No-UV/Blue	0.01	1.48	5.39	233.90	727.35
	No-UV	0.00	5.64	166.75	265.69	960.75
	No-UVB	0.06	67.77	170.10	268.69	979.87
	Full-Spectrum	1.84	77.78	176.51	279.46	1019.98
	Unfiltered	*2.16*	*88.84*	*198.90*	*317.34*	*1160.47*

Table S2

Initial litter quality, mean and standard errors are shown (n=5)

Trait	Mean	SE
SLA (mm^2mg^{-1})	13.75	0.22
Dry weight (g)	0.30	0.01
Leaf area (cm^2)	82.36	1.24
Chlorophyll (OI)	11.36	0.28
Flavonoids (OI)	1.93	0.01
Anthocyanins (OI)	0.72	0.01
C content (%)	45.96	0.12
N content (%)	0.87	0.03
Ash (%)	4.10	0.15

Table S3

Pairwise comparisons for filter treatment on litter ash free dry mass (AFDM) at the end of the experiment: t- tests, with the Holm's correction for multiple comparisons, were used to calculate the *p* values. Significant contrasts are shown in bold. The number "6" refers to the sample after 6-months of exposure at the end of the experiment.

Treatment combination	Estimate	SE	t-value	*p-value*
Dark,6 - NoUV/Blue/Green,6	12.703	3.628	3.501	0.121
Dark,6 - NoUV/Blue,6	4.322	3.628	1.191	1.000
Dark,6 - NoUV,6	**15.212**	**3.628**	**4.192**	**0.012**
Dark,6 - NoUVB,6	**14.904**	**3.628**	**4.108**	**0.016**
Dark,6 - Full-Spectrum,6	10.701	3.628	2.949	0.599
NoUV/Blue/Green,6 - NoUV/Blue,6	-8.381	3.628	-2.310	1.000
NoUV/Blue/Green,6 - NoUV,6	2.509	3.628	0.691	1.000
NoUV/Blue/Green,6 - NoUVB,6	2.201	3.628	0.606	1.000
NoUV/Blue/Green,6 - Full-Spectrum,6	-2.002	3.628	-0.552	1.000
NoUV/Blue,6 - NoUV,6	10.890	3.628	3.001	0.519
NoUV/Blue,6 - NoUVB,6	10.581	3.628	2.916	0.654
NoUV/Blue,6 - Full-Spectrum,6	6.379	3.628	1.758	1.000
NoUV,6 - NoUVB,6	-0.308	3.628	-0.085	1.000
NoUV,6 - Full-Spectrum,6	-4.511	3.628	-1.243	1.000
NoUVB,6 - Full-Spectrum,6	-4.202	3.628	-1.158	1.000

Table S4

Pairwise comparisons for filter treatments on litter N content according to collection time: t- tests, with the Holm's correction for multiple comparisons, were used to calculate the *p* values. Significant contrasts are shown in bold. The numbers, 1, 3, and 6, after the treatment refer to the number of months of exposure during the experiment after which the litter was sampled.

Treatment combination	**Estimate**	**SE**	**t-value**	***p-value***
Dark,1 - NoUV/Blue/Green,1	9.005	30.936	0.291	1.000
Dark,1 - NoUV/Blue,1	14.160	30.936	0.458	1.000
Dark,1 - NoUV,1	-10.511	30.936	-0.340	1.000
Dark,1 - NoUVB,1	14.273	30.936	0.461	1.000
Dark,1 - Full-Spectrum,1	0.122	30.936	0.004	1.000
NoUV/Blue/Green,1 - NoUV/Blue,1	5.155	30.936	0.167	1.000
NoUV/Blue/Green,1 - NoUV,1	-19.516	30.936	-0.631	1.000
NoUV/Blue/Green,1 - NoUVB,1	5.268	30.936	0.170	1.000
NoUV/Blue/Green,1 - Full-Spectrum,1	-8.883	30.936	-0.287	1.000
NoUV/Blue,1 - NoUV,1	-24.671	30.936	-0.797	1.000
NoUV/Blue,1 - NoUVB,1	0.113	30.936	0.004	1.000
NoUV/Blue,1 - Full-Spectrum,1	-14.038	30.936	-0.454	1.000
NoUV,1 - NoUVB,1	24.785	30.936	0.801	1.000
NoUV,1 - Full-Spectrum,1	10.633	30.936	0.344	1.000
NoUVB,1 - Full-Spectrum,1	-14.151	30.936	-0.457	1.000
Dark,3 - NoUV/Blue/Green,3	-0.911	30.936	-0.029	1.000
Dark,3 - NoUV/Blue,3	1.562	30.936	0.050	1.000
Dark,3 - NoUV,3	1.027	30.936	0.033	1.000
Dark,3 - NoUVB,3	6.585	30.936	0.213	1.000
Dark,3 - Full-Spectrum,3	33.497	30.936	1.083	1.000
NoUV/Blue/Green,3 - NoUV/Blue,3	2.473	30.936	0.080	1.000
NoUV/Blue/Green,3 - NoUV,3	1.938	30.936	0.063	1.000
NoUV/Blue/Green,3 - NoUVB,3	7.495	30.936	0.242	1.000
NoUV/Blue/Green,3 - Full-Spectrum,3	34.407	30.936	1.112	1.000

Treatment combination	**Estimate**	**SE**	**t-value**	***p-value***
NoUV/Blue,3 - NoUV,3	-0.535	30.936	-0.017	1.000
NoUV/Blue,3 - NoUVB,3	5.023	30.936	0.162	1.000
NoUV/Blue,3 - Full-Spectrum,3	31.935	30.936	1.032	1.000
NoUV,3 - NoUVB,3	5.558	30.936	0.180	1.000
NoUV,3 - Full-Spectrum,3	32.470	30.936	1.050	1.000
NoUVB,3 - Full-Spectrum,3	26.912	30.936	0.870	1.000
Dark,6 - NoUV/Blue/Green,6	93.445	30.936	3.021	0.454
Dark,6 - NoUV/Blue,6	53.040	30.936	1.714	1.000
Dark,6 - NoUV,6	**120.890**	**30.936**	**3.908**	**0.029**
Dark,6 - NoUVB,6	**155.865**	**30.936**	**5.038**	**< 0.001**
Dark,6 - Full-Spectrum,6	103.803	30.936	3.355	0.169
NoUV/Blue/Green,6 - NoUV/Blue,6	-40.405	30.936	-1.306	1.000
NoUV/Blue/Green,6 - NoUV,6	27.446	30.936	0.887	1.000
NoUV/Blue/Green,6 - NoUVB,6	62.421	30.936	2.018	1.000
NoUV/Blue/Green,6 - Full-Spectrum,6	10.358	30.936	0.335	1.000
NoUV/Blue,6 - NoUV,6	67.851	30.936	2.193	1.000
NoUV/Blue,6 - NoUVB,6	102.826	30.936	3.324	0.185
NoUV/Blue,6 - Full-Spectrum,6	50.763	30.936	1.641	1.000
NoUV,6 - NoUVB,6	34.975	30.936	1.131	1.000
NoUV,6 - Full-Spectrum,6	-17.088	30.936	-0.552	1.000
NoUVB,6 - Full-Spectrum,6	-52.063	30.936	-1.683	1.000

Table S5

Pairwise comparisons for filter treatments on litter C:N ratio: t- tests, with the Holm's correction for multiple comparisons, were used to calculate the *p* values. Significant contrasts are shown in bold.

Treatment combination	**Estimate**	**SE**	**t-value**	***p-value***
Dark - NoUV/Blue/Green	-3.978	2.060	-1.931	0.689
Dark - NoUV/Blue	-2.344	2.060	-1.138	1.000
Dark - NoUV	-2.266	2.060	-1.100	1.000
Dark - NoUVB	**-7.102**	**2.060**	**-3.448**	**0.014**
Dark - Full-Spectrum	-3.521	2.060	-1.709	0.950
NoUV/Blue/Green - NoUV/Blue	1.634	2.060	0.793	1.000
NoUV/Blue/Green - NoUV	1.712	2.060	0.831	1.000
NoUV/Blue/Green - NoUVB	-3.124	2.060	-1.517	1.000
NoUV/Blue/Green - Full-Spectrum	0.457	2.060	0.222	1.000
NoUV/Blue - NoUV	0.078	2.060	0.038	1.000
NoUV/Blue - NoUVB	-4.758	2.060	-2.310	0.309
NoUV/Blue - Full-Spectrum	-1.177	2.060	-0.571	1.000
NoUV - NoUVB	-4.836	2.060	-2.348	0.303
NoUV - Full-Spectrum	-1.255	2.060	-0.609	1.000
NoUVB - Full-Spectrum	3.581	2.060	1.739	0.950

Table S6

Pairwise comparisons for filter treatments overall on microbial biomass: t- tests, with the Holm's correction for multiple comparisons, were used to calculate the *p* values. Significant contrasts are shown in bold.

Treatment	**Estimate**	**SE**	**t-value**	***p-value***
Dark - NoUV/Blue/Green	-103.792	60.627	-1.712	0.806
Dark - NoUV/Blue	-5.204	60.627	-0.086	1.000
Dark - NoUV	5.993	60.627	0.099	1.000
Dark - NoUVB	117.653	60.627	1.941	0.656
Dark - Full-Spectrum	-27.000	61.381	-0.440	1.000
NoUV/Blue/Green - NoUV/Blue	98.588	60.627	1.626	0.853
NoUV/Blue/Green - NoUV	109.785	60.627	1.811	0.748
NoUV/Blue/Green - NoUVB	**221.445**	**60.627**	**3.653**	**0.006**
NoUV/Blue/Green - Full-Spectrum	76.792	61.381	1.251	1.000
NoUV/Blue - NoUV	11.197	60.627	0.185	1.000
NoUV/Blue - NoUVB	122.857	60.627	2.026	0.584
NoUV/Blue - Full-Spectrum	-21.796	61.381	-0.355	1.000
NoUV - NoUVB	111.659	60.627	1.842	0.748
NoUV - Full-Spectrum	-32.993	61.381	-0.538	1.000
NoUVB - Full-Spectrum	-144.653	61.381	-2.357	0.281

Table S7

Pairwise comparisons for filter treatments overall on fungal biomass: t- tests, with the Holm's correction for multiple comparisons, were used to calculate the *p* values. Significant contrasts are shown in bold.

Treatment	**Estimate**	**SE**	**t-value**	***p-value***
Dark - NoUV/Blue/Green	-82.443	57.423	-1.436	1.000
Dark - NoUV/Blue	10.550	57.423	0.184	1.000
Dark - NoUV	24.352	57.423	0.424	1.000
Dark - NoUVB	127.133	57.423	2.214	0.374
Dark - Full-Spectrum	-10.009	58.137	-0.172	1.000
NoUV/Blue/Green - NoUV/Blue	92.993	57.423	1.619	0.972
NoUV/Blue/Green - NoUV	106.795	57.423	1.860	0.719
NoUV/Blue/Green - NoUVB	**209.576**	**57.423**	**3.650**	**0.006**
NoUV/Blue/Green - Full-Spectrum	72.434	58.137	1.246	1.000
NoUV/Blue - NoUV	13.803	57.423	0.240	1.000
NoUV/Blue - NoUVB	116.583	57.423	2.030	0.535
NoUV/Blue - Full-Spectrum	-20.559	58.137	-0.354	1.000
NoUV - NoUVB	102.780	57.423	1.790	0.760
NoUV - Full-Spectrum	-34.361	58.137	-0.591	1.000
NoUVB - Full-Spectrum	-137.141	58.137	-2.359	0.279

Table S8

Pairwise comparisons for filter treatments overall on bacterial biomass: t- tests, with the Holm's correction for multiple comparisons, were used to calculate the *p* values. Significant contrasts are shown in bold.

Treatment	**Estimate**	**SE**	**t-value**	***p-value***
Dark - NoUV/Blue/Green	**-21.349**	**5.273**	**-4.048**	**0.001**
Dark - NoUV/Blue	**-15.754**	**5.273**	**-2.987**	**0.041**
Dark - NoUV	**-18.359**	**5.273**	**-3.481**	**0.010**
Dark - NoUVB	-9.480	5.273	-1.798	0.748
Dark - Full-Spectrum	**-16.991**	**5.339**	**-3.183**	**0.024**
NoUV/Blue/Green - NoUV/Blue	5.595	5.273	1.061	1.000
NoUV/Blue/Green - NoUV	2.990	5.273	0.567	1.000
NoUV/Blue/Green - NoUVB	11.869	5.273	2.251	0.289
NoUV/Blue/Green - Full-Spectrum	4.358	5.339	0.816	1.000
NoUV/Blue - NoUV	-2.605	5.273	-0.494	1.000
NoUV/Blue - NoUVB	6.274	5.273	1.190	1.000
NoUV/Blue - Full-Spectrum	-1.238	5.339	-0.232	1.000
NoUV - NoUVB	8.879	5.273	1.684	0.854
NoUV - Full-Spectrum	1.368	5.339	0.256	1.000
NoUVB - Full-Spectrum	-7.511	5.339	-1.407	1.000

Table S9

Pairwise comparisons for filter treatments overall on F:B ratio: t- tests, with the Holm's correction for multiple comparisons, were used to calculate the *p* values. Significant contrasts are shown in bold.

Treatment	**Estimate**	**SE**	**t-value**	***p-value***
Dark - NoUV/Blue/Green	1.051	0.683	1.539	0.878
Dark - NoUV/Blue	1.571	0.675	2.329	0.215
Dark - NoUV	**2.613**	**0.675**	**3.873**	**0.002**
Dark - NoUVB	**3.180**	**0.675**	**4.714**	**< 0.001**
Dark - Full-Spectrum	**1.922**	**0.675**	**2.849**	**0.062**
NoUV/Blue/Green - NoUV/Blue	0.521	0.683	0.762	1.000
NoUV/Blue/Green - NoUV	1.562	0.683	2.287	0.216
NoUV/Blue/Green - NoUVB	**2.129**	**0.683**	**3.117**	**0.030**
NoUV/Blue/Green - Full-Spectrum	0.871	0.683	1.275	1.000
NoUV/Blue - NoUV	1.041	0.675	1.543	0.878
NoUV/Blue - NoUVB	1.609	0.675	2.385	0.206
NoUV/Blue - Full-Spectrum	0.351	0.675	0.520	1.000
NoUV - NoUVB	0.567	0.675	0.841	1.000
NoUV - Full-Spectrum	-0.691	0.675	-1.024	1.000
NoUVB - Full-Spectrum	-1.258	0.675	-1.865	0.517

Table S10

Pairwise comparisons for filter treatments overall on Gram-P biomass: t- tests, with the Holm's correction for multiple comparisons, were used to calculate the *p* values. Significant contrasts are shown in bold.

Treatment	**Estimate**	**SE**	**t-value**	***p-value***
Dark - NoUV/Blue/Green	**-17.256**	**4.522**	**-3.816**	**0.003**
Dark - NoUV/Blue	**-14.605**	**4.522**	**-3.230**	**0.019**
Dark - NoUV	**-17.029**	**4.522**	**-3.766**	**0.004**
Dark - NoUVB	-9.769	4.522	-2.161	0.360
Dark - Full-Spectrum	**-16.755**	**4.578**	**-3.660**	**0.005**
NoUV/Blue/Green - NoUV/Blue	2.651	4.522	0.586	1.000
NoUV/Blue/Green - NoUV	0.226	4.522	0.050	1.000
NoUV/Blue/Green - NoUVB	7.486	4.522	1.656	1.000
NoUV/Blue/Green - Full-Spectrum	0.501	4.578	0.109	1.000
NoUV/Blue - NoUV	-2.424	4.522	-0.536	1.000
NoUV/Blue - NoUVB	4.836	4.522	1.069	1.000
NoUV/Blue - Full-Spectrum	-2.150	4.578	-0.470	1.000
NoUV - NoUVB	7.260	4.522	1.606	1.000
NoUV - Full-Spectrum	0.274	4.578	0.060	1.000
NoUVB - Full-Spectrum	-6.986	4.578	-1.526	1.000

Table S11

Pairwise comparisons for filter treatments overall on Gram-N biomass: t- tests, with the Holm's correction for multiple comparisons, were used to calculate the *p* values. Significant contrasts are shown in bold.

Treatment	**Estimate**	**SE**	**t-value**	***p-value***
Dark - NoUV/Blue/Green	-4.093	1.404	-2.915	0.059
Dark - NoUV/Blue	-1.149	1.404	-0.818	1.000
Dark - NoUV	-1.330	1.404	-0.947	1.000
Dark - NoUVB	0.289	1.404	0.206	1.000
Dark - Full-Spectrum	-0.236	1.421	-0.166	1.000
NoUV/Blue/Green - NoUV/Blue	2.944	1.404	2.097	0.457
NoUV/Blue/Green - NoUV	2.764	1.404	1.968	0.565
NoUV/Blue/Green - NoUVB	**4.382**	**1.404**	**3.121**	**0.034**
NoUV/Blue/Green - Full-Spectrum	3.857	1.421	2.713	0.099
NoUV/Blue - NoUV	-0.181	1.404	-0.129	1.000
NoUV/Blue - NoUVB	1.438	1.404	1.024	1.000
NoUV/Blue - Full-Spectrum	0.913	1.421	0.642	1.000
NoUV - NoUVB	1.619	1.404	1.153	1.000
NoUV - Full-Spectrum	1.093	1.421	0.769	1.000
NoUVB - Full-Spectrum	-0.525	1.421	-0.370	1.000

Table S12

Pairwise comparisons for filter treatments overall on Gram-P: Gram-N ratio: t- tests, with the Holm's correction for multiple comparisons, were used to calculate the *p* values. Significant contrasts are shown in bold.

Treatment	**Estimate**	**SE**	**t-value**	***p-value***
Dark - NoUV/Blue/Green	0.0231	0.0254	0.9075	1.0000
Dark - NoUV/Blue	0.0644	0.0236	2.7252	0.0900
Dark - NoUV	0.0584	0.0239	2.4487	0.1836
Dark - NoUVB	0.0567	0.0239	2.3687	0.1963
Dark - Full-Spectrum	**0.0770**	**0.0234**	**3.2964**	**0.0147**
NoUV/Blue/Green - NoUV/Blue	0.0413	0.0222	1.8565	0.6338
NoUV/Blue/Green - NoUV	0.0353	0.0225	1.5708	1.0000
NoUV/Blue/Green - NoUVB	0.0336	0.0226	1.4883	1.0000
NoUV/Blue/Green - Full-Spectrum	0.0539	0.0220	2.4541	0.1836
NoUV/Blue - NoUV	-0.0060	0.0204	-0.2925	1.0000
NoUV/Blue - NoUVB	-0.0077	0.0205	-0.3766	1.0000
NoUV/Blue - Full-Spectrum	0.0126	0.0198	0.6379	1.0000
NoUV - NoUVB	-0.0017	0.0207	-0.0841	1.0000
NoUV - Full-Spectrum	0.0186	0.0201	0.9258	1.0000
NoUVB - Full-Spectrum	0.0204	0.0202	1.0085	1.0000

Table S13

Pairwise comparisons for filter treatments PLFA biomarkers with function pairwise.adonis() with similarity index Bray-Curtis and *p*-value correction Holm. Significant contrasts are shown in bold.

Treatment	**F Model**	**R^2**	***p-value***
NoUV/Blue/Green vs Full-Spectrum	2.495	0.054	0.850
NoUV/Blue/Green vs Dark	2.716	0.058	0.850
NoUV/Blue/Green vs NoUV/Blue	2.888	0.060	0.850
NoUV/Blue/Green vs NoUVB	**11.956**	**0.210**	**0.015**
NoUV/Blue/Green vs NoUV	4.399	0.089	0.384
Full-Spectrum vs Dark	1.071	0.024	1.000
Full-Spectrum vs NoUV/Blue	0.383	0.008	1.000
Full-Spectrum vs NoUVB	6.414	0.125	0.084
Full-Spectrum vs NoUV	1.068	0.023	1.000
Dark vs NoUV/Blue	0.944	0.021	1.000
Dark vs NoUVB	6.196	0.121	0.117
Dark vs NoUV	0.916	0.020	1.000
NoUV/Blue vs NoUVB	3.500	0.071	0.539
NoUV/Blue vs NoUV	0.334	0.007	1.000
NoUVB vs NoUV	2.932	0.060	0.850

Table S14

SIMPER contrast between the No-UV/Blue/Green and the No-UVB treatments, showing the PLFA biomarker c18:2ω6,9 to contribute the most to the dissimilarity between the two treatments. Analysis done with the function simper() from the 'vegan' package using the Bray-Curtis dissimilarity index.

Contrast: NoUV/Blue/Green_NoUVB

	average	sd	ratio	ava	avb	cumsum
C18.2w6.9	**0.228854**	**0.1525756**	**1.4999**	**808.584**	**565.7148**	**0.8436**
i16.0	0.010478	0.0076464	1.3703	20.032	19.4208	0.8822
C16.1w5.1	0.005885	0.0026736	2.2011	9.569	0.6451	0.9039
i17.0	0.005726	0.0040680	1.4075	16.813	15.9284	0.9250
a17.0	0.004851	0.0042215	1.1491	16.203	13.1626	0.9429
a15.0	0.004166	0.0038494	1.0822	9.295	6.9331	0.9583
cy17.0	0.004082	0.0033502	1.2185	15.913	10.6197	0.9733
i15.0	0.003624	0.0030458	1.1898	8.438	7.3125	0.9867
cy.19.0	0.002777	0.0021720	1.2783	6.032	7.0863	0.9969
C16.1w5	0.000833	0.0008443	0.9866	1.237	0.2756	1.0000

Table S15

Pairwise comparisons for filter treatments PLFA biomarkers after 1 month in the field, with function pairwise.adonis() with similarity index Bray-Curtis and *p*-value correction Holm. Significant contrasts are shown in bold.

Treatment	**F Model**	**R^2**	***p-value***
NoUV/Blue/Green vs Full-Spectrum	1.334	0.118	1.000
NoUV/Blue/Green vs Dark	0.142	0.014	1.000
NoUV/Blue/Green vs NoUV/Blue	4.121	0.292	0.320
NoUV/Blue/Green vs NoUVB	10.189	0.505	0.104
NoUV/Blue/Green vs NoUV	**26.031**	**0.722**	**0.042**
Full-Spectrum vs Dark	1.439	0.126	1.000
Full-Spectrum vs NoUV/Blue	0.826	0.076	1.000
Full-Spectrum vs NoUVB	2.462	0.198	0.896
Full-Spectrum vs NoUV	3.028	0.294	0.792
Dark vs NoUV/Blue	4.160	0.294	0.308
Dark vs NoUVB	9.370	0.484	0.108
Dark vs NoUV	**21.127**	**0.679**	**0.030**
NoUV/Blue vs NoUVB	0.362	0.035	1.000
NoUV/Blue vs NoUV	0.435	0.042	1.000
NoUVB vs NoUV	0.260	0.025	1.000

Table S16

SIMPER contrast for significant pairwise comparisons at collection time = 1 month, showing the PLFA biomarker c18:2ω6,9 to contribute the most to the dissimilarity between the treatments. Analysis done with the function simper() from the 'vegan' package using the Bray-Curtis dissimilarity index.

Contrast: NoUV/Blue/Green_NoUV

	average	sd	ratio	ava	avb	cumsum
C18.2w6.9	**0.178883**	**0.0637904**	**2.8042**	**634.207**	**420.345**	**0.8739**
a17.0	0.004279	0.0033065	1.2940	10.692	9.661	0.8948
i17.0	0.004171	0.0036894	1.1305	12.159	10.000	0.9152
C16.1w5.1	0.003694	0.0031852	1.1596	7.769	3.873	0.9332
cy17.0	0.003234	0.0028088	1.1514	17.134	13.752	0.9490
a15.0	0.002904	0.0028569	1.0164	5.583	5.368	0.9632
cy.19.0	0.002627	0.0027777	0.9457	3.019	5.506	0.9761
i16.0	0.002488	0.0018510	1.3443	5.233	4.013	0.9882
C16.1w5	0.001271	0.0007948	1.5987	2.249	2.685	0.9944
i15.0	0.001141	0.0010312	1.1067	4.800	3.837	1.0000

Contrast: Dark_NoUV

	average	sd	ratio	ava	avb	cumsum
C18.2w6.9	**0.180551**	**0.0744714**	**2.4244**	**637.592**	**420.345**	**0.8767**
i17.0	0.004793	0.0043039	1.1136	14.848	10.000	0.9000
a17.0	0.003495	0.0040387	0.8653	8.377	9.661	0.9169
C16.1w5.1	0.003431	0.0026571	1.2911	5.134	3.873	0.9336
cy.19.0	0.003354	0.0031096	1.0787	1.633	5.506	0.9499
C16.1w5	0.002635	0.0035411	0.7441	4.621	2.685	0.9627
cy17.0	0.002378	0.0016009	1.4856	15.266	13.752	0.9742
i16.0	0.002306	0.0017759	1.2984	4.102	4.013	0.9854
a15.0	0.001918	0.0015535	1.2349	5.021	5.368	0.9947
i15.0	0.001085	0.0005848	1.8552	2.526	3.837	1.0000

Table S17

ANOVA results for two fixed factors (Filter treatment: with 2 levels and Time with 3 levels) and their interactions on single dependent variables: Ash Free Dry Mass (AFDM) remaining, carbon content, nitrogen content and C:N ratio Degrees of freedom (d.f.), sum of squares (SS), mean square (MS), F statistic (F) and *p*-value (*p*) are presented. Significant terms are shown in bold. Non-significant terms were retained since dropping them did not significantly affect the model.

Variable: AFDM					
	d.f.	**SS**	**MS**	**F**	***p***
Filter treatment	1	7.53	7.53	0.384	0.541
Time	**2**	**280.08**	**140.04**	**7.142**	**0.004**
Filter treatment x Time	2	11.26	5.63	0.287	0.752
Residuals	24	470.62	19.61		
Variable: Carbon content					
	d.f.	**SS**	**MS**	**F**	***p***
Filter treatment	1	0.46	0.46	0.020	0.888
Time	**2**	**269.62**	**134.81**	**5.905**	**0.008**
Filter treatment x Time	2	6.84	3.42	0.150	0.862
Residuals	24	547.94	22.83		
Variable: Nitrogen content					
	d.f.	**SS**	**MS**	**F**	***p***
Filter treatment	1	1551.60	1551.60	2.559	0.123
Time	**2**	**25081.30**	**12540.70**	**20.680**	**< 0.001**
Filter treatment x Time	2	94.20	47.10	0.078	0.926
Residuals	24	14554.10	606.4		
Variable: C:N ratio					
	d.f.	**SS**	**MS**	**F**	***p***
Filter treatment	**1**	**123.16**	**123.16**	**5.817**	**0.024**
Time	**2**	**1024.83**	**512.41**	**24.203**	**< 0.001**
Filter treatment x Time	2	40.77	20.38	0.963	0.396
Residuals	24	508.12	21.17		

Table S18

Transmittance (%) of mesh used in classical litterbags and polyethene filter used for the full-spectrum treatment.

Spectral region	Full-Spectrum	Mesh
PAR	92.18	73.50
UV-B	82.81	66.84
UV-A	87.08	72.27
Blue	91.87	74.47
Green	92.23	73.95

FIGURES

Figure S1

Measured spectral irradiance under the six filter treatments used in the experiment and ambient sunlight (no filter).

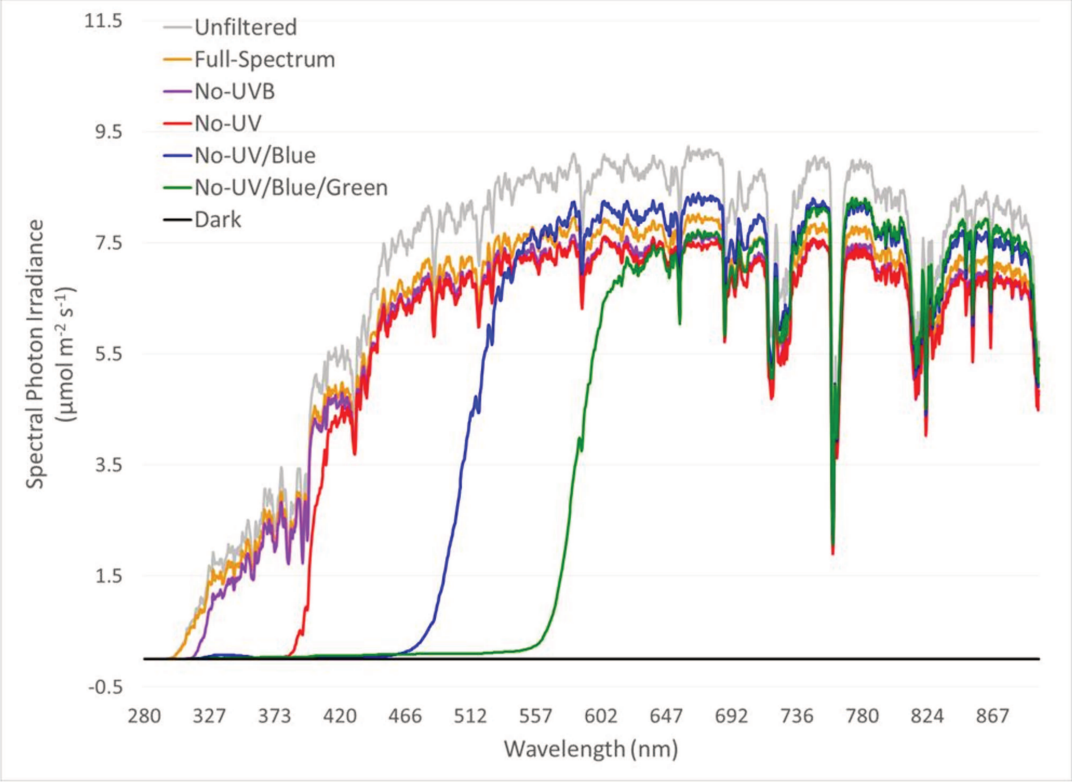

Figure S2

Time series of (A) photosynthetically active radiation (PAR), blue and green light and (B) UV-A and UV-B radiation in the understorey at the study site.

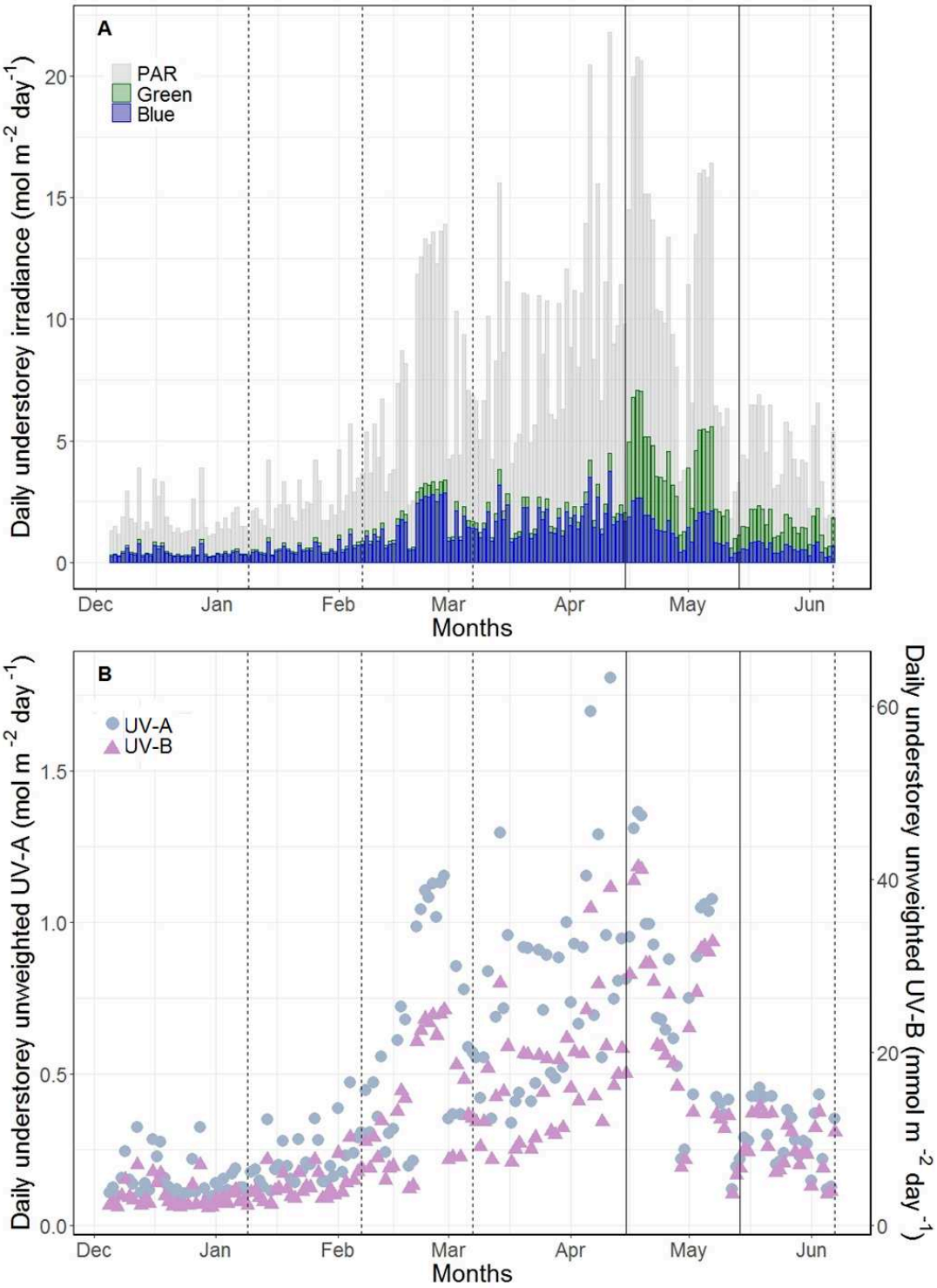

Figure S3

Daily photosynthetically active radiation (PAR) in the understorey (in green) and above the canopy (in grey) over the time of the experiment. Time series of modelled PAR reconstructed using radiative transfer modelling of solar irradiance and global light index (GLI) calculated from hemispherical photos taken at the site during the experiment. Vertical dashed lines show collection times and solid lines show the period of spring flush from bud burst to canopy closure.

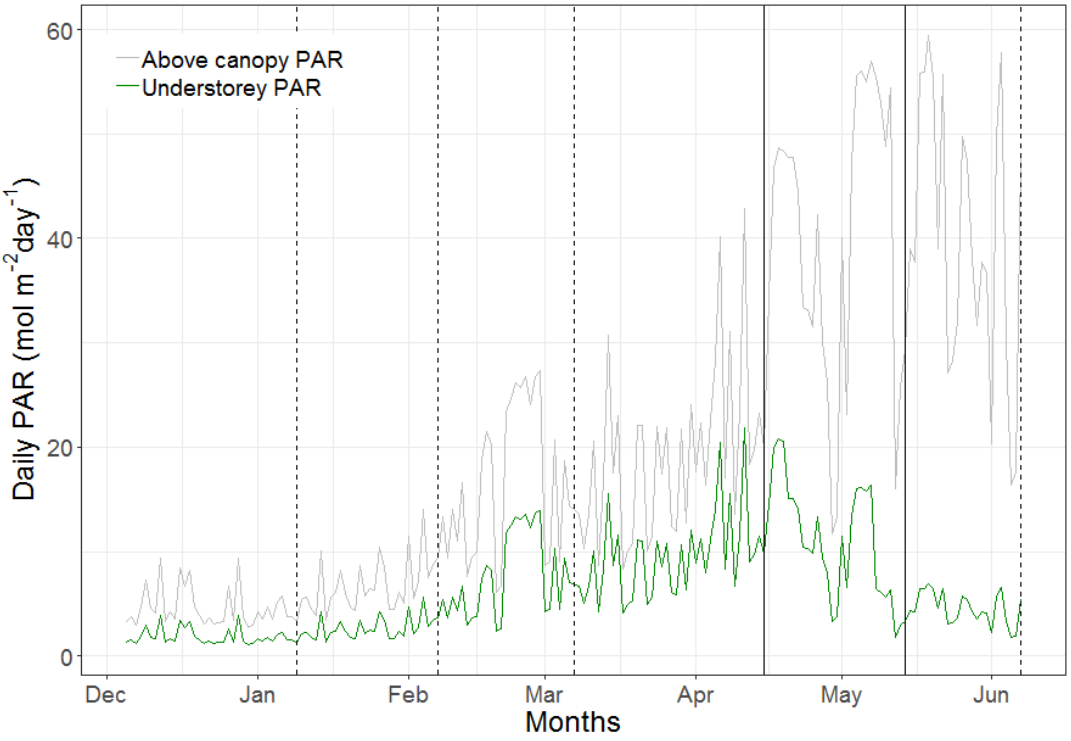

Figure S4

Average daily temperature inside the litterbags of the six filter treatment installed at the field site.

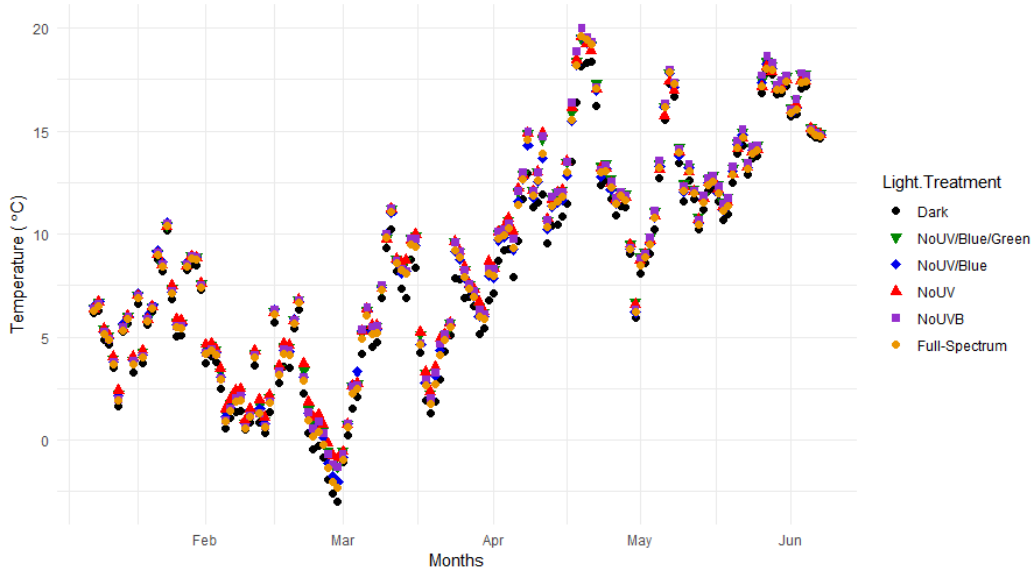

Figure S5

Photo of the field site with the litterbags at the beginning of the experiment.

Figure S6

Photos of the leaf litter stapled to the mesh (A) and ready to be attached to the filters (B).

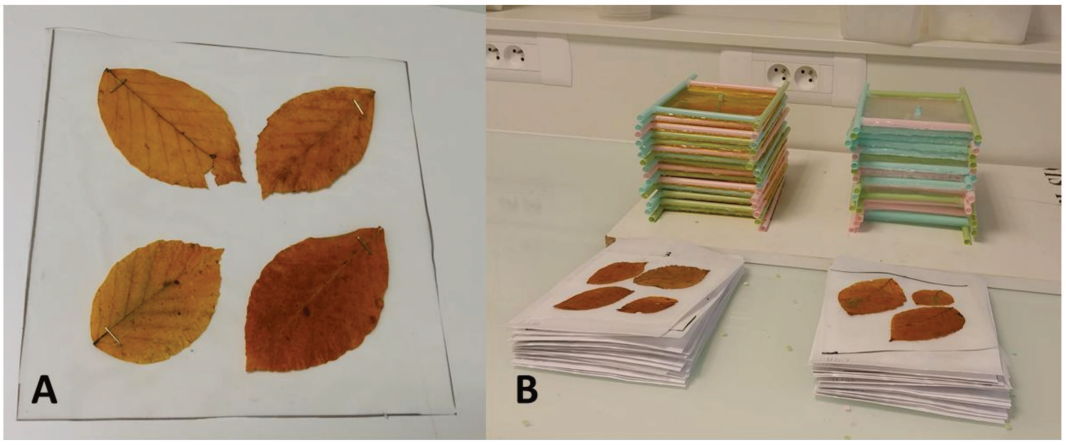

Figure S7

Microbial biomass, bacterial biomass, fungal biomass, F:B ratio, Gram-P biomass and Gram-N biomass for each filter treatment and time. Means ± SE are shown (n = 6).

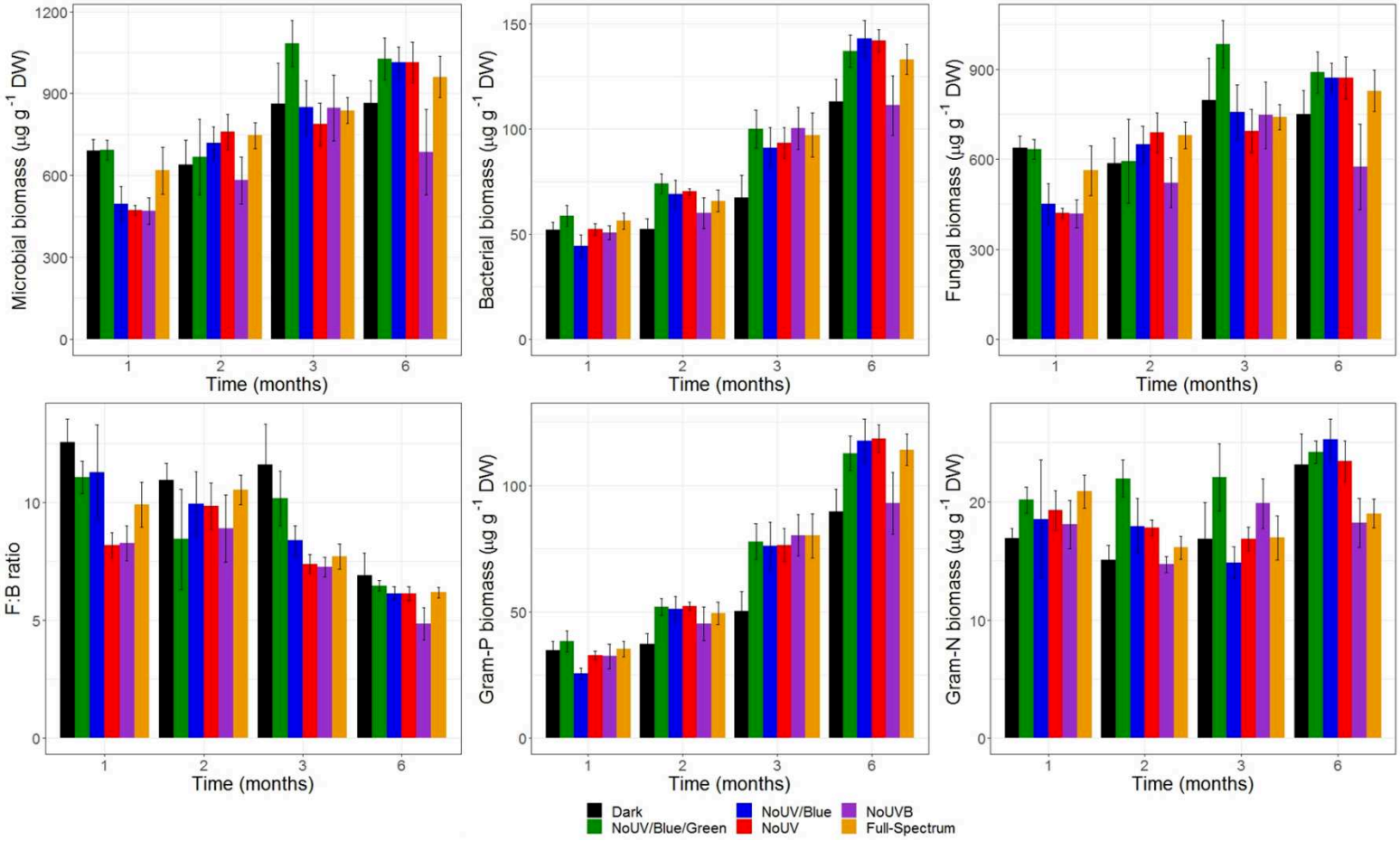

Figure S8

Bacterial biomass separate for Gram-P and Gram-N biomass for each filter treatment and time (months). Means ± SE are shown (n = 6).

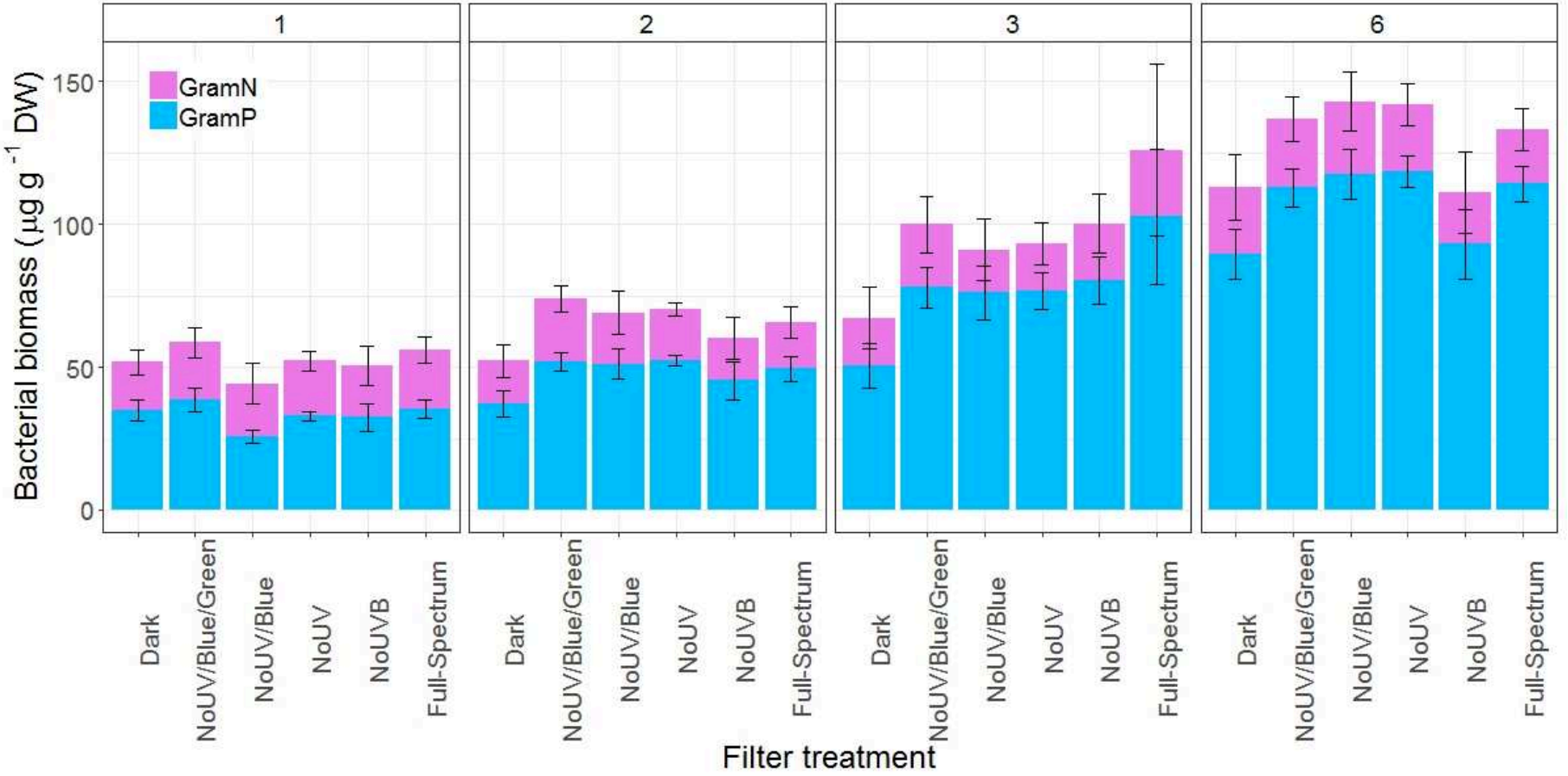

Figure S9

NLFA 16:1ω5:PLFA 16.1ω5 ratio for each filter treatment and collection time. Means ± SE are shown (n = 6).

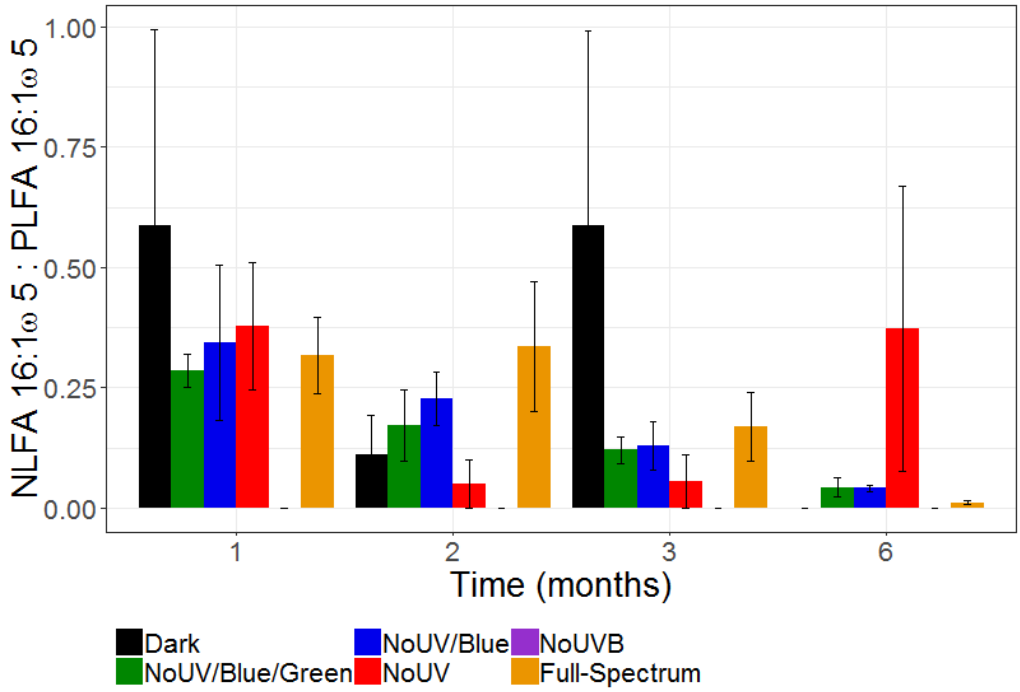

Figure S10

Gram-P:Gram-N ratio for each filter treatment. Means ± SE are shown (n = 6). Capital letters show significant differences between filter treatments. Pairwise comparisons were performed with the function glht in package Multicomp applying Holm's adjustment.

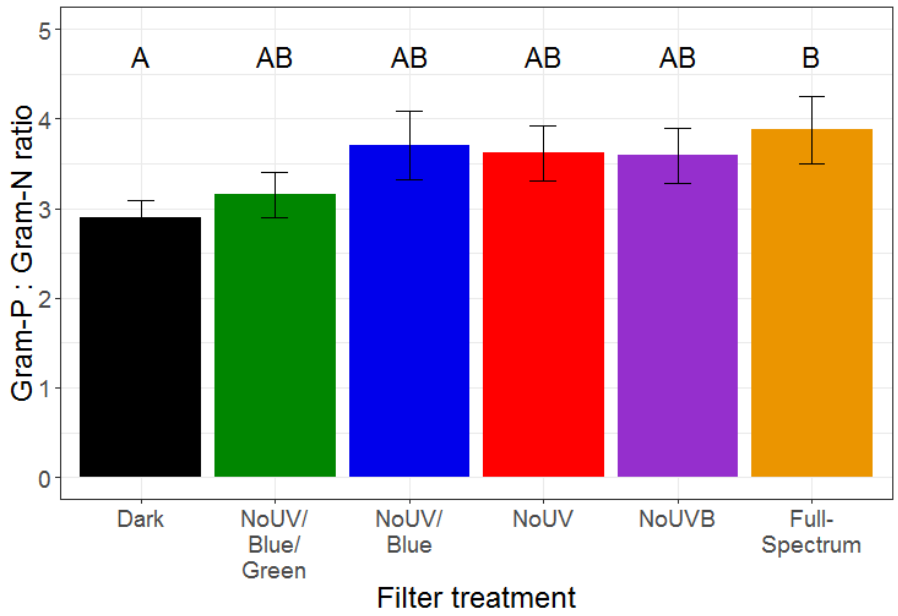

Figure S11

Patterns of PLFA-biomarker composition mapped against explanatory variables: Filter treatment (A) and Time (B), using non-metric multidimensional scaling (nMDS). Two axes were used and the stress was 0.036.

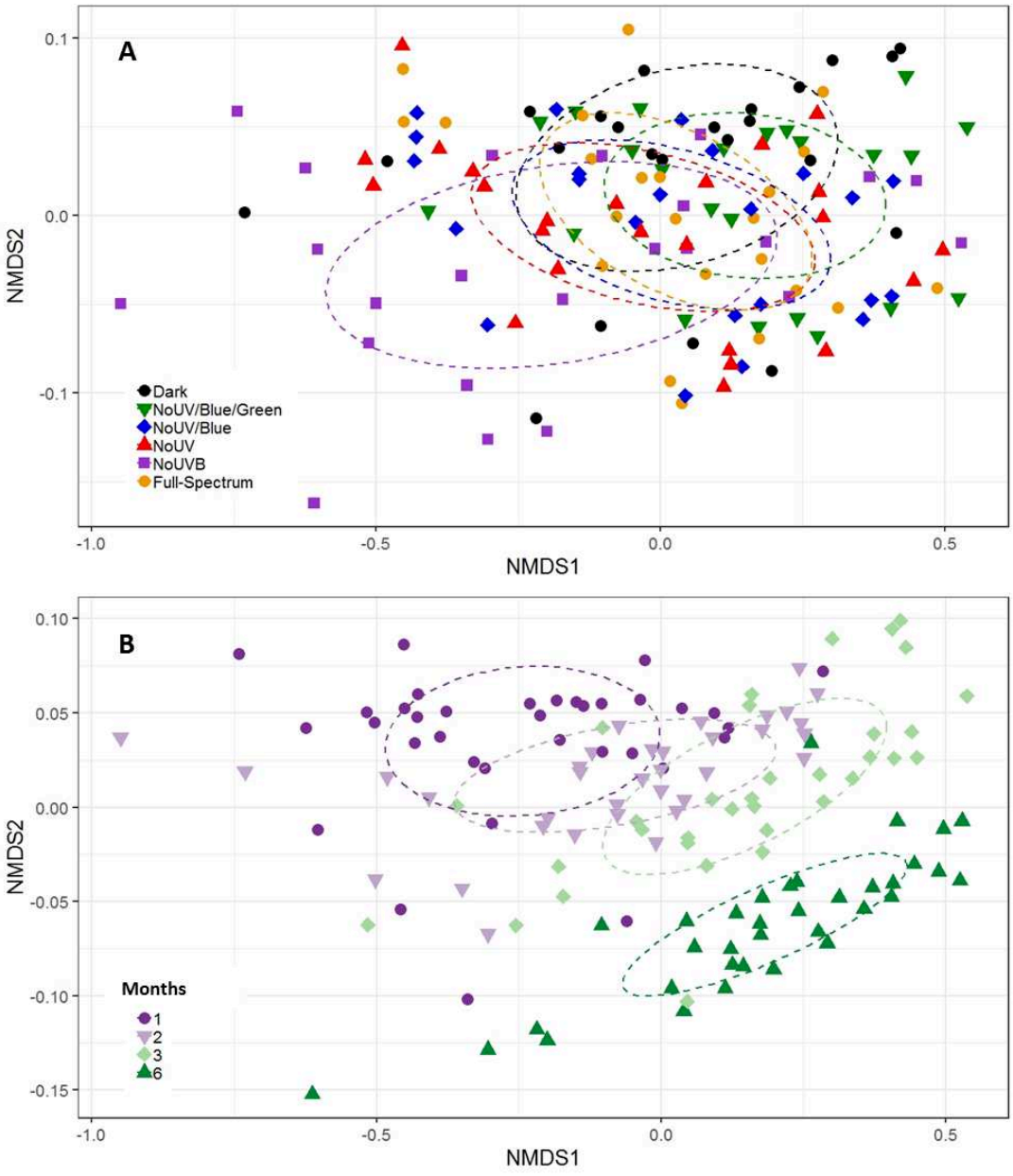

Figure S12

Correlation matrix between different variables. Colours indicate the strength and the direction of the correlations (red = positive, blue = negative). Significance of the correlations are shown in plot A with stars (*p*-values: *** ≤ 0.001; ** ≤ 0.01; * ≤ 0.05) while white squares represent non-significant correlations. Adjusted R^2 are shown in plot B.

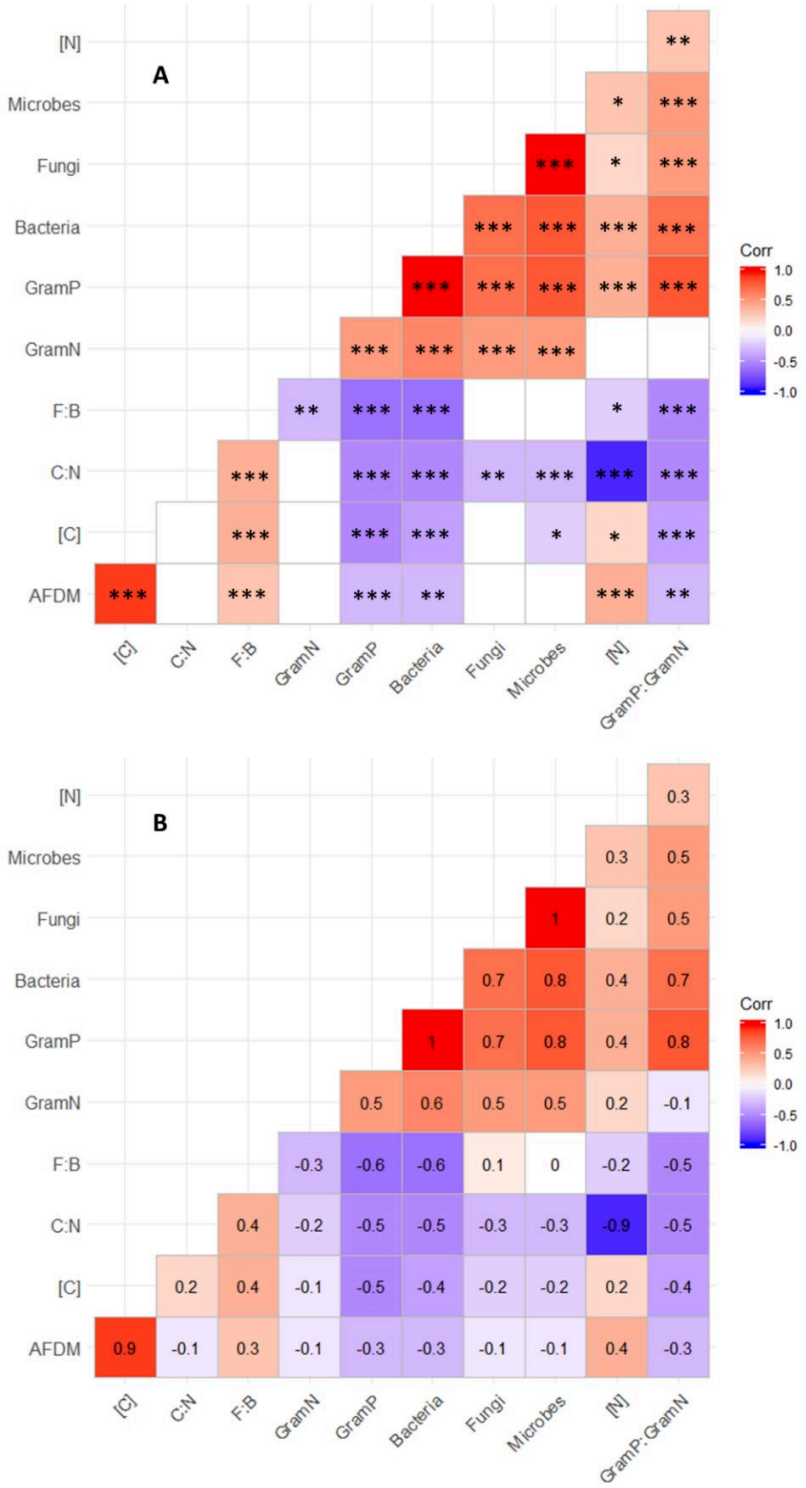

Figure S13

Final AFDM, [C], [N] and C:N in the full spectrum treatment compared with a classical litterbag (mesh). Mean ± SE are shown (n = 5). Significant differences are shown (*p*-values: *** ≤ 0.001; ** ≤ 0.01; * ≤ 0.05, ns ≥ 0.05).

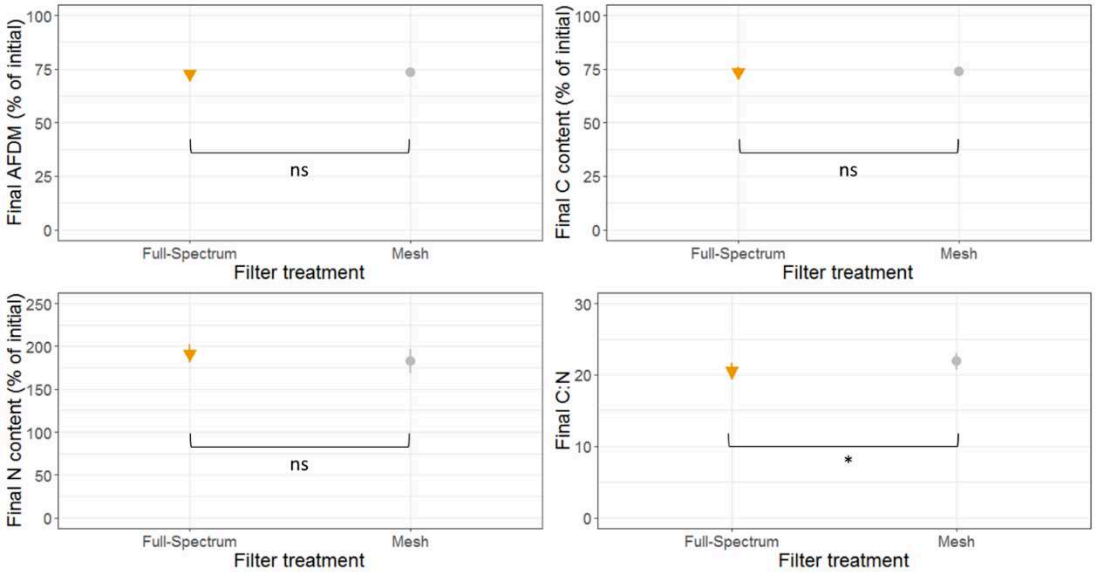

CHAPTER IV

TITLE PAGE

TITLE: The crucial role of blue light as a driver of photodegradation in terrestrial ecosystems on the global scale: a meta-analysis

AUTHORS: Marta Pieristè[1,2*], Qing-Wei Wang[3, 4*], Titta K. Kotilainen[5], Estelle Forey[2], Matthieu Chauvat[2], Hiroko Kurokawa[4], T Matthew Robson[1], Alan G Jones[6]

AFFILIATIONS: [1] Organismal and Evolutionary Biology (OEB), Viikki Plant Science Centre (ViPS), P.O. Box 65 (Viikinkaari1), 00014, University of Helsinki, Finland

[2] Normandie Université, UNIROUEN, IRSTEA, ECODIV, FR Scale CNRS 3730, Rouen, France

[3]CAS Key Laboratory of Forest Ecology and Management, Institute of Applied Ecology, Chinese Academy of Sciences, Shenyang 110016, China

[4] Forestry and Forest Products Research Institute, 1 Matsunosato, Tsukuba, Ibaraki 305-8687, Japan

[5] Natural Resources Institute Finland, Itäinen Pitkäkatu 4a, 20520, Turku, Finland

[6] Forest Systems, Scion. 49 Sala Street, Private Bag 3020, Rotorua 3046, New Zealand

***CORRESPONDING AUTHORs:** Marta Pieristè, marta.pieriste@helsinki.fi, +31 (0)6 83568944

Qing-Wei Wang, wangqingwei@iae.ac.cn, wangqw08@gmail.com; +86 (0)2483970329

DECLARATION OF AUTHORSHIP:
MP and QWW formulated the initial idea, MP and QWW designed the study, MP collected the data, MP and QWW analysed the data. MP wrote the draft of the manuscript and the remaining co-authors revised the manuscript.

ABSTRACT

Wherever sunlight reaches litter there is potential for photodegradation to contribute to decomposition. Typically, ultraviolet (UV) radiation has been considered the main driver of this process and has been broadly studied in many biomes. However, short-wavelength visible light was lately identified as biologically active in litter photodegradation along with UV radiation. Whilst several reviews have attempted to identify how photodegradation affects decomposition, we aimed to tease apart the extent to which different spectral regions contribute to this process globally. We performed a meta-analysis of studies that assessed photodegradation through spectrally selective attenuation of solar radiation, to identify the impact of waveband-dependent photodegradation on litter mass loss across all studied biomes under ambient sunlight. We found the full-spectrum of sunlight to significantly increase litter mass loss by 14% ± 1% across all studies. When accounting for spectral composition, blue light-driven photodegradation alone was responsible for most of this increase in mass loss (12% ± 1%). This highlights the crucial role of blue light in the photodegradation process. On the other hand, any effects of UV and its constituent UV-B radiation were not significant at the global scale only at a local scale, while UV-A radiation reduced mass loss by 5% ± 1% globally. These waveband-dependent effects were modulated by climate, ecosystem type and decay period. Relating photodegradation rates with initial litter traits, we did not find any of the classical litter traits to predict photodegradation on a global scale, suggesting different traits to be relevant in different biomes. However, there have been too few studies to make confident general inferences about

photodegradation at high latitudes and in ecosystems characterized by high canopy cover, where further investigation is needed to better explain the role of photodegradation globally.

KEY WORDS

Decomposition, spectral composition, UV, litter traits, biogeochemical cycling

INTRODUCTION

The capability of sunlight to impact litter decomposition in terrestrial ecosystems, through the process of photodegradation, is by now well established (Bais et al., 2018). Photodegradation involves three main mechanisms: photochemical mineralization, consisting of the direct breakdown of organic matter (Gallo et al., 2006), photofacilitation, meaning the facilitation of microbial decomposition following the photomineralization of complex polymers (Baker and Allison, 2015), and photoinhibition, referring to the inhibition of microbial decomposition (Barnes et al., 2015). Which of these processes is dominant depends not only on the spectral region considered, but also on other environmental factors, such as temperature and precipitation, interacting with photodegradation (King et al., 2012). In some cases, the positive (photochemical mineralization and consequent photofacilitation) and negative (photoinhibition) effects offset each other (Bais et al., 2018).

Since the 1990s, when the study of photodegradation began, research has largely focused on the effects of supplemental UV radiation (280-400 nm), and more specifically UV-B radiation (280-315 nm), in an attempt to evaluate their impact on litter decomposition after the formation of the stratospheric ozone hole (Zepp et al., 1995, Caldwell and Flint, 1994). Consequently, photodegradation under ambient sunlight did not receive much attention until recently (reviewed by King et al., 2012). This shift in focus has led researchers to realise that the short-wavelength regions of the visible spectrum, blue (420-490 nm, Sellaro et al., 2010 and green (500-570 nm, Sellaro et al., 2010) light, are also important as drivers of photodegradation (Austin and Ballaré, 2010).

Photodegradation has a role in litter decomposition in terrestrial ecosystems, not only in arid and semiarid environments at low latitudes (Day et al., 2007, Almagro et al., 2015), as originally thought, but also at higher latitudes (Jones et al., 2016, Zaller et al., 2009) and in mesic environments (Brandt et al., 2010). Recently, forests have been added to the list of ecosystems where photodegradation affects biogeochemical cycling, extending the reach of this process beyond those areas with low canopy cover and exposed to high solar radiation (Pieristè et al., 2019, Pieristè et al., 2020, Méndez et al., 2019). However, photodegradation does not always impact litter decomposition in the same way, and whether it accelerates or decelerates the decomposition process is thought to depend on both the spectral composition and irradiance of incident radiation and the biome in question (Bais et al., 2018). This could be explained by the interaction of photodegradation with other abiotic factors, such as temperature, precipitation and soil moisture, as the relative importance of photodegradation is reported to be enhanced in dryer conditions (Brandt et al., 2007, Brandt et al., 2010, Almagro et al., 2017). Moreover, photodegradation rate increases with those factors that change the exposure of litter to sunlight, such as season, canopy structure and phenological stage, litter layer thickness or litter position (Moody et al., 2001, Rutledge et al., 2010, Bravo-Oviedo et al., 2017, Almagro et al., 2015, Henry et al., 2008, Mao et al., 2018). Additionally, the incident irradiance and spectral composition of solar radiation changes on a spatial scale according to several factors, such as latitude, elevation and sun angle, meaning that underlying patterns of photodegradation should vary consistently across the globe (Aphalo et al., 2012, Aphalo, 2018, Gallo et al., 2009).

Photodegradation is also thought to be moderated by litter traits, in particular lignin content was suggested as a good predictor of the photodegradation rate in arid and semiarid environments, due to its capacity to absorb UV radiation (Austin and Ballaré, 2010, Méndez et al., 2019). However, other studies have found the photodegradation rate to be correlated with specific leaf area (SLA) and initial hemicellulose and cellulose content but not with lignin content (King et al., 2012, Day et al., 2018, Pan et al., 2015). This suggests that we do not yet understand the underlying mechanisms of photodegradation, but it appears that there is the potential for different plant morphological and biochemical traits to be important as predictors of photodegradation driven by different spectral regions.

Effects of UV-B-driven photodegradation were reviewed in a meta-analysis by Song et al., 2013 and, under ambient sunlight, UV-B radiation was found to have no significant, direct or indirect, effects on litter decomposition at the global scale. King et al., 2012 reviewed the effects of UV radiation and visible light below 450 nm, finding that these spectral regions can increase litter mass loss. However, these two studies (Song et al., 2013 and King et al., 2012) included both experiments employing supplemental and ambient radiation and did not analyse the effect of the separate spectral regions (e.g. UV-B, UV-A, blue light). To date, the contrasting results from studies on the effects of photodegradation driven by different spectral regions under ambient sunlight, have not been comprehensively synthesised and generalized at the global scale. Knowledge of the impact of waveband-dependent photodegradation on litter mass loss on a global scale could represent the first step towards quantifying the impact of sunlight on decomposition and later carbon loss across the globe, as

we know that photodegradation is responsible for the release of carbon compounds, such as methane (CH4), carbon dioxide (CO2) and carbon monoxide (CO), into the atmosphere(Brandt et al., 2009, Day et al., 2019).

This study aims to analyse the effect of photodegradation driven by UV radiation, its constituent UV-B and UV-A radiation, and blue light on mass loss from litter at the global scale and to assess whether photodegradation rates are modulated by climate, ecosystem type, length of the exposure period and litter habit (evergreen or deciduous). We expect blue light- and UV-A radiation-driven photodegradation to enhance litter mass loss, due to the ability of these spectral regions to degrade lignin (Austin and Ballaré, 2010) while having lower potential than UV-B radiation for photoinhibition of microbial decomposers (Austin et al., 2016, King et al., 2012). This ability of UV-B radiation to inhibit microbial decomposition (Ball et al., 2019, Day et al., 2018), mitigating the direct photochemical mineralisation of litter, leads us to expect photodegradation driven by this spectral region to have no net effect on litter mass loss in accordance with the findings of Song et al., 2013. Moreover, we expect photodegradation to be more relevant (1) in arid than mesic conditions, where precipitation is likely to be the main driver of the decomposition process (Bais et al., 2018), as well as (2) in ecosystems with low canopy cover which allow most of the incident solar radiation to penetrate to the litter layer.

In addition, we aim to identify initial litter traits that could predict the impact of photodegradation driven by each spectral region. Previous studies (Day et al., 2018, Méndez et al., 2019, Austin and Ballaré, 2010, Pan et al., 2015, King et al., 2012) found different traits to be good predictors of the photodegradation rate when applying

different spectral treatments to attenuate several parts of the solar spectrum. In light of this finding, we expect different traits to predict photodegradation rates driven by different spectral regions.

MATERIAL AND METHODS

Data collection

Data for the meta-analysis were extracted from published literature and two unpublished studies from the research groups of the authors of this meta-analysis. Literature, published between 1980 and July 2019, was collected from Web of Science, Google Scholar, and Scopus database (see ESM Appendix-1 for details of the keywords used). We selected studies that spectrally selectively attenuated solar radiation to measure the photodegradation of surface leaf litter in terrestrial ecosystems. Since one of our aims is to understand the effects of spectral composition on mass loss under ambient sunlight, all studies employing supplemental radiation were excluded. Moreover, as we aimed to examine the correlation between photodegradation rate and litter traits, we retained only studies employing leaf litter from a single species, while we excluded studies using litter mixtures (see ESM Appendix-1 for more details about study selection). We extracted data concerning litter mass loss and initial litter traits. Where data were not presented in tables, we extracted them directly from the figures using WebPlotDigitizer 4.2 (Rohatgi, 2019). We retained a total of 25 papers (see Appendix-2 for list of retained studies) with a total of 1483 datapoints. Several papers included comparisons of multiple plant species (see ESM Appendix-3 for the list of litter

species), field sites and spectral treatments, so the number of trials exceeded the number of studies. The global dataset was divided into five categories according to the spectral treatment: the effect of excluding 1) UV radiation; 2) UV-B radiation; 3) UV-A radiation; 4) blue light and 5) the full spectrum of visible light and UV radiation. There were too few studies to be able to test the effects of green light. The effect of each spectral region was obtained by comparison of pairs of spectral treatments applied in the original studies: the effects of excluding UV radiation, UV-B radiation and the full-spectrum were obtained by comparison of the control treatment with the no-UV, no-UVB and dark treatments respectively; while the effect of UV-A radiation was obtained by comparison between the no-UV and the no-UVB treatment and the effect of blue light by contrasting the no-UV/blue and no-UV treatments as in (Wang et al., 2020).

Additionally, we extracted complementary information from each study: ecosystem (grassland, shrubland, woodland, open area); length of the decay period (months); habit (evergreen or deciduous), litter form (herbaceous; shrub, tree), latitude (see ESM Appendix-4 for more details about data and complementary information included in the dataset). The climate of each study site was defined according to the updated Koppen-Geiger climate classification through the map provided by (Beck et al., 2018), dividing the globe into five main climate zones further separated in subdivisions based on temperature and precipitation (see ESM Appendix-5 for more details about the climate classification). We could not consider subdivisions in temperate and continental zones because of the small amount of data from these climates.

In order to deliver estimate global-scale quantities of C released from surface litter by photodegradation, we extracted data from the SRDB database (Bond-Lamberty and Thomson, 2010) for the annual litter carbon fluxes from each of the biomes corresponding to the locations of studies retained in the meta-analysis (see ESM Appendix-7). These data allowed us to roughly estimate the carbon flux in each of these biomes attributable to litter mass loss due to photodegradation.

Statistical analysis

The effect sizes expressed as log response ratio (lnRR) of mass loss were computed with the function escalc() from the package 'metafor' (ver. 2.1-0) (Viechtbauer, 2019), which uses sample sizes, standard deviations and means of the original studies and presents bias correction for small sampling. We used a three-level random mixed effect model with variables "Ecosystem", "Decay", "Climate", "Habit", "Life form" and "Latitude" as fixed factors and "Study" and "Trial" as random factors. "Trial" represents the series of measurements of mass loss from each species in each study. We used this method to test the overall effect of exclusion of each spectral region and the effect of the categorical variables, with the function rma.mv() from the package 'metafor' (ver. 2.1-0) (Viechtbauer, 2019), employing the Knapp and Hartung method correction for random meta-analyses (Knapp and Hartung, 2003, Assink and Wibbelink, 2016). From these models we obtained the estimated average lnRR which we used to calculate the percentage change to better interpret the magnitude effect with the formula as in (Pustejovsky, 2018).

We analysed possible correlations between the rate of photodegradation (effect size = lnRR) and the initial litter traits, as reported by the authors in their studies: carbon

content (C); nitrogen content (N); carbon to nitrogen ratio (C:N); lignin content; lignin to nitrogen ratio (Lig:N) and specific leaf area (SLA). To evaluate the potential correlation between photodegradation driven by each spectral region and the initial litter traits, we used a mixed-effect model with the function lme() from the package 'nlme' (ver. 3.1-141) (Pinheiro et al., 2019). We used the initial traits as covariates, the study and trial as random effects and the sample size as weight in order to obtain an estimate of the mean slope, its standard error and the statistical significance of the relationship (Cornwell et al., 2008). We then calculated the regression coefficients with the function r.squaredGLMM from package 'MuMIn' (ver. 1.43.6) (Bartoń, 2019). Following the same method, we also analysed relationships between photodegradation driven by each spectral region and latitude; mean annual temperature (MAT) and precipitation (MAP) at the experimental sites.

There is potential for bias due to the paucity of published studies from certain climates, ecosystems, latitude, etc. To better understand the risk of bias, we explored the dataset of retained studies to identify over- and under-represented categories. To evaluate literature bias we employed an Egger's test (Egger et al., 1997) by using the variance of the effect size as a moderator of a meta regression clustered by trial and study (Viechtbauer, 2010). This allowed us to account for the dependency among the effect sizes.

RESULTS

Effect of full-spectrum-driven photodegradation on litter mass loss

Full-spectrum of sunlight significantly increased litter mass loss overall (+14% ± 1%, p = 0.040, Fig.2a, Table 1), however, this effect varied significantly depending on climate (p = 0.001, Table 2), ecosystem type (p < 0.001, Table 2) and decay period (p < 0.001, Table 2). Specifically, the full spectrum significantly increased mass loss effect only in arid (+36%, p < 0.001, Fig.2a) and semiarid (+26%, p < 0.001, Fig.2a) climates. In terms of ecosystem types, receipt of the full-spectrum of sunlight increased mass loss only in open areas (+37%, p = 0.013, Fig.2a) and shrublands (+34%, p < 0.001, Fig.2a), while it had no significant effect in grasslands (p = 0.534, Fig.2a) or woodlands (p = 0.293, Fig.2a). Furthermore, the full spectrum of sunlight significantly increased litter mass loss between three and twelve months of decomposition (3 to 6 months: +21%, p = 0.016; 6 to 12 months: +22%, p = 0.001, Fig.2a), but it had no significant effect during the initial three months of decomposition (p = 0.251, Fig.2a) nor after twelve months (p = 0.529, Fig.2a).

Effect of blue light-driven photodegradation on litter mass loss

Blue light caused an increase in mass loss overall (+12% ± 1%, p = 0.037, Fig.2b, Table 1) and this effect was dependent on climate (p = 0.003, Table 2) and ecosystem type (p < 0.001, Table 2). Blue light significantly increased litter mass loss in arid (+10%, p < 0.001, Fig.2a) and semiarid (+27%, p < 0.001, Fig.2b) climates but had no significant effect on litter mass loss in temperate (p = 0.302, Fig.2b) and continental climates (p = 0.782, Fig.2b). Moreover, blue light significantly increased litter mass loss in open

areas (+50%, $p < 0.001$, Fig.2b) and shrublands (+10%, $p < 0.001$, Fig.2b), but not in woodlands ($p = 0.091$, Fig.2b).

Effect of UV-driven photodegradation on litter mass loss

The total UV radiation (UV-B + UV-A) had no significant effect on mass loss overall ($p = 0.255$, Fig. 2e, Table 1). However, there was an interactive effect of UV radiation modulated by the decay period ($p < 0.001$, Table 2), which increased with the length of decay period reaching a peak between 24 and 36 months, when UV radiation increased mass loss by 40% (Fig.2c). UV-B radiation, similarly to the total UV radiation, did not have a significant overall effect on litter mass loss ($p = 0.872$, Fig. 2d, Table 1). However, the effect of UV-B radiation changed according to climate ($p < 0.001$, Table 2), decay period ($p < 0.001$, Table 2) and habit ($p = 0.048$, Table 2). UV-B radiation significantly increased mass loss in semiarid climates (+10%, $p < 0.001$, Fig.2d), while it reduced mass loss in polar climates (-23%, $p < 0.001$, Fig.2d). Furthermore, UV-B radiation between 6 and 12 months of decomposition (+8%, $p = 0.007$, Fig.2d), while it had no significant effect during the other periods of decomposition (Fig.2d). Moreover, UV-B radiation increased mass loss of evergreen trees' litter (+17%, $p = 0.006$, Fig.2d), while it had no significant effect on mass loss of deciduous trees' litter ($p = 0.602$, Fig.2d). In contrast to UV-B radiation, solar UV-A radiation significantly reduced mass loss overall (-5% ± 1%, $p = 0.019$, Fig.2e) and this effect was dependent on the decay period ($p = 0.012$, Table 2), being limited to the first three months of decomposition (-9%, $p = 0.023$, Fig.2e).

Relationship between photodegradation and abiotic factors

Photodegradation driven by blue light, UV-A and UV radiation did not correlate with any of abiotic factors (MAT, MAP and latitude). However, photodegradation attributable to the full-spectrum of sunlight was significantly positively correlated with MAP (slope = 0.001, R^2 = 0.292, *p* = 0.009, Fig.3, Table S1) and UV-B radiation was significantly negatively correlated with latitude (slope = -0.003, R^2 = 0.244, *p* = 0.027, Fig.3, Table S1).

Relationship between Initial litter traits and photodegradation

Photodegradation attributable to the full-spectrum, blue light and UV-A radiation did not correlate with any of these traits (Table S2). On the other hand, photodegradation attributable to the total UV and UV-B radiation were significantly negatively correlated with initial C (*p*: 0.025 & 0.043 respectively, Fig.4, TableS2), however the correlations were very weak (slope = -0.015 & -0.013, R^2 = 0.080 & 0.167, Fig.4, Table S2).

Bias analysis and bias exploration

We did not find bias in the datasets for the following spectral regions: blue light ($F_{1,195}$ = 0.597, *p*-value = 0.441); UV-A radiation ($F_{1,116}$ = 0.010, *p*-value = 0.921); UV-B radiation ($F_{1,127}$ = 1.223, *p*-value = 0.271) and UV radiation ($F_{1,355}$ = 0.741, *p*-value = 0.390); except for the full spectrum ($F_{1,251}$ = 13.371, *p*-value < 0.001). UV radiation was the most studied spectral region, while blue light and UV-A radiation were under-represented in our dataset (Fig.1a). Most studies were carried out at latitudes between 30° and 50°North and South, while data from high latitudes were lacking

(Fig.1b). Grassland and shrubland ecosystems were more studied than woodlands and open areas (Fig.1c). Arid and semiarid climates were the most studied, while polar and subtropical climates were the least studied followed by continental and temperate climates (Fig.1d). In terms of the decay period, the first 12 months of decomposition were the most studied (Fig.1e). The retained studies were located in six biomes: “boreal forests/taiga”, “deserts and xeric shrublands”, “Mediterranean forests, woodlands and scrub”, “montane grasslands and shrublands”, “temperate broadleaf and mixed forests” and “temperate grasslands, savannas and shrublands” (Fig.1h, see ESM Appendix-6 and Appendix-7 for further details).

DISCUSSION

Photodegradation across the globe: a waveband-dependent process

Exposure to the full-spectrum of sunlight increased litter mass loss by 14% ± 1% overall (Table 1, Fig.2a), confirming the importance of sunlight among the suite of abiotic factors driving the decomposition process across the globe. This result is in agreement with previous findings analysing the effect of the full-spectrum of sunlight on litter mass loss (Day et al., 2015, Ma et al., 2017, Pan et al., 2015). However, the magnitude of the effect is smaller than found in the meta-analysis from King et al., 2012, which calculated an increase in mass loss of 23% due to sunlight. Our meta-analysis includes studies that were carried out in temperate and hemi-boreal forest environments, including one as yet unpublished study (Pieristè et al., 2019, Pieristè et al., 2020). This type of ecosystem was not represented in the meta-analysis by King et al., 2012. In temperate and boreal forests, sunlight tends to have the opposite net

effect on photodegradation compared with forests at lower latitudes (Ma et al., 2017), decreasing litter mass loss in some litter species (Pieristè et al., 2019, Pieristè et al., 2020). Hence, the inclusion of studies from these biomes may explain the lower contribution of photodegradation to decomposition on the global scale from our meta-analysis compared with previous analyses.

Overall, blue light explained the large part of mass loss through an increase of 12% ± 1% (Table 1, Fig.2b), while we found no significant effect of UV and UV-B radiation on litter mass loss, in agreement with a previous meta-analysis showing no effect of UV-B radiation overall (Song et al., 2013). On the other hand, UV-A radiation decreased mass loss by 5% ± 1% (Table 1, Fig.2e), suggesting that this spectral region reduces litter decomposition. The potential of UV and UV-B radiation to slow down microbial decomposition, due to their high energetic capacity to cause oxidative stress in living organisms, has been reported in previous studies (Moody et al., 2001, Moody et al., 1999, Verhoef et al., 2000) as well as their potential for photochemical mineralization (Gallo et al., 2009). Moreover, past studies found UV and UV-B radiation to have contrasting effects in different climates: for instance their positive effect on decomposition in arid and semiarid climates was not found to extend to temperate and continental climates (Pieristè et al., 2019, Pieristè et al., 2020, Gallo et al., 2009, Gallo et al., 2006). On the other hand, while blue light has proved to be effective in terms of photochemical mineralization, photoinhibition was not apparent in litter exposed to this spectral region (Austin et al., 2016); this is likely to be the reason for the overall positive effect of blue light on litter decomposition. A similar argument could be made to explain the effect of UV-A radiation, supposing that UV-A-photoinhibition,

known to occur in some fungi (Yamazaki et al., 1996), could outweigh photochemical mineralization. The effect of UV-A radiation on decomposer organisms needs further investigation, in order to better understand the role of this spectral region in litter decomposition. The high irradiance of blue light and UV-A radiation compared to UV-B radiation in ambient sunlight may provide another reason for their stronger effect on global decomposition in natural conditions (Aphalo et al., 2012).

We estimated annual carbon flux from litter attributable to photodegradation driven by different spectral regions applying the percentage contributed by photodegradation to the gross annual carbon flux lost from litter. This produced an estimate of photodegradation driven by the full spectrum could contribute 20-35 g C m^{-2} per year according to biome type (Table S3). While blue light would potentially be responsible for 16-26 g C m^{-2} per year according to biome type (Table S3). On the other hand, UV-A radiation could offset the annual carbon flux by 6-12 g C m^{-2} according to biome type (Table S3). Our estimate suggests that at a global scale, photodegradation due to the full spectrum of sunlight may contribute 1.82 Pg to the annual global terrestrial carbon flux in the six biomes studied, corresponding to 0.01 – 0.65 Pg according to the type of biome.

Climate moderated photodegradation driven by blue light, UV-B radiation and the full-spectrum of sunlight, with the highest photodegradation rates occurring in arid and semiarid climates. This is likely due to the high irradiance and dry climatic conditions that promote photodegradation, together with reduced microbial activity in these kind of environments (Gallo et al., 2006, Brandt et al., 2007), while in temperate and continental climates decomposition is likely to be driven by factors promoting

biotic processes, such as precipitation and temperature cycles (Adair et al., 2008, Aerts, 1997, Meentemeyer, 1978). However, in this meta-analysis we did not find a significant correlation between the rate of photodegradation and the mean annual precipitation (MAP) for any of the spectral regions, except for the full-spectrum of sunlight. It is possible that using MAP, an average estimate calculated over 30 years, failed to capture any fine-scale variability in the weather conditions during the experiments in these studies. Cumulative precipitation during the experiment, seasonality of rainfall and rainfall intensity and duration might prove better predictors, however these data were not available for many of the studies included in the meta-analysis, so could not be used. Most arid and semiarid environments studied were at low latitudes, typically receiving high irradiance, and proportionally high UV-B radiation, compared with higher latitudes, potentially increasing the importance of photodegradation among factors controlling decomposition in these biomes.

In our meta-analysis the decay period played an important role in moderating the photodegradation rate, with different spectral regions acting at different periods during decomposition. For instance, the effect of UV radiation on mass loss increased after 12 months, while the importance of blue light decreased after 12 months. As previously suggested by Wang et al., 2015 and Lin et al., 2018, the contribution of photofacilitation depends on the duration of exposure and phase of decomposition. The role of UV radiation as inhibitor of microbial decomposition is likely to be the reason why the net effect of UV on mass loss is less important during the initial stages of decomposition when microbial decomposers play an important role (Voříšková and

Baldrian, 2013). The opposite may be true for blue light which is known to photodegrade lignin (Austin and Ballaré, 2010) facilitating subsequent microbial activity without itself being responsible for microbial photoinhibition (Austin et al., 2016, King et al., 2012).

Initial litter traits fail to predict photodegradation rate at the global scale

In our meta-analysis, those litter traits typically employed as predictors of litter decomposition, such as C:N or Lig:N, failed to predict photodegradation rates driven by specific spectral regions. Past studies from several biomes have found photodegradation rate to correlate with various traits. For instance, the photodegradation rate correlated with initial N and SLA in an arid shrubland (Pan et al., 2015), while a correlation with initial lignin content was found in a semiarid grassland (Austin and Ballaré, 2010) and in a semiarid forest (Méndez et al., 2019). On the other hand, in the Sonoran Desert, characterised by bare soil and sparse shrubs, photodegradation was correlated with initial hemicellulose and cellulose content (Day et al., 2018). These trends together with our results suggest that different traits predict the photodegradation rate in different biomes. As a consequence, photodegradation at the global scale is likely to be mainly driven by climate, while initial litter traits tend to be more relevant at the local scale, due to their interaction with other abiotic factors such as temperature and precipitation which are able to drive microbial decomposition and shape microbial assemblages (Yao et al., 2017, Classen et al., 2015, Hawkes et al., 2011). Unfortunately, the number of studies from each biome is too small to be able to test the importance of each trait for each biome

separately. Moreover, as litter traits are partly determined by the climatic conditions during plant growth (Fortunel et al., 2009), climatic regimes (or biomes) are auto-correlated and therefore difficult to disentangle. This could be another potential reason for the lack of correlation between initial litter traits and photodegradation. Nevertheless, it is likely that the interaction of photodegradation with factors such as temperature and precipitation, and with the microbial pool, is more important than the initial litter traits in determining the rate of photodegradation.

Potential bias and further considerations

Every meta-analysis is subjected to bias, for this reason results must be interpreted with care, even if we tried to minimize potential biases as much as possible. Exploring the literature published about photodegradation under ambient sunlight, we identified some over- and under-represented categories that could potentially affect our results. For instance, UV-driven photodegradation is the most studied, while not much attention has focused on blue and green light and UV-A radiation, despite their relevance in the photodegradation process (Austin et al., 2016). We might expect that as more studies focus on these under-represented spectral regions whose importance only recently came to prominence, our results would change. Moreover, studies of photodegradation were mainly located at latitudes between 30° and 50° North and South (Fig.1b), with high latitudes being under-represented. As photodegradation has even proved relevant even under relatively low irradiances (Pieristè et al., 2019, Pieristè et al., 2020), the study of photodegradation in biomes at high latitudes and with a dynamic vegetation structure is fundamental to understand the real impact of photodegradation at the global scale. Moreover, woodlands are

by far less studied than shrublands and grasslands and these studies are located at higher latitudes in temperate and continental climates, while grasslands have mainly been studied in arid and semiarid climates at lower latitudes. This segregation might partially explain the higher importance attributed to photodegradation in arid conditions.

Something more to consider, which is a particularly contentious subject in photobiology, is the method used to manipulate the solar spectrum. In photodegradation studies, there is no standard method of filtering solar radiation and this makes it hard to compare multiple studies where different methods create different micro-environments and exclude different classes of decomposers from reaching the litter, consequently altering the decomposition rates (King et al., 2012). Agreement on a standard method for the manipulation of solar radiation in photodegradation studies would allow a better comparison between them.

CONCLUSION

We performed a meta-analysis to test the impact on litter mass loss at the global scale of those spectral regions biologically active in photodegradation. Our results confirmed the importance of sunlight as an abiotic driver of litter decomposition through the process of photodegradation at the global scale. The full-spectrum of sunlight increased litter mass loss by 14% ± 1% at the global scale, suggesting important consequences of relationships with photodegradation for the global terrestrial carbon flux. Furthermore, our meta-analysis highlights the important role of blue light in litter decomposition globally, as this spectral region alone is

responsible for an increase in mass loss of 12% ± 1%. On the other hand, any effects of UV and its constituent UV-B radiation were not significant at the global scale only at a local scale, while UV-A radiation reduced mass loss by 5% ± 1% globally. In addition, none of the classical litter traits seemed to predict photodegradation on a global scale, suggesting the possibility that different traits could be relevant in different biomes. Further investigation is needed into the role of photodegradation at high latitudes and under tree canopies, as these categories are at present understudied; this will allow us to have a better understanding of the role of photodegradation across the globe and would represent a first step towards estimating its impact on the global carbon cycles.

FUNDING

This research was funded by Academy of Finland decisions #266523, #304519 and #324555 to TMR, personal EF project and a grant from the Region "Haute-Normandie" through the GRR-TERA SCALE (UFOSE Project) to MP, and by the National Natural Science Foundation of China (nos. 41971148, 41701052) to QWW, by the Japan Society for the Promotion of Science (KAKENHI, 17F17403) to QWW and HK.

REFERENCES

Adair, E. C., Parton, W. J., Del Grosso, S. J., Silver, W. L., Harmon, M. E., Hall, S. A., Burke, I. C. & Hart, S. C. 2008. Simple three-pool model accurately describes patterns of long-term litter decomposition in diverse climates. *Global Change Biology,* 14**,** 2636-2660.

Aerts, R. 1997. Climate, Leaf Litter Chemistry and Leaf Litter Decomposition in Terrestrial Ecosystems: A Triangular Relationship. *Oikos,* 79**,** 439-449.

Almagro, M., Maestre, F. T., Martínez-López, J., Valencia, E. & Rey, A. 2015. Climate change may reduce litter decomposition while enhancing the contribution of photodegradation in dry perennial Mediterranean grasslands. *Soil Biology and Biochemistry,* 90**,** 214-223.

Almagro, M., Martínez-López, J., Maestre, F. T. & Rey, A. 2017. The Contribution of Photodegradation to Litter Decomposition in Semiarid Mediterranean Grasslands Depends on its Interaction with Local Humidity Conditions, Litter Quality and Position. *Ecosystems,* 20**,** 527-542.

Aphalo, P. J. 2018. Exploring temporal and latitudinal variation in the solar spectrum at ground level with the TUV model. *UV4Plants Bulletin,* 2018**,** 45-56.

Aphalo, P. J., Albert, A., Mcleod, A., Heikkilä, A., Gómez, I., López Figueroa, F., Robson, T. M. & Strid, Å. 2012. *Beyond the visible: a handbook of best practice in plant UV photobiology,* Helsinki, University of Helsinki, Division of Plant Biology.

Assink, M. & Wibbelink, C. J. J. T. Q. M. F. P. 2016. Fitting three-level meta-analytic models in R: A step-by-step tutorial. *The Quantitative Methods for Psychology,* 12**,** 154-174.

Austin, A. T. & Ballaré, C. L. 2010. Dual role of lignin in plant litter decomposition in terrestrial ecosystems. *Proceedings of the National Academy of Sciences,* 107**,** 4618.

Austin, A. T., Méndez, M. S. & Ballaré, C. L. 2016. Photodegradation alleviates the lignin bottleneck for carbon turnover in terrestrial ecosystems. *Proceedings of the National Academy of Sciences,* 113**,** 4392.

Bais, A. F., Lucas, R. M., Bornman, J. F., Williamson, C. E., Sulzberger, B., Austin, A. T., Wilson, S. R., Andrady, A. L., Bernhard, G., Mckenzie, R. L., Aucamp, P. J., Madronich, S., Neale, R. E., Yazar, S., Young, A. R., De Gruijl, F. R., Norval, M., Takizawa, Y., Barnes, P. W., Robson, T. M., Robinson, S. A., Ballaré, C. L., Flint, S. D., Neale, P. J., Hylander, S., Rose, K. C., Wängberg, S. Å., Häder, D. P., Worrest, R. C., Zepp, R. G., Paul, N. D., Cory, R. M., Solomon, K. R., Longstreth, J., Pandey, K. K., Redhwi, H. H., Torikai, A. & Heikkilä, A. M. 2018. Environmental effects of ozone depletion, UV radiation and

interactions with climate change: UNEP Environmental Effects Assessment Panel, update 2017. *Photochemical & Photobiological Sciences,* 17**,** 127-179.

Baker, N. R. & Allison, S. D. 2015. Ultraviolet photodegradation facilitates microbial litter decomposition in a Mediterranean climate. *Ecology,* 96**,** 1994-2003.

Ball, B. A., Christman, M. P. & Hall, S. J. 2019. Nutrient dynamics during photodegradation of plant litter in the Sonoran Desert. *Journal of Arid Environments,* 160**,** 1-10.

Barnes, P. W., Throop, H. L., Archer, S. R., Breshears, D. D., Mcculley, R. L. & Tobler, M. A. 2015. Sunlight and Soil–Litter Mixing: Drivers of Litter Decomposition in Drylands. *In:* LÜTTGE, U. & BEYSCHLAG, W. (eds.) *Progress in Botany: Vol. 76.* Cham: Springer International Publishing.

Bartoń, K. 2019. MuMIn: Multi-Model Inference.

Beck, H. E., Zimmermann, N. E., Mcvicar, T. R., Vergopolan, N., Berg, A. & Wood, E. F. 2018. Present and future Köppen-Geiger climate classification maps at 1-km resolution. *Scientific data,* 5**,** 180214.

Bond-Lamberty, B. & Thomson, A. M. 2010. A Global Database of Soil Respiration Data. *Biogeosciences,* 7**,** 1915-1926.

Brandt, L. A., Bohnet, C. & King, J. Y. 2009. Photochemically induced carbon dioxide production as a mechanism for carbon loss from plant litter in arid ecosystems. *Journal of Geophysical Research: Biogeosciences,* 114.

Brandt, L. A., King, J. Y., Hobbie, S. E., Milchunas, D. G. & Sinsabaugh, R. L. 2010. The Role of Photodegradation in Surface Litter Decomposition Across a Grassland Ecosystem Precipitation Gradient. *Ecosystems,* 13**,** 765-781.

Brandt, L. A., King, J. Y. & Milchunas, D. G. 2007. Effects of ultraviolet radiation on litter decomposition depend on precipitation and litter chemistry in a shortgrass steppe ecosystem. *Global Change Biology,* 13**,** 2193-2205.

Bravo-Oviedo, A., Ruiz-Peinado, R., Onrubia, R. & Del Río, M. 2017. Thinning alters the early-decomposition rate and nutrient immobilization-release pattern of foliar litter in Mediterranean oak-pine mixed stands. *Forest Ecology and Management,* 391**,** 309-320.

Caldwell, M. M. & Flint, S. D. 1994. Stratospheric ozone reduction, solar UV-B radiation and terrestrial ecosystems. *Climatic Change,* 28**,** 375-394.

Classen, A. T., Sundqvist, M. K., Henning, J. A., Newman, G. S., Moore, J. a. M., Cregger, M. A., Moorhead, L. C. & Patterson, C. M. 2015. Direct and indirect effects of climate

change on soil microbial and soil microbial-plant interactions: What lies ahead? *Ecosphere,* 6**,** art130.

Cornwell, W. K., Cornelissen, J. H. C., Amatangelo, K., Dorrepaal, E., Eviner, V. T., Godoy, O., Hobbie, S. E., Hoorens, B., Kurokawa, H., Pérez-Harguindeguy, N., Quested, H. M., Santiago, L. S., Wardle, D. A., Wright, I. J., Aerts, R., Allison, S. D., Van Bodegom, P., Brovkin, V., Chatain, A., Callaghan, T. V., Díaz, S., Garnier, E., Gurvich, D. E., Kazakou, E., Klein, J. A., Read, J., Reich, P. B., Soudzilovskaia, N. A., Vaieretti, M. V. & Westoby, M. 2008. Plant species traits are the predominant control on litter decomposition rates within biomes worldwide. *Ecology,* 11**,** 1065-1071.

Day, T. A., Bliss, M. S., Placek, S. K., Tomes, A. R. & Guénon, R. 2019. Thermal abiotic emission of CO2 and CH4 from leaf litter and its significance in a photodegradation assessment. *Ecosphere,* 10**,** e02745.

Day, T. A., Bliss, M. S., Tomes, A. R., Ruhland, C. T. & Guénon, R. 2018. Desert leaf litter decay: Coupling of microbial respiration, water-soluble fractions and photodegradation. *Global Change Biology,* 24**,** 5454-5470.

Day, T. A., Guénon, R. & Ruhland, C. T. 2015. Photodegradation of plant litter in the Sonoran Desert varies by litter type and age. *Soil Biology and Biochemistry,* 89**,** 109-122.

Day, T. A., Zhang, E. T. & Ruhland, C. T. 2007. Exposure to solar UV-B radiation accelerates mass and lignin loss of Larrea tridentata litter in the Sonoran Desert. *Plant Ecology,* 193**,** 185-194.

Egger, M., Smith, G. D., Schneider, M. & Minder, C. 1997. Bias in meta-analysis detected by a simple, graphical test. *BMJ,* 315**,** 629.

Fortunel, C., Garnier, E., Joffre, R., Kazakou, E., Quested, H., Grigulis, K., Lavorel, S., Ansquer, P., Castro, H., Cruz, P., Doležal, J., Eriksson, O., Freitas, H., Golodets, C., Jouany, C., Kigel, J., Kleyer, M., Lehsten, V., Lepš, J., Meier, T., Pakeman, R., Papadimitriou, M., Papanastasis, V. P., Quétier, F., Robson, M., Sternberg, M., Theau, J.-P., Thébault, A. & Zarovali, M. 2009. Leaf traits capture the effects of land use changes and climate on litter decomposability of grasslands across Europe. *Ecology,* 90**,** 598-611.

Gallo, M. E., Porras-Alfaro, A., Odenbach, K. J. & Sinsabaugh, R. L. 2009. Photoacceleration of plant litter decomposition in an arid environment. *Soil Biology and Biochemistry,* 41**,** 1433-1441.

Gallo, M. E., Sinsabaugh, R. L. & Cabaniss, S. E. 2006. The role of ultraviolet radiation in litter decomposition in arid ecosystems. *Applied Soil Ecology,* 34**,** 82-91.

Hawkes, C. V., Kivlin, S. N., Rocca, J. D., Huguet, V., Thomsen, M. A. & Suttle, K. B. 2011. Fungal community responses to precipitation. *Global Change Biology,* 17**,** 1637-1645.

Henry, H. a. L., Brizgys, K. & Field, C. B. 2008. Litter Decomposition in a California Annual Grassland: Interactions Between Photodegradation and Litter Layer Thickness. *Ecosystems,* 11**,** 545-554.

Jones, A. G., Bussell, J., Winters, A., Scullion, J. & Gwynn-Jones, D. 2016. The functional quality of decomposing litter outputs from an Arctic plant community is affected by long-term exposure to enhanced UV-B. *Ecological Indicators,* 60**,** 8-17.

King, J. Y., Brandt, L. A. & Adair, E. C. 2012. Shedding light on plant litter decomposition: advances, implications and new directions in understanding the role of photodegradation. *Biogeochemistry,* 111**,** 57-81.

Knapp, G. & Hartung, J. 2003. Improved tests for a random effects meta-regression with a single covariate. *Statistics in Medicine,* 22**,** 2693-2710.

Lin, Y., Karlen, S. D., Ralph, J. & King, J. Y. 2018. Short-term facilitation of microbial litter decomposition by ultraviolet radiation. *Science of The Total Environment,* 615**,** 838-848.

Ma, Z., Yang, W., Wu, F. & Tan, B. 2017. Effects of light intensity on litter decomposition in a subtropical region. *Ecosphere,* 8**,** e01770.

Mao, B., Zhao, L., Zhao, Q. & Zeng, D. 2018. Effects of ultraviolet (UV) radiation and litter layer thickness on litter decomposition of two tree species in a semi-arid site of Northeast China. *Journal of Arid Land,* 10**,** 416-428.

Meentemeyer, V. 1978. Macroclimate and Lignin Control of Litter Decomposition Rates. *Ecology,* 59**,** 465-472.

Méndez, M. S., Martinez, M. L., Araujo, P. I. & Austin, A. T. 2019. Solar radiation exposure accelerates decomposition and biotic activity in surface litter but not soil in a semiarid woodland ecosystem in Patagonia, Argentina. *Plant and Soil*.

Moody, S. A., Newsham, K. K., Ayres, P. G. & Paul, N. D. 1999. Variation in the responses of litter and phylloplane fungi to UV-B radiation (290–315 nm). *Mycological Research,* 103**,** 1469-1477.

Moody, S. A., Paul, N. D., Björn, L. O., Callaghan, T. V., Lee, J. A., Manetas, Y., Rozema, J., Gwynn-Jones, D., Johanson, U., Kyparissis, A. & Oudejans, A. M. C. 2001. The direct effects of UV-B radiation on Betula pubescens litter decomposing at four European field sites. *Plant Ecology,* 154**,** 27-36.

Pan, X., Song, Y.-B., Liu, G.-F., Hu, Y.-K., Ye, X.-H., Cornwell, W. K., Prinzing, A., Dong, M. & Cornelissen, J. H. C. 2015. Functional traits drive the contribution of solar radiation to leaf litter decomposition among multiple arid-zone species. *Scientific Reports,* 5**,** 13217.

Pieristè, M., Chauvat, M., Kotilainen, T. K., Jones, A. G., Aubert, M., Robson, T. M. & Forey, E. 2019. Solar UV-A radiation and blue light enhance tree leaf litter decomposition in a temperate forest. *Oecologia,* 191**,** 191-203.

Pieristè, M., Neimane, S., Solanki, T., Nybakken, L., Jones, A. G., Forey, E., Chauvat, M., Ņečajeva, J. & Robson, T. M. 2020. Ultraviolet radiation accelerates photodegradation under controlled conditions but slows the decomposition of senescent leaves from forest stands in southern Finland. *Plant Physiology and Biochemistry,* 146**,** 42-54.

Pinheiro, J., Bates D, Debroy S, Sarkar D & Team, R. C. 2019. nlme: Linear and Nonlinear Mixed Effects Models. 3.1-141 ed.: R-Core project.

Pustejovsky, J. E. 2018. Using response ratios for meta-analyzing single-case designs with behavioral outcomes. *Journal of School Psychology,* 68**,** 99-112.

Rohatgi, A. 2019. WebPlotDigitizer. 4.2 ed. San Francisco, California, USA.

Rutledge, S., Campbell, D. I., Baldocchi, D. & Schipper, L. A. 2010. Photodegradation leads to increased carbon dioxide losses from terrestrial organic matter. *Global Change Biology,* 16**,** 3065-3074.

Sellaro, R., Crepy, M., Trupkin, S. A., Karayekov, E., Buchovsky, A. S., Rossi, C. & Casal, J. J. 2010. Cryptochrome as a Sensor of the Blue/Green Ratio of Natural Radiation in Arabidopsis. *Plant Physiology,* 154**,** 401.

Song, X., Peng, C., Jiang, H., Zhu, Q. & Wang, W. 2013. Direct and Indirect Effects of UV-B Exposure on Litter Decomposition: A Meta-Analysis. *PLOS ONE,* 8**,** e68858.

Verhoef, H. A., Verspagen, J. M. H. & Zoomer, H. R. 2000. Direct and indirect effects of ultraviolet-B radiation on soil biota, decomposition and nutrient fluxes in dune grassland soil systems. *Biology and Fertility of Soils,* 31**,** 366-371.

Viechtbauer, W. 2010. Conducting meta-analyses in R with the metafor package. *Journal of statistical software,* 36**,** 1-48.

Viechtbauer, W. 2019. Meta-Analysis Package for R. 2.1-0 ed.

Voříšková, J. & Baldrian, P. 2013. Fungal community on decomposing leaf litter undergoes rapid successional changes. *The ISME Journal,* 7**,** 477-486.

Wang, J., Liu, L., Wang, X. & Chen, Y. 2015. The interaction between abiotic photodegradation and microbial decomposition under ultraviolet radiation. *Global Change Biology,* 21**,** 2095-2104.

Wang, Q.-W., Robson, T. M., Pieristè, M., Oguro, M., Oguchi, R., Murai, Y. & Kurokawa, H. 2020. Testing trait plasticity over the range of spectral composition of sunlight in forb species differing in shade tolerance. *Journal of Ecology,* n/a.

Yamazaki, Y., Kataoka, H., Miyazakl, A., Watanabe, M. & Ootakl, T. 1996. Action Spectra for Photoinhibition of Sexual Development in Phycomyces blakesleeanus. *Photochemistry and Photobiology,* 64**,** 387-392.

Yao, M., Rui, J., Niu, H., Heděnec, P., Li, J., He, Z., Wang, J., Cao, W. & Li, X. 2017. The differentiation of soil bacterial communities along a precipitation and temperature gradient in the eastern Inner Mongolia steppe. *CATENA,* 152**,** 47-56.

Zaller, J. G., Caldwell, M. M., Flint, S. D., Ballaré, C. L., Scopel, A. L. & Sala, O. E. 2009. Solar UVB and warming affect decomposition and earthworms in a fen ecosystem in Tierra del Fuego, Argentina. *Global Change Biology,* 15**,** 2493-2502.

Zepp, R. G., Callaghan, T. V. & Erickson, D. J. 1995. Effects of increased solar ultraviolet radiation on biogeochemical cycles. *Ambio,* 24**,** 181-187.

TABLES

Table 1

Overall estimated log response ratio (lnRR) of mass loss, 95% confidence interval and *p*-value for each spectral region.

Spectral region	Estimate	95% CI		*p*-value	*% change*
Full-spectrum	**-0.138**	**-0.270**	**-0.007**	**0.040**	**14.798**
Blue light	**-0.116**	**-0.225**	**-0.007**	**0.037**	**12.299**
UV-A radiation	**0.048**	**0.008**	**0.089**	**0.019**	**4.917**
UV-B radiation	0.008	-0.086	0.101	0.872	0.803
UV radiation	-0.104	-0.283	0.075	0.255	10.960

Table 2

Heterogeneity between groups (Qb) and *p*-values of the moderators for each spectral region. Values in bold indicate statistical-significance.

Spectral region	Variable	Qb	*p*-value
Full-spectrum	**Climate**	**4.76**	**0.001**
	Decay period	**3049.09**	**< 0.001**
	Ecosystem	**9.77**	**< 0.001**
	Habit	0.41	0.526
	Life form	2.08	0.128
Blue	**Climate**	**4.81**	**0.003**
	Decay period	1.49	0.206
	Ecosystem	**46.74**	**< 0.001**
	Habit	0.02	0.898
	Life form	0.30	0.738
UV- A	Climate	0.64	0.529
	Decay period	**3.83**	**0.012**
	Ecosystem	2.46	0.090
	Habit	0.70	0.405
	Life form	0.22	0.805
UV- B	**Climate**	**11.85**	**< 0.001**
	Decay period	**11.17**	**< 0.001**
	Ecosystem	2.51	0.062
	Habit	**4.04**	**0.048**
	Life form	0.19	0.83
UV	Climate	0.39	0.763
	Decay period	**8.78**	**< 0.001**
	Ecosystem	2.15	0.094
	Habit	0.07	0.799
	Life form	2.66	0.071

FIGURES LIST

Figure 1

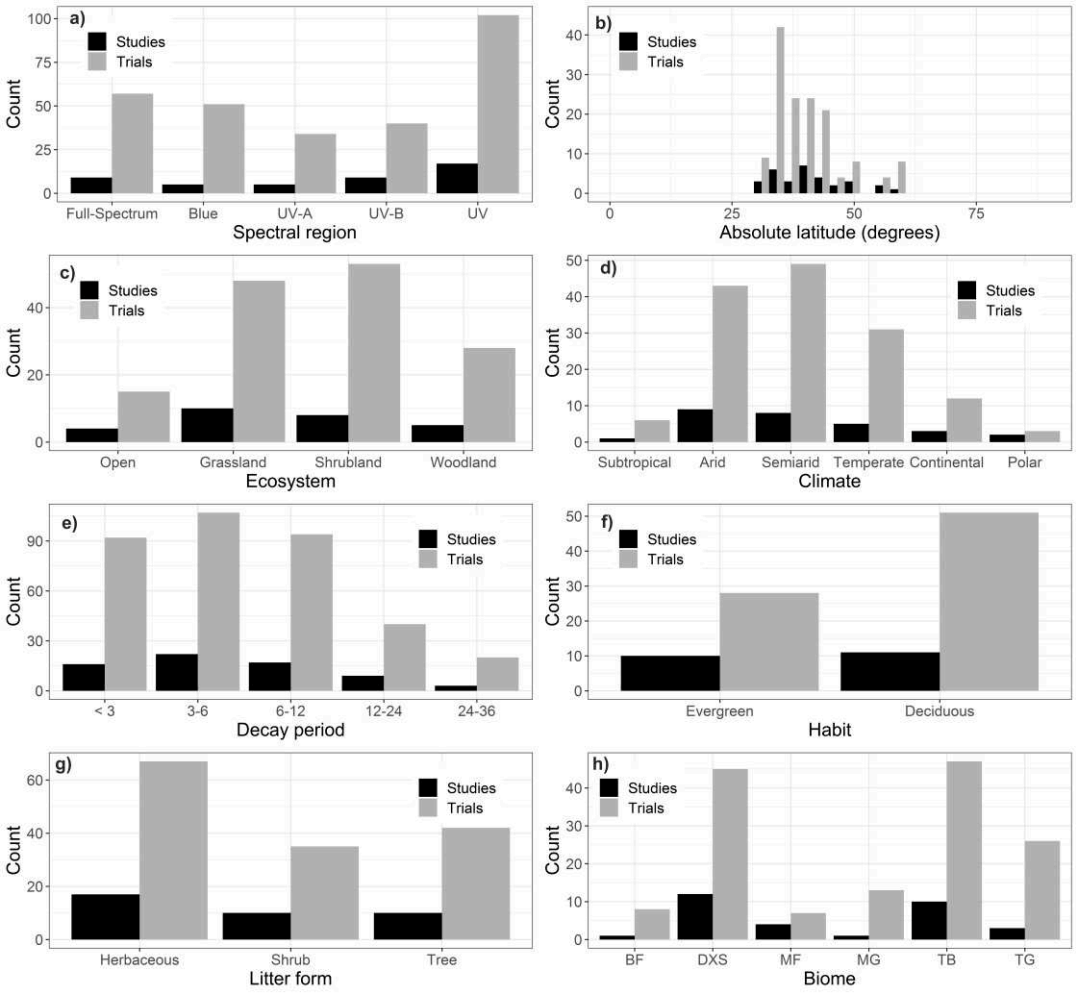
a)
Studies
Trials
Count
Full-Spectrum
Blue
UV-A
UV-B
UV
Spectral region
b)
Absolute latitude (degrees)
c)
Open
Grassland
Shrubland
Woodland
Ecosystem
d)
Subtropical
Arid
Semiarid
Temperate
Continental
Polar
Climate
e)
< 3
3-6
6-12
12-24
24-36
Decay period
f)
Evergreen
Deciduous
Habit
g)
Herbaceous
Shrub
Tree
Litter form
h)
BF
DXS
MF
MG
TB
TG
Biome

Figure 2

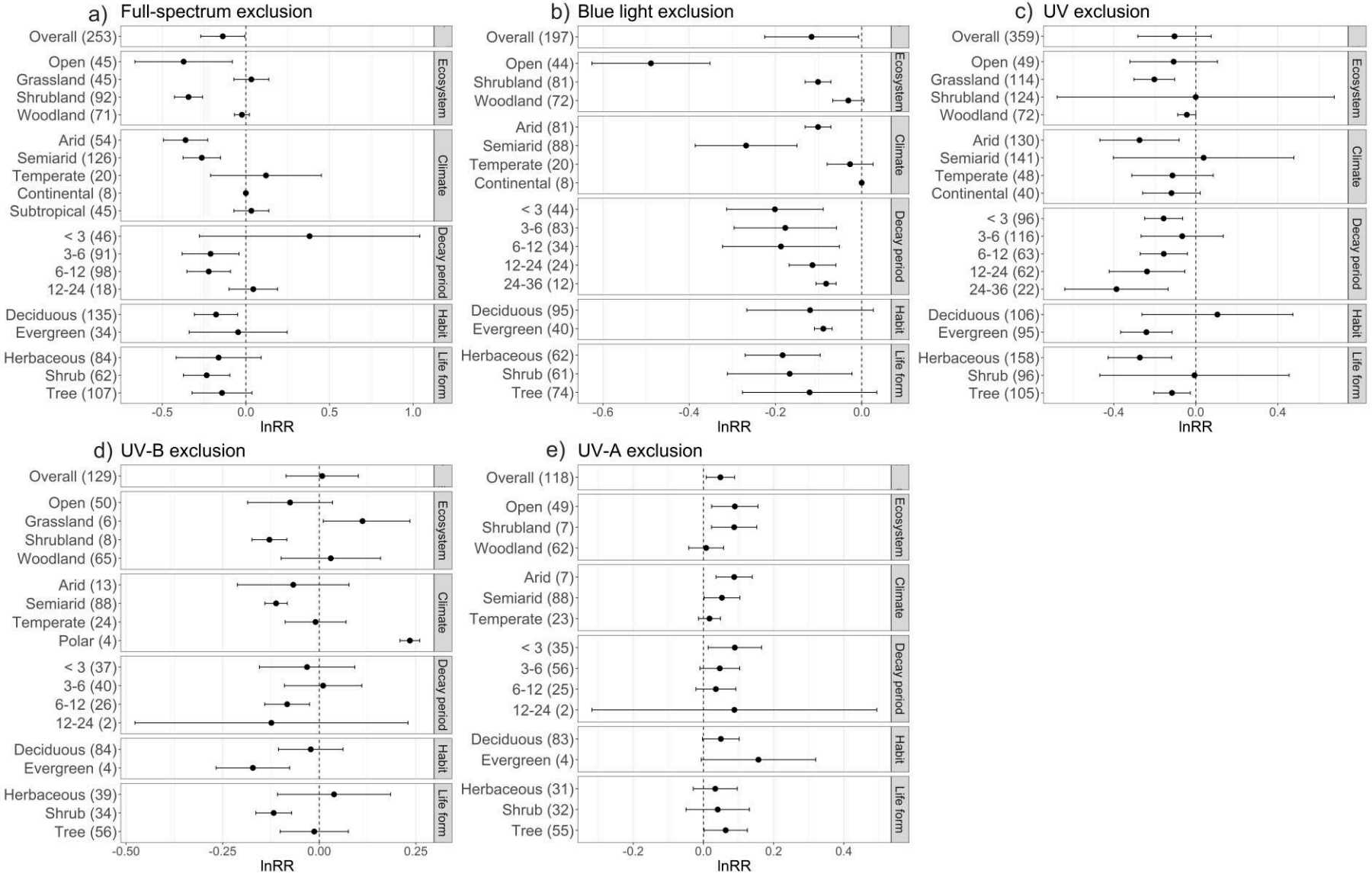
a) Full-spectrum exclusion
Overall (253)
Open (45)
Grassland (45)
Shrubland (92)
Woodland (71)
Ecosystem
Arid (54)
Semiarid (126)
Temperate (20)
Continental (8)
Subtropical (45)
Climate
< 3 (46)
3-6 (91)
6-12 (98)
12-24 (18)
Decay period
Deciduous (135)
Evergreen (34)
Habit
Herbaceous (84)
Shrub (62)
Tree (107)
Life form
-0.5
0.0
0.5
1.0
lnRR
b) Blue light exclusion
Overall (197)
Open (44)
Shrubland (81)
Woodland (72)
Ecosystem
Arid (81)
Semiarid (88)
Temperate (20)
Continental (8)
Climate
< 3 (44)
3-6 (83)
6-12 (34)
12-24 (24)
24-36 (12)
Decay period
Deciduous (95)
Evergreen (40)
Habit
Herbaceous (62)
Shrub (61)
Tree (74)
Life form
-0.6
-0.4
-0.2
0.0
lnRR
c) UV exclusion
Overall (359)
Open (49)
Grassland (114)
Shrubland (124)
Woodland (72)
Ecosystem
Arid (130)
Semiarid (141)
Temperate (48)
Continental (40)
Climate
< 3 (96)
3-6 (116)
6-12 (63)
12-24 (62)
24-36 (22)
Decay period
Deciduous (106)
Evergreen (95)
Habit
Herbaceous (158)
Shrub (96)
Tree (105)
Life form
-0.4
0.0
0.4
lnRR
d) UV-B exclusion
Overall (129)
Open (50)
Grassland (6)
Shrubland (8)
Woodland (65)
Ecosystem
Arid (13)
Semiarid (88)
Temperate (24)
Polar (4)
Climate
< 3 (37)
3-6 (40)
6-12 (26)
12-24 (2)
Decay period
Deciduous (84)
Evergreen (4)
Habit
Herbaceous (39)
Shrub (34)
Tree (56)
Life form
-0.50
-0.25
0.00
0.25
lnRR
e) UV-A exclusion
Overall (118)
Open (49)
Shrubland (7)
Woodland (62)
Ecosystem
Arid (7)
Semiarid (88)
Temperate (23)
Climate
< 3 (35)
3-6 (56)
6-12 (25)
12-24 (2)
Decay period
Deciduous (83)
Evergreen (4)
Habit
Herbaceous (31)
Shrub (32)
Tree (55)
Life form
-0.2
0.0
0.2
0.4
lnRR

Figure 3

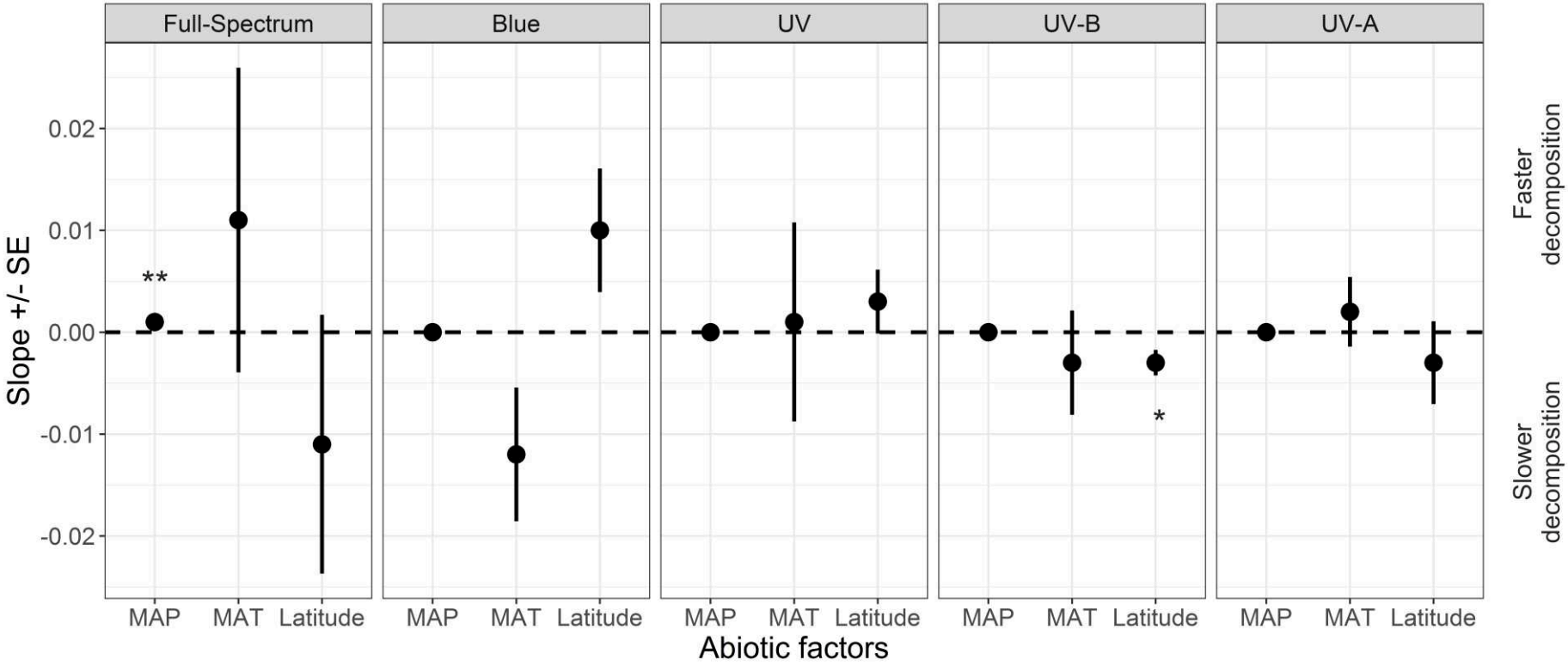
Full-Spectrum
Blue
UV
UV-B
UV-A
Slope +/- SE
0.02
0.01
0.00
-0.01
-0.02
**
*
MAP
MAT
Latitude
Abiotic factors
Faster decomposition
Slower decomposition

Figure 4

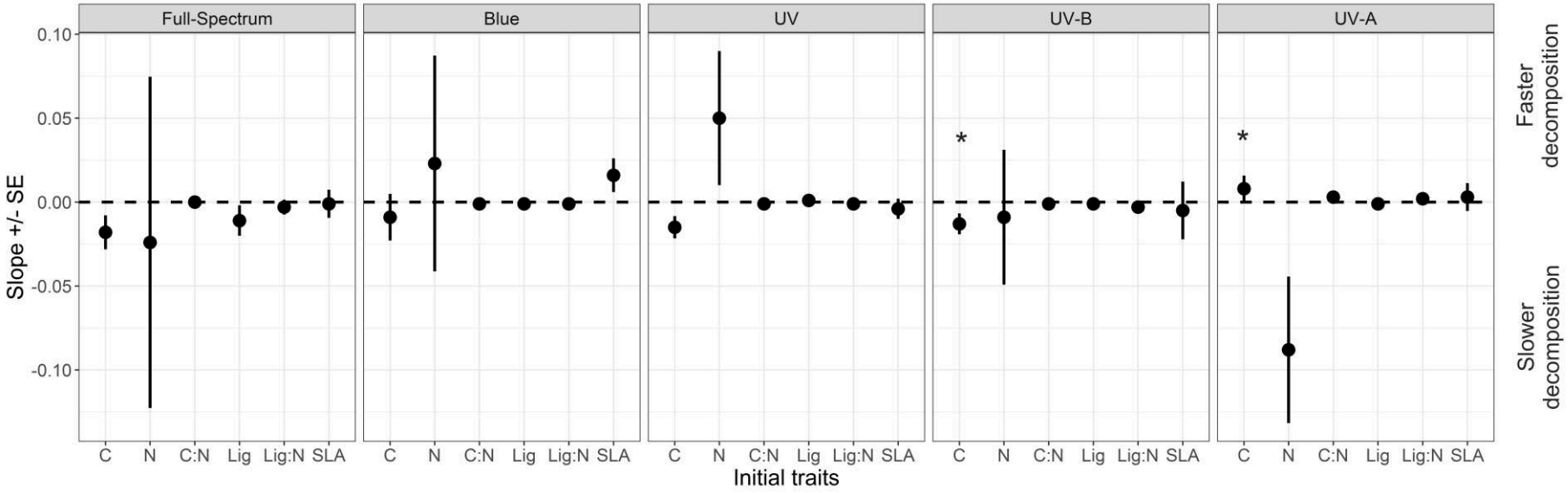
Full-Spectrum
Blue
UV
UV-B
UV-A
Slope +/- SE
0.10
0.05
0.00
-0.05
-0.10
C
N
C:N
Lig
Lig:N
SLA
Initial traits
*
*
Faster decomposition
Slower decomposition

Electronic supplementary material

Appendix 1 – Literature collection and selection criteria

Literature, published between 1980 and July 2019, was collected from Web of Science, Google Scholar, and Scopus database. Keywords used for literature search were as follow:

(1) TS= (“blue light”) AND TS= (litter* OR decomposition* OR “leaf litter”* OR photodegradation) AND TS= plant*

(2) TS= (“green light”) AND TS= (litter* OR decomposition* R “leaf litter”* OR photodegradation) AND TS= plant*

(3) TS= (“red light” OR “far-red”) AND TS= (litter* OR decomposition* OR “leaf litter”* OR photodegradation) AND TS= plant*

(4) TS= (Ultraviolet OR UV-B OR UV-A) AND TS= (litter* OR decomposition* OR “leaf litter”* OR photodegradation) AND TS= plant*

(5) TS=(“light quality” OR “spectral composition”) AND TS= (litter* OR decomposition* OR “leaf litter”* OR photodegradation) AND TS= plant*

The few studies from controlled environments were excluded due to the difficulties in comparing them with field studies. All studies employing litter resulting from a mixture of different species were excluded as they were impractical to relate to standard litter traits measured for single species. For the same reason, only studies using leaf litter were considered, while studies employing mixtures of stems and twigs or woody debris were excluded. Studies in which litterbags were buried were excluded. All studies employing supplemental radiation were excluded since the meta-analysis aimed to produce results representative of natural conditions (ambient solar spectral irradiance).

Appendix 2 - List of papers retained in the meta-analysis

1. Almagro, María, Fernando T. Maestre, Javier Martínez-López, Enrique Valencia, and Ana Rey. 2015. "Climate Change May Reduce Litter Decomposition While Enhancing the Contribution of Photodegradation in Dry Perennial Mediterranean Grasslands." *Soil Biology and Biochemistry* 90 (November): 214–23. doi:10.1016/j.soilbio.2015.08.006.

2. Almagro, María, Javier Martínez-López, Fernando T. Maestre, and Ana Rey. 2017. "The Contribution of Photodegradation to Litter Decomposition in Semiarid Mediterranean Grasslands Depends on Its Interaction with Local Humidity Conditions, Litter Quality and Position." *Ecosystems* 20 (3): 527–42. doi:10.1007/s10021-016-0036-5.

3. Austin, Amy T., M. Soledad Méndez, and Carlos L. Ballaré. 2016. "Photodegradation Alleviates the Lignin Bottleneck for Carbon Turnover in Terrestrial Ecosystems." *Proceedings of the National Academy of Sciences* 113 (16): 4392–97. doi:10.1073/pnas.1516157113.

4. Baker, Nameer R., and Steven D. Allison. 2015. "Ultraviolet Photodegradation Facilitates Microbial Litter Decomposition in a Mediterranean Climate." *Ecology* 96 (7): 1994–2003.

5. Brandt, L. A., J. Y. King, S. E. Hobbie, D. G. Milchunas, and R. L. Sinsabaugh. 2010. "The Role of Photodegradation in Surface Litter Decomposition Across a Grassland Ecosystem Precipitation Gradient." *Ecosystems* 13 (5): 765–81. doi:10.1007/s10021-010-9353-2.

6. Day, T.A., Bliss, M.S., Tomes, A.R., Ruhland, C.T. and Guénon, R., 2018. "Desert leaf litter decay: Coupling of microbial respiration, water-soluble fractions and photodegradation." Global change biology, 24(11), pp.5454-5470.

7. Day, Thomas A., René Guénon, and Christopher T. Ruhland. 2015. “Photodegradation of Plant Litter in the Sonoran Desert Varies by Litter Type and Age.” *Soil Biology and Biochemistry* 89 (October): 109–22. doi:10.1016/j.soilbio.2015.06.029.

8. Day, Thomas A., Elisa T. Zhang, and Christopher T. Ruhland. 2007. “Exposure to Solar UV-B Radiation Accelerates Mass and Lignin Loss of Larrea Tridentata Litter in the Sonoran Desert.” *Plant Ecology* 193 (2): 185–94. doi:10.1007/s11258-006-9257-6.

9. Gaxiola, Aurora, and Juan J. Armesto. 2015. “Understanding Litter Decomposition in Semiarid Ecosystems: Linking Leaf Traits, UV Exposure and Rainfall Variability.” *Frontiers in Plant Science* 6 (March). doi:10.3389/fpls.2015.00140.

10. Henry, H.A., Brizgys, K. and Field, C.B., 2008. “Litter decomposition in a California annual grassland: interactions between photodegradation and litter layer thickness.” Ecosystems, 11(4), pp.545-554.

11. Huang, Gang, Hong-mei Zhao, and Yan Li. 2017. “Litter Decomposition in Hyper-Arid Deserts: Photodegradation Is Still Important.” *Science of The Total Environment* 601–602 (December): 784–92. doi:10.1016/j.scitotenv.2017.05.213.

12. Lin, Yang, Rachel D. Scarlett, and Jennifer Y. King. 2015. “Effects of UV Photodegradation on Subsequent Microbial Decomposition of Bromus Diandrus Litter.” *Plant and Soil* 395 (1–2): 263–71. doi:10.1007/s11104-015-2551-0.

13. Liu, G., Wang, L., Jiang, L., Pan, X., Huang, Z., Dong, M. and Cornelissen, J.H., 2018. Specific leaf area predicts dryland litter decomposition via two mechanisms. *Journal of Ecology*, *106*(1), pp.218-229.

14. Ma, Zhiliang, Wanqin Yang, Fuzhong Wu, and Bo Tan. 2017. “Effects of Light Intensity on Litter Decomposition in a Subtropical Region.” *Ecosphere* 8 (4): e01770. doi:10.1002/ecs2.1770.

15. Mao, B., Zhao, L., Zhao, Q. and Zeng, D., 2018. “Effects of ultraviolet (UV) radiation and litter layer thickness on litter decomposition of two tree species in a semi-arid site of Northeast China.” Journal of Arid Land, 10(3), pp.416-428.

16. Messenger, David J., Stephen C. Fry, Sirwan Yamulki, and Andrew R. McLeod. 2012. “Effects of UV-B Filtration on the Chemistry and Decomposition of Fraxinus Excelsior Leaves.” *Soil Biology and Biochemistry* 47 (April): 133–41. doi:10.1016/j.soilbio.2011.12.010.

17. Pan, Xu, Yao-Bin Song, Guo-Fang Liu, Yu-Kun Hu, Xue-Hua Ye, William K. Cornwell, Andreas Prinzing, Ming Dong, and Johannes H.C. Cornelissen. 2015. “Functional Traits Drive the Contribution of Solar Radiation to Leaf Litter Decomposition among Multiple Arid-Zone Species.” *Scientific Reports* 5 (August): 13217. doi:10.1038/srep13217.

18. Pancotto Verónica A., Osvaldo E. Sala, Marta Cabello, Nancy I. López, T. Matthew Robson, Carlos L. Ballaré, Martyn M. Caldwell, and Ana L. Scopel. 2003. “Solar UV-B Decreases Decomposition in Herbaceous Plant Litter in Tierra Del Fuego, Argentina: Potential Role of an Altered Decomposer Community.” *Global Change Biology* 9 (10): 1465–1474.

19. Pieristè, M., Chauvat, M., Kotilainen, T.K., Jones, A.G., Aubert, M., Robson, T.M. and Forey, E., 2019. Solar UV-A radiation and blue light enhance tree leaf litter decomposition in a temperate forest. Oecologia, 191(1), pp.191-203.

20. Pieristè, M, Neimane, S, Solanki, T, Nybakken, L, Jones, AG, Forey, E, Chauvat, M, Jevgenija, N, Robson, TM, 2020. “Ultraviolet radiation accelerates photodegradation under controlled conditions but slows the decomposition

of senescent leaves from forest stands in southern Finland." Plant Physiology and Biochemistry, 146, pp. 42-54

21. Pieristè, M, Forey, E, Laruelle, F, Lounès-Hadj Sahraoui, A, Meglouli, H, Delporte, P, Robson, TM, Chauvat, M, "Spectral composition of sunlight affects the microbial functional structure of beech leaf litter" *under review in Plant and Soil*

22. Uselman, S.M., Snyder, K.A., Blank, R.R. and Jones, T.J., 2011. "UVB exposure does not accelerate rates of litter decomposition in a semi-arid riparian ecosystem." Soil Biology and Biochemistry, 43(6), pp.1254-1265.

23. Wang, J., Yang, S., Zhang, B., Liu, W., Deng, M., Chen, S. and Liu, L., 2017. Temporal dynamics of ultraviolet radiation impacts on litter decomposition in a semi-arid ecosystem. Plant and soil, 419(1-2), pp.71-81.

24. Wang, Q.W., Pieristè M, Kenta T, Liu C, Robson, T. M., Kurokawa, H. Quantifying the contribution of photodegradation to litter decomposition in a temperate forest gap and understorey. *Unpublished*

25. Zaller, Johann G., Martyn M. Caldwell, Stephan D. Flint, Carlos L. Ballaré, Ana L. Scopel, and Osvaldo E. Sala. 2009. "Solar UVB and Warming Affect Decomposition and Earthworms in a Fen Ecosystem in Tierra Del Fuego, Argentina." *Global Change Biology* 15 (10): 2493–2502. doi:10.1111/j.1365-2486.2009.01970.x.

Appendix 3 – Litter species

ID	Species	Life form	Habit
1	*Acer carpinifolium*	Tree	Deciduous
2	*Achnatherum sibiricum*	Herbaceous	
3	*Agriophyllum arenarium*	Herbaceous	
4	*Agriophyllum pungens*	Herbaceous	
5	*Agropyron cristatum*	Herbaceous	
6	*Alhagi sparsifolia*	Herbaceous	
7	*Ambrosia deltoidea*	Shrub	Evergreen
8	*Andropogon gerardii*	Herbaceous	
9	*Araucaria auraucana*	Tree	Evergreen
10	*Aristida pennata*	Herbaceous	
11	*Aristida purpurea*	Herbaceous	
12	*Avena sativa*	Herbaceous	
13	*Baileya multiradiata*	Herbaceous	
14	*Betula pendula*	Tree	Deciduous
15	*Betula platyphylla*	Tree	Deciduous
16	*Bouteloua gracilis*	Herbaceous	
17	*Bromus diandrus*	Herbaceous	
18	*Bromus pictus*	Herbaceous	
19	*Bromus rubens*	Herbaceous	
20	*Calligonum mongolicum*	Shrub	Deciduous
21	*Caragana korshinskii*	Shrub	Deciduous
22	*Carduus acanthoides*	Herbaceous	
23	*Carex curta*	Herbaceous	
24	*Carex decidua*	Herbaceous	
25	*Chusquea culeou*	Shrub	Evergreen
26	*Cinnamomum camphora*	Tree	Deciduous
27	*Cleistogenes squarrosa*	Herbaceous	

28	*Cryptomeria fortunei*	Tree	Evergreen
29	*Cunninghamia lanceolata*	Tree	Evergreen
30	*Cynanchum sibiricum*	Herbaceous	
31	*Cynodon dactylon*	Herbaceous	
32	*Dactylis glomerata*	Herbaceous	
33	*Echinops gmelinii*	Herbaceous	
34	*Echinops sphaerocephalus*	Herbaceous	
35	*Elymus condensatus*	Herbaceous	
36	*Encelia farinosa*	Shrub	Evergreen
37	*Encelia frutescens*	Shrub	Evergreen
38	*Ephedra distachya*	Shrub	Evergreen
39	*Eragrostis curvula*	Herbaceous	
40	*Erodium oxyrhinchum*	Herbaceous	
41	*Fagus crenata*	Tree	Deciduous
42	*Fagus sylvatica*	Tree	Deciduous
43	*Fallopia japonica*	Herbaceous	
44	*Filipendula camtschatica*	Herbaceous	
45	*Fraxinus americana*	Tree	Deciduous
46	*Fraxinus excelsior*	Tree	Deciduous
47	*Glycine max*	Herbaceous	
48	*Gunnera magellanica*	Herbaceous	
49	*Haloxylon ammodendron*	Shrub	Evergreen
50	*Hedysarum laeve*	Shrub	Deciduous
51	*Helianthus annuus*	Herbaceous	
52	*Krascheninnikovia ceratoides*	Shrub	Deciduous
53	*Larrea tridentata*	Shrub	Evergreen
54	*Lepidium latifolium*	Herbaceous	
55	*Lespedeza bicolor*	Shrub	Deciduous
56	*Lespedeza davurica*	Herbaceous	
57	*Leymus chinensis*	Herbaceous	

58	*Lindera obtusiloba*	Shrub	Deciduous
59	*Lolium multiflorum*	Herbaceous	
60	*Maytenus boaria*	Shrub	Evergreen
61	*Mulgedium tataricum*	Herbaceous	
62	*Mulinum spinosum*	Shrub	Evergreen
63	*Nitraria sibirica*	Herbaceous	
64	*Nitraria tangutorum*	Shrub	Deciduous
65	*Nothofagus antarctica*	Tree	Deciduous
66	*Nothofagus dombeyi*	Tree	Evergreen
67	*Nothofagus nervosa*	Tree	Deciduous
68	*Nothofagus obliqua*	Tree	Deciduous
69	*Olneya tesota*	Tree	Evergreen
70	*Paspalum quadrifarium*	Herbaceous	
71	*Peganum harmala*	Herbaceous	
72	*Pertya trilobata*	Herbaceous	
73	*Phragmites australis*	Herbaceous	
74	*Pinus massoniana*	Tree	Evergreen
75	*Pinus ponderosa*	Tree	Evergreen
76	*Pinus sylvestris var. Mongolica*	Tree	Evergreen
77	*Poa ligularis*	Herbaceous	
78	*Populus nigra*	Tree	Deciduous
79	*Populus x xiaozhuanica*	Tree	Evergreen
80	*Porlieria chilensis*	Shrub	Evergreen
81	*Prosopis velutina*	Tree	Deciduous
82	*Quercus acutissima*	Tree	Deciduous
83	*Quercus crispula*	Tree	Deciduous
84	*Quercus robur*	Tree	Deciduous
85	*Retama sphaerocarpa*	Shrub	Evergreen
86	*Salix cheilophila*	Tree	Deciduous
87	*Salix gordejevii*	Shrub	Deciduous

88	*Schisandra chinensis*	Shrub	Deciduous
89	*Schizachyrium scoparium*	Herbaceous	
90	*Simmondsia chinensis*	Shrub	Evergreen
91	*Stipa krylovii*	Herbaceous	
92	*Stipa speciosa*	Herbaceous	
93	*Stipa tenacissima*	Herbaceous	
94	*Tamarix chinensis*	Shrub	Deciduous
95	*Toona ciliata*	Tree	Deciduous
96	*Triticum aestivum*	Herbaceous	
97	*Vitis coignetiae*	Shrub	Deciduous
98	*Zea mays*	Herbaceous	

Appendix 4 – Data extracted from the papers

The following data were extracted from the studies where present for each plant species (directly from tables or from the plots through web plot digitizer):

- Initial dry weight (g)
- Decomposition rate k
- Initial LMA (g/m^2)
- Initial SLA (cm^2/g) -> then transformed in LMA
- Initial carbon content (%)
- Initial nitrogen content (%)
- Initial C:N
- Initial lignin content (%)
- Initial cellulose content (%)
- Initial hemicellulose content (%)
- Duration (months)
- Number of replicates
- Remaining dry mass (%), average and std error
- Mass lost (%), average and std error
- Final carbon content (%)
- Final nitrogen content (%)
- Final C:N
- Final lignin content (%)

Complementary information extracted:

- Author
- Year of publication
- Coordinates of the study site
- Elevation of the study site
- Ecosystem (grassland, scrubland, open area, woodland,..)
- Climate (arid, temperate, semi-arid…)

- Spectral manipulation
- Light environment (representing the light treatment)
- Average annual precipitation (mm)
- Average annual temperature (°C)
- Plant species
- Functional group (herbaceous, shrub, tree)
- Habit (evergreen, deciduous)
- Duration of the treatment (months).

Appendix 5 – Climate categories – Köppen-Geiger updated classification

- **Subtropical:** group A

  Am = Tropical monsoon climate
- **Arid:** group B

  BWh = Hot desert climate
- **Semiarid:** group B

  BSh = Hot semi-arid climate
- **Temperate:** group C

  Cfb = Temperate oceanic climate

  Csb = Warm-summer Mediterranean climate

  Csc = Cold-summer Mediterranean climate
- **Continental:** group D

  Dfa = Hot-summer humid continental climate

  Dfb = Warm-summer humid continental climate

  Dwb = Monsoon-influenced warm-summer humid continental climate
- **Polar:** group E

  ET = Tundra climate

Appendix 6 – List of biomes in which the retained studies are located

Biome	N of experimental sites
Boreal forests / Taiga	1
Deserts and xeric shrublands	12
Mediterranean Forests, Woodlands and Scrub	4
Montane grasslands and shrublands	1
Temperate broadleaf and mixed forests	10
Temperate grasslands, savannas and shrublands	3

Appendix 7 – Map showing the locations of studies retained in the meta-analysis

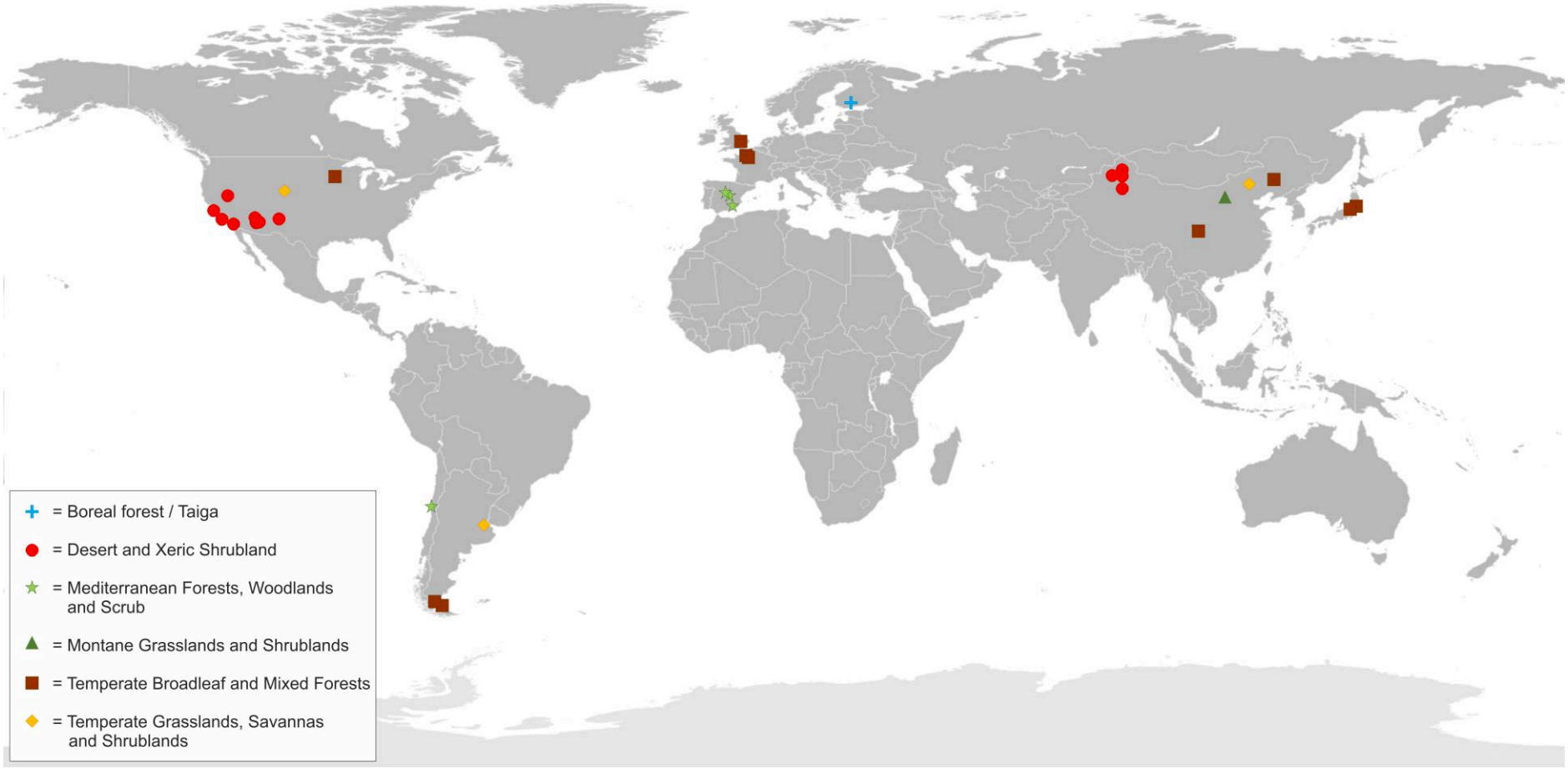

Map of the study sites of retained studies divided according to the WWF biome classification.

Appendix 8 – Supplementary Tables

Table S1

Average slope, *p*-value and R^2 of the relationship of MAT, MAP and latitude with photodegradation. *p*-values in bold indicate statistically significant differences ($P < 0.05$).

Spectral region	**Full-spectrum**			**Blue light**			**UV-A radiation**			**UV-B radiation**			**UV radiation**		
Variable	**Slope**	***p*-value**	**R^2**	**Slope**	***p*-value**	**R^2**	**Slope**	***p*-value**	**R^2**	**Slope**	***p*-value**	**R^2**	**Slope**	***p*-value**	**R^2**
MAP	**0.001**	**0.009**	**0.292**	0.000	0.551	0.013	0.000	0.508	0.031	0.000	0.403	0.045	0.000	0.315	0.038
MAT	0.011	0.495	0.045	-0.012	0.169	0.059	0.002	0.627	0.011	-0.003	0.521	0.032	0.001	0.879	0.002
Latitude	-0.011	0.376	0.032	0.010	0.091	0.060	-0.003	0.509	0.018	**-0.003**	**0.027**	**0.244**	0.003	0.403	0.028

Table S2

Average slope, p-value and R^2 of the relationship between initial litter traits and photodegradation. *p*-values in bold indicate statistically significant differences ($P < 0.05$).

Spectral region	**Full-spectrum**			**Blue light**			**UV-A radiation**			**UV-B radiation**			**UV radiation**		
Variable	**Slope**	***p*-value**	**R^2**	**Slope**	***p*-value**	**R^2**	**Slope**	***p*-value**	**R^2**	**Slope**	***p*-value**	**R^2**	**Slope**	***p*-value**	**R^2**
Carbon	-0.018	0.084	0.061	-0.009	0.539	0.011	0.008	0.283	0.044	**-0.013**	**0.043**	**0.167**	**-0.015**	**0.025**	**0.080**
Nitrogen	-0.024	0.810	0.001	0.023	0.718	0.004	*-0.088*	*0.053*	*0.140*	-0.009	0.818	0.002	0.050	0.209	0.024
C:N	0.000	0.998	0.000	-0.001	0.780	0.002	*0.003*	*0.052*	*0.136*	-0.001	0.510	0.018	*-0.001*	*0.074*	*0.046*
Lignin	-0.011	0.217	0.059	-0.001	0.705	0.005	-0.001	0.820	0.004	-0.001	0.331	0.047	0.001	0.670	0.015
Lig:N	-0.003	0.558	0.006	-0.001	0.512	0.013	0.002	0.172	0.090	-0.003	0.150	0.132	-0.001	0.439	0.014
SLA	-0.001	0.907	0.000	0.016	0.120	0.142	0.003	0.756	0.038	-0.005	0.768	0.030	-0.004	0.498	0.004

Table S3

Average carbon flux in g C m^{-2} and corresponding standard error (SE) attributable to photodegradation in each biome divided according to spectral regions. Contribution to carbon emission (+) and retention (-).

Biome	Full-spectrum		Blue light		UV-A radiation	
	Average	SE	Average	SE	Average	SE
Boreal forests / Taiga	+ 20.28	7.19	+ 17.38	6.16	- 7.24	2.57
Deserts and xeric shrublands	+ 23.38	4.77	+ 20.04	4.09	- 8.35	1.71
Mediterranean Forests, Woodlands and Scrub	+ 30.10	3.80	+ 25.80	3.26	- 10.75	1.36
Montane grasslands and shrublands	+ 35.09	10.96	+ 30.08	9.40	- 12.53	3.92
Temperate broadleaf and mixed forests	+ 29.89	0.70	+ 25.62	0.60	- 10.67	0.25
Temperate grasslands, savannas and shrublands	+ 19.17	2.46	+ 16.43	2.11	- 6.85	0.88